Wnt signalling in the Ewing's sarcoma family of tumours

Lucy Abigail Shaw

Submitted in accordance with the requirements for the degree of Doctor of Philosophy

The University of Leeds

Leeds Institute of Cancer and Pathology

School of Medicine

July, 2014

The candidate confirms that the work submitted is her own and that appropriate credit has been given where reference has been made to the work of others.

Acknowledgments

I would like to thank my colleagues at the Leeds Institute of Cancer and Pathology for their help over the past 4 years. I am grateful to Dr Andrew Gaffney for producing the Shef4 human embryonic stem (hES) cell line with inducible EWS-FLI1 expression, and for technical advice on the culture of hES cells. I am also very grateful to Andrea Berry for providing the reprogrammed TTC466 and control (GFP) cell lines, and for her advice and assistance throughout my PhD. I would like to thank Dr Georgia Mavria for kindly providing the *E.coli* expressing pGEX GST-PBD used for the Rac1/Cdc42 pull-down assays, and to Dr Margherita Scarcia for technical assistance with these assays. Statistical analysis of the Wnt signalling array data was performed by Mr John Alexander and Dr Helene Thygesen and I am grateful for their assistance.

I would like to thank all members of Lab 4, past and present for their support and guidance over the past 4 years, especially to Dr Elizabeth Roundhill for assistance with the lentiviral and cloning experiments and to Samantha Brownhill and Dr Virginie Viprey for assistance with the planning and analysis of the RTqPCR experiments.

I am extremely thankful to my supervisor Professor Sue Burchill for her continued advice, support and encouragement both in the lab and in the writing of this thesis. I would also like to thank my co-supervisor Dr Helen Payne for her guidance.

Finally thanks to my wonderful friends and to my partner Phil, for his tireless support particularly over the past 6 months, and to my mum Carol, for everything.

Abstract

Ewing's sarcoma family of tumours (ESFT) are aggressive tumours with a tendency to metastasise, which is associated with poor outcome. ESFT are characterised by an *EWS-ETS* gene rearrangement, most commonly *EWS-FLI1*. However, the mechanism of tumour formation is poorly understood and the cell of origin unclear. Since Wnt signalling is frequently deregulated in pathological conditions including cancer I have examined the potential role of Wnt signalling in ESFT cell lines and two novel *in vitro* models of ESFT development.

Components of the Wnt signalling pathway were expressed in all 6 ESFT cell lines studied. A lentiviral-based luciferase assay measuring TCF/LEF mediated signalling was successfully developed and demonstrated that the canonical Wnt signalling pathway is active in ESFT cell lines. Assays developed to investigate the activity of the noncanonical Wnt signalling pathway indicated that active Rac1 is expressed in some ESFT cell lines, and that ESFT cell lines are highly migratory.

Two complementary model systems were utilised to investigate Wnt signalling in the initiation of ESFT. Firstly, analysis of reprogrammed ESFT cells showed an increase in response of the canonical Wnt signalling pathway to Wnt3A, and an increase in active Rac1 expression. Furthermore Wnt signalling components were differentially expressed in reprogrammed cells. The induction of EWS-FLI1 expression in human embryonic stem (hES) cells increased canonical Wnt signalling and expression of active Cdc42. These cells had an altered phenotype and were more migratory. EWS-FLI1 expression also resulted in differential expression of Wnt signalling components including DKK2, DKK4, FZD8, Wnt4 and Wnt5A.

These data demonstrate that both the canonical and noncanonical Wnt signalling pathways may be important in the initiation of ESFT. Further elucidation of the role of these pathways and the individual components in tumour development could inform the development of novel therapeutics that could prevent tumour metastasis and relapse.

Table of Contents

Acknowledgments ..... **iii**

Abstract ..... **iv**

Figures ..... **xii**

Tables ..... **xv**

Abbreviations ..... **xvi**

1. Introduction **1**

1.1 Cancer 1

1.1.1 Biology of cancer 1

1.1.2 Metastasis 3

1.1.3 Cancer initiating cells (CICs) 3

1.1.4 Cancer treatment 5

1.2 Ewing's sarcoma family of tumours (ESFT) 7

1.2.1 Biology of ESFT 7

1.2.2 Genetic abnormalities in ESFT 7

1.2.3 Model systems to study ESFT initiation and development 9

1.2.4 Treatment of ESFT 12

1.3 Wnt signalling 16

1.3.1 Wnt ligands 16

1.3.2 Wnt signalling pathways 17

1.3.2.1 Canonical Wnt signalling 17

1.3.2.2 Noncanonical Wnt signalling 20

1.3.2.3 Alternative Wnt receptors 20

1.3.3 Wnt signalling in normal cells 22

1.3.4 Wnt signalling in cancer 23

1.3.4.1 Canonical Wnt signalling in cancer 23

1.3.4.2 Noncanonical Wnt signalling in cancer 24

1.3.4.3 Wnt signalling in cancer initiating cells (CICs) 25

1.3.5 Wnt signalling in ESFT 25

1.4 Hypothesis and aims 27

2. Expression of Wnt signalling components in ESFT cell lines **29**

2.1 Introduction 29

2.2 Materials and methods 33

2.2.1 Tissue culture 33

2.2.2 Determination of viable cell number 35

2.2.3 SDS-PAGE and western blotting 35
2.2.3.1 Preparation of protein extracts 35
2.2.3.2 Determination of protein concentration 36
2.2.3.3 SDS-Polyacrylamide Gel Electrophoresis (SDS-PAGE) 36
2.2.3.4 Electrophoretic transfer of proteins 37
2.2.3.5 Immunodetection of proteins 37
2.2.4 Subcellular fractionation 39
2.2.5 Flow cytometry 41
2.2.6 RTqPCR 41
2.2.6.1 Extraction of RNA from cell lines 41
2.2.6.2 Spectrophotometric measurement of nucleic acid quantity and quality 42
2.2.6.3 Preparation of cDNA 42
2.2.6.4 Taqman gene expression array 44
2.2.6.5 Assays-on-Demand™ 45
2.2.7 Statistics 46
2.3 Results 48
2.3.1 mRNA expression of Wnt signalling components in ESFT cell lines 48
2.3.1.1 Profile by TaqMan® Wnt Pathway Array 48
2.3.2 Expression of Wnt ligands in ESFT cell lines 52
2.3.2.1 Expression of Wnt1 protein 52
2.3.2.2 Expression of Wnt3A protein 58
2.3.2.3 Expression of Wnt5A protein 60
2.3.3 Subcellular localisation of β-catenin in ESFT cell lines 64
2.3.4 Expression of active β-catenin in ESFT cell lines 66
2.4 Discussion 68
3. Developing an assay to measure the activity of the canonical Wnt signalling pathway in ESFT cell lines 76
3.1 Introduction 76
3.2 Materials and Methods 79
3.2.1 Cell lines and tissue culture 79
3.2.2 Lentiviral transduction of cells 79
3.2.2.1 Production of vector DNA 79
3.2.2.2 Generation of lentiviral vectors in HEK293T cells 80
3.2.2.3 Infecting target cells with lentiviral vectors 81
3.2.3 Measuring GFP expression in cells by flow cytometry 81

3.2.4 Titration of lentiviral vectors 82
3.2.5 Luciferase assay 83
3.2.6 L cell conditioned media 83
3.2.6.1 Generating L cell conditioned media 83
3.2.6.2 The effect of L cell conditioned media on the viability of ESFT cell lines 84
3.2.6.3 Quantifying the concentration of Wnt3A in L-Wnt3A conditioned media 84
3.2.7 Measuring 7TGP reporter activity in cells 84
3.2.8 Measuring 7TFP reporter activity in cells 85
3.2.9 Viable cell number of ESFT cells treated with Wnt ligands 85
3.2.10 Detection of total and active β-catenin by western blot 85
3.2.11 Statistics 85
3.3 Results 86
3.3.1 Developing and optimising a lentiviral TCF reporter assay 86
3.3.1.1 Titration of lentiviral vector 86
3.3.1.2 Infection of ESFT cell lines with lentiviral GFP plasmid 88
3.3.1.3 Optimising measurement of canonical Wnt signalling activity using 7TGP and 7TFP reporter plasmids 90
3.3.2 Measuring the activity of the canonical Wnt signalling pathway in ESFT cell lines 100
3.3.2.1 7TGP reporter activity in ESFT cell lines 100
3.3.2.2 7TFP reporter activity in ESFT cell lines 102
3.3.3 Effect of recombinant Wnt3A and Wnt5A on the viable cell number of ESFT cell lines 104
3.3.4 Confirmation of downstream activation of the canonical Wnt signalling pathway 105
3.3.4.1 Optimising conditions to detect increase in total and active β-catenin after treatment with Wnt3A 105
3.3.4.2 Level of total and active β-catenin in ESFT cells after Wnt3A treatment 107
3.4 Discussion 109
4. Developing assays to measure the activity of the noncanonical Wnt signalling pathway in ESFT cells 116
4.1 Introduction 116
4.2 Materials and Methods 119
4.2.1 Rac1/Cdc42 pull-down assay 119
4.2.1.1 Preparing PAK-CRIB protein 119

4.2.1.2 Binding GST-PAK-CRIB protein to beads 119
4.2.1.3 Quantification of GST-PAK-CRIB protein bound to beads..... 120
4.2.1.4 Performing Rac1/Cdc42 pull-down assay 120
4.2.1.5 Determining the specificity of Rac1 and Cdc42 antibodies.... 121
4.2.2 Generation of spheroids from cell lines 121
4.2.3 3D migration assay using cell spheroids..... 121
4.2.4 3D invasion assay using cell spheroids..... 122
4.3 Results..... 123
4.3.1 Optimisation of Rac1/Cdc42 pull-down assay..... 123
4.3.1.1 Quantification of PAK-CRIB protein 123
4.3.1.2 Validation of Rac1 and Cdc42 antibodies..... 124
4.3.1.3 Stimulation of cells with recombinant Wnt5A..... 125
4.3.2 Measuring active Rac1/Cdc42 in ESFT cell lines..... 128
4.3.3 Optimisation of 3D migration assay..... 130
4.3.3.1 Validation of 3D migration assay in U87MG cells 130
4.3.3.2 Formation of spheroids from ESFT cell lines..... 132
4.3.3.3 Migration of ESFT cell lines on different substrates 133
4.3.4 ESFT cell line migration in response to Wnt5A and Wnt3A 135
4.3.5 Correlation between pull-down and migration assays 137
4.3.6 Measuring the invasion of ESFT cells 138
4.4 Discussion..... 140
5. Wnt signalling in reprogrammed ESFT cells 147
5.1 Introduction 147
5.2 Materials and methods 149
5.2.1 Feeder-free stem cell culture 149
5.2.1.1 Coating plastics with hESC-qualified Matrigel™..... 149
5.2.1.2 Routine culture of cells maintained in mTeSR™1 149
5.2.1.3 Formation of single cell suspension from cells maintained in mTeSR™1 150
5.2.2 Routine culture of GFP control cells..... 150
5.2.3 Determining viable cell number of OSCK4 and GFP cell lines 150
5.2.4 Analysis of Wnt signalling components using RTqPCR..... 150
5.2.5 Cloning of 7TFH vector 151
5.2.5.1 Plasmid digestion 151
5.2.5.2 Agarose gel electrophoresis..... 151
5.2.5.3 DNA extraction from an agarose gel..... 152

5.2.5.4 Calf-intestinal alkaline phosphatase (CIP) treatment 152
5.2.5.5 DNA ligation 152
5.2.5.6 Bacterial Transformation 153
5.2.5.7 DNA isolation by minipreparation..... 153
5.2.5.8 Identifying correctly cloned vector constructs 154
5.2.6 Generation of cell lines transduced with 7TFH vector..... 155
5.2.7 Luciferase assay..... 155
5.2.8 Migration assay 155
5.2.9 Rac1/Cdc42 pull-down assay..... 155
5.2.10 Statistics..... 156
5.3 Results..... 157
5.3.1 Determining optimal growth conditions for OSCK and GFP cell lines 157
5.3.2 mRNA expression of Wnt signalling components in OSCK and GFP cells 160
5.3.2.1 Profile by TaqMan® Wnt Pathway Array..... 160
5.3.2.2 Validation of expression by RTqPCR..... 165
5.3.3 Activity of the canonical Wnt signalling pathway in OSCK and GFP cells 167
5.3.3.1 Cloning of Hygromycin resistance gene into 7TFP vector..... 167
5.3.3.2 Confirming the luciferase reporter function of 7TFH plasmid 169
5.3.3.3 Measuring the activity of the canonical Wnt signalling pathway in OSCK and GFP cells 170
5.3.4 Activity of the noncanonical Wnt signalling pathway in OSCK and GFP cells 171
5.3.4.1 Migration of OSCK and GFP cells..... 171
5.3.4.2 Expression of active Rac1/Cdc42 in OSCK and GFP cells..... 172
5.4 Discussion..... 173
6. Wnt signalling in hES cells with inducible EWS-FLI1 expression 179
6.1 Introduction 179
6.2 Materials and Methods..... 181
6.2.1 Feeder-free embryonic stem cell culture..... 181
6.2.2 Culture of Shef4$^{EWS\text{-}FLI1.ON}$ cells 181
6.2.2.1 Inducing EWS-FLI1 expression in Shef4$^{EWS\text{-}FLI1}$ cells 181
6.2.2.2 Passage of Shef4$^{EWS\text{-}FLI1.ON}$ cells 181
6.2.3 Detection of EWS-FLI1 in Shef4$^{EWS\text{-}FLI1}$ cells..... 181

6.2.3.1 RTqPCR 181
6.2.3.2 Western blot 182
6.2.4 Immunofluorescence 182
6.2.5 Determining viable cell number of Shef4 cells 183
6.2.6 Analysis of Wnt signalling components using RTqPCR 183
6.2.7 Generation of cell lines transduced with 7TFH vector 183
6.2.8 Luciferase assay 183
6.2.9 Detection of total and active β-catenin by western blot 184
6.2.10 Migration assay 184
6.2.11 Rac1/Cdc42 pull down assay 184
6.2.12 Statistics 184
6.3 Results 185
6.3.1 Characterising Shef4 cells with inducible EWS-FLI1 expression 185
6.3.1.1 Expression of EWS-FLI1 mRNA in Shef4$^{EWS-FLI1}$ cells 185
6.3.1.2 Expression of EWS-FLI1 protein in Shef4$^{EWS-FLI1}$ cells 186
6.3.1.3 Growth characteristics of Shef4$^{EWS-FLI1}$ cells with EWS-FLI expression 187
6.3.2 mRNA expression of Wnt signalling components in Shef4$^{EWS-FLI1}$ cells 195
6.3.2.1 Profile by TaqMan® Wnt Pathway Array 195
6.3.3 Activity of the canonical Wnt signalling pathway in Shef4 cells with EWS-FLI1 expression 197
6.3.3.1 Optimisation of luciferase reporter assay in Shef4 cells 197
6.3.3.2 Effect of doxycycline treatment on canonical Wnt signalling activity in Shef4$^{EWS-FLI1}$ cells with time 198
6.3.3.3 Activation of canonical Wnt signalling in Shef4 cells with and without EWS-FLI1 expression after treatment with Wnt ligands 199
6.3.3.4 Effect of doxycycline on canonical Wnt signalling in Shef4 parental cells 200
6.3.3.5 Confirmation that stimulation of Wnt signalling in Shef4$^{EWS-FLI}$ cells activates downstream targets 201
6.3.4 Activity of the noncanonical Wnt signalling pathway in Shef4 cells with EWS-FLI1 expression 203
6.3.4.1 Migration of Shef4 cells with EWS-FLI1 expression 203
6.3.4.2 Expression of active Rac1/Cdc42 in Shef4 cells with and without EWS-FLI1 expression 208
6.3.5 Effect of Wnt ligands on the growth of Shef4 cells with and without EWS-FLI1 expression 210

6.4 Discussion 211

7. Final Discussion 219

7.1 EWS-FLI1 activates canonical Wnt signalling 220

7.2 Role of DKK proteins in the initiation of ESFT 223

7.3 Noncanonical Wnt signalling in ESFT 225

7.4 Use of model systems to investigate ESFT initiation 227

7.5 Biological and clinical significance 229

7.6 Wnt signalling inhibition 231

6.4.1 Wnt signalling inhibition in the treatment of ESFT 231

7.7 Final conclusions and future work 233

Appendix 234

References 236

Figures

Figure 1.1 The process of cancer development including the hallmarks of cancer 2

Figure 1.2 The dynamic cancer initiating cell (CIC) model 5

Figure 1.3 Overview of canonical Wnt signalling 19

Figure 1.4 Overview of noncanonical Wnt signalling 21

Figure 1.5 Wnt signalling in the regulation of MSC differentiation 23

Figure 1.6 Summary of thesis hypothesis 28

Figure 2.1 Cellular fractionation by differential centrifugation 40

Figure 2.2 RNA expression of components of the Wnt signalling pathway in ESFT cell lines 49

Figure 2.3 Heat map of expression of components of the Wnt signalling pathway in ESFT cell lines. 51

Figure 2.4 Wnt1 protein expression in ESFT cells determined by western blot. 53

Figure 2.5 Wnt1 protein expression in ESFT cells determined by flow cytometry 55

Figure 2.6 Wnt1 mRNA expression determined by RTqPCR 57

Figure 2.7 Wnt3A protein was not detected in ESFT cells Total 58

Figure 2.8 Wnt3A mRNA is not expressed in ESFT cell lines as determined by RTqPCR 59

Figure 2.9 Wnt5A protein expression in ESFT cells determined by western blot. 61

Figure 2.10 Protein expression of Wnt5A in ESFT determined by flow cytometry 63

Figure 2.11 Subcellular localisation of β-catenin in ESFT cell lines. 65

Figure 2.12 Expression of the active form of β-catenin in ESFT cell lines. 67

Figure 3.1 Calculating the lentiviral titre in HEK293T cells 87

Figure 3.2 Infection of ESFT cell lines with lentiviral GFP plasmid 89

Figure 3.3 Activation and stability of 7TGP and 7TFP plasmids in HEK293T cells 91

Figure 3.4 Stimulation of 7TGP cell lines with L-cell conditioned media 93

Figure 3.5 Growth of ESFT cell lines in L-cell conditioned media 94

Figure 3.6 Stimulation of HEK293T 7TGP cells with L-cell CM and recombinant Wnt3A protein 96

Figure 3.7 Activation of GFP and luciferase reporter plasmids in HEK293T cells after treatment with L-Wnt3A CM and recombinant Wnt3A protein 97

Figure 3.8 Quantifying the concentration of Wnt3A in L-Wnt3A CM 99

Figure 3.9 GFP reporter activation in ESFT cell lines 101

Figure 3.10 Firefly luciferase reporter activation in ESFT cell lines 103

Figure 3.11 ESFT viable cell number after treatment with Wnt3A and Wnt5A 104

Figure 3.12 Downstream activation of canonical Wnt signalling in HEK293T cells following treatment with Wnt3A 106

Figure 3.13 Downstream activation of canonical Wnt signalling in ESFT cells after treatment with Wnt3A 108

Figure 4.1 Quantification of PAK-CRIB bound to glutathione-sepharose beads 123

Figure 4.2 Specificity of anti-Rac1 and anti-Cdc42 antibodies 124

Figure 4.3 Expression of active Rac1 after in HeLa and SKES-1 cells after treatment with Wnt5A over time 126

Figure 4.4 Expression of active Rac1 in SKES-1 cells after treatment with increasing concentrations of Wnt5A SKES 127

Figure 4.5 Expression of active Rac1 and Cdc42 in ESFT cell lines 129

Figure 4.6 Quantifying migration in U87MG cells 131

Figure 4.7 Spheroids formed by ESFT cell lines 132

Figure 4.8 ESFT cell migration on different substrates 133

Figure 4.9 Migration of ESFT cell lines with and without treatment with Wnt3A and Wnt5A 136

Figure 4.10 Correlation between active Rac1 and migration index ESFT cells 137

Figure 4.11 Invasion of ESFT cells in Collagen I and Matrigel™ 139

Figure 5.1 Growth of GFP and OSCK cells on different substrates and in different media 158

Figure 5.2. Light microscope images of GFP and OSCK cells cultured on different substrates and in different media 159

Figure 5.3 RNA expression of components of the Wnt signalling pathway in OSCK and GFP cells 161

Figure 5.4 Clustering of Wnt signalling components in OSCK and GFP cells. 163

Figure 5.5 sFRP5, Wnt16, FGF4 and DKK2 mRNA expression determined by RTqPCR 166

Figure 5.6 Cloning of 7TFH plasmid 168

Figure 5.7 Confirming the functional activity of the cloned 7TFH reporter plasmid 169

Figure 5.8 Luciferase reporter activity in GFP and OSCK cells. 170

Figure 5.9 Migration of OSCK and GFP cells 172

Figure 5.10 Expression of active Rac1 and Cdc42 in GFP and OSCK cell lines 172

Figure 6.1 Induction of EWS-FLI1 expression using the TetON Advanced inducible expression system 180

Figure 6.2 Expression of EWS-FLI mRNA in Shef4$^{EWS\text{-}FLI}$ cells treated with DOX 185

Figure 6.3 Expression of EWS-FLI protein in Shef4$^{EWS\text{-}FLI1}$ cells treated with DOX 186

Figure 6.4 Light microscopy of Shef4$^{EWS\text{-}FLI.OFF}$ and Shef4$^{EWS\text{-}FLI.ON}$ cells 188

Figure 6.5 Actin cytoskeleton in Shef4$^{EWS\text{-}FLI.OFF}$ and Shef4$^{EWS\text{-}FLI.ON}$ cells 189

Figure 6.6 Effect of doxycycline on Shef4 and Shef4$^{EWS\text{-}FLI1}$ viable growth 191

Figure 6.7 Effect of doxycycline treatment on Shef4 viable cell number with time.....191

Figure 6.8 Shef4$^{EWS\text{-}FLI1.ON}$ viable cell number in mTeSR-™1 and RPMI.....193

Figure 6.9 Light microscopy of Shef4$^{EWS\text{-}FLI1.ON}$ cells in mTeSR™1 and RPMI.....194

Figure 6.10 RNA expression of components of the Wnt signalling pathway in Shef4$^{EWS\text{-}FLI1}$ cells.....196

Figure 6.11 Effect of time in culture on the activity of luciferase reporter activity in Shef4 7TFH cells.....197

Figure 6.12 Luciferase reporter activity in Shef4$^{EWS\text{-}FLI1.ON}$ cells.....198

Figure 6.13 Luciferase reporter activity in Shef4 cells with and without EWS-FLI1 expression after treatment with Wnt ligands.....199

Figure 6.14 Effect of exposure to doxycycline on the activity of luciferase reporter plasmid in Shef4 cells.....200

Figure 6.15 Expression of β-catenin in Shef4$^{EWS\text{-}FLI1}$ cells after stimulation with Wnt ligands.....202

Figure 6.16 Formation of spheroids from Shef4 cells.....204

Figure 6.17 Migration of Shef4 cells with and without EWS-FLI1 expression on different substrates.....205

Figure 6.18 Migration of Shef4 cells with and without EWS-FLI1 expression in response to Wnt ligands.....207

Figure 6.19 Expression of active Rac1 and Cdc42 in Shef4 cells with and without EWS-FLI1 expression.....208

Figure 6.20 Actin cytoskeleton in Shef4$^{EWS\text{-}FLI.OFF}$ and Shef4$^{EWS\text{-}FLI.ON}$ cells treated with Wnt5A.....209

Figure 6.21 Viable cell number of Shef4 cell lines following treatment with Wnt3A and Wnt5A.....210

Tables

Table 1.1 EWS fusion types in ESFT 8

Table 2.1 Components of the Wnt signalling pathways which have been detected in ESFT cell lines and samples 31

Table 2.2 Characteristics of ESFT and cell lines used as controls 34

Table 2.3 Antibodies and optimised antibody concentrations for western blots 38

Table 2.4 Reagents in RT+ and RT- reactions 43

Table 2.5 PCR mix reagents for RTqPCR using Assay-on-Demand™ (Applied Biosystems) and PPIA housekeeping gene 45

Table 2.6 Inter-assay variance of different housekeeping genes on the Wnt signalling array 48

Table 2.7 Summary of expression of canonical and noncanonical Wnt signalling components in ESFT cell lines 71

Table 3.1 Summary of results of assays used to measure canonical Wnt signalling in ESFT cell lines 88

Table 4.1 Phenotype of ESFT cell spheroid migration over 72h 135

Table 4.2 Summary of the results of the assays used to measure the activity of the noncanonical Wnt signalling pathway in ESFT cell lines 131

Table 5.1 Wnt signalling component TaqMan® Assay-on-Demand primer/probe product information 151

Table 5.2 Primers used to sequence clones 7TFH vector 155

Table 5.3 Genes with significantly different mRNA expression in OSCK cells compared to GFP cells 164

Table 6.1 PCR mix reagents for RTqPCR to detect EWS-FLI1 182

Table 6.2 Genes with significantly different mRNA expression in Shef4$^{EWS\text{-}FLI1.ON}$ cells compared to Shef4$^{EWS\text{-}FLI1.OFF}$ 195

Abbreviations

3D	three- dimensional
AML	acute myeloid leukaemia
amp	ampicillin
ANOVA	analysis of variance
APC	adenomatous polyposis coli
ATTC	American Type Tissue Collection
bp	base pair
Ca^{2+}	calcium
CamKII	calmodulin-dependent protein kinase II
CBP	CREB-binding protein
CCND-1	cyclin D1
cDNA	complementary DNA
ChIP	chromatin immunoprecipitation
CIC	cancer initiating cell
CIP	Calf-intestinal alkaline phosphatase
CKI	casein kinase-I
CM	conditioned media
CO_2	carbon dioxide
CRIB	Cdc42/Rac Interactive Binding
CSC	cancer stem cell
Ct	cycle threshold
ddH_2O	double distilled H_2O
dH_2O	distilled water
DKK	Dickkopf
DMEM	Dulbecco's Modified Eagle Medium
DNA	deoxyribonucleic acid
dNTP	deoxyribonucleotide triphosphate
DOX	doxycycline
DTT	dithiothreitol
Dvl	Dishevelled
E1AF	Early region 1A enhancer binding protein

EDTA	ethylenediaminetetracetate
EGFR	epidermal growth factor receptor
EMT	epithelial-to-mesenchymal transition
ERG	ETS related gene
ESFT	Ewing's sarcoma family of tumours
ETS	E26 transformation-specific
ETV1	ETS translocation variant 1
Euro-EWING	European Ewing Tumour Working Initiative of National Groups
FACS	fluorescence-activated cell sorting
FCS	foetal calf serum
FEV	Fifth Ewing variant
Ffluc	Firefly luciferase
FGF	fibroblast growth factor
FLI1	Friend leukemia integration 1 transcription factor
FZD	Frizzled
GDP	guanosine diphosphate
GFP	green fluorescent protein
GFP	green fluorescent protein
GOI	gene of interest
GSK	glycogen synthase kinase
GST	glutathione-*S*-transferase
GTP	guanosine triphosphate
GTPases	guanosine triphosphate-ases
h	hour(s)
HDAC	histone deacetylase
hES	human embryonic stem
HIV	human immunodeficiency virus
hNCSC	human neural crest stem cells
HSPG	heparin sulfate proteoglycan
Hygro	hygromycin
IF	immunofluorescence
IGF1	Insulin-like growth factor 1
IGFBP3	IGF binding protein 3
IHC	immunohistochemistry

iPS	induced pluripotent stem
IPTG	isopropyl β-D-1-thiogalactopyranoside
IVF	*in vitro* fertilization
JNK	c-Jun N-terminal kinase
kb	kilobase
kDa	kilodalton
KO	knock out
L	litre
LAR	luciferase assay reagent
LDL	low density lipoprotein
LDLR	low-density lipoprotein receptor
LEF	lymphoid enhancer-binding protein
LRP	LDL receptor related proteins
LTR	long terminal repeat
M	molar
MAPK	mitogen-activated protein kinase
MAPT	microtubule-associated protein tau
MEF	mouse embryonic fibroblast
MET	mesenchymal-to-epithelial transition
$MgCl_2$	magnesium chloride
MI	migration index
min	minute(s)
miRNA	micro RNA
ml	mililitre
MOI	multiplicity of infection
MPC	mesenchymal progenitor cell
mRNA	messenger RNA
MSC	mesenchymal stem cell
MS-PCR	methylation specific PCR
MW	molecular weight
MZ	migration zone
N/A	not applicable
NEB	New England Biolabs
NFAT	nuclear factor of activated T-cells
NGS	next-generation sequencing

NLK	nemo like kinase
ng	nanogram
nm	nanometre
NSAID	non steroidal anti-inflammatory drug
NSCLC	non-small cell lung cancer
O_2	oxygen
^oC	degrees Celsius
OSCK	Oct4, Sox2, c-Myc and Klf-4
PAGE	polyacrylamide gel electrophoresis
PAK	p21 activated kinase I
PARP	poly ADP ribose polymerase
PBS	phosphate buffered saline
PBST	PBS containing 0.1% Tween-20
PCP	planar cell polarity
PCR	polymerase chain reaction
PDAC	pancreatic ductal adenocarcinoma
PDGF	platelet derived growth factor
PFA	paraformaldehyde
PI3K	phosphatidylinositol 3-kinase
PKC	Protein kinase C
PLB	passive lysis buffer
PMSF	phenymethylsulfonyl
PPIA	Peptidylprolyl isomerise A
pPNET	peripheral primitive neuroectodermal tumour
pRB	retinoblastoma protein
Puro	puromycin
r	recombinant
Ras	rat sarcoma
RIPA	Radio Immuno Precipitation Assay
RLU	Relative Light Units
RNA	ribonucleic acid
RNAi	RNA interference
RNAseq	RNA sequencing
ROCK	Rho-associated kinase
RRE	*rev*-response element

RT	room temperature
RT	reverse transcriptase
RT-	RT negative
RT+	RT positive
rTetR	reverse Tet Repressor
RT-PCR	reverse-transcriptase PCR
RTqPCR	reverse-transcriptase quantitative PCR
rtTA	reverse tetracycline transactivator
s	second(s)
SDS	sodium dodecyl sulphate
SEM	standard error of the mean
sFRP	secreted Frizzled-related protein
SOC	Super Optimal broth with Catabolite repression
TAK1	TGF-beta-activated kinase 1
TBP	TATA-binding protein
TBS	Tris-Buffered Saline
TCF	T-cell factor
TEMED	N, N, N', N'- Tetramethylethylenediamine
tetO	tet operator sequence
TetON	rtTA-Advanced transactivator
TetR	Tet Repressor
TGFβRII	Transforming growth factor-beta receptor 2
TRE	transcriptional response element
TRE	Tet Response Element
TSG	tumour suppressor gene
TU	transduction units
U	unit
UK	United Kingdom
UV	ultraviolet
v/v	volume/volume
VAC	vincristine-actinomycin-cyclophosphamide
VAI	vincristine-actinomycin-ifosfamide
VIDE	Vincristine-ifosfamide-doxorubicin-etoposide
VSV-G	Vesicular Stomatitis Virus
w/v	weight/volume

WB	western blot
WHO	World Health Organization
WIF	Wnt inhibitory factor
yr	years old
μg	microgram
μl	microlitre

1. Introduction

1.1 Cancer

1.1.1 Biology of cancer

Cancer is responsible for more than 10% of deaths worldwide. In 2012 there was an estimated 14.1 million new cases of cancer worldwide, and 8.2 million people died from the disease (GLOBOCAN 2014). The number of cases is expected to rise by 70% over the next two decades to 25 million per year. There are over 200 different cancers currently described that, from both a clinical and scientific view point, appear remarkably diverse reflecting the complexity and intricate nature of cancer development and progression. Despite this, a set of common capabilities have been described which are acquired by almost all types of cancers (Figure 1.1). These hallmarks were first proposed by Hanahan and Weinberg in 2000, and have recently been updated as a result of continued research and understanding to include; a metabolic switch to from oxidative phosphorylation to glycolysis, and also evasion of immune system surveillance (Hanahan and Weinberg 2000, Hanahan and Weinberg 2011).

Cancer is a genetic disease caused by inherited or acquired mutations in deoxyribonucleic acid (DNA). Traditionally cancer development has been considered clonal, akin to the theory of Darwinian evolution, whereby a genetic change gives a selective advantage to a cell and its progeny. Over time, subsequent mutations develop so that eventually cancer occurs (Foulds 1954, Nowell 1976). It is now understood that most cancers develop due to mutations in two types of genes; tumour suppressor genes (TSG) and oncogenes. Tumour suppressor genes such as p53 (Lane and Crawford 1979, Linzer and Levine 1979), retinoblastoma protein (pRB) (Friend et al. 1987) and PTEN (Li et al. 1997) encode proteins which function to suppress the cancer phenotype, for example by maintaining correct control of the cell cycle (Harris, 1971). Therefore mutations resulting in loss of expression of TSG are common in cancer. In contrast, oncogenes are mutated or overexpressed forms of genes (known as proto-oncogenes) that can cause cancer by mechanisms such as promoting increased proliferation or preventing apoptosis. Examples include the myc family of transcription factors (Paynes et al, 1982) and the Rat sarcoma (Ras) family of regulatory guanosine triphosphate-ases (GTPases) (Chang et al. 1982).

In most cases, cancer does not result from a single mutation. It is hypothesised that there may be a single oncogenic driver such as a mutation in a TSG or oncogene that results in the accumulation additional mutations, for example through disruption of cell cycle control or of DNA repair mechanisms. Early *in vitro* experiments showed that cells require at least two genetic aberrations before they are transformed, and work in familial cancer syndromes led Knudson to propose the 'two hit' hypothesis where patients with one inherited mutation in *RB1* require one additional mutation to occur for cancer to develop (Knudson 1971). More recently it has been hypothesised that 5 mutations are required for non-inheritable cancers to occur (Weinberg 2014). As these additional mutations occur, the cell acquires the capabilities described as the hallmarks of cancer.

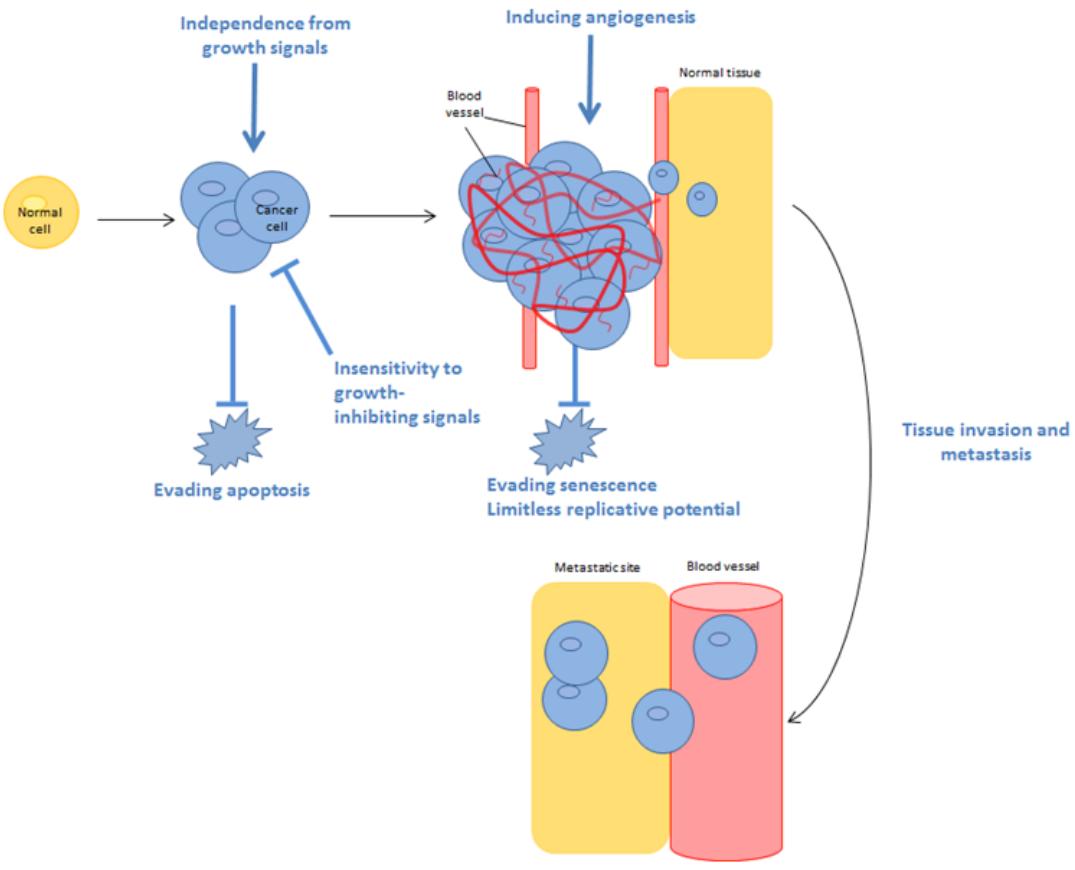

Figure 1.1 The process of cancer development including the hallmarks of cancer The key characteristics or 'hallmarks' of a cancer cell are shown in blue. Adapted from Hanahan and Weinberg (2000) and Pelengaris and Kahn (2013).

1.1.2 Metastasis

The spread of cancer to other regions of the body is known as metastasis, this process is one of the hallmarks of cancer (Figure 1.1). Patients may present with metastatic disease, or may develop metastasis sometimes decades after the primary tumour was excised and/or treated. For metastasis to occur, cancer cells must acquire capabilities for local invasion, intravasation into a blood vessel, transport through the circulation, extravasation out of the vessel, formation of micrometastases and finally colonisation in the new site (Fidler 2003). In the case of carcinomas this process involves the cancerous polarised epithelial cells undertaking a dramatic change in morphology and dissolving intercellular connections to become invasive and motile, often known as the epithelial-to-mesenchymal transition (EMT). The reverse process, mesenchymal-to-epithelial transition (MET) is thought to be important in seeding tumour cells at distant metastatic sites (Wells et al. 2008). In non-epithelial cancers the process of metastasis is less well documented, however MET has been described in sarcoma and linked to a better prognosis (Yang et al. 2014), highlighting the importance of mesenchymal characteristics in the process of migration. Metastatic disease is responsible for 90% of deaths from cancer (Weinberg 2014) therefore understanding this process and the cells involved is extremely important to increase treatment success and cure of cancer patients.

1.1.3 Cancer initiating cells (CICs)

The clonal evolution model of cancer suggests that each cell within the tumour has an equal potential to acquire mutations which lead to growth advantage and therefore generate new tumours. This hypothesis was challenged in the 1970s when it was shown that only a subpopulation of cells have the ability to initiate and maintain tumour growth (Hamburger and Salmon 1977). This led to the development of a hierarchical model, where a subpopulation of cells have the ability to self-renew, differentiate and regenerate tumours. These cells have many similar properties to normal stem cells such as the ability to self-renew, multipotent differentiation potential and the expression of stem cell-associated markers such as CD133 (Zhu et al. 2009). For this reason these cells were termed cancer stem cells (CSC); or more accurately, since they do not represent true stem cells, cancer initiating cells (CIC).

The first definitive evidence for CICs was in acute myeloid leukaemia (Bonnet and Dick 1997), this was followed by the demonstration of CICs in solid tumours of the breast (Al-Hajj et al. 2003) and brain (Singh et al. 2003). To date, CICs have been identified in

numerous other tumour types including prostate (Collins et al. 2005), pancreatic (Li et al. 2007), colon (O'Brien et al. 2007) and more recently the Ewing's sarcoma family of tumours (ESFT) (Suvà et al. 2009).

There still remains much controversy over the origin of CICs (Figure 1.2). Studies have suggested they may arise from normal stem cells that have gained malignant mutations (Bonnet and Dick 1997, Schepers et al. 2012), or from progenitor cells which acquire self-renewal capacity (Cozzio et al. 2003). It has also been shown that differentiated cancer cells can re-acquire self-renewal capacity and stem-like characteristics, and this may occur upon exposure to microenvironmental factors (Vermeulen et al. 2010, Chaffer et al. 2011). Therefore it is possible that CICs arise from different cells in different tumour types.

Whatever the origin of CICs, they have important implications for the successful treatment of cancer. It has been suggested, at least in some cancer types such as pancreatic cancer (Hermann et al. 2007), that CICs are responsible for metastasis. This hypothesis is supported by the fact that the process of metastasis requires stem-cell characteristics such as self-renewal. Importantly, CICs have also been shown to be more resistant to current cancer treatment. This is likely due to a variety of different mechanisms. CICs have been shown to have increased expression of ABC drug transporters and intracellular detoxification enzymes. CICs have also been shown to have more efficient DNA repair mechanisms and may upregulate anti-apoptotic proteins (Alison et al. 2012). In addition, CICs share another stem-cell phenotype in that they are relatively quiescent, meaning cytotoxic agents that target rapidly dividing cells do not kill the CICs. Indeed it has been shown experimentally and in patient samples that chemotherapy targets the non-CIC cells and therefore enriched for a more aggressive CIC population that can go on and recapitulate the tumour (Hermann et al. 2007, Dylla et al. 2008, Li et al. 2008). Therefore in many cancers it is believed that CICs are responsible for the failure of treatment, relapse and progression.

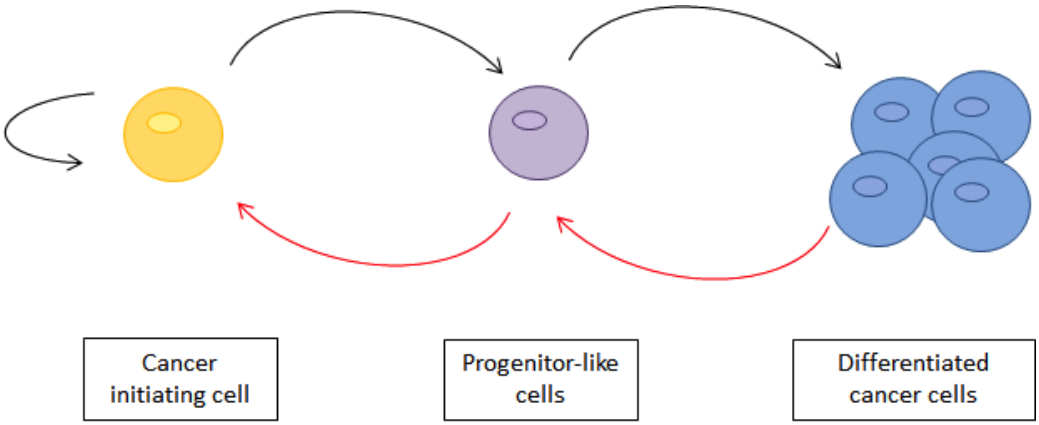

Figure 1.2 The dynamic cancer initiating cell (CIC) model CICs differentiate to give rise to the bulk of the tumour (black arrows). Alternatively (or additionally) signals from the microenvironment lead to dedifferentiation of tumour cells (red arrows). Adapted from Vermeulen et al. (2012)..

1.1.4 Cancer treatment

The clinical treatment of cancer depends on the type of cancer and location of the tumour(s), as well as the stage of disease (Pelengaris and Khan 2013). Surgery was once the only treatment for cancer and still offers the best chance of a cure for many patients. Surgery is most often used in combination with radiotherapy and/or systemic chemotherapy. In some cases chemotherapy is given to reduce tumour bulk prior to surgical excision to improve the ease of surgery and reduce the risk of disease spread resulting from surgery (DeVita and Chu 2008). Chemotherapy may also be given after complete surgical resection in an attempt to target remaining cancer cells including subclinical micrometastases (Weinberg 2014). For most cancer patients cytotoxic drugs remain the only current chemotherapy treatment option available. Cytotoxic agents non-specifically target highly proliferating cells, exploiting the lack of growth regulation in cancer cells (DeVita and Chu 2008). These drugs are classed according to their mode of action which may include alkylating the DNA (e.g. alkylating agents such as cyclophosphamide), forming interstrand cross-links between DNA (e.g. platinum compounds such as cisplatin), intercalating between base pairs within DNA (e.g. anthracyclines such as doxorubicin), destabilising microtubules (e.g. vincristine) or interacting with DNA-associated proteins such as topoisomerases (e.g. Topoisomerase II inhibitors such as etoposide). Most cytotoxic agents are given in combination as their synergistic or additive actions increase the amount of cancer cell kill (DeVita and Chu

2008). In addition, some cytotoxic agents may have more than one mode of action, for example doxorubicin is an alkylating agent but can also intercalate DNA and inhibit topoisomerase II function (Gewirtz 1999). Although cytotoxic agents have been used for many years, their non-specific action means they also target highly proliferative normal cells such as those of the immune system and lining the gastrointestinal tract. This leads to side effects such as tiredness, hair loss, vomiting, diarrhoea and susceptibility to infection. These effects may be dose-limiting or even lethal. Furthermore, many cytotoxic agents work by inducing irreversible damage in DNA, with the hope this will induce apoptosis in cancer cells (DeVita and Chu 2008). However, if the cells survive, then this damage could increase the number of mutations meaning cytotoxic treatment could actually select for more aggressive clones that may repopulate the tumour (Weinberg 2014). In addition, some cancer patients, especially children are at increased risk of developing a second cancer during their lifetime (Wasilewski-Masker et al. 2009, Friedman et al. 2010) indicating that cytotoxic agents also damage the DNA of normal cells.

Our knowledge of the molecular alterations within cancer cells has increased dramatically over the past few decades. One of the fundamental reasons for this is the development of new technologies such as next-generation sequencing (NGS) which has enabled whole cancer genomes to be mapped, and provided valuable information about the specific mutations which occur in each individual tumour. However, interpreting this data, understanding the biological implications and translation of this knowledge to more effective and less toxic treatments has proved challenging. For example recent whole genome sequencing of one melanoma revealed 33,000 different somatic mutations (Pleasance et al. 2010). One challenge is understanding which of these are driver mutations promoting tumour growth and which are simply passenger mutations that have occurred but that do not contribute to the tumorigenic phenotype. However in some cancer types, identification of mutations that are common in (at least a subset) of patients has resulted in the generation of novel targeted therapies. For example, approximately 20% of lung cancer patients have mutations in the *EGFR* gene (Rosell et al. 2009), and up to 70% of these patients exhibit a clinical response when treated with EGFR inhibitors such as gefitinib or erlotinib (Mok et al. 2009, Rosell et al. 2012). Another example of targeted therapy is in melanoma in which the *BRAF* gene is mutated in up to a third of tumours, and these patients respond to vemurafenib, a BRAF inhibitor (Flaherty et al. 2010). Unfortunately tumours often become resistant to targeted therapies, by acquiring additional mutations or by upregulating alternative signalling pathways (Remon et al. 2014). Importantly research has shown that even within tumours heterogeneity exists

meaning different mutations may be present in different parts of the tumour (Gerlinger et al. 2012). This raises the issue of how patients should be stratified to receive personalised therapy, since if a single tumour biopsy is taken this may not represent the biology and genetics of the entire tumour mass. Nevertheless, the goal of further understanding the biology of individual tumours in order to deliver personalised therapy remains important for the future treatment of cancer patients

1.2 Ewing's sarcoma family of tumours (ESFT)

1.2.1 Biology of ESFT

Ewing's sarcoma family of tumours (ESFT) are rare solid tumours including Ewing's sarcoma, peripheral primitive neuroectodermal tumours (pPNET) and Askin's tumour. ESFT most frequently arise in children and young adults between the ages of 10 and 24 years, with an incidence of approximately 1.8 per million 0-49 year olds. There is slightly higher incidence in males than females (ratio 1.4 : 1) (McNally et al. 2012). Most ESFT arise in the bone, commonly in the pelvis (26%), long bones of the lower extremities such as the femur (20%) or the bones of the chest wall (16%) (Bernstein et al. 2006). However, in around 15% of cases the primary tumours arise in a variety of extra osseous sites (Grier 1997).

Morphologically, ESFT consists of sheets of small, poorly differentiated round cells with scant cytoplasm and large nuclei with little mitotic activity. Immunohistochemisty shows that in more than 90% of cases ESFT cells express the cell surface membrane protein CD99 (Ambros et al. 1991). Membrane expression of CD99 is used to diagnose ESFT and distinguish them from other small round cell tumours (Weidner and Tjoe 1994).

1.2.2 Genetic abnormalities in ESFT

ESFT are characterised by a unique non-random chromosomal translocation between the *EWS* gene on chromosome 22q12 with a member of the *ETS* gene family of transcription factors. In 85% of ESFT this is *FLI1* on chromosome 11q24, which generates the chimeric EWS-FLI1 fusion protein (Delattre et al. 1992). Other *EWS-ETS* translocations have been identified in the remaining 15% of cases including *EWS-ERG* or very rarely *EWS-ETV, EWS-E1AF1* or *EWS-FEV* (Burchill 2008) (Table 1.1). The identification of these gene rearrangements has led to the classification of Ewing's sarcoma, pPNET and Askin's tumours into a common group with similar histogenesis known at the ESFT. More recently, the World Health Organization (WHO) have renamed this family 'Ewing Sarcoma'.

However, this term is limited as it doesn't reflect the range of tumours within the family, and in addition, ESFT was first described by James Ewing (Ewing 1921), therefore the term 'Ewing's' sarcoma' is more accurate.

Fusion Transcript	Translocation	Frequency of occurrence
EWS-FLI1 Type I*	t(11;22)(q24;q12)	60%
EWS-FLI1 Type II*	t(11;22)(q24;q12)	25%
EWS-ERG	t(21;22)(q22;q12)	10%
EWS-ETV1	t(7;22)(q22;q12)	<1%
EWS-E1AF	t(17;22)(q12;q12)	<1%
EWS-FEV	t(2;22)(q33;q12)	<1%

Table 1.1 EWS fusion types in ESFT *Alternative fusion types have been identified depending on where the breakpoint arises in different exons of the FLI1 gene. *EWS*= Ewing Sarcoma Breakpoint Region 1, *FLI1*= Friend leukemia integration 1 transcription factor *ERG*= ETS related gene, *ETV1* = ETS translocation variant 1, *E1AF* = Early region 1A enhancer binding protein, *FEV* = Fifth Ewing variant.

All reported fusion proteins contain at least the N-terminal 7 exons of *EWS* containing the EWS activation domain (Herrero-Martin et al. 2011), and the DNA-binding domain of the *ETS* fusion partner. Both domains are required for the oncogenic function. The fusion proteins are known to localise to the nucleus and bind DNA in a site-specific manner and are thought to function as aberrant transcription factors.

Being the most common, EWS-FLI1 is the most studied fusion protein and has been shown to have numerous downstream targets that contribute to the pathogenesis of ESFT. Microarray analyses have revealed EWS-FLI1 both up- and down-regulates downstream targets (Hancock and Lessnick 2008, Kauer et al. 2009). Interestingly, initial studies suggested EWS-FLI downregulates many more genes than it upregulates (Prieur et al. 2004, Smith et al. 2006). The fusion protein has been reported consistently to upregulate genes involved in proliferation and survival including *PDGFC, IGF1, MYC, CCND-1, NKX2-2* and suppress genes involved in apoptosis and growth inhibition for example *p21, p57^{kip}, TGFβRII* and *IGFBP3* (Riggi and Stamenkovic 2007, Ross et al. 2013). EWS-FLI1 can also initiate oncogenic pathways even when the DNA-binding domain of *FLI1* is mutated,

indicating that the fusion protein activates pathways independent of FLI1 DNA binding (Welford et al. 2001). A variety of different signalling pathways have been linked to pathogenesis of ESFT, although it is not clear if this is due to expression of the fusion protein or cooperating mutations which have occurred. A number of studies have shown that the insulin-like growth factor 1 (IGF-1) pathway is important in ESFT (Yee et al. 1990, Scotlandi et al. 1996, Toretsky et al. 1997). More recently the Wnt signalling pathway has also been linked to the pathogenesis of ESFT (discussed in Section 1.3.5).

Although the EWS-ETS fusion proteins have been identified as the main genetic drivers of malignancy, secondary genetic abnormalities have been described in over 80% of ESFT (Burchill 2008). Chromosome gain is observed more frequently than loss in ESFT, with more complex karyotypes associated with a worse prognosis (Roberts et al. 2008). In particular, gains of chromosomes and 8 and 12 are common and can occur together (Maurici et al. 1998). However the prognostic implication of these chromosomal abnormalities is not clear (Roberts et al. 2008). The most common secondary aberrations detected in ESFT are deletions of the *CDKN2A* locus on chromosome 9p and in genes that regulate the G1 cell cycle checkpoint. For example, inactivation of the *CDKN2A* region which codes for *p16* occurs between 13-39% of primary ESFT (Tsuchiya et al. 2000, Maitra et al. 2001, Lopez-Guerrero et al. 2001, Brownhill et al. 2007). The primary mechanism of this inactivation appears to be homozygous deletion, the *p16* promoter is rarely methylated (Tsuchiya et al. 2000, Lopez-Guerrero et al. 2001, Brownhill et al. 2007). Some studies have associated mutation or deletion of *p16* with worse survival (Tsuchiya et al. 2000, Wei et al. 2000), although other studies have reported no prognostic significance of deletion of *p16* gene (Brownhill et al. 2007, Lopez-Guerrero et al. 2011). In contrast to *p16*, deletions or mutations of the tumour suppressor gene *TP53* are rare in ESFT. However, when present *TP53* aberrations are associated with poor overall survival (de Alava et al. 2000, Lopez-Guerrero et al. 2001).

1.2.3 Model systems to study ESFT initiation and development

Unlike other sarcomas such as osteosarcoma that show some lineage-specific differentiation, ESFT present as undifferentiated tumours that reveal little insight into the cell of origin. When first described in 1921, Ewing proposed an endothelial origin (Ewing 1921). However early studies found that cell surface antigens associated with the neuroectodermal lineage were expressed on ESFT (Lipinski et al. 1986). Most Ewing's sarcomas arise in the bone, but about 15% of primary ESFTs arise in extra osseous sites. The wide range of organs and tissues from which ESFTs can arise, along with their

histological features of poor differentiation and both mesenchymal and neuroectodermal characteristics has fuelled a debate as to their cell of origin.

Although characterised by the presence of an EWS-ETS fusion such as EWS-FLI, it is not known how or in what cell type these fusion proteins lead to ESFT formation. It is understood that EWS-FLI1 acts an aberrant transcription factor, and has been shown to regulate genes that are critical for ESFT tumorigenesis. Therefore many researchers have developed systems to induce expression of the fusion protein in different cell types in an approach to understand the process of tumour initiation, with the hope this may lead to the development of improved therapeutics.

Initial experiments used murine fibroblast NIH/3T3 cells that can be readily transformed by EWS-FLI1, to identify genes regulated by the fusion protein (May et al. 1993, Braun et al. 1995). However, more recently it has been shown that the gene expression profile of NIH/3T3 cells does not accurately represent the expression profile of ESFT tumour samples (Braunreiter et al. 2006, Hancock and Lessnick 2008). Therefore researchers have developed model systems in which EWS-FLI1 is expressed in human cell types, and it has been shown that the phenotype and gene expression changes that occur when EWS-FLI1 is expressed appear to be cell type specific. This has lead to the hypothesis that there is a specific permissive cellular environment in which the EWS-FLI fusion protein is tolerated and this leads to the initiation of ESFT. For example, in some human cells such as fibroblasts, rather than being oncogenic, EWS-FLI1 induces cell cycle arrest (Lessnick et al. 2002). In other cell types such as neuroblastoma (Rorie et al. 2004) and rhabdomyosarcoma (Hu-Lieskovan et al. 2005) expression of EWS-FLI1 has been shown to induce an ESFT phenotype along with upregulating genes associated with neuronal differentiation (that are also expressed in ESFT) such as *MAPT*. It has therefore been suggested that the neuroectodermal characteristics observed in ESFT may be acquired though the upregulation and downregulation of EWS-FLI1 target genes, rather than reflecting the cell of origin.

A recently emerged concept is that ESFT may arise from a pluripotent or multipotent progenitor cell, and that EWS-FLI1 may interfere with normal differentiation thus inducing the tumour phenotype. Many reports have suggested that the cell of origin may be a mesenchymal stem cell (MSC). The term MSC is generally used to describe cells which can differentiate towards mesodermal lineages including osteoblasts, chondrocytes and adipocytes. However, there is still controversy over how these cells are defined therefore these cells are also often referred to as mesenchymal progenitor cells (MPCs) or bone

marrow stromal cells. MSCs are found in the bone marrow and a number of other tissue sites therefore it is believed that the MSC-origin theory could explain the broad tissue distribution of ESFT. A number of model systems have been used to support the hypothesis that MSCS are the ESFT cell of origin. For example, unlike other cell types, human MSCs tolerate the forced expression of the EWS-FLI1 fusion protein. Importantly it has been observed that ESFT cell lines where EWS-FLI1 has been inhibited with RNAi display a MSC gene expression profile, and these cells have the ability to differentiate into osteoblasts and adipocytes (Tirode et al. 2007). It has been reported that the gene expression profile of MSCs expressing EWS-FLI1 is similar to ESFT, but not to other bone and soft tissue tumours (Riggi et al. 2008). Interestingly, it has been shown that MSCs derived from paediatric rather than adult donors display different expression profiles upon EWS-FLI1 induction. Paediatric MSCs containing EWS-FLI1 have increased expression of EWS-FLI1 target genes such as *IGF1* and *NKX2.2*, and have an expression profile that more closely resembles that of ESFT, compared to adult MSCs (Riggi et al. 2010).

Importantly however, so far none of the populations of MSCs with EWS-FLI1 expression have been reported to form tumours *in vivo*. Consequently it is not clear whether MSCs are simply tolerant of EWS-FLI1 expression, and the genetic and phenotypic alterations observed are a manifestation of the EWS-FLI1 fusion itself, or if additional genetic abnormalities are required for ESFT initiation. In support of the latter hypothesis, in a transgenic mouse model of ESFT with conditional expression of EWS-FLI1 in the mesoderm-derived tissues of the limb, sarcomas did not spontaneously form unless *p53* was also deleted. This suggests that expression of EWS-FLI1 alone may not be enough to induce transformation *in vivo*. Interestingly, these transgenic mice also had shortened limbs and muscle atrophy, supporting the hypothesis that EWS-FLI1 impairs differentiation of cells. Indeed, in mouse MSCs it has been reported that expression of EWS-FLI1 blocks differentiation along osteogenic and adipogenic lineages (Torchia et al. 2003), although in human MSCs with EWS-FLI1 expression some degree of differentiation has been reported (Riggi et al. 2008).

Despite this evidence, there is still controversy as to the definitive cell of origin of ESFT. For example, another recent study has demonstrated that neural crest stem cells (derived from human embryonic stem cells) and neuromesenchymal stem cells can tolerate expression of EWS-FLI1, and this leads to an alteration in EWS-FLI1 target genes (von Levetzow et al. 2011). However, this could be explained by the finding that at least the

initial population of MSCs that form during development derive from neuroepithelim and neural crest cells rather than mesoderm (Takashima et al. 2007).

The hypothesis that EWS-FLI1 contributes to a pluripotent, undifferentiated state is supported by the fact that expression of EWS-FLI1 in paediatric MSCs induces expression of the stem cell markers CD133, Oct4, Sox2 and Nanog (Riggi et al. 2010). This primitive state may be further understood by the study of 'reprogrammed' ESFT cells. The reprogramming of cells to induced pluripotent stem (iPS) cells was first described in mice, and subsequently in human cells using adult dermal fibroblasts by lentiviral transduction of the key pluripotency genes Oct4, Sox2, Klf4 and c-Myc (Takahashi and Yamanaka 2006, Takahashi et al. 2007). Since iPS cells exhibit many characteristics of human embryonic stem (hES) cells, including self-renewal and pluripotency, they are being used extensively in the field of regenerative medicine and in modelling human disease.

Such model systems have provided important insights into how ESFT initiates and develops. Even so, is it not currently understood precisely what genetic events are required for initiation of ESFT or in what specific cell type ESFT initiates. It may be that ESFT can arise in multiple cell types i.e. there may be several permissive cells of origin. This would also explain the wide range of sites in which ESFT arises.

Further understanding of the cell of origin of ESFT is important, particularly as CICs have recently been identified in ESFT based on expression of the cell surface marker CD133 (Suvà et al. 2009). These CICs express the stem cell markers Oct4, Sox2 and Nanog and importantly, like MSCs, can differentiate along adipogenic, osteogenic, and chondrogenic lineages. Although it was subsequently shown that CD133 expression is very heterogeneous in ESFT, and CD133+ cells are not consistently more resistant to therapeutics (Jiang et al. 2010), work in other cancer types has suggested that CICs cells may be responsible for disease relapse (Section 1.1.3). Therefore further investigation into the biology of these cells in ESFT may improve our understanding of how to prevent relapse and resistance to therapy in patients.

1.2.4 Treatment of ESFT

The outcome of patients with ESFT has been significantly improved since the implementation of multimodal therapy, and patients with localised disease now have up to 75% chance of long-term survival (Thacker et al. 2005). In most cases complete surgical resection is the standard treatment where possible, with chemotherapy given both pre- and postoperatively. There are no randomized control trials comparing radiotherapy and

surgery for local control. However, radiotherapy is suggested when complete surgical resection is not possible (Schuck et al. 2003). Unfortunately, ESFT display an aggressive behaviour with a tendency to metastasise primarily to the lung, bone and bone marrow. Approximately 25% of patients have overt metastases at presentation (Grier 1997, Cotterill et al. 2000, Thacker et al. 2005, Bernstein et al. 2006) but up to 50% of patients without clinically detectable metastasis at diagnosis will relapse with distant metastatic disease after surgery if systemic chemotherapy is not given.

Metastatic disease is considered the most adverse prognostic factor for ESFT and patients with metastasis to the bone or bone marrow have a 5-year survival rate of less than 25% (Paulussen et al. 1998, Cotterill et al. 2000). In addition, despite aggressive treatment, 30-40% of patients have a recurrence and of these only 50-60% achieve partial or complete remission to second line treatment (Shankar et al. 2003, Barker et al. 2005).

ESFT are treated with chemotherapy regimens including actinomycin D, doxorubicin, etoposide, cyclophosphamide, vincristine and ifosfamide. There is no internationally defined standard treatment for ESFT and in the UK, patients are treated as part of clinical trials. In the recently completed Euro-EWING 99 trial patients received vincristine, ifosfamide, doxorubicin and etoposide (VIDE) induction chemotherapy and were then randomised according to disease-risk. Standard risk patients received either vincristine, actinomycin D and ifosfamide (VAI) or vincristine, actinomycin D and cyclophosphamide (VAC). High risk patients receiving VAI or high-dose busulfan-melphalan megatherapy followed by autologous stem-cell transplantation. Although the high risk arm did not recruit the expected number of patients, the study recommended the VAC regimen for consolidation treatment of standard risk patients. Unfortunately there was a high degree of toxicity associated with the VIDE induction regimen, including stomatitis (inflammation of the mouth and lips) and infections (Juergens et al. 2006). Some secondary malignancies have also been reported although the complete data has not been published. The newly opened Euro-EWING 2012 trial will compare the VIDE regimen to the standard chemotherapy regimen used in the USA, where much fewer side effects have been reported. In the USA patients receive alternating cycles of vincristine-doxorubicin-cyclophosphamide followed by ifosfamide-etoposide and finally vincristine-cychlophosphamide (VDC/IE/VC) as induction chemotherapy. The Euro-EWING 2012 trial will also compare treatment with the bisphosphonate Zoledronic acid. Biphosphonates inhibit bone resorption and are therefore used extensively to treat osteoporosis and local bone loss (Bone et al. 2004). Biphosphonates have also been used for the treatment of

bone metastasis in patients with breast (Powles et al. 2006) and prostate (Berry 2006) cancer. Zoledronic acid has been shown to inhibit the growth of ESFT cell lines *in vitro*, and also inhibit the growth of bone tumours in mouse models of ESFT (Odri et al. 2010). Interestingly, when combined with ifosfamide, zoledronic acid exerted synergistic effects resulting in an inhibition of tumour growth that was similar to three cycles of ifosfamide alone.

Despite ongoing clinical trials, the survival rate of patients with recurrent or metastatic disease has not improved for many years. In addition, such aggressive treatment can result in debilitating side effects and even secondary cancers. Survivors of ESFT have been shown to be particularly at risk of developing thyroid and breast cancers and sarcoma, especially when radiotherapy has been given (Kuttesch et al. 1996, Wasilewski-Masker et al. 2009). Therefore there remains a real need to gain understanding of the biology of ESFT in order to develop more selective, effective and less toxic agents.

As the EWS-ETS fusion proteins are specific to ESFT cells they are an attractive target for therapy. Although it may not be possible or financially attractive to pharmaceutical companies to target the fusion specifically, drug screens have identified existing agents that target the fusion proteins. For example, the antibiotic mithramycin can inhibit EWS-FLI1 (Grohar et al. 2011). This drug suppresses tumour growth in ESFT xenograft models and is currently being investigated in a phase I/II trial in children with ESFT. Other drugs targeting EWS-FLI1 are also in pre-clinical development such as the small molecule YK-4-279. This compound interferes with the interaction between EWS-FLI1 and RNA helicase A, a critical mediator of EWS-FLI1 activity (Erkizan et al. 2009).

An alternative approach to identify useful therapeutic options is to develop our understanding of the cellular mechanisms and pathways affected by the fusion proteins. The IGF signalling pathway has been known to be have a role in ESFT tumorigenesis for a number of years. Emerging evidence has suggested that this pathway may actually be directly regulated by EWS-FLI. It has been shown that EWS-FLI downregulates IGFBP3 (IGF binding protein 3) (Prieur et al. 2004), and it is suggested this increases the amount of free IGF-1, thus stimulating tumour growth. In addition, data has shown that a group of microRNAs that negatively modulate the IGF pathway, are repressed by EWS-FLI expression (McKinsey et al. 2011). In the clinic, targeting the IGF pathway in ESFT patients has resulted in modest responses. A phase II clinical trial using a humanised IGF-1R antibody showed an overall response rate of just 10-15% (Pappo et al. 2011). However this study indicated that the response rate was better in patients with bone based primary

tumours, which are more common in younger patients. A more recent study has reported a 30% response rate when a monoclonal IGF-1R antibody (cixutumumab) was combined with a mTOR inhibitor (temsirolimus), including a complete response in a patient previously resistant to IGF-1R antibody therapy (Naing et al. 2012). Despite perhaps disappointing initial clinical results, there is strong evidence for the role of IGF signalling in ESFT so future work is ongoing to predict patients who will respond to this type of therapy and to target resistance networks (Kovar et al. 2012).

Recently, there have been a number of studies demonstrating that poly ADP ribose polymerase (PARP) inhibitors may be effective against ESFT. Research was performed at the Wellcome Trust Sanger Institute to screen over 600 cancer cell lines for sensitivity to 130 different drugs currently in preclinical or clinical evaluation (Garnett et al. 2012). A surprising result was the sensitivity of some ESFT cell lines to the PARP inhibitor olaparib (AZD2281). This observation has been confirmed by other researchers and it has also been demonstrated that EWS-FLI1 expression directly increases sensitivity of cells to PARP1 inhibition (Brenner et al. 2012). Importantly, olaparib was not effective as a single agent in xenograft models of ESFT, though combination with temozolamide showed regression of tumour growth (Brenner et al. 2012). A phase II clinical trial is ongoing to study the effect of olaparib in adults with recurrent or metastatic ESFT, and a phase I trial is recruiting to investigate the combination of olaparib and temozolamide in younger ESFT patients (Grohar and Helman 2013).

Although exciting, novel therapeutics have not yet shown dramatic responses in ESFT patients. There is still research ongoing to identify other signalling pathways which may be targeted, especially in metastatic disease. For example, a recent study by Schaefer et al. (2008) used Affymetrix microarray technology to compare the gene expression profile of 20 localised tumours to 7 metastatic tumours, and found that components of the Wnt signalling were differentially expressed. In addition, Wnt signalling was associated with resistance to chemotherapeutics used in the VIDE regimen (Schaefer et al. 2008). Studies have also shown that when EWS-FLI1 expression is induced in cells, components of the Wnt signalling pathway are upregulated (Hu-Lieskovan et al. 2005). Wnt signalling is important in normal mesenchymal stem cell development and differentiation. Therefore further investigation of this signalling pathway in ESFT may help us to understand the molecular mechanisms behind ESFT initiation, metastasis and response to therapy (Section 1.3.5).

1.3 Wnt signalling

Wnt proteins are a family of secreted lipid-modified glycoproteins that are evolutionally conserved in metazoan organisms (H. Clevers 2006). Wnt proteins act as cell-cell communication molecules and function as morphogens that are secreted from one cell or tissue type to activate surface receptors and signal transduction components in neighbouring cells (Zecca et al. 1996), thereby regulating processes such as cell proliferation, survival and differentiation (H. Clevers 2006). Signalling by Wnt proteins is one of the fundamental mechanisms that controls key developmental processes such as tissue patterning, cell migration and cell proliferation. In the adult, Wnt signalling regulates hematopoiesis, osteogenesis, angiogenesis and adipogenesis and is therefore critical to maintain tissue homeostasis (Wend et al. 2010).

1.3.1 Wnt ligands

In humans 19 Wnt ligands have been identified. They are cysteine-rich proteins of approximately 350-400 amino acids that share 20-85% amino acid identity (MacDonald et al. 2009). The cysteine residues are thought to form disulfide bonds, ensuring correct folding of the proteins, and all Wnts have an N-terminal signal peptide for secretion; therefore all Wnt ligands are predicted to be secreted (Willert and Nusse 2012). Early studies showed that Wnts are highly hydrophobic and adhere tightly to membranes and the extracellular matrix. Murine Wnt3A was the first Wnt protein to be purified and biochemically analysed, in part due to its relatively efficient secretion (Willert et al. 2003). Wnt3A has been found to undergo two types of lipid modifications, firstly a palmitate attached to the N-terminal cysteine (Willert et al. 2003), which has subsequently been identified in most other Wnt proteins. In addition, a palmitoleoyl attached to serine at position 209 (Takada et al. 2006); this is also believed to be conserved amongst the Wnts. These lipid modifications have been shown to be essential for Wnt secretion and signalling activity (Takada et al. 2006), and are the reason that Wnts are so hydrophobic. They are believed to anchor Wnts to the lipid bilayer, possibly to create a high enough concentration for secretion to take place. Wnt proteins also have multiple glycosylations which is believed in part to explain their solubility despite having lipid modifications (Willert and Nusse 2012). The number of glycosylation events varies between ligands; Wnt1 has four and Wnt3A has two *N*-linked glycosylations (Willert et al. 2003, Willert and Nusse 2012) and secretion of Wnt3A and Wnt5A is impaired if the glycosylation sides are mutated (Komekado et al. 2007, Kurayoshi et al. 2007). Although Wnt proteins have been

described to activate either canonical or noncanonical pathways, there is no structural or sequence basis for this distinction (Willert and Nusse 2012). It is likely that the cellular context dictates which pathway is activated rather than any inherent property of the Wnt ligands. For example, Wnt5A is generally considered a 'noncanonical' ligand, but has been shown to activate the canonical pathway in certain contexts (Mikels and Nusse 2006).

Once secreted, Wnts can become both short- and long-range signalling molecules, with the capacity to reach up to 20 cell diameters away (Zecca et al. 1996). Considering they are largely insoluble and membrane bound it is not fully understood how Wnts diffuse and distribute through the aqueous extracellular space. However, various theories have been suggested. For example, Wnts may form multimers or 'micelles' that shield the hydrophobic lipid adducts. Alternatively or possibly in addition, Wnts could bind to lipoprotein particles or form a matrix with heparin sulfate proteoglycans (HSPGs) and distribute by lateral diffusion (MacDonald et al. 2009). There is evidence that several of these mechanisms are active, and seem to depend on cellular context and developmental status.

1.3.2 Wnt signalling pathways

Wnt signalling is generally divided into three main pathways; the canonical Wnt/β-catenin and the noncanonical pathways; Wnt/Ca^{2+} and planar cell polarity (PCP). The canonical pathway is the most widely studied and best understood of the three pathways (Moon et al. 2004).

1.3.2.1 Canonical Wnt signalling

The canonical Wnt signalling pathway involves the regulation of the key mediator, β-catenin. In the absence of Wnt ligands, β-catenin is recruited to a 'destruction complex' that contains the scaffolding proteins, adenomatous polyposis coli (APC) and Axin (Farr et al. 2000). Two kinases also residing in the complex, glycogen synthase kinase (GSK)-3β and casein kinase (CK)-I, sequentially phosphorylate a set of conserved serine and threonine residues in the amino terminus of β-catenin, which targets it for proteosomal degradation (Yost et al. 1996, Amit et al. 2002). In the absence of Wnt this destruction complex is constitutively active, resulting in the degradation of β-catenin, and maintaining low levels in the cytoplasm. In this situation, the target genes of β-catenin are kept repressed by interacting with T-cell factor (TCF) and lymphoid enhancer-binding protein (LEF) protein family members, along with co-receptors histone deacetylase (HDAC) and Groucho (Cavallo et al. 1998). Various secreted antagonists such as Dickkopf (DKK) and Frizzled-

related protein (sFRP) family members can interact with extracellular Wnt ligands to prevent activation of the pathway (Kawano and Kypta 2003, Moon et al. 2004). The DKK family of proteins are generally considered to be inhibitors of the canonical Wnt signalling pathway as they bind and sequester the co-receptors low density lipoprotein (LDL)-receptor related proteins (LRP) 5 and 6 (Mao et al. 2001, Semënov et al. 2001). However, it has been shown that DKK2 can either promote or inhibit canonical Wnt signalling depending on the cellular context. It is thought that at low levels of LRP5/6 DKK2 acts as a Wnt inhibitor whereas with high levels of LRP-5/6 DKK2 activates the pathway, possibly because DKK2 can bind directly to LRP-6 to activate canonical Wnt signalling (Li et al. 2002).

For Wnt signalling to occur, a Wnt ligand must bind with a member of the Frizzled (FZD) family of seven-pass transmembrane receptors and one of the co-receptors, LRP 5/6 (Peters et al. 1999, Tamai et al. 2000). There are 10 FZD genes in mammals and it is believed Wnt binding induces the formation of FZD-LRP5/6 complexes, although this has not been demonstrated *in vivo*. Evidence has shown there is functional redundancy among FZD receptors. LRP6 is essential for embryogenesis whereas LRP5 is more important in bone homeostasis (MacDonald et al. 2009). In the canonical Wnt signalling pathway Wnt binding recruits Axin and the destruction complex to the plasma membrane, where Axin binds to the cytoplasmic tail of LRP 5/6. Axin is then degraded, thereby decreasing β-catenin degradation. In addition, Wnt ligand binding also induces activation of the phosphoprotein Dishevelled (Dvl) which prevents GSK3β binding to Axin, further reducing the phosphorylation and degradation of β-catenin, and increasing its post-translational stability (Moon et al. 2004). As levels of β-catenin rise, it accumulates in the nucleus where it interacts with DNA-bound TCF/LEF family members to activate the transcription of target genes. The conversion of the TCF repressor complex into a transcriptional activator complex involves the displacement of Groucho, and recruitment of the histone acetylase CREB-binding protein (CBP) or its closely related homolog, p300 (Takemaru and Moon 2000). Canonical Wnt signalling target genes are diverse with over 100 identified to date. Many are known to be involved in tumorigenesis, others in development and stem cell maintenance (H. Clevers 2006). Many of the Wnt signalling components themselves are TCF/LEF targets such as DKK1, Wnt3A, Axin and LRP6, which highlights the ability of Wnt/β-catenin to regulate itself and the importance of keeping the Wnt signalling pathway under tight control.

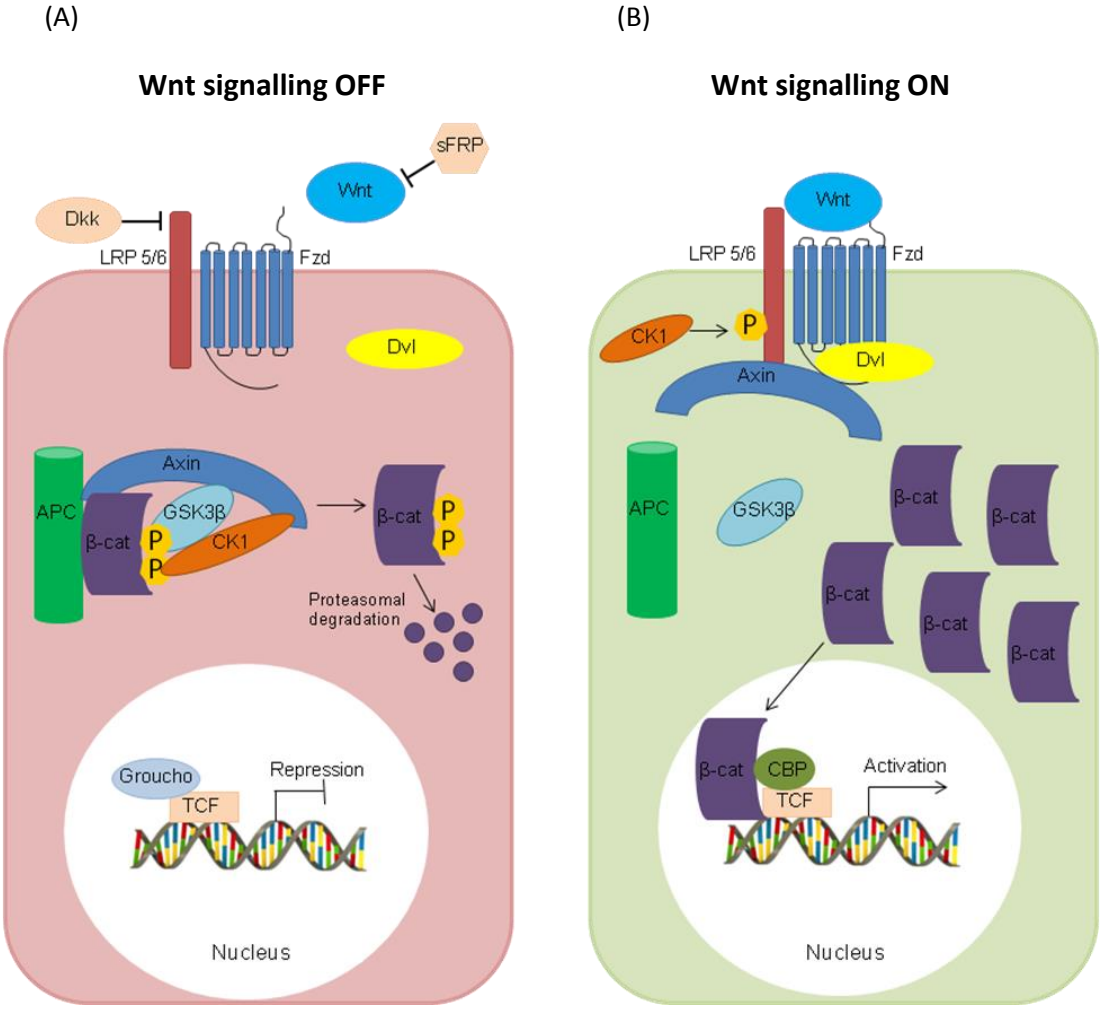

Figure 1.3 Overview of canonical Wnt signalling (A) In the absence of Wnt proteins, β-catenin is recruited to a 'destruction complex' and is phosphorylated and targeted for proteosomal degradation. β-catenin levels in the cytoplasm remain low and the target genes of β-catenin are repressed by interacting with TCF/Lef proteins (B) When a Wnt protein binds to a member of the Fzd family of receptors and one of the co-receptors LRP 5/6, the destruction complex breaks down, β-catenin degradation is reduced and it accumulates in the nucleus where it interacts with DNA-bound TCF/Lef family members to activate the transcription of target genes. APC=adenomatous polyposis coli, CBP=CREB-binding protein, CK1=casein kinase I, DKK=Dickkopf, Dvl=Dishevelled, Fzd=frizzed, GSK3β= glycogen synthase kinase-3β, LDL=low density LRP=low density lipoprotein receptor-related protein, sFRP=secreted frizzled-related protein, TCF=T-cell factor. Adapted from Moon (2004).

1.3.2.2 Noncanonical Wnt signalling

The noncanonical Wnt signalling pathways are β-catenin-independent and are generally thought to be involved in cell migration and polarity (Sugimura and Li 2010a). The two major pathways are the Wnt/PCP pathway and Wnt/Ca^{2+} pathway. Wnt proteins that play a role in these pathways include Wnt5A, Wnt4, Wnt11 and Wnt7A (Wang 2009). In the Wnt/PCP signalling pathway Wnt ligands and FZD interact with an alternative co-receptor, ROR2, which recruits Dvl to the membrane. Dvl is also important in canonical Wnt signalling and different domains within Dvl, including DIX, PDZ and DEP, diverge different downstream pathways (Habas and Dawid 2005). Activation of the DEP domain leads to activation of small GTPases such as RhoA and Rac (Oishi et al. 2003). These in turn activate c-Jun N-terminal kinase (JNK) signals which have cytoskeletal effects and ultimately control cell polarity and motility (Boutros et al. 1998, Wang 2009).

Wnt5A and Wnt11 are also known to activate Wnt/Ca^{2+} signalling. Here, Wnt binding to FZD results in the activation of heterotrimeric G proteins and the release of calcium from its intracellular stores (Malbon et al. 2001). The increase in intracellular calcium results in the activation of calcium dependent signalling molecules and the activation of calcium dependent effector proteins. Protein kinase C (PKC) may be activated which regulates many cellular processes including the small GTPase Cdc42 (Schlessinger et al. 2007). Cdc42 is one of the key effectors of actin remodelling in the cytoskeleton, therefore this pathway has some overlap with the PCP pathway. An influx of intracellular calcium ions also activates calmodulin-dependent protein kinase II (CamKII) (Kuhl et al. 2000) which induces activation of TAK1 and NLK kinases in the MAPK pathway (Ishitani et al. 2003) (Figure 3). A further branch of the calcium pathway is calmodulin-mediated activation of calcineurin, a protein phosphatase known to activate the NFAT transcription factor (Saneyoshi et al. 2002). The calcineurin-NFAT pathway is one of the major noncanonical pathways in vertebrates and is known to be involved in numerous diseases, including cancer. Both CaMKII-TAK1-NLK and NFAT-mediated transcription can antagonize β-catenin- dependent canonical Wnt signalling, meaning the canonical and noncanonical pathways are not usually active in the same cell (Ishitani et al. 2003).

1.3.2.3 Alternative Wnt receptors

To add another level of complexity to Wnt signalling, there are also membrane proteins other than FZD receptors that contain Wnt-binding domains, and these may be equally important receptors for Wnts. The atypical tyrosine kinase Ryk possesses a Wnt inhibitory

factor (WIF) domain and is also important in transducing Wnt signals during axon guidance, and can bind both canonical and non-canonical Wnts (van Amerongen et al. 2008). Ryk can bind Wnt1 and activate TCF/LEF dependent transcription. However, Ryk can also signal via the release of intracellular calcium when bound to Wnt5A and activate src (Wouda et al. 2008). The complexity of Wnt signalling, and the fact that Wnts can induce a variety of different responses in different cell types could be due to the complexity of receptor configurations that are possible. It may be receptor configuration and not the intrinsic properties of the Wnt family members that dictate which pathway is activated.

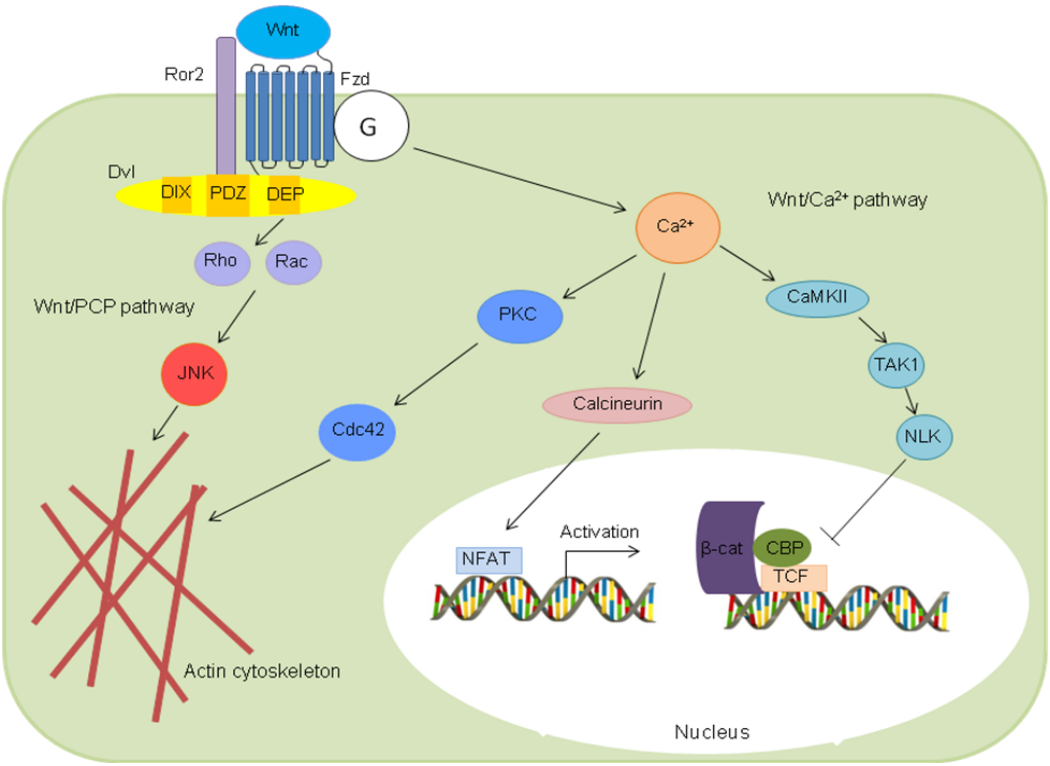

Figure 1.4 Overview of noncanonical Wnt signalling In the Wnt/PCP signalling pathway, Wnt ligands and FZD interact with an alternative co-receptor, ROR2. This leads to activation of small GTPases such as RhoA and Rac, and these in turn activate c-Jun N-terminal kinase (JNK) signals which have cytoskeletal effects and ultimately control cell polarity and motility. In the Wnt/Ca^{2+} signalling pathway, Wnt binding to FZD results in the activation of heterotrimeric G proteins and the release of calcium from its intracellular stores. This leads to activation of calcium dependent signalling molecules such as PKC which activates the small-GTPase Cdc42. CamKII is also activated which induces activation of TAK1 and NLK in the MAPK pathway. This antagonises β-catenin-dependent canonical Wnt signalling. Calcium signalling also activates calcineurin, a protein phosphatase known to activate the NFAT transcription factor. PKC=protein kinase C, CamKII=calmodulin-dependent protein kinase II, NLK=nemo-like kinase, TAK1=TGF-beta-activated kinase 1, NFAT=nuclear factor of activated T-cells, MAPK=mitogen-activated protein kinase. Adapted from Sugimura and Li (2010).

1.3.3 Wnt signalling in normal cells

Through its role in directing cell proliferation, cell polarity, fate determination and tissue patterning, Wnt signalling is known to regulate development of many of the tissues and organs in the body (van Amerongen and Nusse 2009). Wnt signalling remains essential throughout life in self-renewing tissues such as the gut, hair follicles and haematopoietic cells (H. Clevers 2006). These tissues all contain stem cells which have the unique ability to self-renew and to differentiate into more specialised cells.

The role of Wnt signalling in stem cell biology varies according to the cellular context. In some circumstances Wnt appears to be important for maintenance of multi- or pluripotency but has also been implicated in the differentiation of stem and progenitor cells. Wnt signalling is particularly important in the stem cells of the intestine. Mutation of the TCF family member TCF4 in mice results in the absence of the stem/progenitor cell compartment in crypts of the small intestine (Korinek et al. 1998). In addition, inhibition of Wnt signalling by transgenic expression of the endogenous inhibitor DKK1 in adult mice induces the complete loss of crypts (Kuhnert et al. 2004).

Wnt signalling is also important in bone development due to its role in controlling MSC differentiation. MSCs can differentiate into osteoblasts and adipocytes and their fate is determined by transcription factors Runx2 and PPAR-γ, respectively (Sugimura and Li 2010b). The Wnt signalling pathways act at different stages in the process of differentiation (Figure 1.5). Recently, it has been shown that the noncanonical ligand Wnt5A is important in the fate determination of MSCs. Wnt5A promotes osteogenesis by suppressing PPARγ activation and activating Runx2 in the ST2 mesenchymal progenitor cell line (Takada et al. 2007). In contrast, the canonical ligand Wnt3A has been shown to maintain a proliferating MSC population, and suppress osteogenesis (Boland et al. 2004). Wnt/β-catenin signalling also appears to suppress adipogenesis by suppressing expression of PPARγ and inducing osteogenesis by increasing RUNX2 expression. Interestingly, the canonical Wnt inhibitor DKK1 is secreted from mature osteoblasts which indicates a feedback loop exists to regulate osteogenesis (Qiang et al. 2008).

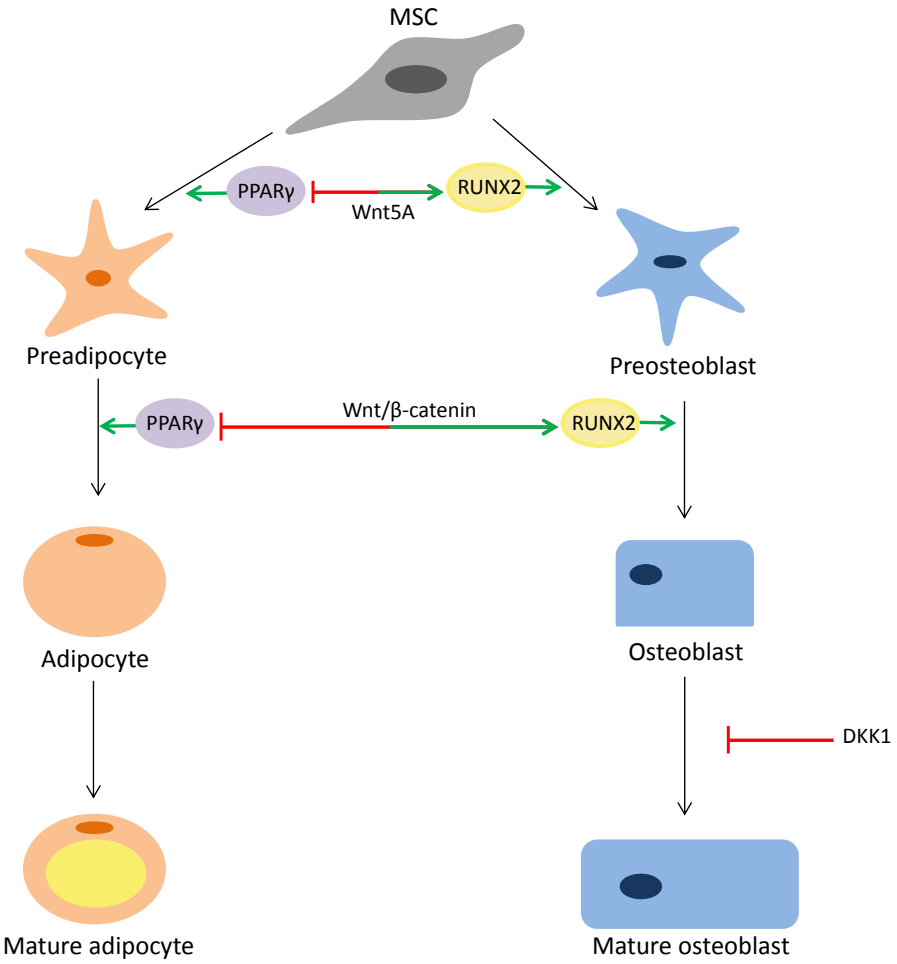

Figure 1.5 Wnt signalling in the regulation of MSC differentiation MSCs can differentiate into osteoblasts and adipocytes and this is regulated by transcription factors Runx2 and PPAR-γ, respectively. Wnt5A is important in fate determination and promotes osteogenesis and inhibits adipogenesis. The canonical Wnt signalling pathway is important at later stages of differentiation and promotes the maturation of preosteoblasts. The Wnt inhibitor DKK1 is secreted from mature osteoblasts to regulate osteogenesis. Adapted from Takada et al. 2009.

1.3.4 Wnt signalling in cancer

During development and normal adult homeostasis, the activity of Wnt signalling is tightly regulated. Disruption of this balance is frequently linked to development of pathological conditions such as cancer.

1.3.4.1 Canonical Wnt signalling in cancer

Nuclear accumulation of β-catenin demonstrated by immunohistochemistry has been used as evidence of an activated canonical pathway in a variety of human tumours including colorectal, lung, breast, cervical, skin and liver (Camilli and Weeraratna 2010). In

hepatocellular carcinoma, nuclear β-catenin accumulation has been linked to poorly differentiated morphology, high proliferation and poor prognosis (Endo et al. 2000, Inagawa et al. 2002).

This aberrant accumulation of β-catenin has been attributed to mutations or epigenetic variation in various members of the signalling pathway. Activating β-catenin mutations at one of the phosphorylation sites that prevent its degradation have been identified in 50% of colon cancers (Sparks et al. 1998). Mutations in β-catenin have also been reported in brain tumours (Zurawel et al. 1998), ovarian (Palacios and Gamallo 1998) and prostate cancer (Voeller et al. 1998). Many other mutations affecting other members of the signalling cascade have been identified, in particular those that affect the interaction of β-catenin with the destruction complex, leading to an increase in β-catenin levels. For example, truncating mutations in APC leading to loss of function occurs in around 80% of sporadic cancers (Powell et al. 1992), and this leads to inappropriate stabilisation of β-catenin and aberrant transcription of genes including c-myc and cyclin D1.

1.3.4.2 Noncanonical Wnt signalling in cancer

The noncanonical signalling pathway is less frequently investigated in cancer. In part this is because it is more difficult to ascertain the role of noncanonical signalling since the downstream effector molecules are involved in many other signalling pathways.

The ligand most widely studied in noncanonical signalling is Wnt5A which can have either a tumour suppressive or oncogenic function depending on the cancer type. It is possible that Wnt5A plays a role in tumour suppression by inhibiting the canonical Wnt signalling pathway (Ishitani et al. 2003). Consistent with this hypothesis expression of Wnt5A is decreased in colorectal cancer (Ying et al. 2008), neuroblastoma (Blanc et al. 2005), ductal breast cancer (Jonsson et al. 2002) and leukaemia (Ying et al. 2007). Furthermore, Wnt5A has been shown to inhibit migration of thyroid (Kremenevskaja et al. 2005) and colon cancer (Dejmek et al. 2005) cell lines. However, in contrast overexpression of Wnt5A has been reported in pancreatic (Ripka et al. 2007), prostate (Wang et al. 2007) and gastric cancer, where it enhances the motility of malignant cells, promotes tumour invasion and correlates with advanced disease and poor prognosis (Kurayoshi et al. 2006). Studies have also shown increased motility and migration of melanoma cells when Wnt5A is overexpressed, and in melanoma tissue samples there is a correlation between high expression of Wnt5A and higher grade of tumour (Weeraratna et al. 2002).

1.3.4.3 Wnt signalling in cancer initiating cells (CICs)

As previously discussed (Section 1.1.4), CICs have been identified in a number of different cancer types and have been shown to have stem-cell characteristics. This has lead to the suggestion that the same signalling pathways, including Wnt, may be involved in their maintenance and proliferation. Interestingly, many of the cell surface markers that have been used to identify and isolate potential CICs such as LGR5, CD44, CD24 and Epcam are direct Wnt targets (Takahashi-Yanaga and Kahn 2010). High canonical Wnt signalling has been shown to identify CICs in colorectal cancer (Vermeulen et al. 2010) and lung cancer (Teng et al. 2010). Canonical Wnt signalling has also been shown to increase the clonogenic potential and self-renewal in putative leukemic stem cells in acute myeloid leukaemia (AML) (Ysebaert et al. 2006, Kawaguchi-Ihara et al. 2008). In addition, Wnt signalling is associated with the CIC population in breast cancer (Li et al. 2003, Li et al. 2008), squamous cell carcinoma (Malanchi et al. 2008) and hepatocellular carcinoma (Yang et al. 2008).

1.3.5 Wnt signalling in ESFT

Expression of components of the Wnt signalling pathway have previously been detected in ESFT cell lines using RT-PCR analysis. In a panel of nine ESFT cell lines Wnt10B mRNA was detected in all cell lines, along with Wnt5A, Wnt11 and Wnt13 in at least 7 of the cell lines. In addition, mRNA expression of the receptors FZD2, FZD3, FZD4, FZD7 and FZD8 and the co-receptors LRP-5 and -6 were reported (Üren et al. 2004).

More recent studies have also identified that Wnt signalling may be important in the development of ESFT. For example, Wnt signalling targets/components such as c-myc, cyclin D1 and Wnt5A have been shown to be highly associated with primary ESFT, and also differentially expressed when EWS-FLI1 was induced in rhabdomyosarcoma cells (Hu-Lieskovan et al. 2005). Other studies have used microarray analysis in an attempt to understand the differences between localised and metastatic disease, and have shown that Wnt signalling or Wnt signalling components may be important. Firstly, Schaefer et al. (2008) compared the gene expression profile of 20 localised to 7 metastatic tumours, and demonstrated Wnt signalling was the pathway most significantly different between the two groups of tumours, indicating different Wnt signalling may have a role in ESFT metastasis. In addition, the authors investigated the response of ten ESFT cell lines to drugs commonly used in the treatment of ESFT and reported that Wnt signalling was one of 77 pathways that was altered following treatment with all four drugs in the VIDE regimen. In a different study, the microarray profile of 30 primary and seven metastases

were investigated and linked to event-free survival. It was found that the small GTPase *Rac1,* which is involved in PCP noncanonical signalling, could discriminate patients with a poor or good prognosis (Scotlandi et al. 2009). Taken together these studies suggest that Wnt signalling could be involved in both the initiation and progression of ESFT.

There are some reports detailing the response of ESFT cells to exogenous Wnt ligands. For example, treatment of the TC32 ESFT cell line with the canonical ligand Wnt3A induces morphological changes in these cells, with the presence of long cytoplasmic extensions resembling neuronal axons (Üren et al. 2004, Endo et al. 2008). Wnt3A treatment also increases migration of TC32 cells by more than five-fold. However, importantly Wnt3A treatment does not lead to any change in proliferation, survival or growth of TC32 cells in soft agar (Üren et al. 2004). It has also been shown that treatment of ESFT cell lines with the noncanonical Wnt ligand Wnt5A increases migration (Zhe et al. 2012).

Interestingly a number of different studies have identified that the DKK family of proteins, in particular DKK1 and DKK2, may be important in ESFT. In ESFT DKK1 mRNA is reported to be downregulated, and DKK2 mRNA upregulated in both ESFT cell lines and tumours (Staege et al. 2004, Miyagawa et al. 2009, Navarro et al. 2010, Hauer et al. 2013). It has been suggested that this upregulation of DKK2 may be a direct consequence of EWS-ETS fusion proteins directly interacting with the promoter region of DKK2 (Miyagawa et al. 2009). However, this has been disputed since knockdown of EWS-FLI1 in ESFT cell lines has no effect on DKK2 expression (Hauer et al. 2013). Nevertheless, an increase in DKK2 mRNA expression has been measured when EWS-ETS fusion proteins (including EWS-FLI1, EWS-ERG and EWS-E1AF) are expressed in mesenchymal progenitor cells (Miyagawa et al. 2009). More recently, it has been shown by constitutive knockdown of DKK2 in cell lines (by retroviral RNAi), that DKK2 increases migration and invasiveness of ESFT, and mediates osteolysis (Hauer et al. 2013). The same study reported that DKK2 stimulates rather than inhibits canonical Wnt signalling, as constitutive knockdown decreased nuclear β-catenin and decreased downstream targets of canonical Wnt signalling such as cyclin D1.

In contrast to DKK2, in non-ESFT cell lines including HeLa and HEK293T cells, EWS-FLI1 has been shown to inhibit DKK1 expression (Navarro et al. 2010). Since DKK1 is itself a target of canonical Wnt signalling, the authors of this study investigated if EWS-FLI1 had more general effects of Wnt target genes. They found that the fusion protein directly interacts with the TCF/LEF family member LEF1, potentially interfering with the formation of β-catenin/LEF complexes, and therefore repressing canonical Wnt signalling. The study also demonstrated that canonical Wnt signalling could not be stimulated in ESFT cell lines

unless EWS-FLI1 was knocked down. In agreement with this other studies have reported no cytoplasmic or nuclear staining of β-catenin immunohistochemistry in patient tumour samples (Üren et al. 2004), and no nuclear β-catenin in TC32 ESFT cells (Hu-Lieskovan et al. 2005). Furthermore, using a canonical Wnt signalling reporter assay, no β-catenin mediated gene expression was reported in ESFT cell lines (Hu-Lieskovan et al. 2005).

The current literature suggests that Wnt signalling may be an important pathway both in the initiation and progression of ESFT. However, the precise role of the different pathways in these processes has not been fully elucidated.

1.4 Hypothesis and aims

The hypothesis of my thesis is that, Wnt signalling is important in the initiation and progression of ESFT (Figure 1.6). More specifically that the canonical Wnt signalling pathway is important in the initiation of ESFT, and that the noncanonical pathway may become dominant in the progression and metastasis of ESFT due to its role in promoting migration and invasiveness, as has been demonstrated in other cancer types.

The objectives of my research have therefore been to;

1. Examine the expression profile of Wnt signalling components in ESFT cell lines (Chapter 2).
2. Develop a functional assay to measure the activity of the canonical Wnt signalling pathway (Chapter 3).
3. Optimise functional assays to investigate the activity of the noncanonical Wnt signalling pathway (Chapter 4).
4. Investigate the activity of the Wnt signalling pathways in two model systems of ESFT initiation. Firstly, in reprogrammed ESFT cells (Chapter 5) and in human embryonic stem cells with inducible EWS-FLI1 expression (Chapter 6).

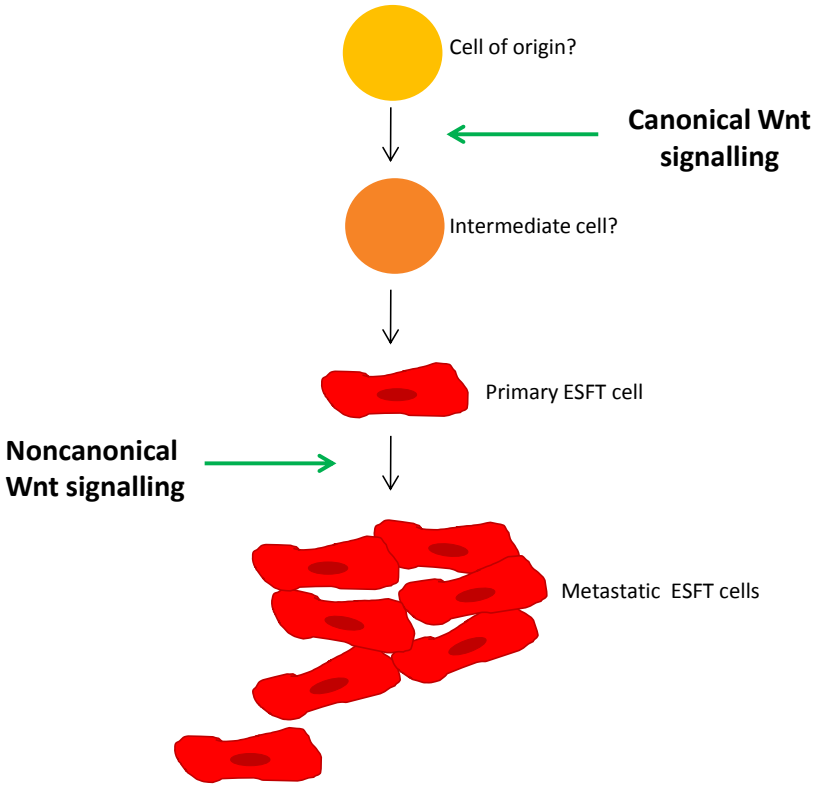

Figure 1.6 Summary of thesis hypothesis that canonical Wnt signalling is important in the initiation of ESFT and noncanonical Wnt signalling becomes dominant during disease progression by promoting invasion and migration.

2. Expression of Wnt signalling components in ESFT cell lines

2.1 Introduction

Aberrant Wnt signalling has been implicated in the initiation and progression of various different cancer types. The role of the Wnt signalling pathways in the development and progression of ESFT has not been widely studied. However the expression of various components of the Wnt signalling pathway have been described in ESFT samples and cell lines as summarised in Table 2.1.

Component	Function in Wnt signalling	Source	Detection method	Reference
Wnt4, Wnt10B, Wnt13,	Canonical Wnt ligands	Cell lines	RT-PCR	(Üren et al. 2004)
Wnt5A	Noncanonical Wnt ligand	Cell lines Tumour samples	RT-PCR WB RTqPCR Microarray	(Üren et al. 2004) (Jin et al. 2012) (Jin et al. 2012) (Hu-Lieskovan et al. 2005)
sFRP1	Secreted inhibitor of both pathways	Cell lines Tumour samples	RT-PCR MS-PCR	(Üren et al. 2004) (Jin et al. 2012)
sFRP2	Secreted inhibitor of both pathways	Cell lines Tumour samples	RT-PCR MS-PCR	(Üren et al. 2004) (Jin et al. 2012)
sFRP3	Secreted inhibitor of both pathways	Cell lines	RT-PCR	(Üren et al. 2004)

sFRP4	Secreted inhibitor of both pathways	Cell lines	RT-PCR	(Üren et al. 2004)
LRP5/LRP6	Co-receptors for Frizzled receptors	Cell lines	RT-PCR	(Üren et al. 2004)
FZD2	Receptor for Wnt ligands	Cell lines	RT-PCR	(Üren et al. 2004)
FZD3	Receptor for Wnt ligands	Cell lines	RT-PCR	(Üren et al. 2004) (Endo et al. 2008)
FZD4	Receptor for Wnt ligands	Cell lines	RT-PCR	(Üren et al. 2004) (Endo et al. 2008)
FZD7	Receptor for Wnt ligands	Cell lines	RT-PCR	(Üren et al. 2004) (Endo et al. 2008)
FZD8	Receptor for Wnt ligands	Cell lines	RT-PCR	(Üren et al. 2004)
DKK1	Secreted inhibitor of both pathways	Cell lines	Microarray RTqPCR	(Navarro et al. 2010) (Miyagawa et al. 2009)
DKK2	Secreted inhibitor of both pathways	Cell lines Tumour samples	Microarray RTqPCR RTqPCR	(Navarro et al. 2010) (Miyagawa et al. 2009) (Hauer et al. 2013)
DKK4	Secreted inhibitor of both pathways	Cell lines	Microarray	(Navarro et al. 2010)
CELSR3	Component of noncanonical PCP pathway	Tumour samples	Microarray	(Schaefer et al. 2008)
CTBP2	Transcriptional co-repressor of canonical Wnt signalling	Tumour samples	Microarray	(Schaefer et al. 2008)
TCF1	Member of the TCF/LEF family of transcription factors	Tumour samples	Microarray	(Schaefer et al. 2008)
TCF4 (TCF7L2)	Member of the TCF/LEF family	Tumour samples	Microarray	(Schaefer et al. 2008)

Rac1	Component of noncanonical PCP pathway	Tumour samples	Microarray	(Scotlandi et al. 2009)

Table 2.1 Components of the Wnt signalling pathways which have been detected in ESFT cell lines and samples The role in Wnt signalling and method of detection is shown for each component. RT-PCR=reverse transcriptase polymerase chain reaction (PCR), RTqPCR=quantitative reverse transcriptase PCR, MS-PCR= methylation-specific PCR, WB=western blot.

To investigate Wnt signalling in cells it is common to profile the expression of these components, including protein expression of the Wnt ligands themselves. Of the 19 members of the family, Wnt1 was the first Wnt protein to be identified and was initially linked to the formation of mammary tumours in mice (Nusse and Varmus 1982, Nusse et al. 1984). Indeed Wnt1 expression has been observed in human breast (Wong et al. 2002) , gastric and pancreatic (Katoh 2003) cancer cells, and increased expression linked to poor survival in glioma (Liu et al. 2011). Wnt3A is the most frequently investigated canonical Wnt ligand, in part due to the fact that is one of the few Wnt ligands which has been purified and structure analysed (Willert et al. 2003). Treatment with recombinant Wnt3A protein or Wnt3A conditioned media is the most commonly used method to stimulate the canonical Wnt signalling pathway. In ESFT cell lines, Wnt3A protein has been shown to stimulate the formation of long cytoplasmic extensions, but not to increase proliferation (Üren et al. 2004, Endo et al. 2008). However, it has not been established if ESFT cell lines produce and secrete endogenous Wnt3A protein. The noncanonical ligand Wnt5A has also been successfully purified and is the most extensively studied noncanonical Wnt ligand. The role of Wnt5A in cancer is complex as it can have both tumour suppressive and oncogenic properties depending on the cancer type. In ESFT, Wnt5A has been reported to be a 'signature' gene at diagnosis which is upregulated upon expression of EWS-FLI (Hu-Lieskovan et al. 2005). Expression of Wnt5A has also been reported in ESFT cell lines (Üren et al. 2004) and recombinant Wnt5A protein has been shown to promote migration of ESFT cell lines (Jin et al. 2012).

In addition to investigating the expression of different Wnt ligands, downstream components such as the key mediator β-catenin are also commonly investigated. When canonical Wnt signalling is activated, the degradation complex is inhibited meaning β-catenin is not phosphorylated and therefore not degraded. Levels of β-catenin in the cytoplasm rise, and it translocates to the nucleus where it can bind to TCF/LEF proteins to modulate the expression of target genes; expression of nuclear β-catenin is therefore

frequently used as a marker of activated canonical Wnt signalling (Burkhalter et al. 2011). High levels of nuclear β-catenin (increased canonical Wnt signalling) have been described and reported to predict for poor outcome in breast cancer (Lin et al. 2000) and colorectal cancer (Cheah et al. 2002). In contrast, in paediatric medulloblastoma, nuclear β-catenin and activation of the canonical Wnt signalling pathway is linked to favourable prognosis (Ellison et al. 2005, Fattet et al. 2009). Active (nonphosphoryated) β-catenin can also be detected in cells with active canonical Wnt signalling using antibodies to specifically detect β-catenin dephosphorylayed at residues Ser37 and Thr41 (van Noort et al. 2002).

The aims of the chapter were therefore to:

1. Investigate the mRNA expression of components of the Wnt signalling pathway in a panel of ESFT cell lines by RTqPCR.
2. Optimise antibodies for the detection of canonical and noncanonical Wnt ligands and investigate their protein expression in ESFT cell lines.
3. Investigate the subcellular localisation and phosphorylation status of β-catenin in ESFT cell lines to probe for activation of the canonical Wnt signalling pathway.

2.2 Materials and methods

2.2.1 Tissue culture

Six ESFT cell lines were studied (Table 2.1). All cell lines were substrate adherent and were routinely cultured on Primaria™ plastic (Falcon; BD Biosciences, Oxford, UK) in 75cm^2 flasks. Cells were passaged when they reached 85-90% confluency; media was aspirated from the flask and cells washed with 1X phosphate buffered saline (PBS; w/v, Oxoid Limited, Basingstoke, UK), followed by incubation with 5ml ethylenediaminetetracetate (EDTA, 0.1% in PBS; (w/v), Invitrogen™; Life Technologies, Paisley, UK) for 2 minutes (min). EDTA was removed, cells washed in PBS and then incubated with 5ml 1X Trypsin (0.25% (w/v) (Sigma-Aldrich, Dorset, UK), in 1X PBS) for 5 min, or until cells had completely detached from the plastic, as assessed by light microscopy; Olympus CKX41 (Olympus Microscopy, Essex, UK). For the SKES-1 cell line the EDTA incubation step was omitted. An equal volume of media containing 10% Foetal Calf Serum (FCS; v/v, Harlan Sera-Lab, Loughborough, UK) was added to the cells neutralise the trypsin. The cell suspension was centrifuged at 405g for 5 min and the resulting cell pellet resuspended in appropriate cell line specific media and reseeded into flasks or 6 well plates as required. Cells were maintained in a humidified chamber (Sanyo CO_2 Incubator, MCO-2OAIC, Sanyo Gallenkamp Plc., Loughborough, UK) in 5% CO2 in air at 37°C. Cell lines were screened for mycoplasma contamination every 3 months by technical staff using the EZ-PCR mycoplasma test kit (Geneflow Ltd, Fradley, UK). For ESFT cell lines, expression and type of fusion transcript was verified by technical staff using reverse-transcriptase quantitative polymerase chain reaction (RTqPCR).

Cell line	ESFT	Cell type	Fusion transcript	Origin (source)	Media
A673	Yes	pPNET	EWS-FLI1 Type I	15yr female (ATCC)	DMEM+ 10% FCS + 2mM Glutamine
RD-ES	Yes	Ewing's sarcoma	EWS-FLI1 Type II	19yr male. (ATCC)	RPMI + 10% FCS + 2mM Glutamine
SKES-1	Yes	Ewing's sarcoma	EWS-FLI1 Type II	18yr male. (ATCC)	McCoy's 5a + 15% FCS + 2mM Glutamine
SK-N-MC	Yes	pPNET	EWS-FLI1 Type I	14yr female. (ATCC)	DMEM + F12 + 10% FCS + 2mM Glutamine
TC32	Yes	pPNET	EWS-FLI1 Type I	17yr female. (Gift: Dr Toretsky).	RPMI + 10% FCS + 2mM Glutamine
TTC466	Yes	Ewing's sarcoma (extra osseous)	EWS-ERG	Metastatic. (Gift: Dr Poul Sorenson).	RPMI + 10% FCS + 10% conditioned media + 2mM Glutamine
A431	No	Epidermoid carcinoma	N/A	(Gift: Professor M. Knowles)	DMEM + 10% FCS + 2mM Glutamine
NIH/3T3	No	Mouse fibroblast	N/A	(Gift: Professor Tim Bishop)	DMEM + 10% FCS + 2mM Glutamine
L-Wnt5A	No	Mouse fibroblasts overexpressing human Wnt5A	N/A	(ATCC)	Modified DMEM (ATCC) +10% FCS + 4 mM Glutamine
L-Wnt3A	No	Mouse fibroblasts overexpressing human Wnt3A	N/A	(ATCC)	As for L-Wnt5A
HeLa	No	Cervical adeno-carcinoma	N/A	(Gift: Professor M. Knowles)	DMEM + 10% FCS + 2mM Glutamine

Table 2.2 Characteristics of ESFT and cell lines used as controls Details of the origin of the cell line and media used to maintain cultures are given. The EWS-ETS fusion type is given for ESFT cell lines. All cell lines are human origin unless otherwise stated. All media was purchased from Invitrogen™ unless otherwise stated. pPNET=peripheral primitive neuroectodermal tumour, N/A = not applicable, yr = years old. DMEM= Dulbecco's Modified Eagle Medium. ATTC=American Type Tissue Collection (supplied by LGC Standards, Teddington, UK).

2.2.2 Determination of viable cell number

Viable cell number was assessed using the trypan blue exclusion assay. Cells were trypsinised and resuspended in media as described (Section 2.2.1). Cell suspension (10µl) was added to an equal volume of trypan blue dye (0.4%; v/v, Sigma-Aldrich) and viable cell number assessed using the Neubauer haemocytomter. Non-viable cells appear blue as the permeable membrane allows uptake of the dye. The number of clear (viable) cells in 4 areas of the grid were counted and the mean of these was calculated to give a value x 10^4 cells/ml. Alternatively, the automated Vi-cell (Beckman Coulter, High Wycombe, UK) viable cell counter was used. This machine uses the same principle to measure viable cell number but in this case the addition of trypan blue and cell counting is automated. In this method, 1ml of cell suspension is taken up by the machine, trypan blue added and viable cell number x 10^6 cells/ml, is calculated. All viable cell counts were performed in triplicate.

2.2.3 SDS-PAGE and western blotting

2.2.3.1 Preparation of protein extracts

Cell lines were cultured in 75cm^2 tissue culture flasks until 70% confluent. Media was aspirated, cells washed once with 5ml ice-cold 1X PBS, scraped into 2ml ice-cold PBS using a cell scraper (Sarstedt Ltd., Leicester, UK) and centrifuged at 405g for 5min. The supernatant was aspirated and the pellet resuspended in 200µl of Radio Immuno Precipitation Assay (RIPA) lysis buffer (1X PBS containing 1% (v/v) Nonidet P-40, 10mM sodium deoxycholate, 0.1% (w/v) sodium dodecyl sulphate (SDS)) with protease inhibitor cocktail (0.6mM phenymethylsulfonyl (PMSF), 1mM sodium orthovanadate, 25µM leupeptin, and 30µl/ml Aprotinin, all purchased from Sigma-Aldrich). Samples were incubated on ice for 30 min, and centrifuged at 12,470g at 4°C for 10 min. The resulting supernatant was retained as the soluble protein fraction.

A 5µl aliquot of the cell lysate was added to 45µl deionized distilled (dd)H_20 and retained for protein estimation. The remainder was added to an equal volume of 2X SDS loading buffer (100mM Tris-HCl (pH 8.3), 20% (v/v) Glycerol, 4% SDS, 0.2% (w/v) bromophenol blue (Sigma-Aldrich), 200mM dithiothreitol (DTT, Sigma-Aldrich)), stored in single use aliquots at -20°C. Where non-reduced samples were required, DTT was omitted from the buffer.

2.2.3.2 Determination of protein concentration

The BioRad DC Protein Assay (Bio-Rad Laboratories Ltd, Hemel Hempstead, UK) based on the Lowry Assay (Lowry et al. 1951) was used to estimate protein concentration of all samples. All reagents are company proprietary. Briefly, a standard dilution curve was prepared of bovine serum albumin (BSA, Sigma-Aldrich) ranging from 0 to 2mg/ml in 10% RIPA lysis buffer. Each sample or standard (5µl) was pipette in triplicate into wells of a 96 well microtitre place (Nunc-Immuno™, Nalge Nunc Intl., supplied by Fisher Scientific, Loughborough, UK). Working reagent SA was prepared by adding Reagent S (20µl) to Reagent A (1ml) and added to each well (25µl). Reagent B was then added (200µl) to each well and the plate was agitated for 10 seconds (s) followed by 15 min incubation at room temperature (RT). Absorbance of each well was read at 690 nm using a microplate reader (Titertek-Berthold Instruments, supplied by GeneFlow) Protein concentration in samples was determined from the standard curve generated from the BSA dilutions.

2.2.3.3 SDS-Polyacrylamide Gel Electrophoresis (SDS-PAGE)

Mini-Protean II cell apparatus (Bio-Rad) was used throughout. The appropriate percentage acrylamide gel was chosen according to the molecular weight of the protein of interest; for most proteins a 10% resolving gel solution was utilised. Acrylamide (10%; v/v, Severn Biotech. Ltd, Kidderminster, UK), 1.5M Tris (pH 8.8, MP Biomedicals Inc., supplied by Fisher Scientific), 0.1% SDS (w/v, BDH Laboratory Supplies, supplied by VWR Int. Ltd., Lutterworth, UK), 0.1% ammonium persulphate (w/v, Sigma-Aldrich), 0.006% N, N, N', N'-Tetramethylethylenediamine (v/v, TEMED, Sigma-Aldrich)) were mixed and poured into the gel apparatus. The resolving gel was then overlayed with 2-methyl-2-butanol (Sigma-Aldrich) until polymerized (approximately 30 min). The 2-methyl-2-butanol was removed and the resolving gel rinsed with ddH_2O. The resolving gel was overlayed with a stacking gel (5% (v/v) acrylamide, 1 M Tris (pH6.8), 0.1% (w/v) SDS, 0.1% (w/v) ammonium persulphate, 0.01% (v/v) TEMED) and a comb placed in the solution taking care to avoid introduction of air bubbles. Once polymerised, the comb was removed and the wells washed with ddH_2O to remove any non-polymerised acrylamide.

The gel was transferred to the electrophoresis tank containing 2X SDS running buffer (25mM Tris-HCl (MP Biomedicals), 250mM Glycine (Sigma-Aldrich), 0.1% (w/v) SDS). Protein extracts (50µg) in 2 x SDS loading buffer were heated to 95°C for 5 min, centrifuged briefly at 12,470g to bring down any condensation from the tube lid, and loaded into the well alongside 5µl of LI-COR molecular weight marker (LI-COR Biosciences, supplied by

VWR). The gel was electrophorised at a constant voltage of 100 V until the bromophenol blue dye had reached the bottom of the gel.

2.2.3.4 Electrophoretic transfer of proteins

After completion of SDS-PAGE electrophoresis the stacking gel was removed and resolving gel placed in transfer buffer (25mM Tris, 192mM glycine, 20% (v/v) methanol, 0.01% SDS) for 5 min. The Bio-Rad transfer kit was assembled using Hybond C-extra supported nitrocellulose membrane (Amersham Biosciences, Little Chalfont, UK) against the gel, 3mm filter paper (Whatmann, supplied by GE Healthcare, Chalfont St Giles, UK) and two filter pads (Bio-Rad). Proteins were immunoblotted from the gel onto the nitrocellulose membrane at 100 V, with constant stirring using a magnetic flea, for 90 min at RT.

2.2.3.5 Immunodetection of proteins

The membrane was incubated in LI-COR blocking buffer (LI-COR Biosciences) with rapid agitation on an orbital shaker at RT for 1 hour (h): the content of the LI-COR locking buffer is company proprietary. The membrane was incubated in primary antibody diluted in an incubation solution (50% (v/v) LI-COR blocking buffer and 50% (v/v) PBS with 0.1% (v/v) Tween-20 (v/v; Sigma-Aldrich) (PBST)) overnight at 4°C with shaking on an orbital shaker. The specificity and concentration of primary antibodies (Table 2.3) to minimise background nonspecific binding were optimised using positive control cell extracts. Membranes were washed 3 x 5 min with PBS containing 0.1% Tween-20 (v/v, PBST) and subsequently incubated in the dark for 1 h in the appropriate secondary antibody at a concentration of 1:5000, prepared in incubation solution as above. Membranes were washed 3 x 5 min in PBST and 1 x 5 min in PBS to remove Tween-20 residue. Membranes were visualised using the LI-COR Odyssey infrared imaging system (LI-COR Biosciences). Where quantification was required the intensity of the band of interest was assessed by densitometry using the LI-COR Odyssey software and protein expression was expressed as a ratio of the densitometry value of the target protein band relative to the value of the corresponding loading control protein, β-actin (Table 2.3). To check the efficiency of immunoblotting, membranes were stained using Ponceau S (Sigma-Aldrich) solution for 5 minutes, and rinsed using ddH_2O to reveal the transferred proteins. Alternatively the Pierce Reversible Protein Stain Kit (Fisher Scientific) was used; membranes were washed in dH_2O, stained for 30s then washed 3 times in destain followed by a 5 min wash in destain. Finally membranes were washed once in dH_2O.

Antibody	Species	Optimised concentration	Positive control extract	Supplier (Product code)
Wnt1	Mouse monoclonal	0.5 µg/ml	NIH/3T3	Abcam Plc (Cambridge, UK; ab91191)
Wnt5A	Rat monoclonal	2 µg/ml	HeLa	R&D Systems (Abingdon, UK; MAB645)
Wnt3A	Mouse monoclonal	1 µg/ml	L-Wnt3A	R&D Systems (MAB1324)
Total β-catenin	Rabbit monoclonal	0.2 µg/ml	HeLa or A431	Abcam Plc (ab32572)
Active β-catenin	Mouse monoclonal	1 µg/ml	A431	Millipore (supplied by Fisher Scientific; 05-665)
α- tubulin	Mouse monoclonal	0.4 µg/ml	N/A	Santa Cruz (supplied by Insight Biotechnology, Wembley, UK; sc-5286)
β- actin (reduced samples)	Rabbit polyclonal	0.06 µg/ml	N/A	Abcam Plc (ab8227)
β- actin (non-reduced samples)	Mouse monoclonal	0.5 µg/ml	N/A	Abcam Plc (ab8226)
TATA-binding protein (TBP)	Mouse monoclonal	1.9 µg/ml	N/A	Abcam Plc (ab818)
Secondary antibodies; anti-mouse (A21065), anti-rabbit (A21076)	N/A	0.4 µg/ml	N/A	Alexa fluor 680; Molecular probes, Invitrogen™

Table 2.3 Antibodies and optimised antibody concentrations for western blots Concentrations of antibodies for western blot was determined empirically. All incubations with primary antibody were overnight at 4°C, secondary antibody incubations were for 1 h at RT unless otherwise stated. N/A = not applicable.

2.2.4 Subcellular fractionation

Subcellular fractions were prepared by differential centrifugation (Figure 2.1) modified from a method previously optimised for ESFT cells (Westwood et al. 2002). Cells were seeded onto Primaria™ 10 cm^2 dishes and harvested at 70% confluency by washing with 5ml ice cold 1X PBS and scraping into 1ml ice cold 1X PBS using a cell scraper. Cells were collected into 1.5ml eppendorf and pelleted by centrifugation at 160g for 5 min. Pellets were resuspended in 50µl iso-osmotic buffer (0.3M sucrose (Sigma-Aldrich), 10mM Tris.HCl (pH 7.5), 1mM EDTA) and a total protein sample was removed. The remaining solution was incubated for 5 min on ice before being passed through a 25 gauge needle for 30 strokes. Samples were then centrifuged at 4°C at 1000g for 10 min. The resulting supernatant was centrifuged at 4°C at 100,000g for 1 h, and this supernatant retained as the cytoplasmic fraction. The pellet from the first (1000g) centrifugation step was resuspended and centrifuged again at 4°C at 1000g for 10 min; this was repeated three times and the final pellet was retained as the nuclear fraction (Figure 2.1). All samples were resuspended in iso-osmotic buffer, a 5µl aliquot taken for protein estimation and the remaining sample combined with in an equal volume of 2X SDS loading buffer and stored at -20°C in single use aliquots The purity of fractions was confirmed by western blotting for α-tubulin (cytoplasmic) and TATA-binding protein (TBP, nuclear).

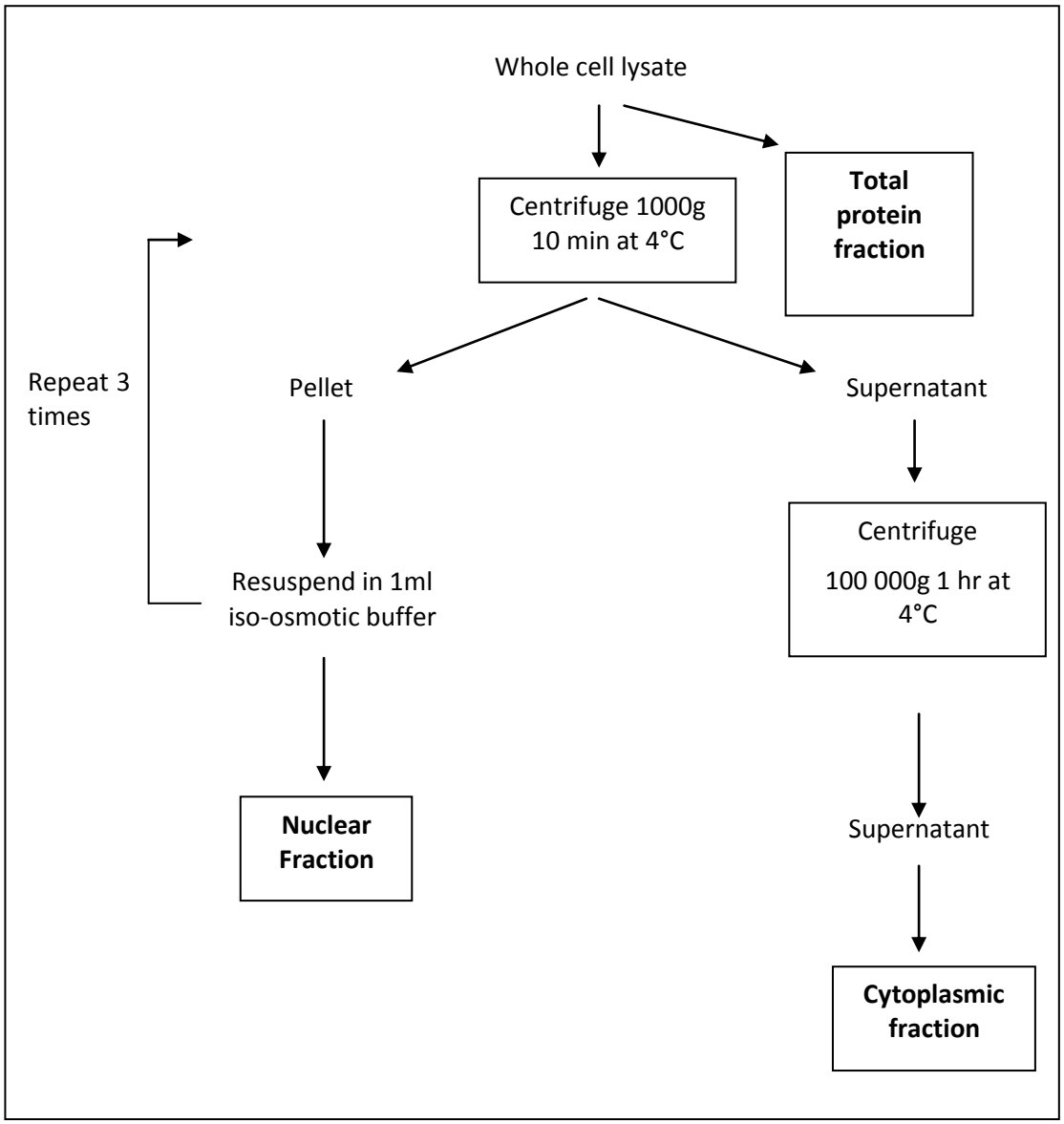

Figure 2.1 Cellular fractionation by differential centrifugation Cells were harvested, total protein extracted and fractions separated by differential centrifugation. Method previously optimized for ESFT cells (Westwood et al. 2002).

2.2.5 Flow cytometry

The same antibodies previously used to detect Wnt1 and Wnt5A by western blot were also used for flow cytometry (Table 2.3). ESFT cells were seeded into Primaria™ 6-well plates at a concentration of 2 x 10^5 cells/well (1 x 10^5 cells/well for A673 cells). After 48 h cells were harvested as previously described (Section 2.2.1). Cells were fixed prior to staining by resuspending the pellet in 500µl 4% (w/v) paraformaldehyde (PFA; Sigma-Aldrich) in 1X PBS and incubating for 10 min at RT. All centrifugation steps were performed at 405g for 5 min at RT. The cell suspension was centrifuged and resuspended in 200µl PBS, centrifuged, and the supernatant aspirated. In all cases cells were permeabilised by adding 500µl 0.1% (v/v) Triton X-100 (Amersham, GE Healthcare; in 5% FCS/PBS) and incubated on ice for 30 min, followed by a wash in PBS as above. Cell pellets were subsequently resuspended in 50µl primary antibody at the optimised concentration diluted in FACS buffer (10% (w/v) FCS in 1 xPBS) and incubated for 30 min at 4°C. Cells were centrifuged and the supernatant aspirated. Cells were washed by resuspending in 200µl FACS buffer, centrifuged and the supernatant aspirated. The cell pellet was then resuspended in 50µl fluorescent secondary antibody (goat anti-mouse, rabbit anti-rat both 1.25µl/ml; Southern Biotech supplied by Cambridge Bioscience, Cambridge, UK) diluted in FACS buffer for 30 min at 4°C, in the dark to protect the fluorescent tag from degradation by light. The cells were washed as described above and the resulting pellet resuspended in 500µl FACS buffer and analysed on the FACSCalibur™ (BD Biosciences) using an excitation laser of 480nm. A total of 10,000 events for each sample were analysed and all experiments performed in triplicate. A no primary antibody control was used to assess non-specific binding of the secondary antibody. Data was analysed using BD Cell Quest™ (BD Biosciences). The fold change was calculated as the fluorescence of the target stained cells divided by the fluorescence of cells stained with secondary antibody only.

2.2.6 RTqPCR

2.2.6.1 Extraction of RNA from cell lines

Cells were harvested from a 75cm^2 flask when 70% confluent (unless otherwise stated), as previously described (Section 2.2.1), and the cell pellet stored at -80°C in single use aliquots. RNA was extracted using the RNeasy® mini kit (Qiagen, Crawley, UK). All buffers are company proprietary. Briefly, cells were resuspended in buffer RLT (600µl) and vortexed to ensure complete mixing. The lysate was passed through a QIAshredder spin column, centrifuged at 13,000 g for 2 min. The supernatant was added to an equal volume

of 70% ethanol and mixed well by pipetting. The sample was then added to an RNeasy spin column and centrifuged for 15 s at 8,000 g. The flow through was discarded and the column washed by adding buffer RW1 (350 µl) and centrifuged at 8 000 g for 15 s. To eliminate any contaminating genomic DNA, buffer RDD containing DNase I was added to the column membrane (80µl) and incubated for 15 min at RT. The column was washed by adding buffer RW1 (350µl) and centrifuged at 8,000g for 15 s. Buffer RPE (500µl) was added to the column and the column centrifuged at 8,000g for 15 s, the flow through was discarded and the same volume of buffer RPE added to the column and centrifuged at 8,000g for 2 min. Finally the column was centrifuged at 13,000g for 1 min to remove residual flow through and RNase-free H_20 (40µl; Sigma-Aldrich) added directly to the membrane and centrifuged for 1 min at 8,000g to elute the RNA.

2.2.6.2 Spectrophotometric measurement of nucleic acid quantity and quality

Absorbance of nucleic acids was measured at 260nm and 280nm using the Nanodrop (Labtech, Ringmer, UK). An absorbance ratio of 1.8-2.0 at 260/280 nm indicated the sample was free from any contaminants such as proteins or chemicals used in the extraction procedure. The quantity of RNA was determined assuming that a 40µg/ml RNA solution has an absorbance of 1 at 260 nm.

2.2.6.3 Preparation of cDNA

To generate complementary DNA (cDNA) the required concentration of RNA made up in 10µl of RNase-free H_2O was added to the reverse transcriptase (RT) reaction (5µl for RT-reactions). An RT negative (RT-) sample was prepared alongside each sample to ensure that any amplification detected is from the synthesised cDNA and not contaminating genomic DNA. The RNA was denatured by heating to 95°C for 5 min, cooled on ice for 5 min and added to RT+ (30µl) and RT- (15µl) mixes (Table 2.4) Samples were incubated using the Techne TC-500 Thermal Cycler (Bibby Scientific Ltd, Staffordshire, UK) at 25°C for 5 min, 50°C for 60 min and 70°C for 15 min, cooled on ice for 2 min and stored at -20°C.

	RT+		RT-	
Reagent	Volume (µl, per sample)	Final concentration	Volume (µl, per sample	Final concentration
RNase-free H_20	7.8		4.9	
1 x First-Strand Buffer (Invitrogen™)	8	1X	4	1X
dNTPs (Amersham Biosciences)	4	1mM	2	1mM
$MgCl_2$	3.2	8mM	1.6	8mM
Random Hexamer Primers (Invitrogen™)	2	0.3µg	1	0.3µg
RNasin® Plus RNase Inhibitor (Promega, Southampton, UK),	1	16 units	0.5	16 units
DTT (Invitrogen™)	2	0.1M	1	0.1M
Superscript™ III Reverse Transcripase (Invitrogen™)	2	200 units	N/A	N/A
Total mix volume per sample (µl)	30		15	

Table 2.4 Reagents in RT+ and RT- reactions dNTP = deoxyribonucleotide triphosphate, $MgCl_2$ = magnesium chloride, DTT = dithiothreitol

2.2.6.4 Taqman gene expression array

Gene expression of components of the Wnt signalling pathway were analysed using the TaqMan® Array Human WNT Pathway 96-well plate (Applied Biosystems; Life Technologies). cDNA was prepared as described previously (Section 2.2.5.3). Only an RT+ reaction was performed using a total concentration of 100ng RNA for each cell line. A PCR mix was made containing the RT mix (40µl), 1X Taqman® Universal PCR Master Mix (1080µl, Invitrogen™) made up in RNase free H_2O (1040µl). The plate was centrifuged at 154g for 1 min before removing the lid and adding 20µl of PCR/cDNA mix to each well; each well contained cDNA generated from 10ng of RNA. MicroAmp® Optical Adhesive Film (Applied Biosystems) was used to cover the plate which was centrifuged at 154g for 1 min. Real time PCR was conducted using the 7500 Real-Time PCR System (Applied Biosystems); PCR/cDNA mix was incubated for 10 min at 95°C to activate the DNA polymerase followed by 40 cycles of denaturation at 95°C for 15 s and annealing/extension at 60°C for 1 min. Results were analysed using the 7500 system software (Applied Biosystems) and cycle threshold (C_t) values calculated. Changes in expression of Wnt signalling pathway genes were determined using the comparative C_t method (Livak and Schmittgen 2001). The expression of each gene on the array was normalised to the expression of the housekeeping gene HRPT1 using the formula

$2^{-\Delta Ct}$

Where $\Delta C_t = C_t$ [gene] - C_t [HRPT1].

Two-way hierarchical clustering of cell lines using complete linkage was carried out according to expression, using Gene Cluster 3.1 and visualised as a heat map using Java TreeView.

2.2.6.5 Assays-on-Demand™

cDNA was prepared as described previously (Section 2.2.5.3). The RT+ (cDNA) and RT- control sample were added to PCR mixes for amplification of the target gene and the housekeeping gene PPIA (Table 2.5). Samples (25µl/well) were transferred in triplicate to MicroAmp® Optical 96-well plates (Applied Biosystems) and sealed with MicroAmp® Optical Adhesive Film. Real time PCR was conducted using the 7500 Real-Time PCR System and Ct values generated as described previously (Section 2.2.5.4). The target gene expression was normalised to the expression of PPIA, and made relative to a reference sample using the formula;

$2^{-\Delta\Delta Ct}$

Where ΔCt = Ct [target gene] – Ct [PPIA]

and ΔΔCt = ΔCt [test sample] – ΔCt [reference sample]

Target Mix	Volume (µl, per sample)	Final concentration
TaqMan Universal PCR Master Mix	50	1X
20X Assay-on-Demand™ primer/probe mix (Applied Biosystems)	5	1X
RNase free H_2O	25	-

PPIA Mix	Volume (µl, per sample)	Final concentration
TaqMan Universal PCR Master Mix	50	1X
10µM PPIA Forward Primer 5'-GGACCCAACACAAATGGTTCC-3'	2	200nM
10µM PPIA Reverse Primer 5'-CTTTCACTTTGCCAAACACCA-3'	2	200nM
20µM PPIA probe 5'ATGCTTGCCATCCAACCACTCAGTCTTG-3'	0.5	100nM
RNase free H_2O	22.5	-

Table 2.5 PCR mix reagents for RTqPCR using Assay-on-Demand™ (Applied Biosystems) and PPIA housekeeping gene

2.2.7 Statistics

For the array analysis the inter-assay variance of housekeeping genes was analysed by one-way analysis of variance (ANOVA) using statistical software R (Version 3.0.2 for OS 6) by Dr Helene Thygesen (University of Leeds). The average variance (across non-household genes) was calculated between the cells lines (explained variance) and between technical repeats (unexplained variance). The optimal household gene would be one where the most variance is between the cell lines, giving the highest F-value, and the least variance between the technical repeats. All other analyses were undertaken by me using GraphPad prism 6 software. Wnt ligand (Wnt1/Wnt5A) protein expression detected by flow cytometry was analysed by one-way ANOVA when comparing all 6 cell lines. Variation between means of cell lines were compared using Bonferroni's post hoc multiple comparison test and differences were considered significant when $p<0.05$.

2.3 Results

2.3.1 mRNA expression of Wnt signalling components in ESFT cell lines

2.3.1.1 Profile by TaqMan® Wnt Pathway Array

The mRNA expression of components of the Wnt signalling pathway were investigated using TaqMan® Wnt Pathway Arrays (Applied Biosystems). The gene expression array contains 4 housekeeping genes; *18S, GAPDH, HRPT1* and *GUSB*. It was first necessary to determine which was the optimal housekeeping gene against which to normalise the expression of Wnt signalling components in ESFT cell lines. An ideal housekeeping gene is one that is ubiquitously expressed, whose expression is regulated in the same way as the target gene but whose expression is generally considered as constant, regardless of experimental conditions. *18S* is a ribosomal RNA subunit and is highly abundant. Although it can be a reliable reference for total RNA mass, its synthesis is independent from the synthesis of mRNA therefore it was excluded (Radonić et al. 2004). It has been reported that *GAPDH* has many putative pseudo-genes (Sun et al. 2012) therefore this housekeeping gene was also disregarded. The variance of normalisation using *HRPT1* and *GUSB* over each technical replicate was investigated, to examine the stability of expression across the replicates. Studies have shown that normalising to the mean of multiple housekeeping genes may be more accurate therefore the inter-assay variance was also calculated for the mean of *HRPT1* and *GUSB* (Table 2.6).

Housekeeping gene	Inter-assay variance (F-value)*
HRPT1	1.23
GUSB	1.16
Mean of *HRPT1* and *GUSB*	0.99

Table 2.6 Inter-assay variance of different housekeeping genes on the Wnt signalling array. * Inter-assay variance calculated using ANOVA as the ratio of the variance observed between the cell lines (explained variance) to the variance between the replicates (unexplained variance). The optimal housekeeping gene to use would be one where the variance between cell lines is greatest and between replicates minimal, therefore giving the highest F-value.

The inter-assay variance was lowest for *HRPT1* (as this gave the highest F-value). Therefore this housekeeping gene was used to normalise expression of the Wnt signalling components in all subsequent experiments.

Wnt signalling components were defined as being expressed if they had a Ct value of less than 40. Components of both the canonical and noncanonical Wnt signalling pathways were detected in ESFT cell lines, including those which have been reported to both promote and inhibit Wnt signalling (Figure 2.2 A). mRNA expression of all 19 Wnt ligands was detected in at least one ESFT cell line. However, Wnt3A mRNA was only detected in RD-ES cells. All six ESFT cell lines expressed mRNA for all 9 Frizzled receptors (Figure 2.2 B). There was low expression of the Wnt ligands in all ESFT cell lines except for Wnt5A which had high, heterogeneous expression in all ESFT cell lines; RD-ES having the highest expression and A673 the lowest.

Critical components of the canonical Wnt signalling pathway such as the key mediator β-catenin (*CTNNB1*), GSK3β**,** a component of the destruction complex and the co-receptors LRP5/6 were highly expressed in all six ESFT cell lines. Many of the FZD receptors were also highly expressed including FZD4 and FZD8. High levels of c-myc mRNA were also detected in ESFT cell lines consistent with previous studies reporting an increase in c-myc protein in ESFT cells (McKeon et al. 1988).

Generation of a heat map using hierarchical clustering showed that the ESFT cell lines share expression of over 70% of Wnt signalling mRNAs (Figure 2.3). Overall, when considering all 91 components of the pathways which are represented on the array, there was high (red) expression of 22%, moderate (black) expression of 27% and low (green) expression of 42% of components in all the cell lines. Genes with marked differential expression between the six cell lines included the inhibitors sFRP2 and FRZB and DKK2. Other components with differential expression included Porcn, which is involved in the production of Wnt ligands and LEF1, involved in transcription following activation of the canonical pathway.

Figure 2.2 RNA expression of components of the Wnt signalling pathway in ESFT cell lines. Cells were harvested, total RNA extracted and expression level determined using the Taqman® Wnt signalling gene expression array. Data is presented as mRNA expression relative to the housekeeping gene HRPT1. (A) Expression of genes previously reported to be involved in the canonical, noncanonical pathways or both, separated into those that promote or inhibit the pathways. (B) Log expression of the above data focussing on the expression of Wnt ligands and Frizzled receptors. Results show the mean of two independent experiments, n=2 (±SEM)

(A) Components of the canonical and noncanonical Wnt signalling pathway

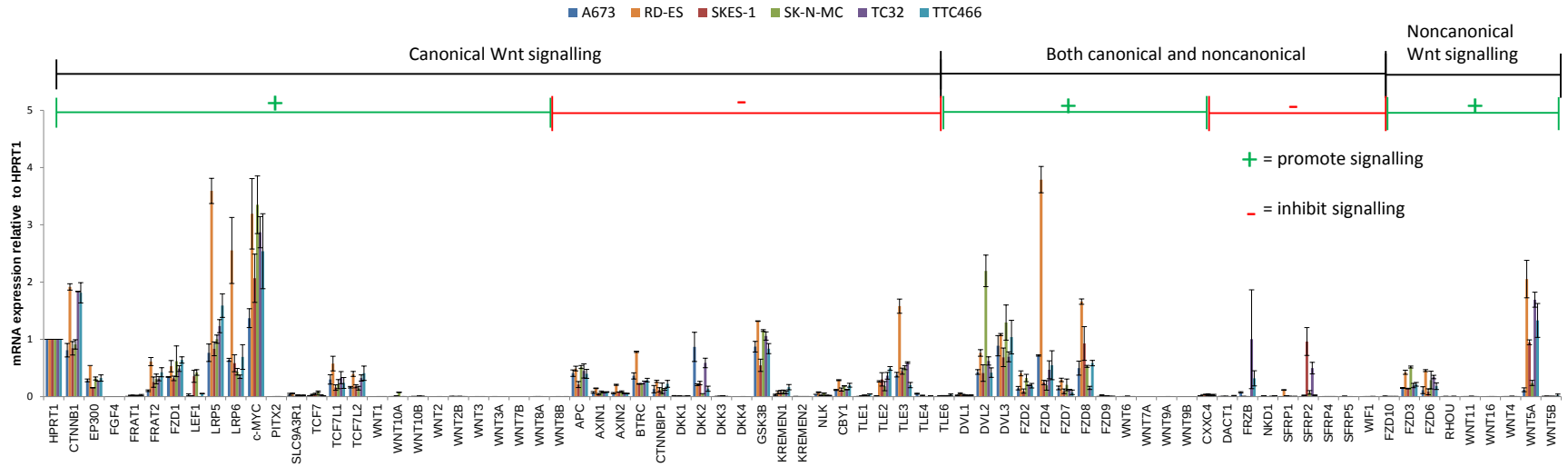

(B) Expression of Wnt ligands and frizzled receptors (presented on the Log scale)

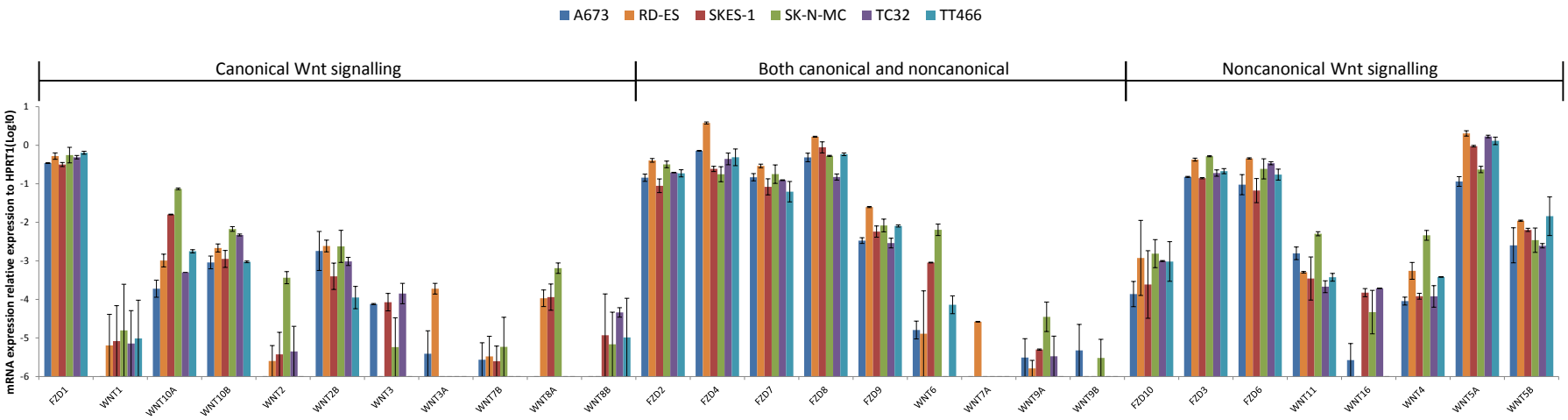

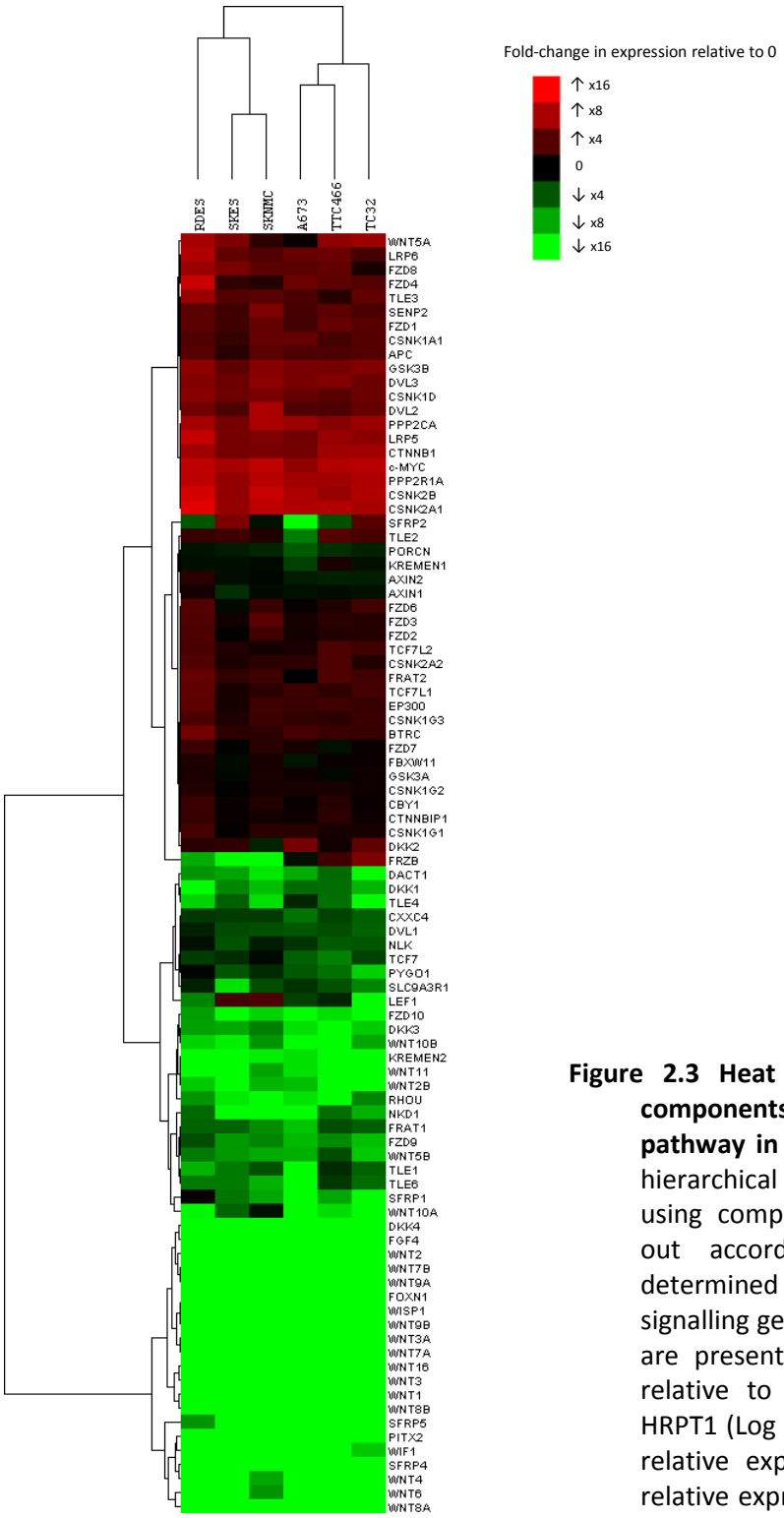

Figure 2.3 Heat map of expression of components of the Wnt signalling pathway in ESFT cell lines. Two-way hierarchical clustering of cell lines using complete linkage was carried out according to expression as determined by the Taqman® Wnt signalling gene expression array. Data are presented as mRNA expression relative to the housekeeping gene HRPT1 (Log scale). Colour shows high relative expression in red and low relative expression in green, with a 4 fold change in expression represented by each of the 7 colours in between red (high) and green (low). Heat map is derived from the mean of two independent datasets.

2.3.2 Expression of Wnt ligands in ESFT cell lines

To confirm the correlation between mRNA detected using the Wnt signalling array and protein, the expression of three Wnt ligand proteins was investigated in ESFT cell lines.

2.3.2.1 Expression of Wnt1 protein

2.3.2.1.1 Expression of Wnt1 protein by western blot

Wnt1 was the first Wnt ligand to be identified and is a classic marker of the canonical Wnt signalling pathway, although its expression has not previously been described in ESFT (Üren et al. 2004). A band of 42 kDa corresponding to the predicted size of Wnt1 protein was detected in all ESFT cell lines (Figure 2.4 A). Expression of β-actin was used to check protein expression on the blot; expression was quantified by densitometry. There was comparable expression levels of Wnt1 in all ESFT cell lines, and in the positive control cell line NIH/3T3 (Figure 2.4 B).

(A)

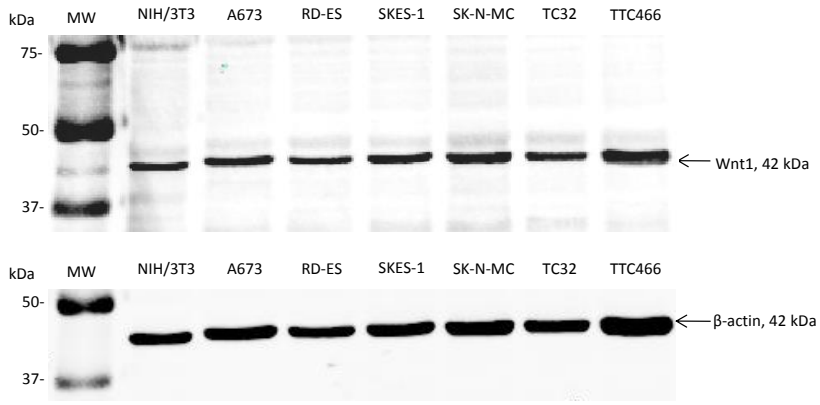

(B)

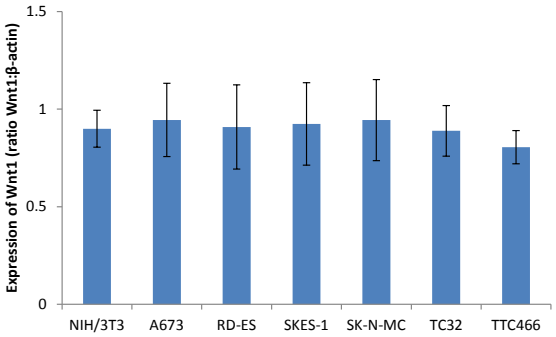

Figure 2.4 Wnt1 protein expression in ESFT cells determined by western blot. (A) Total protein was extracted and expression of Wnt1 in 50ng of extract determined by western blot. β-actin was used to check for equal amounts of protein (control). Image shows a representative example (B) Protein expression was quantified by densitometry and expression calculated as the ratio of intensity of the Wnt1 to β-actin band. Results shown are the mean of three independent experiments (± SEM). NIH/3T3= positive control cell line, MW= molecular weight marker in kDa.

2.3.2.1.2 Expression of Wnt1 protein by flow cytometry

To confirm the expression of Wnt1 observed by western blot and investigate the heterogeneity of Wnt1 expression within cell lines, Wnt1 expression was also examined in ESFT cell lines by flow cytometry.

There was heterogeneous expression of Wnt1 protein between ESFT cell lines when analysed by flow cytometry (Figure 2.5 A and B). Highest expression of Wnt1 was detected in A673 (median fluorescence; 27±5.5) and SK-N-MC (median fluorescence; 25±1) cell lines. The lowest levels of Wnt1 expression were detected in TC32 cells (median fluorescence; 16±1.3). Statistical analysis using a one-way ANOVA confirmed cell lines had significantly different levels of Wnt1 expression ($p=0.046$).

In all ESFT cell lines, when 10,000 events per sample were analysed, over 85% of permeabilised cells expressed Wnt1. This ranged from 85±0.8% in the TC32 cell line to 95±0.6% in the SK-N-MC cell line. In all ESFT cell lines single expression peaks were observed, indicating homogeneous expression of Wnt1 within each cell line (Figure 2.5, top panel).

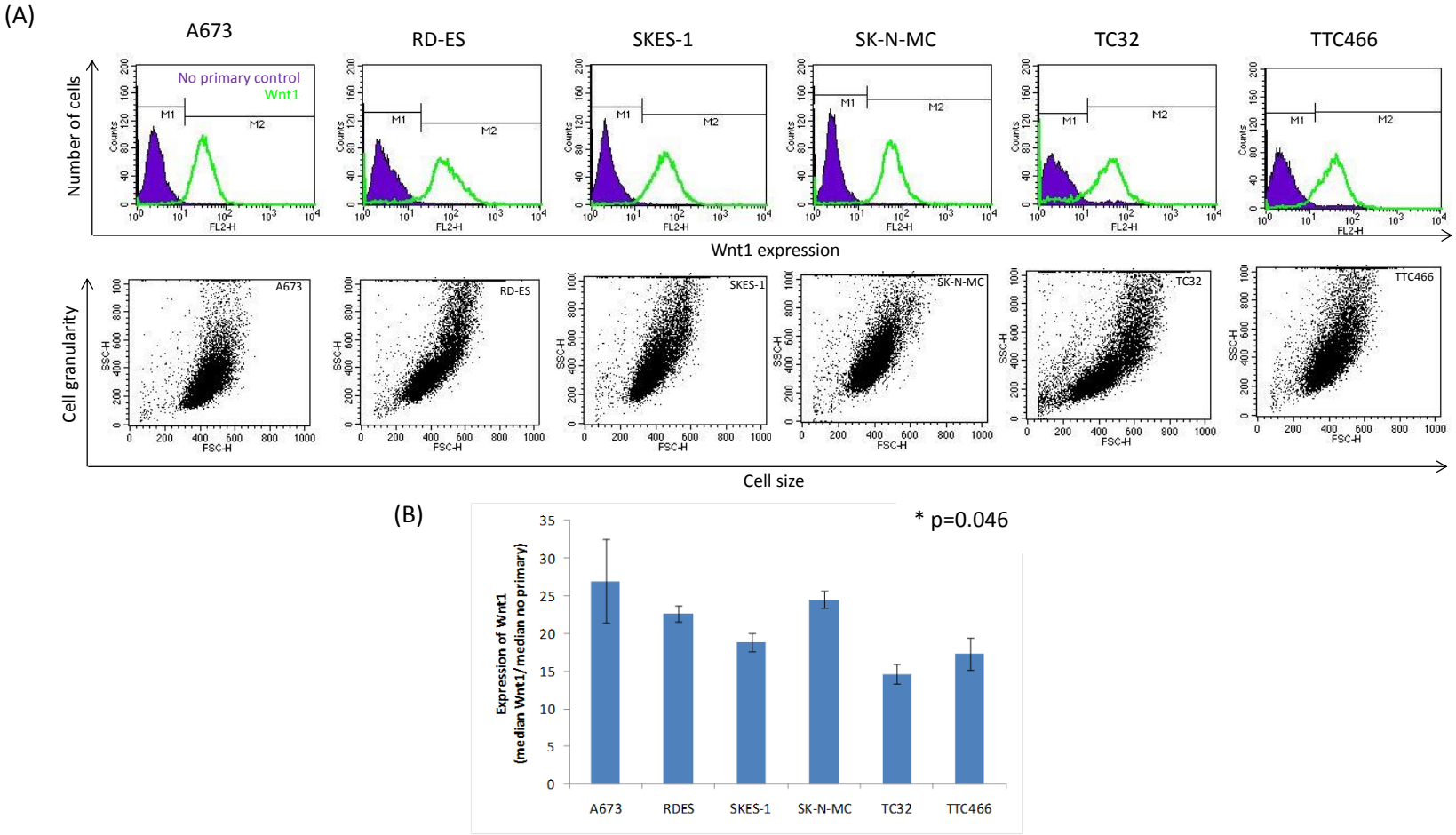

Figure 2.5 Wnt1 protein expression in ESFT cells determined by flow cytometry ESFT cells were harvested, permeabilised and labelled for analysis of Wnt1 expression by flow cytometry. (A) Representative cell scatter and fluorescence plots show cells in the presence (green) or absence (purple) of Wnt1 primary antibody. The M1 region designates negative events and the M2 region positive events. (B) The median fluorescence of each peak was calculated and used to generate a mean fold level of Wnt1 expression relative to the no primary antibody control. Results are presented as the mean of three independent experiments, with three replicates per experiment (n=9) analysing 10,000 events per sample (± SEM).

2.3.2.1.3 Confirmation of Wnt1 mRNA detection by RTqPCR

Wnt1 protein was detected in all ESFT cell lines by western blot and FACS, however Wnt1 mRNA was only consistently detected in A673 cells by RTqPCR using the Wnt signalling pathway array. To confirm the results of the array I performed RTqPCR on RNA (100ng) extracted from all ESFT cell lines using a Wnt1 Assay-on-Demand™ (Applied Biosystems). These studies confirmed that Wnt1 mRNA was expressed by all ESFT cell lines (Figure 2.6A). When RTqPCR was performed using cDNA generated from 100ng RNA, Wnt1 mRNA could be detected in all ESFT cell lines (Figure2.6 A). Results are expressed as relative gene expression using the ΔΔCt method (as described in Section 2.2.5.5). Although Wnt1 mRNA expression appears heterogeneous, with highest expression in SK-N-MC and lowest in SKES-1 cells, the Ct values are all within 2 Ct values (range= 36.4-37.8) indicating Wnt1 mRNA expression is similar between all six ESFT cell lines. This is in agreement with the pattern of Wnt1 protein expression observed by western blot analysis.

The differences in mRNA expression observed between the Wnt signalling pathway arrays and Assay-on-Demand™ could be due to the fact that the arrays were performed using cDNA generated from 10ng RNA. When performing RTqPCR using the Assay-on-Demand™, Wnt1 mRNA could be detected in both SKES-1 cells and the positive control cell line, MCF7. However, when cDNA generated from 100ng RNA was used, the Ct values decreased from 38 to 37.6 and from 37.6 to 38.8 in SKES-1 and MCF7 cells, respectively (a lower Ct Value indicates increased expression) (Figure 2.6 B). This indicates the differences observed were due to the sensitivity of the Wnt signalling array at the concentration of RNA used in those experiments.

A) Wnt1 mRNA expression in ESFT cell lines relative to MCF7 cells

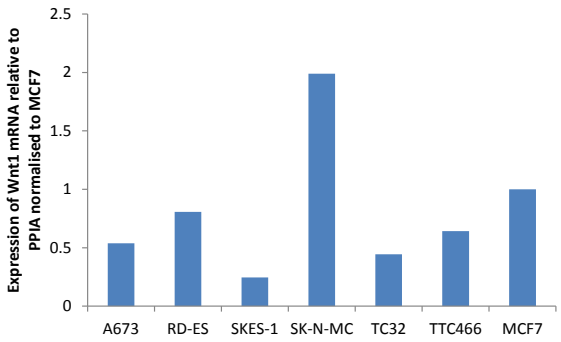

B) Ct values generated in MCF7 and SKES-1 cells using cDNA generated from 10 or 100ng of RNA

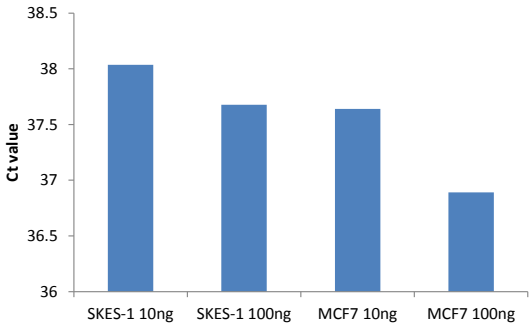

Figure 2.6 Wnt1 mRNA expression determined by RTqPCR RNA was extracted, RT performed and expression of Wnt1 determined by RTqPCR using a Wnt1 Assay-on-Demand™ (Applied Biosystems) A) Wnt1 mRNA expression in ESFT cell lines using cDNA generated from 100ng RNA. B) Ct values determined from SKES-1 and MCF7 (positive control) cells when cDNA generated from 10ng and 100ng of RNA was added to the RTqPCR reaction. Data presented as Wnt1 expression relative to the expression of the housekeeping gene PPIA, normalised to the positive control cell line MCF7. Results show the mean of triplicate wells in one experiment.

2.3.2.2 Expression of Wnt3A protein

2.3.2.2.1 Expression of Wnt3A protein by western blot

Wnt3A is the most commonly studied canonical Wnt ligand and overexpression has been shown to increase chemotactic migration in ESFT cells (Üren et al. 2004). Using an anti-Wnt3A monoclonal antibody (MAB1324, R&D) a single band of 39 kDa was detected in mouse L-cells which overexpress human Wnt3A (L-Wnt3A; control) (Figure 2.7). However, no expression of Wnt3A was detected in any of the ESFT cell lines studied. Attempts to confirm the lack of Wnt3A protein expression in ESFT cells lines using an alternative antibody (ab81614, Abcam) were unsuccessful due to a large number of nonspecific bands (data not shown). Various optimisation steps were made in an attempt to improve the specificity of the antibody including testing a range of antibody dilutions (1:500-1:2000), extra washes with 0.1% PBST and executing SDS-PAGE electrophoresis at 4°C rather than room temperature, however these failed to eliminate the nonspecific bands.

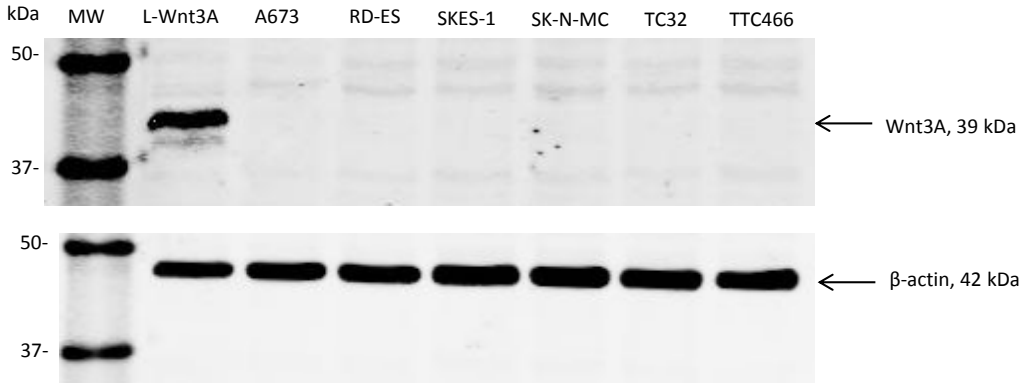

Figure 2.7 Wnt3A protein was not detected in ESFT cells Total protein was extracted and expression of Wnt3A in 50ng of extract determined by western blot. β-actin was used to check equal loading of protein in each well (loading control). L-Wnt3A = mouse L cells overexpressing human Wnt3A (positive control cell line). MW= molecular weight marker in kDa.

2.3.2.2.1 Confirmation of Wnt3A mRNA detection by RTqPCR

Wnt3A mRNA was only detected in RD-ES cells, at low levels (Ct value=37) using the Wnt signalling pathway array. This is consistent with the lack of protein expression. However, I demonstrated that Wnt1 mRNA could be detected if cDNA generated from 100ng RNA was analysed using RTqPCR. When RTqPCR was performed specifically for Wnt3A mRNA using cDNA generated from 100ng RNA, expression was not detected in any ESFT cell line (Figure 2.8 A). Although Ct values lower than 40 were detected in some cells lines, this was not consistent across the three wells in any cell line (Figure 2.8 B). The variance observed suggests that Wnt3A mRNA is not expressed in the ESFT cell lines studied.

(A)

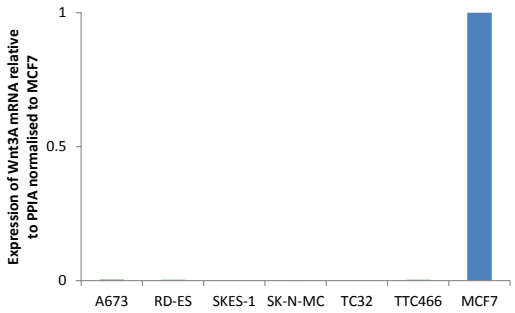

(B)

Wnt3A

Cell Line	Well 1 (Ct)	Well 2 (Ct)	Well 3 (Ct)	Ct Mean
A673	37.75	36.05	40	37.9
RD-ES	36.44	40	38.39	38.2
SKES-1	40	40	40	40
SK-N-MC	40	39.01	39.45	39.4
TC32	40	40	38.01	39.3
TTC466	40	35.56	37.79	37.7
MCF7	29.32	29.46	29.36	29.3

PPIA

Well 1 (Ct)	Well 2 (Ct)	Well 3 (Ct)	Ct Mean
20.76	21.02	20.83	20.87
20.93	21.07	21.00	21.00
18.86	18.84	18.89	18.86
21.38	21.46	21.22	21.35
20.39	20.36	20.20	20.31
20.71	20.57	20.59	20.62
20.44	20.21	20.06	20.24

Figure 2.8 Wnt3A mRNA is not expressed in ESFT cell lines as determined by RTqPCR RNA was extracted, RT performed and expression of Wnt3A determined by RTqPCR A) Wnt3A mRNA expression in ESFT cell lines using cDNA generated from 100ng of RNA. Data presented as Wnt3A expression relative to the expression of the housekeeping gene PPIA, normalised to the positive control cell line MCF7. Results show the mean of triplicate wells in one experiment. B) Ct values obtained from the RTqPCR for both Wnt3A and PPIA. A higher Ct value corresponds to low expression, a Ct value of 40 is considered no detection.

2.3.2.3 Expression of Wnt5A protein

2.3.2.3.1 Expression of Wnt5A protein by western blot

Wnt5A is the most commonly studied noncanonical Wnt ligand, and had the highest mRNA expression out of the Wnt ligands detected using the Wnt signalling pathway array (Section 2.3.1.1). Protein expression of Wnt5A was determined using a monoclonal antibody (MAB645, R&D) which only detects epitopes in an oxidised form, therefore the reducing agent DTT was omitted from the SDS loading buffers. Wnt5A protein was detected as a band at 42 kDa and expression was heterogeneous between ESFT cell lines (Figure 2.9 A). To check the amount of protein on the membrane expression of β-actin was examined using an anti- β-actin antibody which detects oxidised protein (ab8226, Abcam). Protein expression was quantified by densitometry and revealed RD-ES, SKES-1 and TC32 cells had higher expression of Wnt5A protein, than A673, SK-N-MC and TTC466 cell lines, when expression was normalised to that in the positive control cell line L-Wnt5A (Figure 2.9 B and C). These results are consistent with the Wnt signalling array data which showed mRNA expression of Wnt5A was highest in RD-ES and TC32 cell lines and lowest in A673 and SK-N-MC (Figure 2.2).

(A)

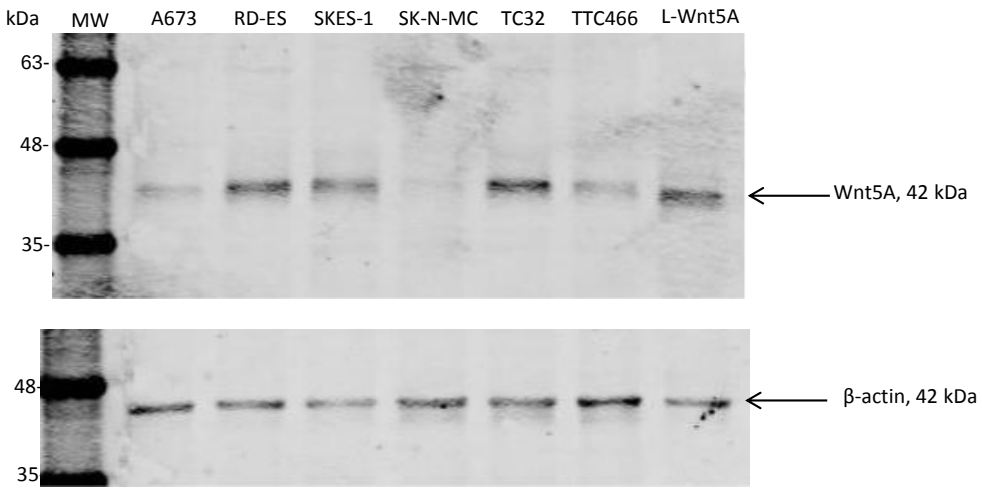

(B) Ratio of Wnt5A to β-actin

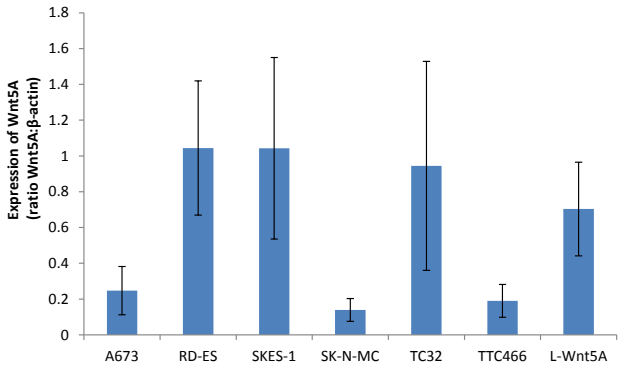

(C) Ratio of Wnt5A to β-actin, normalised to expression in L-Wnt5A

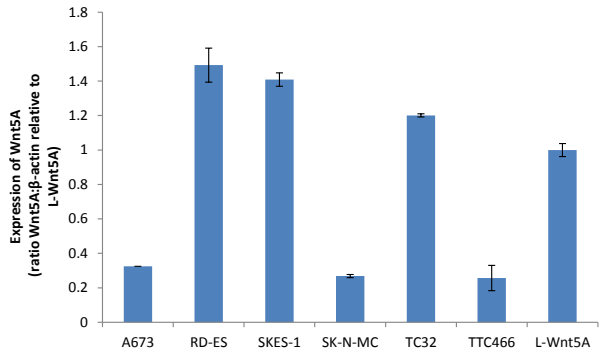

Figure 2.9 Wnt5A protein expression in ESFT cells determined by western blot. (A) Total protein extract was prepared without DTT and expression of Wnt5A in 25µg extract determined by western blot. Expression of β-actin was used as a loading control. Representative of three independent experiments (B) Band intensity was quantified by densitometry and expression levels calculated as the ratio of the intensity of the Wnt5A band to that of the β-actin band and (C) normalised to the positive control cell line L-Wnt5A; L-cells overexpressing Wnt5A. Results in (B) and (C) show the mean of three independent experiments (± SEM). MW= molecular weight marker in kDa.

2.3.2.3.2 Expression of Wnt5A protein by flow cytometry

Expression of Wnt5A protein was also investigated in ESFT cell lines by flow cytometry. There was less heterogeneity of Wnt5A expression between cell lines than that observed by western blot (Figure 2.10 A and B). Expression of Wnt5A was significantly higher in RD-ES (median fluorescence; 10±0.5 compared to the other cell lines (median fluorescence range; 3.6 to 6.2). This is consistent with both the array and western blot data which demonstrated RD-ES had the highest expression of Wnt5A mRNA and protein, respectively.

In ESFT cell lines, when 10,000 events per sample were analysed, there was a range in the percentage of cells expressing Wnt5A. In the TTC466 cell line only 45±2.9% of cells expressed Wnt5A whereas in the A673 cell line 67±3.6% of cells were positive for Wnt5A expression. In all ESFT cell lines single tight expression peaks were observed, indicating Wnt5A expression was similar between cells within each cell line (Figure 2.10, top panel).

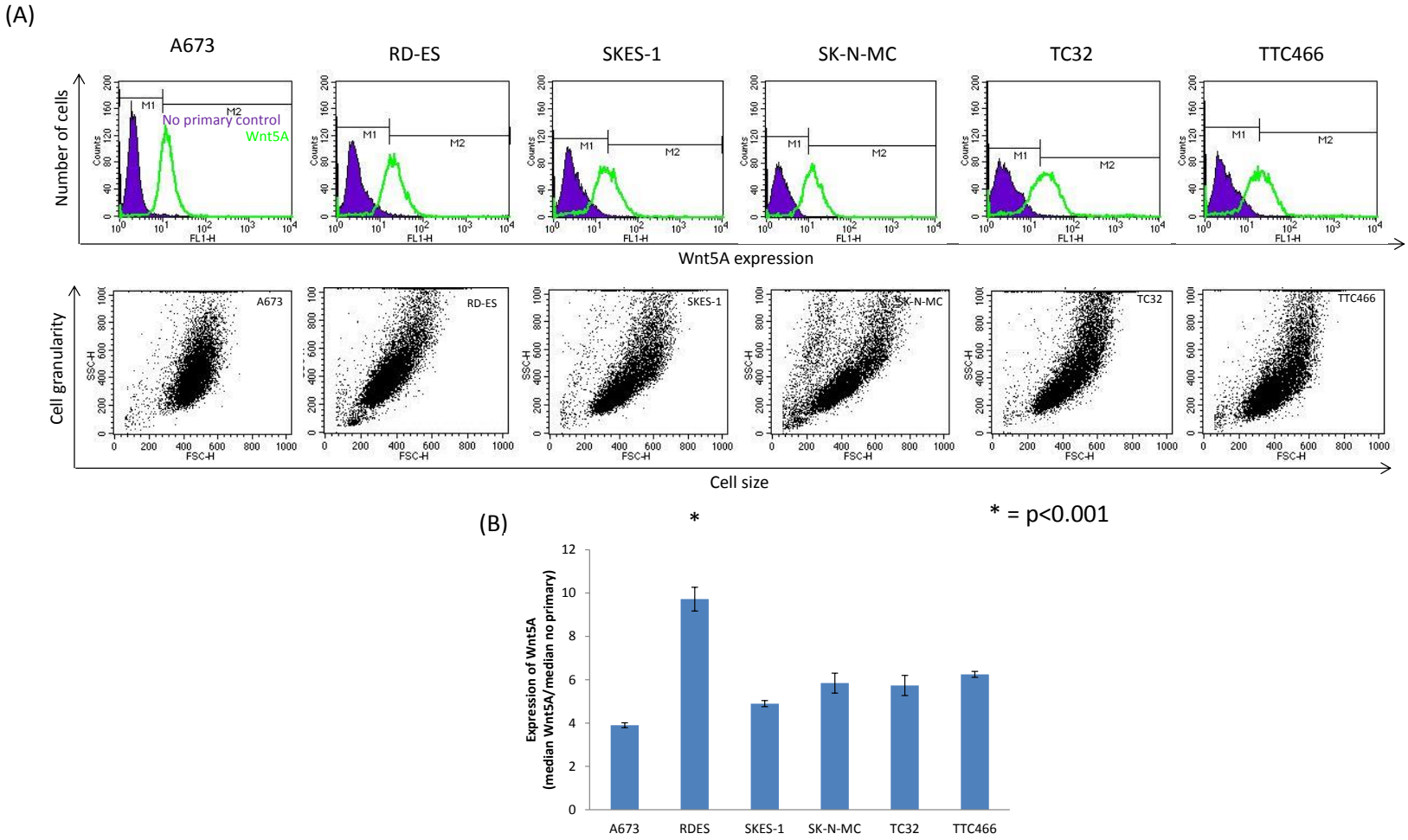

Figure 2.10 Protein expression of Wnt5A in ESFT determined by flow cytometry ESFT cells were harvested, permeabilised and labelled for analysis of Wnt5A expression by flow cytometry. (A) Representative cell scatter and fluorescence plots show cells in the presence (green) or absence (purple) of Wnt5A primary antibody. The M1 region designates negative events and the M2 region positive events. (B) The median fluorescence of each peak was calculated and used to generate a mean fold level of Wnt5A expression relative to the no primary antibody control. Results are presented as the mean of three independent experiments, with three replicates per experiment (n=9) analysing 10,000 events per sample (± SEM).

2.3.3 Subcellular localisation of β-catenin in ESFT cell lines

Possible activation of the canonical Wnt signalling pathway was investigated by measuring the expression of β-catenin in the cytoplasm and the nucleus in ESFT cell lines by western blot of enriched nuclear and cytoplasmic fractions (Section 2.2.4, Figure 2.11). Enrichment of fractions was confirmed by western blot for the specific nuclear and cytoplasmic proteins TBP and α-tubulin, respectively (Figure 2.11 A). As there is no single protein expressed in all fractions, equal protein on the blot was confirmed by staining membranes with Ponceau S (Figure 2.11 B). Expression of β-catenin protein was identified in the nuclear fractions of all ESFT cell lines by western blot (Figure 2.11 A). Nuclear β-catenin expression was heterogeneous with the highest expression in the TC32 cell line and lowest expression in SKES-1 and RD-ES cells. Expression of β-catenin protein was low in the cytoplasmic fractions of all cell lines, consistent with the conclusion that β-catenin is translocated from the cytoplasm to the nucleus; and the hypothesis that the canonical Wnt signalling pathway is active in ESFT cell lines.

(A)

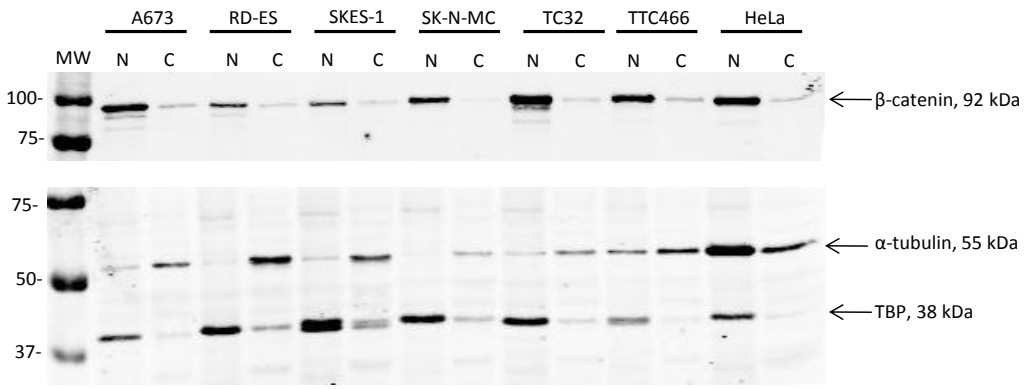

(B) Ponceau S staining of the membrane to confirm equal protein across samples

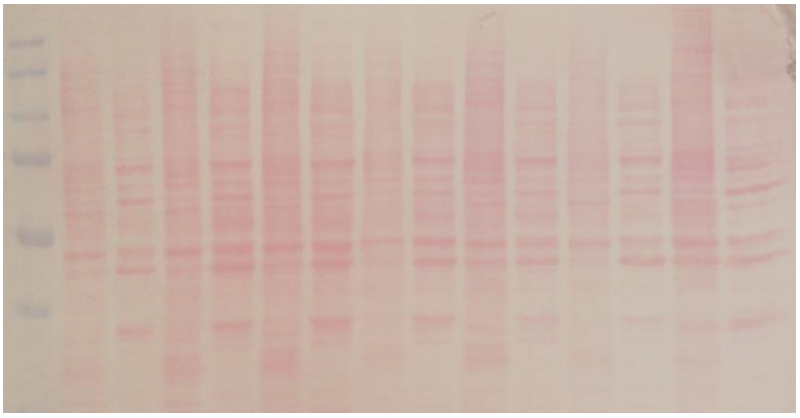

Figure 2.11 Subcellular localisation of β-catenin in ESFT cell lines. (A) Subcellular fractions were prepared by differential centrifugation and expression of β-catenin in 25µg of each fraction determined by western blot. Expression of TATA-binding protein (TBP) was used as a loading control for nuclear fractions and α-tubulin for cytoplasmic fractions. N= nuclear, C= cytoplasmic. (B) Ponceau S staining of membranes was used to check the amount of protein across each fraction. HeLa = positive control cell line. MW = molecular weight in kDa. Representative of two independent experiments.

2.3.4 Expression of active β-catenin in ESFT cell lines

To further investigate activation of the canonical Wnt signalling pathway in ESFT cells, expression of the active form of β-catenin was determined by western blot. This was achieved using an antibody that specifically detects β-catenin in its active form; nonphosphorylated on Ser37 or Thr41 (Millipore, 05-665; (van Noort et al. 2002)). Expression of β-actin was used to confirm equal protein levels, and protein expression was quantified by densitometry. Total β-catenin was detected in all ESFT cell lines with heterogeneous expression; the highest levels were detected in A673 cells and lowest in SKES-1 (Figures 2.12 A and B). Nonphosphorylated (i.e. active) β-catenin was also detected in all ESFT cell lines (Figure 2.12 A). The percentage β-catenin that was nonphosphorylated was variable between biological repeats, as evidenced by the large error bars observed on Figure 2.12 C. The percentage of nonphosphorylated β-catenin ranged from 22-40% depending on the cell line with the greatest percentage in TC32 cells and the lowest in SKES-1. This is consistent with the nuclear localisation assay in which expression of β-catenin was greatest in the nuclear fraction of TC32 cells, and lowest in SKES-1 cells.

(A)

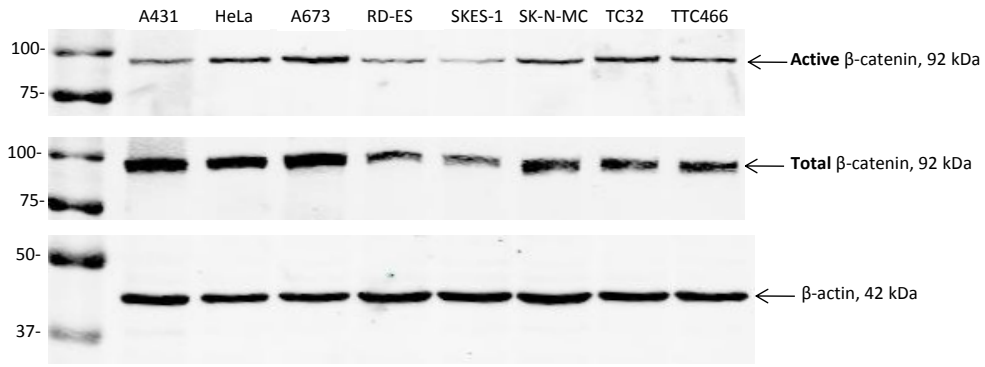

(B) Expression of total β-catenin

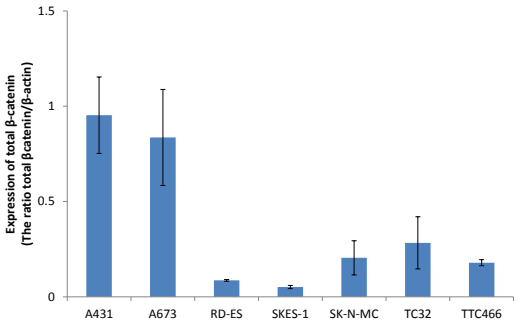

(C) Ratio of active β-catenin compared to total level

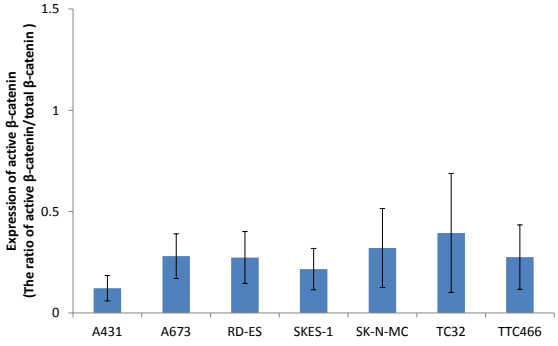

Figure 2.12 Expression of the active form of β-catenin in ESFT cell lines. (A) Total protein was extracted and expression of total and active β-catenin in 50µg extract determined by western blot. Expression of the active form of β-catenin was investigated using an antibody (05-665, Millipore) which specifically detects the nonphosphorylated form. Expression of β-actin was used as a loading control. Representative of three independent repeats. (B) Protein band intensity was quantified by densitometry and total β-catenin expression calculated as the ratio of β-catenin to β-actin. Expression of active β-catenin was calculated as the ratio of active β-catenin to total β-catenin. Results in (B) and (C) show the mean of three independent experiments (± SEM). A431 and HeLa = positive control cells. MW = molecular weight in kDa.

2.4 Discussion

In this chapter my data has revealed that components of the Wnt signalling pathway are expressed in ESFT cells lines. I have identified for the first time expression of the canonical Wnt ligand Wnt1, and confirmed expression of the noncanonical Wnt ligand Wnt5A, in all ESFT cell lines studied. In addition, I have shown that Wnt3A is not expressed in any of the ESFT cell lines investigated. Furthermore I have demonstrated that all ESFT cell lines studied expressed β-catenin in the nucleus and expressed the nonphosphorylated (active) form of β-catenin. Taken together this suggests that the canonical Wnt signalling pathway is active in ESFT cell lines grown under normal conditions.

The results generated from the Wnt signalling array confirmed mRNA expression of components of the Wnt signalling pathway in ESFT cell lines. This included expression of Wnt ligands including Wnt4, Wnt10B, Wnt2B (Wnt13) and Wnt5A which have previously been detected in ESFT cell lines (Üren et al. 2004). In addition, in this study Wnt10B, Wnt11 and Wnt5B mRNAs were also detected in all ESFT cell lines; expression of these Wnt ligands has not been previously reported in ESFT. All 19 Wnt ligands were expressed in at least one cell line, most had low expression with the exception of Wnt5A which will be discussed in more detail later in this discussion.

Other components of the Wnt signalling pathways were also detected in ESFT cell lines including high expression of LRP5, LRP6 and FZD4 consistent with previous findings (Üren et al. 2004). A number of studies have suggested that members of the DKK family may be important in ESFT, and several reports have described expression of both DKK1 and DKK2 in ESFT cell lines. Higher expression of DKK2 compared to DKK1 has been reported (Miyagawa et al. 2009, Hauer et al. 2013), which is consistent with my data. DKK2 has been shown to increase migration and invasion of ESFT cells (Hauer et al. 2013), whereas DKK1 is reported to decrease Wnt signalling in ESFT cells (Endo et al. 2008). I have also demonstrated high levels of c-myc mRNA expression in all ESFT cell lines, which is consistent with previous data on c-myc in ESFT (McKeon et al. 1988). Taken together these results suggest that the Wnt signalling array is generating informative results.

My data also demonstrate expression of members of the secreted frizzled-related protein (sFRP) family including sFRP1, sFRP2, FRZB (sFRP3) and sFRP4 in ESFT cell lines consistent with the previous study by Uren et al., (2004). However, I have also identified sFRP5 in A673, RD-ES and SK-N-MC cell lines. This is in contrast to previous literature demonstrating that sFRP5 is methylated and sFRP5 protein is not expressed in these cell lines (Jin et al.

2012). This discrepancy may reflect partial methylation of the sFRP5 gene. The sFRP family are generally considered to be antagonists of both the canonical and noncanonical Wnt signalling pathways. This is because sFRP proteins have significant similarity to the extracellular domain of frizzled receptors, therefore they can bind and sequester Wnt ligands. Indeed, sFRP5 has been shown to inhibit migration of ESFT cell lines, suggesting it may inhibit the noncanonical Wnt signalling pathway (Jin et al. 2012). In this study the expression of some members of the sFRP family, in particular sFRP2 and FRZB (sFRP3) was differentially expressed across the ESFT cell lines. Although this observation could explain the differences in expression of nuclear and active β-catenin that were detected in ESFT cell lines, this does not seem to be the case as relatively high expression of both sFRP2 and FRZB was detected in TC32 cells even though these cells have the highest level of both nuclear and active β-catenin. Therefore other factors are likely to influence the activity of the Wnt signalling pathways.

Heat map analysis revealed that the majority of Wnt signalling components had similar expression in all six ESFT cell lines. One notable exception was the noncanonical ligand Wnt5A which was the Wnt ligand with the highest mRNA expression in ESFT cell lines. Heterogeneous expression of Wnt5A protein was also observed; Wnt5A protein was highest in RD-ES and TC32 cell lines and lowest in A673 and cells. This is consistent with previous reports that Wnt5A expression is heterogeneously expressed in both ESFT cell lines and in ESFT samples, with higher expression detected in metastatic tumour samples (Jin et al. 2012). These observations suggest that the noncanonical Wnt signalling may be more prominent in some ESFT cells than others, as summarised in Table 2.7. In addition to Wnt5A protein, expression of the canonical Wnt ligands Wnt1 and Wnt3A were also investigated. I have demonstrated for the first time that Wnt1 is expressed in ESFT cell lines, although the levels of Wnt1 mRNA detected were low. It is not well understood how Wnt1 transcription is regulated. It has been reported that the homeobox protein Six3 represses Wnt1 transcription by interacting with Groucho-related co-repressors and HDAC (Lagutin et al. 2003). In addition, it has been shown that certain microRNAs including miR-21, miR-34a (Hashimi et al. 2009) and miR-152 (Huang et al. 2014) can repress transcription of Wnt1. My data also suggests that the Wnt1 protein may have a long half-life as high protein levels were detected in all cell lines but RNA expression was very low, although to my knowledge the half-life has not been formally reported for Wnt1.

Analysis of Wnt1 expression by flow cytometry revealed that in all cell lines the percentage of cells expressing this ligand was relatively homogeneous; over 85% of cells expressed Wnt1 in all cell lines. However for Wnt5A expression was more heterogeneous as the

percentage of cells expressing this ligand ranged from 45-67%. It would therefore be interesting to investigate co-expression patterns of these Wnt ligands in ESFT cell lines using flow cytometry. Although Wnt1 expression was not significantly different between the ESFT cell lines, the expression trend was the opposite to that observed for Wnt5A expression; i.e. with the highest expression observed in A673 and SK-N-MC cells. This data is summarised in Table 2.7 and further supports the hypothesis that some ESFT cells may be dominantly canonical or noncanonical, and others may be mixed. My data suggests that A673 and SK-N-MC cell lines may have active canonical Wnt signalling, and RD-ES, SKES-1 and TC32 may primarily have active noncanonical Wnt signalling.

In contrast to Wnt1 and Wnt5A, the canonical Wnt3A protein was not expressed in any ESFT cell line. Good antibodies to Wnt proteins have been very difficult to develop (based on information provided by the Nusse laboratory on the Wnt homepage: http://www.stanford.edu/group/nusselab/cgi-bin/wnt/). Indeed, in this study I struggled to find an antibody which specifically detects Wnt3A although I eventually optimised a monoclonal antibody produced by R&D which detects Wnt3A in L-cells overexpressing this protein. Although previous studies have treated ESFT cell lines with exogenous Wnt3A ligand, no expression of Wnt3A has been reported previously in ESFT cell lines which is consistent with my data.

To investigate if the canonical Wnt signalling is constitutively active in ESFT cell lines, the subcellular localisation of β-catenin was investigated by differential centrifugation (Westwood et al. 2002) and western blot. In all cell lines β-catenin was detected in the nucleus, with low levels detected in the cytoplasm. This is consistent with active canonical Wnt signalling and contradicts previous reports that β-catenin is only found in the cytoplasm of ESFT cells (Hu-Lieskovan et al. 2005, Scannell et al. 2013). Importantly, it has also been previously reported that β-catenin could not be detected in the cytoplasm or the nucleus of patient samples (Üren et al. 2004). It would therefore be interesting to investigate β-catenin localisation in patient samples using the antibody used in my study.

Constitutive activation of the canonical Wnt signalling pathway was also supported by the detection of the active (nonphosphorylated) form of β-catenin in all ESFT cell lines. The antibody used in the current study has previously been shown to specifically detect β-catenin dephosphorylayed at residues Ser37 and Thr41 (van Noort et al. 2002).. However, although total β-catenin levels were heterogeneous between ESFT cell lines, the ratio of active: total β-catenin was similar. This is in contrast to my prediction that, based on the expression of Wnt ligands, A673 and SK-N-MC ESFT cell lines would have increased levels

Cell Line	Canonical or noncanonical ?	Wnt1 expression			Wnt5A expression			β-catenin expression	
		mRNA ($2^{-\Delta\Delta Ct}$)	**Protein by western blot** (ratio to β-actin)	**Protein by flow cytometry** (median fluorescence/% positive)	**mRNA** ($2^{-\Delta Ct}$)	**Protein by western blot** (ratio to β-actin)	**Protein by flow cytometry** (median fluorescence/% positive)	**Nuclear** ?	**Active** (ratio to total β-catenin)
A673	Canonical	0.54	0.94	**Highest** 26.93/94	**Lowest** 0.12	0.25	**Lowest** 3.90/67	Yes	0.28
RD-ES	Noncanonical	0.80	0.91	22.61/94	**Highest** 2.05	**Highest** 1.04	**Highest** 9.7/46	Yes	0.27
SKES-1	Noncanonical	**Lowest** 0.25	0.92	18.87/90	0.94	**Highest** 1.04	4.89/63	Yes	**Lowest** 0.22
SK-N-MC	Canonical	**Highest** 1.99	0.94	24.54/95	0.23	**Lowest** 0.14	5.84/58	Yes	0.32
TC32	Noncanonical ?	0.45	0.89	**Lowest** 14.59/85	1.69	0.95	5.7/63	Yes	**Highest** 0.39
TTC466	Both?	0.64	0.81	17.29/86	1.32	0.19	6.2/45	Yes	0.27

Table 2.7 Summary of expression of canonical and noncanonical Wnt signalling components in ESFT cell lines ESFT cell lines predicted to have active canonical or noncanonical Wnt signalling pathways, based on mRNA and protein expression of Wnt1 (canonical ligand) and Wnt5A (noncanonical ligand). The activity of the canonical Wnt signalling pathway also predicted by expression of nuclear and active β-catenin.

of canonical Wnt signalling (Table 2.7). Nevertheless, taken together with the nuclear β-catenin observed, these results support the hypothesis there may be endogenous activity of the canonical Wnt signalling pathway in ESFT cell lines under normal growth conditions.

In contrast to Wnt1 and Wnt5A, the canonical Wnt3A protein was not expressed in any ESFT cell line. Good antibodies to Wnt proteins have been very difficult to develop (based on information provided by the Nusse laboratory on the Wnt homepage: http://www.stanford.edu/group/nusselab/cgi-bin/wnt/). Indeed, in this study I struggled to find an antibody which specifically detects Wnt3A although I eventually optimised a monoclonal antibody produced by R&D which detects Wnt3A in L-cells overexpressing this protein. Although previous studies have treated ESFT cell lines with exogenous Wnt3A ligand, no expression of Wnt3A has been reported previously in ESFT cell lines which is consistent with my data.

To investigate if the canonical Wnt signalling is constitutively active in ESFT cell lines, the subcellular localisation of β-catenin was investigated by differential centrifugation (Westwood et al. 2002) and western blot. In all cell lines β-catenin was detected in the nucleus, with low levels detected in the cytoplasm. This is consistent with active canonical Wnt signalling and contradicts previous reports that β-catenin is only found in the cytoplasm of ESFT cells (Hu-Lieskovan et al. 2005, Scannell et al. 2013). Importantly, it has also been previously reported that β-catenin could not be detected in the cytoplasm or the nucleus of patient samples (Üren et al. 2004). It would therefore be interesting to investigate β-catenin localisation in patient samples using the antibody used in my study.

Constitutive activation of the canonical Wnt signalling pathway was also supported by the detection of the active (nonphosphorylated) form of β-catenin in all ESFT cell lines. The antibody used in the current study has previously been shown to specifically detect β-catenin dephosphorylayed at residues Ser37 and Thr41 (van Noort et al. 2002).. However, although total β-catenin levels were heterogeneous between ESFT cell lines, the ratio of active: total β-catenin was similar. This is in contrast to my prediction that, based on the expression of Wnt ligands, A673 and SK-N-MC ESFT cell lines would have increased levels of canonical Wnt signalling (Table 2.7). Nevertheless, taken together with the nuclear β-catenin observed, these results support the hypothesis there may be endogenous activity of the canonical Wnt signalling pathway in ESFT cell lines under normal growth conditions.

It is important to note that nuclear localisation does not conclusively mean canonical Wnt signalling is active. It has been reported that the EWS-FLI1 fusion protein can compete with β-catenin for binding to LEF1, thereby inhibiting downstream canonical Wnt signalling.

Therefore simply observing nuclear β-catenin does not necessarily prove that canonical Wnt signalling pathway is active in ESFT cells.

In other cancer types mutations in components of the Wnt signalling pathway such as β-catenin and APC have been detected (Section 1.3.4.1). In this study the mutation status of the cell lines was not investigated since all ESFT cell lines expressed β-catenin. Furthermore it has been shown previously that mutations in *CTNNB1* (β-catenin) are very rare in ESFT (Shukla et al. 2012). Nevertheless, it will be important in future studies to confirm that the cell lines used in this study do not have mutations which may affect the activity of the Wnt signalling pathways, such as truncating (loss of function) mutations in APC or mutations which prevent the phosphorylation (and subsequent degradation) of β-catenin.

To draw reliable conclusions based on the RTqPCR data generated from the Wnt signalling array it is imperative to report mRNA expression relative to the amount of cDNA analysed, to allow for comparisons of expression between samples. It is normal practice to use the expression of so called 'housekeeping' genes involved in cellular maintenance to normalise for differences in RNA input, RNA quality and the efficiency of the RT reaction. Currently there is no gold-standard housekeeping gene and there are conflicting reports as to which is the best housekeeping gene to use, most likely because this will be tissue/cell type dependent. The Wnt signalling array used in this study contains the housekeeping genes *18S, GAPDH, HRPT1* and *GUSB*. *18S* is a ribosomal subunit and is synthesised by RNA polymerase I (Radonić et al. 2004). This means regulation of *18S* synthesis is independent of mRNA synthesis, therefore it is not a suitable reference gene to use and was excluded from the analysis. Studies have also demonstrated that *GAPDH* expression can be affected by various experimental conditions such as serum concentration (Schmittgen and Zakrajsek 2000). In addition, *GAPDH* has been reported to have at least 67 pseudo-genes that share over 80% identity to the parental mRNA (Sun et al. 2012). Since it has been shown that at least some of these may be transcribed (Tso et al. 1985), and therefore potentially detected by RTqPCR, we do not believe *GAPDH* is suitable to use as a housekeeping gene. In addition, both *18S* and *GAPDH* are very highly expressed, ideally a housekeeping gene should have similar expression levels to the mRNAs of interest. An ideal housekeeping gene should also have relatively constant expression regardless of experimental conditions; therefore the inter-assay variability between replicates of the other housekeeping genes on the array was performed. In ESFT cell lines, the housekeeping gene with the lowest inter-assay variability was *HRPT1*. It has been shown previously that in a range of tissue types, expression of *HRPT1* accurately reflects the expression of 10 other

commonly used housekeeping genes (de Kok et al. 2004), hence I have used *HRPT1* against which to normalise my results.

In summary, my results support the hypothesis that Wnt signalling may be active in ESFT. However, in the subcellular localisation studies, TBP and α-tubulin were used to confirm enrichment of the nuclear and cytoplasmic fractions, respectively. This demonstrated that the fractionation protocol was not completely efficient, and there was some contamination of both the nuclear and cytoplasmic fractions in some cell lines. Since my observations are not consistent with previous reports it would be especially important to confirm my observations. This could be performed using confocal microscopy to identify co-localisation of β-catenin with nuclear proteins such as TBP.

The Wnt signalling array used to assess mRNA expression of Wnt components is a very useful high-throughput tool to investigate which components of the Wnt signalling pathway are expressed. However, since it is a pre-made commercial array it is not possible to choose which components are included. Unfortunately there are not many components of the noncanonical Wnt signalling pathway on this array meaning my data is not as informative for this pathway. I have attempted to separate components into those that are predicted to either promote or inhibit Wnt signalling. However, in reality this is very difficult as expression of a particular Wnt ligand or receptor does not definitively reveal which Wnt signalling pathway, if any, is activated. The Wnt signalling network is complicated, with many different components including many possible ligand/receptor complexes and inhibitors and these are still not completely understood. It is becoming evident however that Wnt ligands may activate different pathways depending on the cellular context and receptors present. For example, in *C.elegans* Wnt1 has been shown to inhibit, rather than activate the activity of TCF (Smit et al. 2004) and Wnt5A can activate the canonical Wnt signalling pathway when bound to FZD4 (Mikels and Nusse 2006). Also in endometrial cancer cells, Wnt7A binding to FZD5 has been shown to activate the canonical Wnt signalling whereas Wnt7A binding to FZD10 activates the noncanonical pathway (Carmon and Loose 2008). In addition, inhibitors of the pathway such as members of the DKK family (Niehrs 2006) and sFRP family (Bovolenta, 2008), have been shown to inhibit but also activate Wnt signalling in some situations. I have attempted to investigate the activity of the canonical Wnt signalling pathway by investigating the downstream effector protein β-catenin. However, as discussed although this is the method used by many studies to investigate activation of the canonical Wnt signalling pathway this is not a true measure of the functional activity of the pathway. Furthermore, for the noncanonical Wnt signalling pathways there is no single protein (such as β-catenin) that can be easily be

detected to probe for activation. Therefore, to reliably investigate the activity of the Wnt signalling pathways in ESFT it is important to develop functional assays to measure signalling directly.

3. Developing an assay to measure the activity of the canonical Wnt signalling pathway in ESFT cell lines

3.1 Introduction

In the previous chapter I demonstrated that components of the canonical Wnt signalling pathway are expressed in ESFT cell lines. In addition, nuclear and unphosphorylated β-catenin were detected in all ESFT cell lines, consistent with the hypothesis that the canonical Wnt signalling pathway is constitutively active in ESFT cell lines. However, in order to demonstrate this conclusively, in this chapter I have developed and optimised a reporter to directly measure activation of the canonical Wnt signalling pathway in ESFT cells.

The most widely used technique to directly measure canonical Wnt signalling is to transiently transfect cells with a TOPFlash (or more recently SUPER-TOPFlash) reporter plasmid (Korinek et al. 1997, Veeman et al. 2003). These plasmids contain the firefly luciferase gene under the control of a promoter containing multiple repeats of the TCF/LEF transcriptional response elements (TRE). Therefore, when β-catenin enters the nucleus and binds to the TCF/LEF binding sites, firefly luciferase is expressed which can be detected using a highly sensitive quantitative luciferase assay. Cells are also transfected with a negative control plasmid, FOPFlash, which contains mutated TCF/LEF binding sites to ensure specificity of firefly luciferase expression upon canonical Wnt signalling. Using this approach previous studies observed no or extremely low canonical Wnt signalling activity in ESFT cells (Hu-Lieskovan et al. 2005, Navarro et al. 2010, Vijayakumar et al. 2011).

However, this technique has a number of disadvantages. For example, unless 100% of the cells are transfected then the TOPFlash assay will only detect canonical Wnt signalling in a subpopulation of cells, which may not be representative of the whole population, meaning rare populations of cells could be missed. In addition, this assay relies upon a separate control plasmid constitutively expressing *Renilla* luciferase to control for transfection efficiency. It is therefore assumed that the transfection of TOPFlash and *Renilla* is identical, which may not be the case. Importantly it also relies on the ability to transiently transfect cells. ESFT cells are very difficult to transfect using currently available reagents such as Lipofectamine®2000 and FuGENE® or electroporation (unpublished observations).

More recently, a second method to investigate canonical Wnt signalling in cells using lentiviral reporter vectors has been described (Fuerer and Nusse 2010). Lentiviral vectors are single-stranded RNA viruses derived from the human immunodeficiency virus (HIV) that stably integrate into the host genome. To eliminate the possibility that a wild-type virus will be reconstituted through recombination, various safety alterations have been made. For example the accessory genes *vif, vpr, vpu* and *nef* have been eliminated (Zufferey et al. 1997). In addition, when making virus particles, cells are transfected with three separate plasmids. Firstly, cells are infected with the lentiviral expression plasmid containing the *psi* (ψ) packaging sequence and the transgene inserted between lentiviral long terminal repeats (LTRs) for target cell integration. Self-inactivating lentiviruses have been developed that have a mutation in the 3'LTR to prevent the vector RNA being transcribed in the transduced cells (Zufferey et al. 1998). The second plasmid transfected contains the packaging genes *pol, gag, rev* and *tat* and the *rev*-response element (RRE). In addition, a pseudotyping plasmid containing the G protein of the Vesicular Stomatitis Virus (VSV-G) envelope gene is transfected. This envelope protein allows lentiviruses to infect all mammalian cells, including nondividing cells (Burns et al. 1993, Akkina et al. 1996, Naldini et al. 1996). Lentiviral vectors have been developed which contain 7 repeats of the TCF binding site driving expression of either GFP or firefly luciferase (Fuerer and Nusse 2010). The vectors also contain a puromycin resistance gene to allow for selection of infected cells to generate a stably expressing cell population. These vectors could therefore be used to measure Wnt signalling in entire populations of cells, including cells that are normally difficult to transiently transfect. Endogenous Wnt signalling could be measured in cells as well as the response of cells to Wnt ligands.

Treatment with exogenous Wnt ligands is often used to stimulate Wnt signalling in cells, thereby demonstrating the activity of the pathway. However, Wnt proteins are poorly soluble and when overexpressed in cell lines are largely associated with the extracellular matrix, and not secreted (Bradley and Brown 1990). The first secreted and biologically active Wnt protein to be described was mouse Wnt3A (Shibamoto et al. 1998). It has been possible to purify biologically active mouse Wnt3A (Willert et al. 2003) and mouse Wnt5A (Mikels and Nusse 2006) proteins, however purification of other Wnt proteins has been less successful as they tend to form protein aggregates that are not biologically active (Willert and Nusse 2012). Rather than using purified Wnt proteins, a more cost effective and commonly used alternative is to use conditioned media from cells overexpressing Wnt proteins. Mouse L (L-M [TK^-]) cells have been stably transfected with Wnt3A and Wnt5A, and conditioned media from these cells shown to contain biologically active Wnt3A and

Wnt5A, respectively (Willert et al. 2003, Mikels and Nusse 2006). However, the disadvantage of this approach is that conditioned media from these cells will contain other factors which may make interpretation of the results difficult. Therefore in an attempt to address this issue, conditioned media from the parental L cell line (which does not produce Wnt3A or Wnt5A protein) is used as a control.

In addition to measuring the activity of canonical Wnt signalling using reporter systems, activation can be confirmed by measuring the expression of target genes downstream of the pathway. There are currently over 120 genes known to be downstream targets as listed on the Wnt homepage (http://www.stanford.edu/group/nusselab/cgi-bin/wnt/) and the specific up or down regulated genes appear to be cell type rather than signal specific (H. Clevers 2006). It is not known whether there are genes that are universal targets of canonical Wnt signalling, although it has been suggested this is the case for *Axin2* (Jho et al. 2002). Expression of β-catenin mRNA and protein has also been shown to increase after stimulation of cells with Wnt3A protein (Gujral and MacBeath 2010, Hernandez et al. 2012) suggesting this may also be an informative downstream target gene to investigate.

The aims of this chapter were to:

1. Optimise and validate a lentiviral reporter assay to measure the activity of canonical Wnt signalling.
2. Measure the endogenous activity of Wnt signalling in ESFT cell lines.
3. Investigate if the Wnt signalling pathway is activated by treatment with exogenous Wnt ligands.

3.2 Materials and Methods

3.2.1 Cell lines and tissue culture

ESFT cell lines were cultured as previously described (Section 2.2.1). HEK293T cells were obtained as a gift from Professor M. Knowles and maintained in DMEM supplemented with 10% (v/v) FCS and 2mM glutamine on Corning® tissue-culture plastic HEK293T cells were passaged at least twice after thawing before being used for lentiviral particle production.

L cells (CRL-2648), L Wnt-5A (CRL-2814) and L Wnt-3A (CRL-2647) cell lines were purchased from the ATCC (supplied by LGC Standards). All L cell lines were maintained in modified DMEM (30-2002, ATCC) containing 4 mM L-glutamine, 4.5 g/L glucose, 1 mM sodium pyruvate, and 1.5 g/L sodium bicarbonate and 10% FCS on Corning plastic. L Wnt-5A and L Wnt-3A cell lines were maintained in 0.6mg/ml and 0.4mg/ml G418 (Gibco®, Life Technologies), respectively, for one week upon arrival to confirm selection.

All cell lines were passaged when 70% confluent as described previously (Section 2.2.1) and cultured in a humidified chamber in 5% CO2 in air at 37°C. Cell lines were screened for mycoplasma contamination every 3 months by technical staff using the EZ-PCR mycoplasma test kit (GeneFlow).

3.2.2 Lentiviral transduction of cells

3.2.2.1 Production of vector DNA

Plasmids 7xTcf-eGFP.SV-40-Puro^R (7TGP; plasmid 24305) and 7xTcf-FFLuc.SV40-Puro^R (7TFP; plasmid 24308) (Fuerer and Nusse 2010) were purchased from Addgene (Cambridge, Massachusetts, USA), provided as transformed bacteria in a stab culture.

3.2.2.1.1 Streaking out transformed bacteria

Bacteria were streaked onto an agar plate containing LB agar with 100µg/ml ampicillin (amp; Sigma-Aldrich) using a sterile inoculation loop and incubated for 16 h at 37°C in a dry chamber (Sanyo Incubator). After this time a single colony was picked using a pipette tip, and used to inoculate a 5ml culture of LB medium (+ 100µg/ml amp) which was incubated for 16h at 37°C with vigorous shaking (approximately 300 rpm) in an incubator shaker (Innova® 4200, New Brunswick Scientific, supplied by Eppendorf UK, Stevenage, UK). The culture was then added to 200ml LB medium (+ 100µg/ml amp) and incubated at 37°C with vigorous shaking for a further 16h. The bacteria were harvested by centrifugation (6000 g

for 15 min at 4°C; Beckman Coulter Avanti® J-26 XP Centrifuge) and all traces of supernatant removed.

3.2.2.1.2 Maxipreparation of DNA

Vector DNA was isolated from the bacterial culture using the HiSpeed® Plasmid Maxi Kit (Qiagen). All reagents are company proprietary. The bacterial pellet was lysed by resuspending in 10ml Buffer P1 (containing RNase A). The solution was mixed thoroughly with 10ml Buffer P2 by shaking and incubated for 5 min at RT. An equal volume (10ml) of chilled Buffer P3 was added to the lysate and mixed immediately by inverting the tube 6 times vigorously for the precipitation step to occur. The lysate was poured into the barrel of a QIAfilter Cartridge and incubated at RT for 10 min or until the precipitate containing genomic DNA, proteins and detergent was visible at the top of the cartridge. Meanwhile, a HighSpeed Maxi Tip was equilibrated by applying 10ml Buffer QBT and the column allowed to empty by gravity flow. Once the incubation was complete, the cap from the QIAfilter outlet nozzle was removed and the plunger gently inserted into the QIAfilter Maxi Cartridge and the cell lysate filtered into the equilibrated HiSpeed Tip. The cleared lysate was allowed to enter the resin by gravity flow and the HiSpeed Maxi Tip was washed with 60 ml Buffer QC. Finally, the DNA was eluted with 15ml Buffer QF into a 50ml Falcon™ tube. The DNA was precipitated by adding 10.5ml isopropanol at RT, mixed, and incubated for 5 min at RT. DNA was harvested by centrifugation (1900g for 45 min; Allegra® 6R Centrifuge, Beckman Coulter) and subsequently washed with 5ml 70% ethanol. A final centrifugation (1900g for 15 min) was performed and any residual ethanol removed by pipetting. The pellet was allowed to air-dry and finally resuspended in 300-500µl nuclease-free water, as determined by the size of the pellet. DNA quality and quantity was measured using the Nanodrop as previously described (Section 2.2.5.2).

3.2.2.2 Generation of lentiviral vectors in HEK293T cells

All work with lentiviral vectors was carried out in a Class II tissue culture facility. All used liquids and tissue culture plastics were decontaminated with 10% (v/v) Virusolve® (AMITY Healthcare, Barnsley, UK) for at least 30 min before being disposed by autoclaving. After use the tissue culture cabinet was cleaned using 10% Virusolve. All equipment including gloves, tissues and used plastics were left in the Class II cabinet for at least 30 min after lentiviral vectors had been used, to eliminate any aerosols which may have been generated, prior to decontamination and disposal by autoclaving.

Lentiviral particles were produced using a second generation packaging system kit LENTI-Smart™ (Invivogen, supplied by Source BioScience, Nottingham, UK) using HEK293T cells. This kit includes the packaging plasmids pLV-iVSV-G (encoding the viral envelope gene) and pLV-HELP (containing *gag, pol, rev* and *tat* genes) and LycoVec™ transfection reagent. To produce lentiviral particles, 12µg of the lentiviral cloning plasmid of interest (in 200µl) was added to one vial of Lenti-SMART™, mixed gently and incubated at RT for 15 min, then 800µl of sterile H_2O was added. Meanwhile, HEK293T cells were trypsinised and viable cell number quantified as previously described (Section 2.2.1). A total of 1 x 10^7 cells were added to 12ml of growth media in a 75 cm^2 flask. The LENTI-Smart™ and cloning plasmid mixture was then added and mixed by pipetting. The flask was placed in the incubator, and the media replaced after 16 h. After 24 h the supernatant was collected and stored at 4°C, and 10ml fresh media added. After 48h the supernatant was harvested and pooled with the supernatant collected after 24 h. The combined supernatant was filtered using a 0.45µm Aerodisc® PVDF filter (PALL Life Sciences, supplied by VWR) to remove viral and cell debris. Viral supernatant was stored in 1.5ml single-use aliquots at -80°C in a designated freezer for Class II material.

3.2.2.3 Infecting target cells with lentiviral vectors

Cells were trypsinised and seeded in 25 cm^2 flasks at a density of 6 x 10^5 (except HEK293T and A673 cells which were seeded at 3 x 10^5) so that they would be 30-50% confluent the next day (Section 2.2.1). After 24h, the media was replaced with 1.5ml viral supernatant (prepared as described in Section 3.2.2.2) diluted in growth media as required, containing 1 µg/ml hexadimethrine bromide (Polybrene®, Sigma-Aldrich). After 4h, the viral supernatant was discarded and replaced with normal growth media. After 48h the growth media was replaced with media containing 0.5µg/ml puromycin (Sigma-Aldrich) to select for cells transduced with the vector. Cells were maintained in selection for 1 week. Cells were used for experiments after a minimum period of 72h after infection to allow time for the gene of interest to be produced. Cells were maintained in Class II conditions (as described in Section 3.2.2.2) for at least 10 days after infection or until at least 2 passages had been performed, after this time lentiviral particles were no longer present.

3.2.3 Measuring GFP expression in cells by flow cytometry

Cells expressing GFP were trypsinised (Section 2.2.1) and centrifuged at 405g for 5 min. For cells which were still being maintained in Class II conditions a centrifuge with buckets and lids was used to minimise the release of aerosols, and these were thoroughly cleaned with 10% Virusolve after use. After centrifugation the cell pellet was resuspended in 500µl 1%

PFA to fix the cells, followed by centrifugation (405g for 5 min). The cell pellet was then washed with 1X PBS, centrifuged (405g for 5 min), the supernatant discarded and the pellet resuspended in 1ml fresh PBS. After fixation, cells did not have to be handled in Class II containment. GFP expression was analysed by flow cytometry (FACSCalibur™, BD Biosciences) using an excitation laser of 480nm. A total of 10,000 events were measured for each sample and triplicate samples were analysed for each cell line. GFP expression was compared to control cells which had not been infected with a lentiviral GFP plasmid, and median GFP fluorescence and percentage of cells expressing GFP determined using CellQuest™ software (BD Biosciences).

3.2.4 Titration of lentiviral vectors

The titre of lentiviral vector produced using the LENTI-Smart™ kit was estimated using HEK293T cells infected with pLV-Green vector. HEK293T cells were chosen as they have a doubling time of between 18-25 h and are therefore recommended by the manufacturers of LENTI-Smart™. HEK293T cells were trypsinised (Section 2.2.1) and seeded at 5 x 10^4 cells/well in 24 well plates. After 24h, cells in 3 of the wells were trypsinised and counted using the Vi-cell automated cell counter (Section 2.2.2) to provide a viable cell count at the time of infection. The following dilutions of pLV-Green viral supernatant in DMEM (+10% FCS) containing 1µg/ml Polybrene® were prepared; 1:2, 1:4, 1:8, 1:16, 1:32, 1:64 and 1:128. The media was removed from remaining wells and 500µl of diluted viral supernatant was added (three wells per dilution). The plate was incubated for 4h at 37°C after which time the viral supernatant was removed and 1ml fresh DMEM (+10% FCS) added. The plate was incubated for a further 72h at 37°C to give time for GFP to be expressed. GFP expression was determined as previously described (Section 3.2.3).

The lentiviral titre was calculated for each dilution using the following formula;

$$\frac{(F \times C \times D)}{0.5}$$

where F is the frequency of GFP positive cells (percentage obtained divided by 100), C is the number of cells (calculated as the average from the cell counts performed at the time of infection) and D is the coefficient of dilution (i.e. 64 for 1:64 dilution. This is divided by the volume (in ml) of media used to infect the cells (0.5). The average titre was calculated from values gained from dilutions where the percentage of GFP positive cells was within the range 1-30% (as suggested by the LENTI-Smart™ kit manual) and was presented as transduction units (TU) per ml.

Using this titre the multiplicity of infection (MOI) could be determined in subsequent lentiviral infections. This is defined as the ratio of transduction-competent lentiviral particles to the number of cells being transduced.

3.2.5 Luciferase assay

Luciferase activity was measured using the Luciferase Assay System (E1500, Promega). In this assay, firefly luciferase catalyses the oxidation of luciferin to oxyluciferin. This reaction produces light which is measured using a luminometer. Prior to performing the assay 1X Passive Lysis Buffer (PLB; E1941, Promega) was prepared in dH_20 and equilibrated to RT. Luciferase Assay Reagent (LAR) was prepared by adding Luciferase Assay Buffer (10ml) to one vial of Luciferase Assay substrate. Complete LAR was stored in working aliquots in the dark at -80°C. LAR was diluted 1:1 in dH_20 and equilibrated to RT before use. To perform the assay, media was aspirated from adherent cells in 24-well plates and cells rinsed with 500µl 1X PBS. PBS was aspirated and 100µl of 1X PLB added to each well and plates rocked on a plate shaker for 15 min at RT to lyse cells. Samples were transferred to individual wells of a round-bottomed 96-well plate and centrifuged at 154g for 1min to pellet cell debris. A 20µl aliquot of each sample was transferred to one well of a flat, solid-bottomed white 96-well plate (Falcon®, supplied by Scientific Laboratory Supplies (SLS), Nottingham, UK). Luminescence detection was performed using a luminometer with an auto injector (Mithras LB 940, Berthold, Harpenden, UK). The injector was washed with 70% ethanol (60 cycles) and dH2O (60 cycles) before use. The injector was primed with LAR and the plate containing assay samples loaded onto the luminometer. The luminometer was programmed to dispense 100µl of LAR into each well, shake the plate, perform a 2s measurement delay followed by a 10s measurement read, before moving onto the next well. After use, the injector was unloaded and washed as described above.

Luminescence of samples was reported in Relative Light Units (RLU) relative to the RLU of parental cells not infected with a luciferase reporter plasmid.

3.2.6 L cell conditioned media

3.2.6.1 Generating L cell conditioned media

To prepare conditioned media (CM), L cells, L Wnt-5A and L Wnt-3A cells were trypsinised (Section 2.2.1) and split 1:10 into $10cm^2$ dishes (Primaria™) in 10ml culture media (Section 3.2.1). After 4 days, the media was removed by aspiration and sterile filtered using a 0.2µm Aerodisc® filter (PALL Life Sciences), and 10ml of fresh culture media added to the cells. After 3 more days the media was removed by aspiration and the cells were discarded.

Media was sterile filtered and combined with the media removed after 4 days. The combined CM was frozen in single use (5ml) aliquots at -20°C.

3.2.6.2 The effect of L cell conditioned media on the viability of ESFT cell lines

ESFT and HEK293T cells were trypsinised (Section 2.2.3) and 2×10^5 cells/well seeded into Primaria™ 24 well plates in cell-type specific media. A673 and HEK293T cell lines were seeded at 1×10^5 cells/well. After 24h, media was aspirated and replaced with 1ml of cell-type specific media (control), L-cell CM, L-Wnt5A CM or L-Wnt3A CM. Viable cell number was determined for triplicate wells per condition after 24h and 48h using the trypan blue exclusion assay (measured with the automated vi-cell counter; Section 2.2.2). The viable cell number for wells treated with CM was calculated as a percentage of the viable cell number of wells cultured in cell-type specific media (control).

3.2.6.3 Quantifying the concentration of Wnt3A in L-Wnt3A conditioned media

CM was prepared from L cells and L-Wnt3A cells as previously described (Section 3.2.6.1). CM samples were analysed that had been collected 4 and 7 days after seeding cells, as well as pooled samples collected after 4 and 7 days. Pooled samples were either filtered using a 0.2µm membrane, or left unfiltered. Each CM sample (20µl) was mixed with an equal volume of 2X SDS-loading buffer (Section 2.2.3.1) and loaded onto a 10% acrylamide gel alongside a range of concentrations of recombinant Wnt3A (10-30ng) in 40µl of 1X SDS-loading buffer. SDS-PAGE was performed followed by western blotting for Wnt3A as described previously (Section 2.2.3). The densitometry of the recombinant protein bands was used to generate a concentration curve which was used to estimate the concentration of Wnt3A in the different samples of conditioned media, based on the densitometry of the bands.

3.2.7 Measuring 7TGP reporter activity in cells

Cells were plated into 24 well plates at 1×10^5 cells per well (except HEK293T and A673 which were seeded at 5×10^4 cells well), in cell type specific media. After 24h the media was replaced with 500µl of conditioned media (as appropriate). Optimisation experiments were performed using HEK293T and SKES-1 cell lines. Cells were treated for varying lengths of time with L cell, L Wnt-5A or L Wnt3A CM (Section 3.2.6.1) or with recombinant Wnt5A (200ng/ml; R&D Systems) or varying concentrations of recombinant Wnt3A (R&D Systems). Using optimised conditions ESFT cell lines were treated with recombinant Wnt5A (200ng/ml) or Wnt3A (200ng/ml) for 24h Cells were harvested and GFP expression analysed by flow cytometry (Section 3.2.3).

3.2.8 Measuring 7TFP reporter activity in cells

Cells were plated into 24 well plates at 1 x 10^5 cells per well (except HEK293T and A673 which were seeded at 5 x 10^4 cells well) in cell type specific media. After 24h the media was replaced with 500µl treated media as previously described (Section 3.2.7). In optimised conditions the luciferase assay was performed 48h after seeding cells as previously described (Section 3.2.5).

3.2.9 Viable cell number of ESFT cells treated with Wnt ligands

Cells were trypsinised (Section 2.2.1) and seeded at 5 × 10^4 cells/well in 24-well Primaria™ plates in cell type specific media. After 24h media was replaced with normal growth media (control) or media containing rWtn3A (200ng/ml) or rWnt5A (200ng/ml). After 24, 48 and 72h viable cell number was counted using the trypan blue exclusion assay (using the automated Vi-cell; Section 2.2.2). Triplicate wells were counted for each condition, at each time point.

3.2.10 Detection of total and active β-catenin by western blot

Cells were seeded in 6-well plates in cell type specific media. After 24h, for optimisation experiments HEK293T cells were treated for increasing lengths of time with Wnt3A. In optimised conditions, ESFT cells were treated with Wnt3A (200ng/ml) or Wnt5A (200ng/ml) for 4h. Total protein was extracted and the concentration quantified and samples (25µg) were analysed by SDS-PAGE as previously described using a 10% gel (Section 2.2.3). Expression of total and active β-catenin and β-actin (loading control) were detected using specific antibodies as previously described (Table 2.3).

3.2.11 Statistics

All analyses were undertaken using GraphPad prism 6 software. Data were analysed by ANOVA when comparing 3 or more conditions or cell lines as described previously (Section 2.2.6). Differences in viable growth curves were analysed by linear regression comparing the slopes and intercepts of multiple lines. Differences between two means was analysed using an unpaired t test with Welch's correction. In all cases, differences were considered significant when $p<0.05$.

3.3 Results

3.3.1 Developing and optimising a lentiviral TCF reporter assay

3.3.1.1 Titration of lentiviral vector

Lentiviral vectors were generated using the LENTI-Smart™ kit (Invivogen). The titre of lentiviral vectors created using this method was determined in HEK293T cells using a lentiviral vector with constitutive GFP expression (pLV-Green). This enabled the number of infected cells to be easily quantified by flow cytometry. When HEK293T cells were infected with increasing dilutions of pLV-Green viral supernatant, the percentage of cells with GFP expression decreased in a dilution dependent fashion (Figure 3.1 A). The number of viable cells present was also determined and used to calculate the viral titre (as described in Section 3.2.4). The titre was determined from dilutions where the percentage of GFP positive cells was between 1-30% (as suggested in the LENTI-Smart™ technical manual) and was calculated as 1.5×10^6 TU/ml (Figure 3.1 B). Using this titre the MOI was calculated for subsequent experiments as the ratio of transduction-competent lentiviral vectors to the number of cells being transduced.

(A)

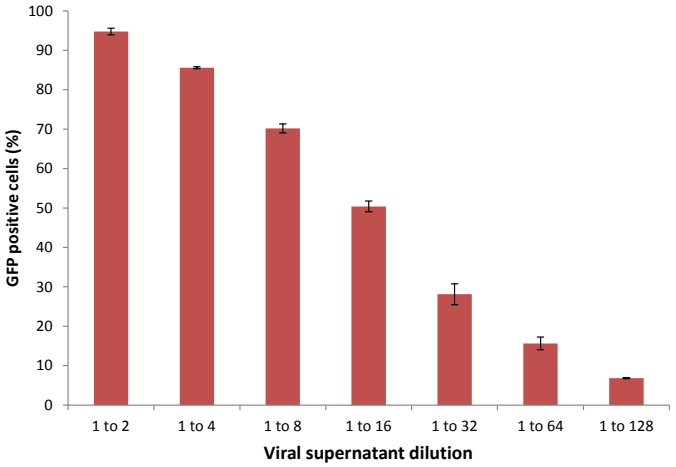

(B)

Lentiviral Dilution	Average % of GFP positive cells	Average cell count ($x10^4$)	Titre
1:2	95	9.3	353360
1:4	86	9.3	638773.3
1:8	69	9.3	1035676
1:16	48	9.3	1444750
1:32	24	9.3	**1450524**
1:64	13	9.3	**1556651**
1:128	7	9.3	**1636693**
		Transduction units (TU) /ml =	**1547956**

Figure 3.1 Calculating the lentiviral titre in HEK293T cells HEK293T cells were infected with pLV-Green lentiviral plasmid using the LentiSmart kit (Invivogen). Increasing dilutions of lentiviral supernatant and media were used to infect the cells for 4h. After 72h the cells were trypsinised, fixed with 1% PFA and analysed by flow cytometry to determine A) the percentage of GFP+ cells achieved by using different viral supernatant dilutions. B) The number of viable cells/well was determined from untreated wells at the time of viral infection by trypan blue exclusion using the automated Vi-cell counter. The percentage of GFP positive cells and the number of cells present were used to determine the viral titre/ml for each dilution (as described in Section 3.2.4). Dilutions where the percentage of GFP positive cells was between 1-30% (shown in bold) were used to calculate the mean transduction units/ml. Results shown as the mean of two independent experiments with 3 replicates per experiment (n=6).

3.3.1.2 Infection of ESFT cell lines with lentiviral GFP plasmid

The lentiviral plasmid containing constitutive GFP expression (pLV-Green) was used to investigate the infection efficiency of lentiviral particles in ESFT cells. Using a MOI of 2, cells expressing GFP could be detected in all ESFT cell lines 72h after infection (Figure 3.2 A). The percentage of cells expressing GFP after infection with a MOI of 2 was 84±0.9% in TC32 cells, but less than 20% in the other ESFT cell lines; ranging from 4±0.9% in SKES-1 cells to 16±0.7% in A673 cells. This could be clearly visualised by fluorescent microscopy (Figure 3.1 C). Using an MOI of 4 rather than 2 did not increase the infection rate in SKES-1 cells (data not shown).

In order to compare the activity of a reporter plasmid between the different cell lines it is important to ensure that the rate of lentiviral particle infection is similar. Ideally, infection rates should be below 20% to reduce the chance of multiple integrations of the reporter into the same cell, which would give an inaccurately high reporter reading (Salmon 2013). For this reason, A673, RD-ES, SKES-1, SK-N-MC and TTC466 cell lines were infected using a MOI of 2. This resulted in a similar level of GFP expression in these cell lines (median fluorescence range 14-22) (Figure 3.2 B). TC32 cells were infected at a MOI of 0.125, as this resulted in 15±0.08 of cells expressing GFP. The level of GFP expression in TC32 cells infected at this MOI was higher than in the other cell lines (median fluorescence= 43±1) (Figure 3.1 B). This may be important when interpreting future experiments as the reporter plasmid may also be expressed at higher levels in TC32 cells.

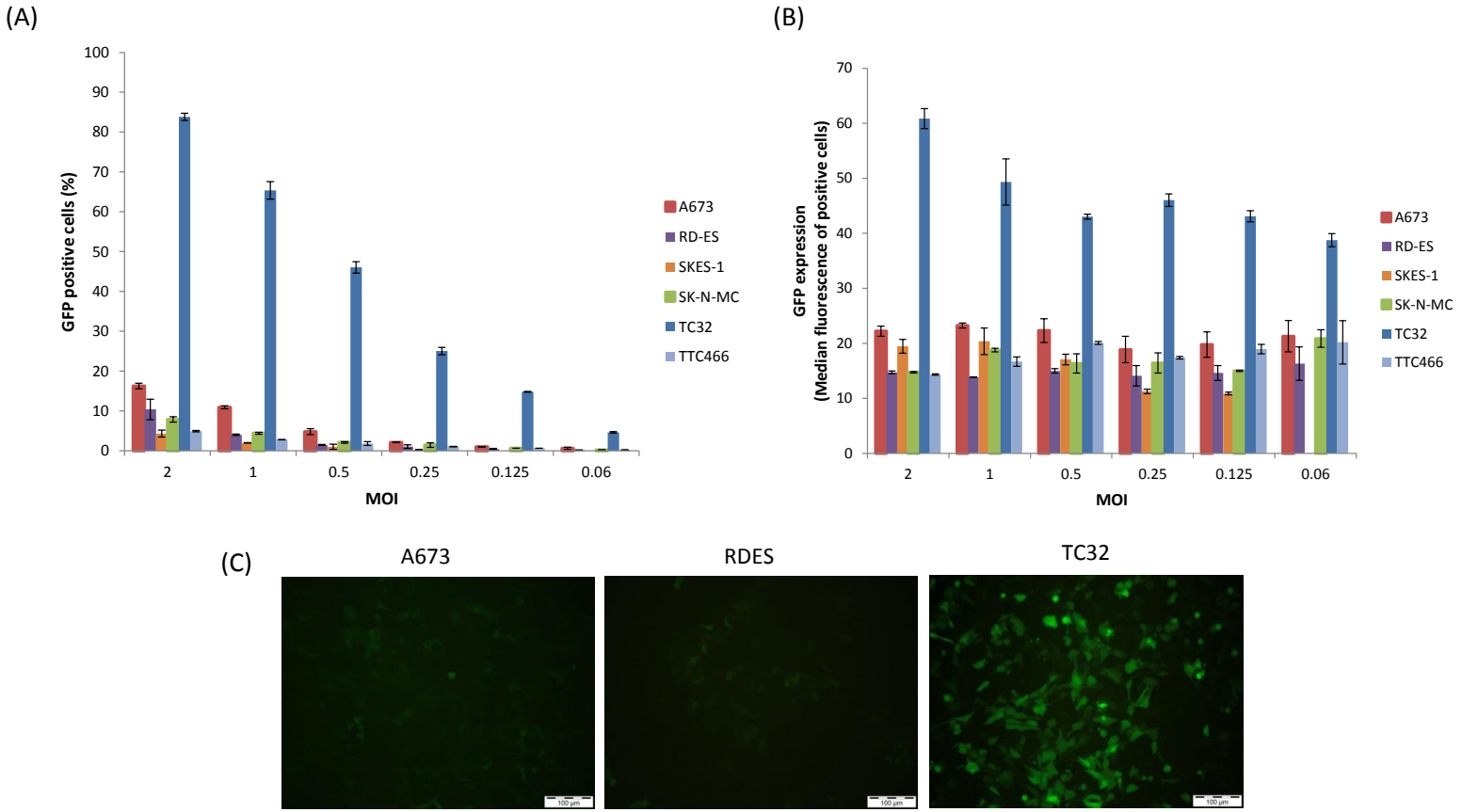

Figure 3.2 Infection of ESFT cell lines with lentiviral GFP plasmid ESFT cell lines were infected with pLV-Green lentiviral plasmid using the LentiSmart kit (Invivogen). MOIs of 0.06-2 were used to infect the cells for 4h. After 72h the cells were trypsinised, fixed with 1% PFA and analysed by flow cytometry. A) The percentage of GFP positive cells and B) the level of GFP expression (median fluorescence) achieved by different MOI's. Results show the mean of two independent experiments with three replicates per experiment (n=6) (±SEM) C) Representative images of GFP expression in A673, RD-ES and TC32 cells, 72h after infection using an MOI of 2, visualised using a fluorescent microscope. MOI= multiplicity of infection.

3.3.1.3 Optimising measurement of canonical Wnt signalling activity using 7TGP and 7TFP reporter plasmids

3.3.1.3.1 Confirming the activity and stability of the 7TGP and 7TFP reporter plasmids

The activity of both the 7TGP (GFP) and 7TFP (firefly luciferase) reporter plasmids was initially tested in HEK293T cells which have been demonstrated to have active canonical Wnt signalling (Veeman et al. 2003).

In HEK293T 7TGP cells, cells expressing GFP could be detected (Figure 3.3 A and B). In control (untreated) cells the percentage of cells expressing GFP was 4±0.1%, and these cells had a median GFP fluorescence of 14.7±0.03. This demonstrates that the 7TGP reporter construct can detect endogenous Wnt signalling in cell lines. When the HEK293T 7TGP cells were treated with the canonical Wnt ligand Wnt3A (200ng/ml, 24h) both the percentage of GFP positive cells (43±2%, $p<0.001$) and the median fluorescence (43.5±6, $p<0.05$) significantly increased; indicating that treatment with Wnt3A protein stimulates canonical Wnt signalling, as measured using the 7TGP reporter. When GFP expression was examined in HEK293T 7TGP cells after the cells had been in culture for 3 months (Nov 2012) there was no significant difference in the results obtained initially (Aug 2012), demonstrating the stability of expression of the 7TGP reporter in selected cell lines.

In HEK293T cells transduced with the luciferase reporter (HEK293T 7TFP), luciferase activity could be detected in control (untreated) cells (8.5±0.1 $x10^6$ RLU), and this significantly ($p<0.0001$) increased after treatment with Wnt3A (200ng/ml, 24h) (223.5 ±1.7 $x10^6$ RLU) (Figure 3.3 C). This demonstrates that the 7TFP vector can also detect endogenous canonical Wnt signalling in cell lines, and the stimulation of canonical Wnt signalling. Again, when the luciferase activity was examined in HEK293T 7TFP cells after 4 months of culture (Feb 2013) the luciferase activity was not significantly different than when first recorded (Oct 2012), indicating the vector expression is stable in cells (Figure 3.3 C)

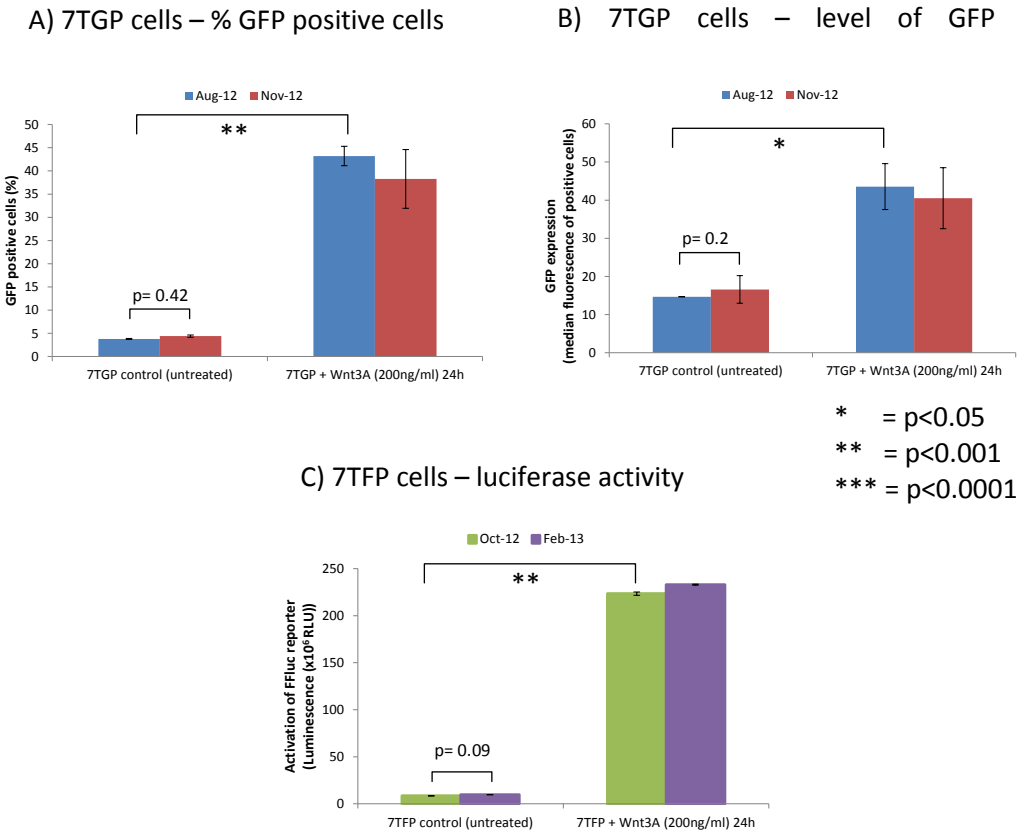

Figure 3.3 Activation and stability of 7TGP and 7TFP plasmids in HEK293T cells HEK293T 7TGP or HEK293T 7TFH cells were seeded into 24 well plates and the next day cultured in media alone (untreated control) or 200ng/ml Wnt3A. After 24h, 7TGP cells were harvested by trypsinisation, fixed in 1% PFA and analysed by flow cytometry to determine A) the percentage of GFP positive cells and B) level of GFP expression (median fluorescence). After 24h, 7TFP cells were C) assayed for luciferase activity using the luciferase assay (Section 3.2.5). Results show the mean of two independent experiments at each time point, with 3 replicates per experiment (n=6) (±SEM). FFLuc = firefly luciferase. RLU = relative light units.

3.3.1.3.2 Optimising stimulation of canonical Wnt signalling in 7TGP cells with Wnt3A conditioned media

Conditions for stimulating cells transduced with the 7TGP vector were optimised using HEK293T cells (positive control) and the SKES-1 ESFT cell line. Endogenous canonical Wnt signalling activity was detected in both cell lines at low levels; median GFP fluorescence was 14.7±0.03 in HEK293T 7TGP cells and 13±0.8 in SKES-1 7TGP cells (Figure 3.4 A). However, only a small percentage of cells expressed GFP in both HEK293T 7TGP (4±0.1%), and SKES-1 7TGP (0.15±0.04%) cells (Figure 3.4 B).

As previously discussed, Wnt3A conditioned media is commonly used to stimulate the canonical Wnt signalling pathway. There was no increase in activity of the GFP reporter, or number of cells expressing GFP, after stimulation with L-cell (control) or L-Wnt5A conditioned media (CM) in either HEK293T 7TGP or SKES-1 7TGP cells (Figure 3.4 A and B). However, consistent with activation of the canonical Wnt signalling pathway, after the addition of L-Wnt3A CM, HEK293T 7TGP cells had increased GFP expression, as early as 4h after treatment (median GFP fluorescence; 25.8±0.29). Maximum GFP expression was observed after 24h (median GFP fluorescence; 109±13), this was a 7.4-fold increase compared to untreated cells. In HEK 293T 7TGP cells the percentage of cells expressing GFP increased after 8h treatment with L-Wnt3A CM (10.7±1.5%) and continued to increase over time until 72±1.5% of cells expressed GFP at 48h. The activation of GFP expression was 3-fold less in SKES-1 7TGP cells, compared to that observed in HEK293T 7TGP cells. In SKES-1 7TGP cells, both the maximum GFP expression level (median fluorescence; 31±0.8) and percentage of cells with GFP expression (54±2.5%) was observed after 48h treatment with L-Wnt3A CM (Figure 3.4 A and B).

In both HEK293T 7TGP and SKES-1 7TGP cell lines the viable cell number was reduced when cells were grown for more than 20h in L-cell CM compared to growth of control cells cultured in normal cell-type specific media (Figure 3.4 C). The viable cell number of SKES-1 7TGP cells was reduced to 60±4.6% when grown in L-cell control CM, 72±4.6% in L-Wnt5A CM and decreased in a time-dependent manner with culture in L-Wnt3A CM to 33±0.7% after 48h. The viable cell growth of HEK293T 7TGP cells was reduced to a lesser extent; decreasing to 51±0.9% compared to that of control cells after 48h culture in L-Wnt3A CM (Figure 3.2 C)

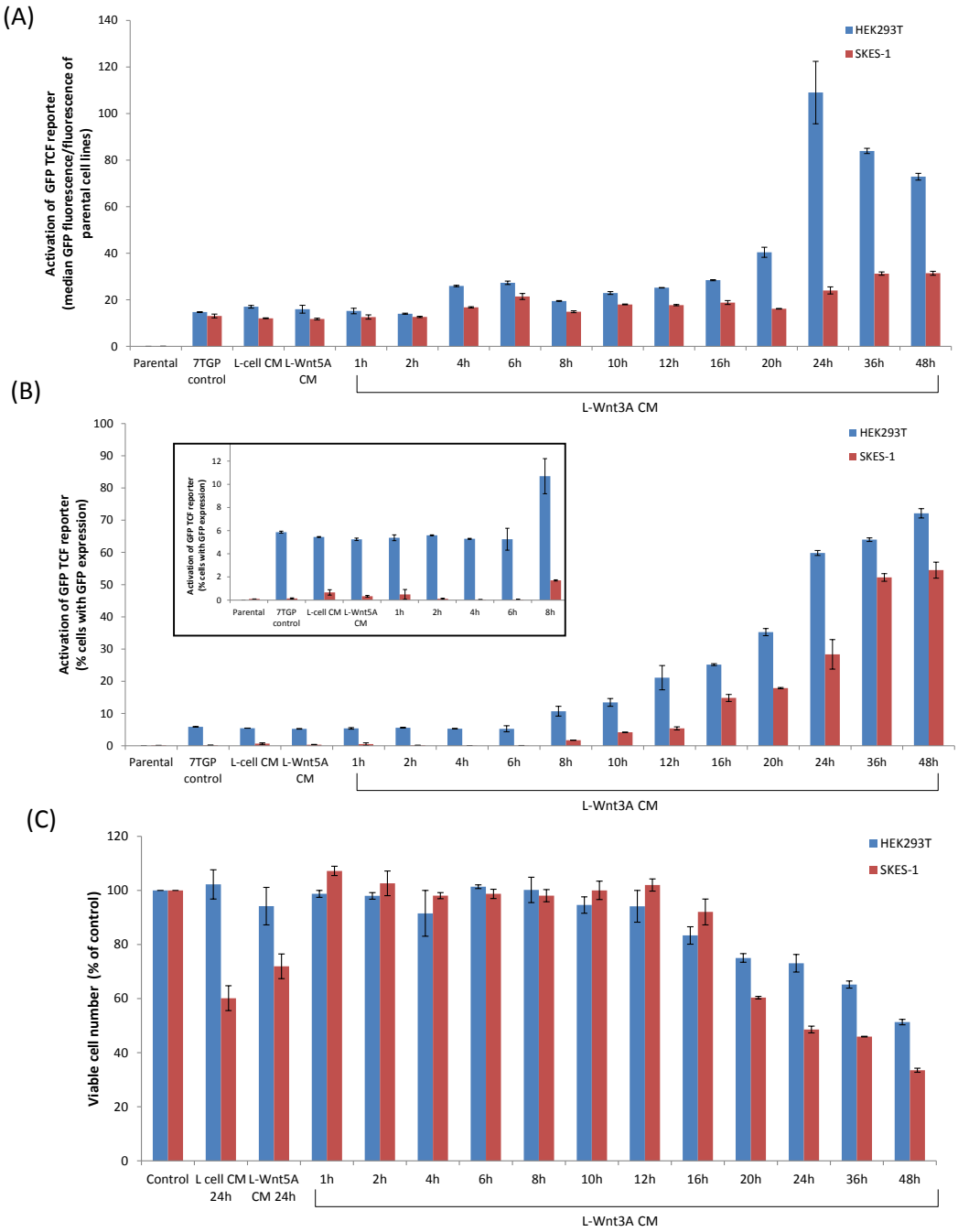

Figure 3.4 Stimulation of 7TGP cell lines with L-cell conditioned media HEK293T 7TGP and SKES-1 7TGP cell lines were cultured in normal cell-specific media (control) or in L-cell conditioned media or L-Wnt5A conditioned media for 24h or L-Wnt3A conditioned media for increasing periods of time. Cells were harvested, fixed with 1% PFA and analysed by flow cytometry to determine A) median fluorescence of GFP+ cells and B) percentage of GFP+ cells. Inset shows a magnified view of the first 9 conditions. C) Identically treated cells were harvested for analysis of viable cell number by trypan blue exclusion using the vi-cell automated cell counter. CM=conditioned media. Results presented from one experiment with three replicate wells (n=3) showing the mean (±SEM).

3.3.1.3.3 Viable cell number of ESFT cell lines cultured in L-cell conditioned media

Culture of cells in L-cell CM reduced the viable cell number of SKES-1 7TGP cells (Section 3.3.1.3.1), therefore the effect of L-cell CM on the growth of other ESFT cell lines was investigated. All ESFT cell lines and HEK293T cells had significantly reduced viable cell number when cultured in all three types of L-cell CM for 48h, compared to cell-type specific media ($p<0.0001$) (Figure 3.5 A and B). When ESFT cell lines were cultured in L-cell control media for 48h, all cell lines had less than 60% viable number compared to control cells (Figure 3.5, red bars). Viable cell number was reduced the least in TTC466 (56±3%) and the most in TC32 cells (23±2%). With the exception of TC32 cells, the decrease in viable cell number was greatest when cells were cultured in L-Wnt3A CM compared to L-cell control CM (Figure 3.5 B). This decrease was significant in A673 and RD-ES cell lines ($p<0.05$).

(A) 24h

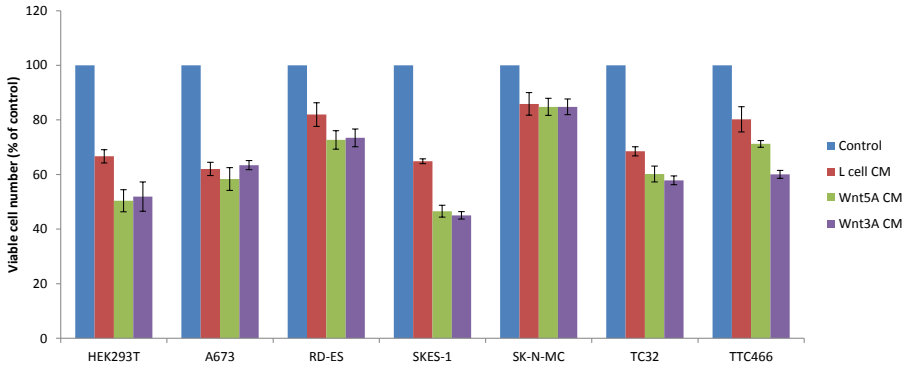

(B) 48h

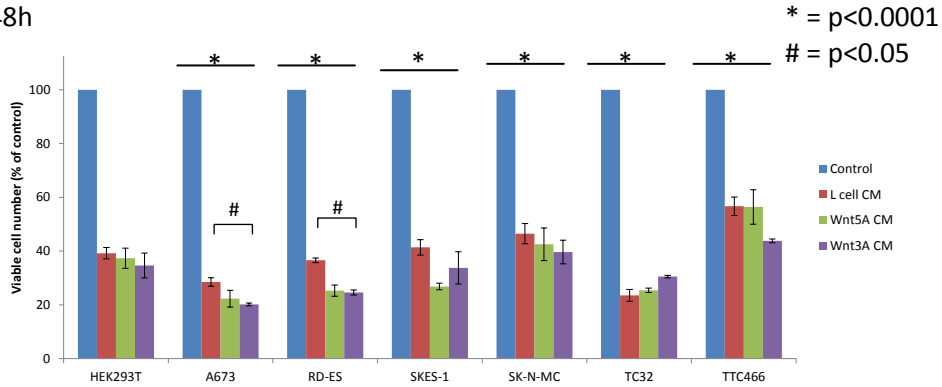

Figure 3.5 Growth of ESFT cell lines in L-cell conditioned media ESFT cell lines and HEK293T cells were cultured in normal, cell-type specific media (control), L-cell CM, L-Wnt5A CM or L-Wnt3A CM for A) 24h and B) 48h. Viable cell number was determined by trypan blue exclusion using the vi-cell automated cell counter. Results show mean of two independent experiments with three replicates per experiment (n=6) (±SEM).

3.3.1.3.4 Optimising stimulation of canonical Wnt signalling in 7TGP and 7TFP cells with recombinant Wnt3A protein.

L-Wnt3A CM was shown to reduce the viable cell number of ESFT cells (Section 3.3.1.3.3). Therefore I investigated the possibility of using recombinant (r) Wnt3A protein (5036-WN/CF, R&D) as an alternative method to stimulate the canonical Wnt signalling pathway but without reducing viable cell number. HEK293T 7TGP cells showed a dose-dependent increase in GFP reporter activation after 24h treatment with rWnt3A (Figure 3.6 A and B). Maximum GFP expression was observed following treatment with 500ng/ml rWnt3A (median fluorescence; 103±1). However, this was 63% less than the expression observed after treatment with L-Wnt3A conditioned media for the same period of time (median fluorescence; 164 ±7) (Figure 3.6 A). When treated with rWnt3A (500ng/ml) 41±1% of HEK293T 7TGP cells expressed GFP after 24h, although this was again less than the percentage of cells expressing GFP after L-Wnt3A CM treatment (58±0.6%). Importantly, however the viable cell number of HEK293T 7TGP cells did not decrease when cells were cultured in 500ng/ml rWnt3A; this compares to a reduction of viable cell number of 25±3% when HEK293T 7TGP cells were grown in L-Wnt3A CM compared to DMEM (normal media) (Figure 3.6 C).

When HEK293T 7TGP cells were treated with rWnt3A (200ng/ml) or L-Wnt3A CM over a time course, maximum activation of the GFP reporter was observed after 24h of treatment (Figure 3.7 B). The activation observed after stimulation with rWnt3A was significantly less than the stimulation observed with L-Wnt3A CM ($p<0.01$, median fluorescence; 51±2 and 109±13, respectively).

HEK293T cells transduced with the luciferase reporter 7TFP (HEK293T 7TFP) were also maximally activated after 24h treatment with rWnt3A (200ng/ml) or L-Wnt3A CM (Figure 3.7 C). Again, stimulation was significantly greater after treatment with L-Wnt3A CM rather than rWnt3A ($p<0.01$, 223 $x10^5$ compared to 283 $x10^5$ relative light units (RLU)). However the fold difference in activation between 7TFP cells treated with rWnt3A and L-Wnt3A CM was only 1.3-fold, this was significantly less($p<0.05$) than the observed difference using the 7TGP reporter (2.7-fold).

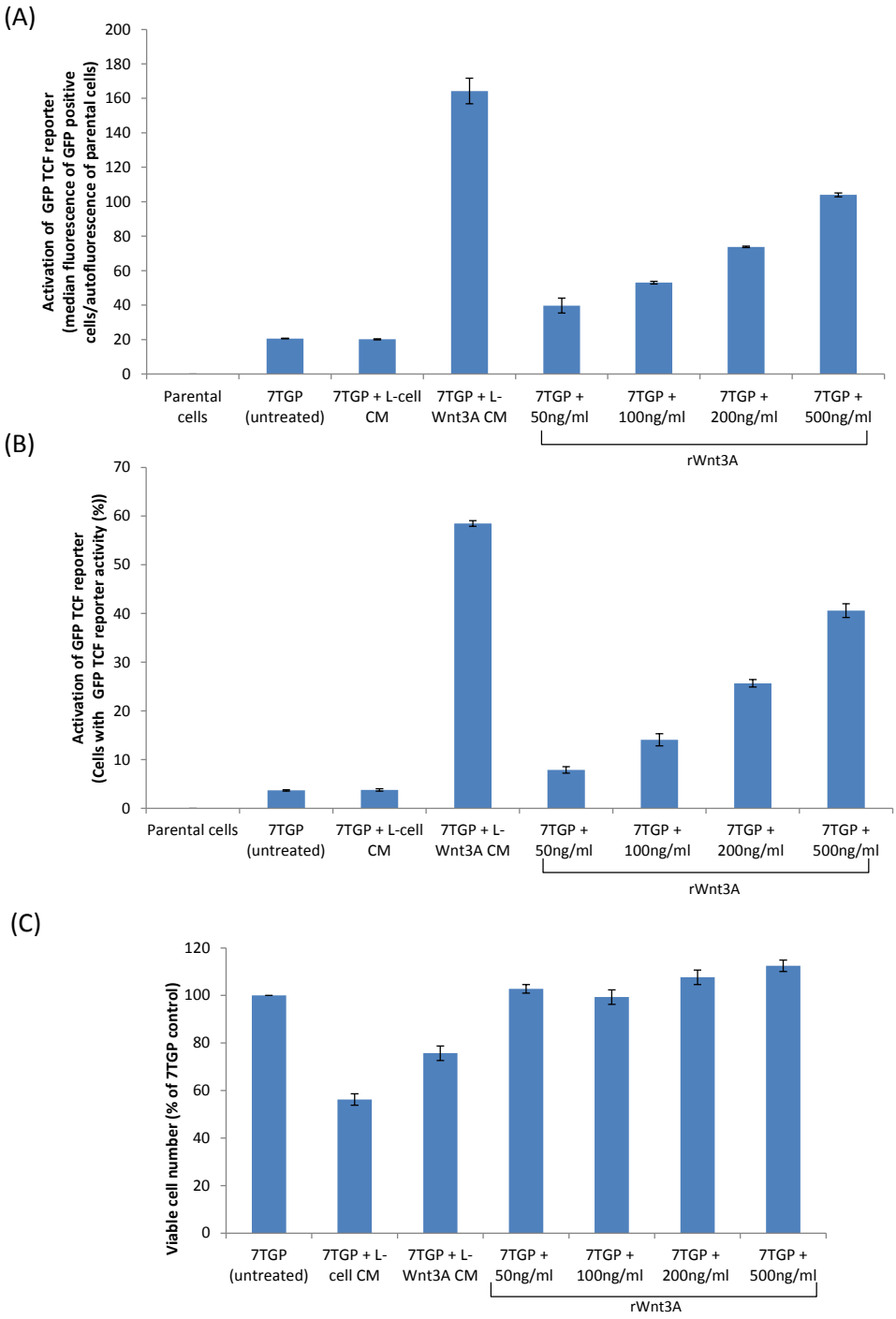

Figure 3.6 Stimulation of HEK293T 7TGP cells with L-cell CM and recombinant Wnt3A protein HEK293T 7TGP cells were treated with L-cell CM, L-Wnt3A CM or increasing concentrations of recombinant Wnt3A protein (50-500ng/ml) for 24h. Cells were harvested, fixed with 1% PFA and GFP expression analysed using flow cytometry to determine A) median GFP fluorescence and B) percentage of GFP+ cells. C) Identically treated cells were harvested for analysis of viable cell number by trypan blue exclusion using the vi-cell automated cell counter and presented as percentage of HEK293T 7TGP control cells cultured in DMEM. Results show the mean of two independent experiments with three replicates per experiment (n=6) (±SEM). CM= conditioned media, r= recombinant.

(A)

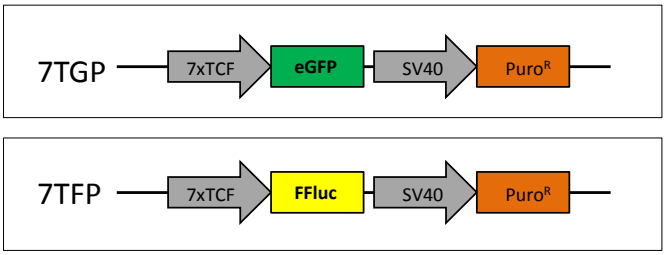

(B) HEK293T 7TGP

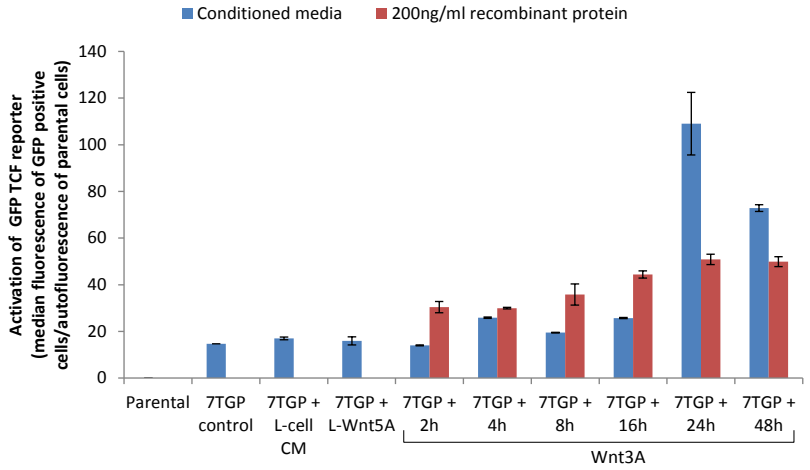

(C) HEK293T 7TFP

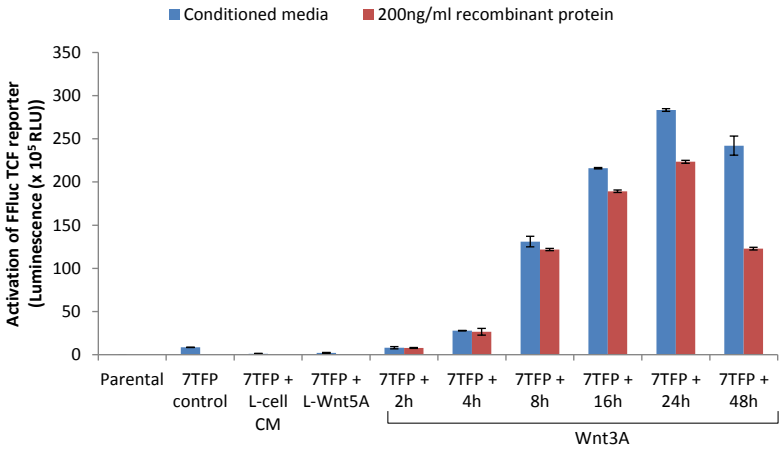

Figure 3.7 Activation of GFP and luciferase reporter plasmids in HEK293T cells after treatment with L-Wnt3A CM and recombinant Wnt3A protein A) Schematic diagram of the 7TGP and 7TFP plasmids. Adapted from Fuerer et al., (2010). B) HEK293T 7TGP and C) HEK293T 7TFP cells were cultured for 24h in normal media (control) or in L-cell CM, L-Wnt5A CM or for increasing lengths of time (2h-48h) in Wnt3A (either L-Wnt3A CM or rWnt3A (200ng/ml)). For HEK293T 7TGP cells GFP activation was analysed by harvesting cells, fixing in 1% PFA and the median fluorescence increase from parental cells quantified by flow cytometry. For HEK 293T 7TFH cells luciferase activity was measured using the Luciferase Assay (Section 3.2.5). Results are shown as the mean of two independent experiments with three replicates per experiment (n=9) (±SEM). CM= conditioned media, r= recombinant, FFluc= firefly luciferase. RLU= relative light units, Puro^R= puromycin resistance.

3.3.1.3.5 Quantification of Wnt3A protein in L-Wnt3A conditioned media

In both HEK293T 7TGP and HEK293T 7TFP cells, activation of canonical Wnt signalling was greater in response to L-Wnt3A conditioned media than in response to Wnt3A recombinant protein (Section 3.3.1.3.4). To investigate this observation further, the concentration of Wnt3A in the L-Wnt3A CM was quantified by western blot. The conditioned media used in previous experiments to treat cells consisted of media collected from L-Wnt3A cells after 4 and 7 days of culture, which was pooled and filtered through a 0.2µm membrane. The effect of pooling and filtering was therefore also investigated.

A band corresponding to Wnt3A (approximately 37 kDa) could be detected in L-Wnt3A CM but not L-cell control CM (Figure 3.8 A). Densitometry was performed and a concentration curve generated from the rWnt3A samples which was used to estimate the concentration of Wnt3A in the L-Wnt3A CM samples (Figure 3.8 B). Analysis showed that CM collected from L-Wnt3A cells after 4 days of culture had the lowest concentration of Wnt3A (534ng/ml), the concentration of Wnt3A was increased to 642ng/ml in CM collected after 7 days of culture. Pooling media collected at day 4 and day 7 did not increase the concentration of Wnt3A (641ng/ml) compared to using only media collected at day 7. Sterile filtering the CM through a 0.2µm membrane resulted in 9% of the Wnt3A protein being lost on the filter; the Wnt3A concentration was reduced from 642ng/ml to 587ng/ml. The concentration of the L-Wnt3A CM used in previous experiments (Day4 + 7, filtered) was estimated to contain 587ng/ml of Wnt5A protein, a much higher concentration than the concentration of rWnt3A used (200ng/ml), which explains why the conditioned media have a greater effect than the recombinant protein.

The rWnt3A bands observed at 37 kDa correspond to the predicted molecular weight of Wnt3A. However, the Wnt3A protein in the L-Wnt3A CM was approximately 41.5 kDa (Figure 3.8 A). This may reflect post transcriptional modifications of the protein and could also contribute to the greater stimulatory effect of L-Wnt3A CM.

(A)

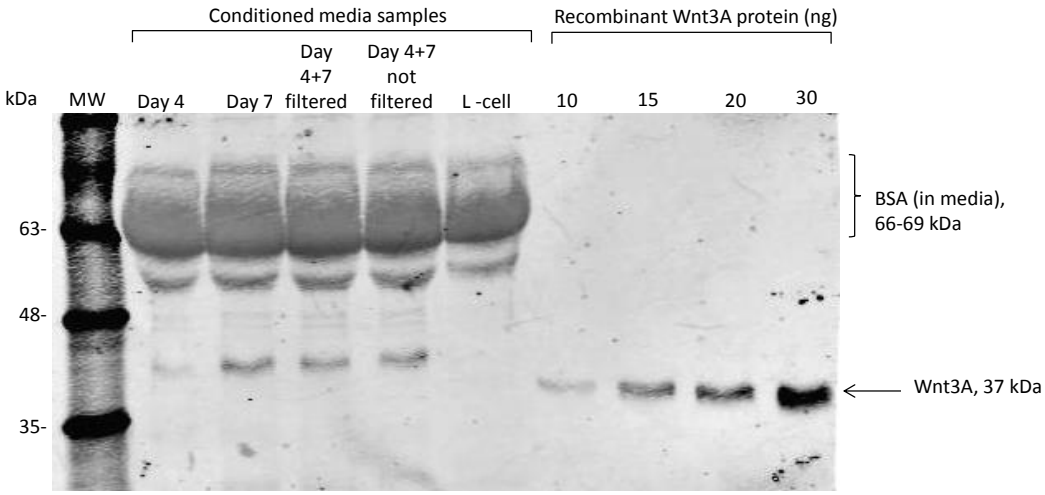

(B)

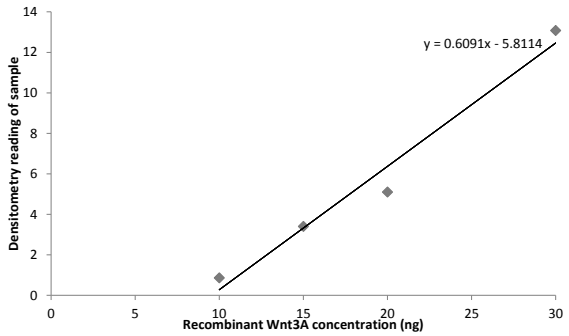

	Day 4	Day 7	Day 4+7 filtered	Day 4+7 not filtered
Densitometry of sample	0.55	1.91	1.21	1.9
Concentration (in 20µl)	10.7	12.8	11.7	12.8
Concentration/ml	533.8	642.3	**586.5**	641.5

Figure 3.8 Quantifying the concentration of Wnt3A in L-Wnt3A CM L-Wnt3A cells were seeded into 10cm^2 dishes and media collected after 4 and 7 days. Media was pooled and filtered through a 0.2µm Aerodisc® filter (PALL Life Sciences) as appropriate. L-cell CM was used as a negative control. A) For quantification, 20µl of each sample of collected CM and increasing concentrations of recombinant Wnt3A protein were analysed by western blot to determine the concentration of Wnt3A. Densitometry was performed and B) a standard curve generated from the values of known concentrations of recombinant protein. The concentration of Wnt3A in the L-Wnt3A CM samples was determined from the standard curve. MW= molecular weight.

3.3.2 Measuring the activity of the canonical Wnt signalling pathway in ESFT cell lines

3.3.2.1 7TGP reporter activity in ESFT cell lines

In ESFT cell lines transduced with the 7TGP reporter plasmid, endogenous activity of the canonical Wnt signalling pathway was detected in RD-ES (fold change from parental cells; 1.3±0.03) and SK-N-MC cells (fold change; 1.2±0.03). The activity of the pathway was low compared to HEK293T 7TGP cells (fold change; 1.9±0.07) (Figure 3.9 A, Parental vs. 7TGP Control). Treatment with rWnt3A (200ng/ml, 24h) significantly increased GFP reporter expression in all the ESFT cell lines, except TC32 and TTC466 ($p<0.05$). Activation was greatest in SK-N-MC cells (3±0.4-fold) and lowest in TTC466 cells (1.3±0.07-fold). The fluorescence plots generated reveal that even after treatment with Wnt3A, there is a population of cells that do not fluoresce consistent with heterogeneous activity of canonical Wnt signalling; some cells with high GFP expression and others with medium, low and no GFP expression. Treatment with recombinant noncanonical ligand Wnt5A (200ng/ml, 24h) did not increase GFP reporter activity in any cell line, confirming the specificity of the reporter to detect canonical Wnt signalling activation.

In all ESFT cell lines, less than 1% of cells had endogenous activity of the GFP reporter, and this was not increased with rWnt5A treatment (Figure 3.9 B). However, after treatment with rWnt3A (200ng/ml, 24h), the percentage of cells expressing GFP was significantly increased in all cell lines ($p<0.05$). After treatment with rWnt3A, the percentage of cells with GFP expression was significantly higher in SK-N-MC ($p<0.05$, 37±2%) and was significantly lower in TC32 (11±2%) and TTC466 (7±0.2%) ($p<0.05$) cells, compared to the other ESFT cell lines, consistent with heterogeneous effects of Wnt3A.

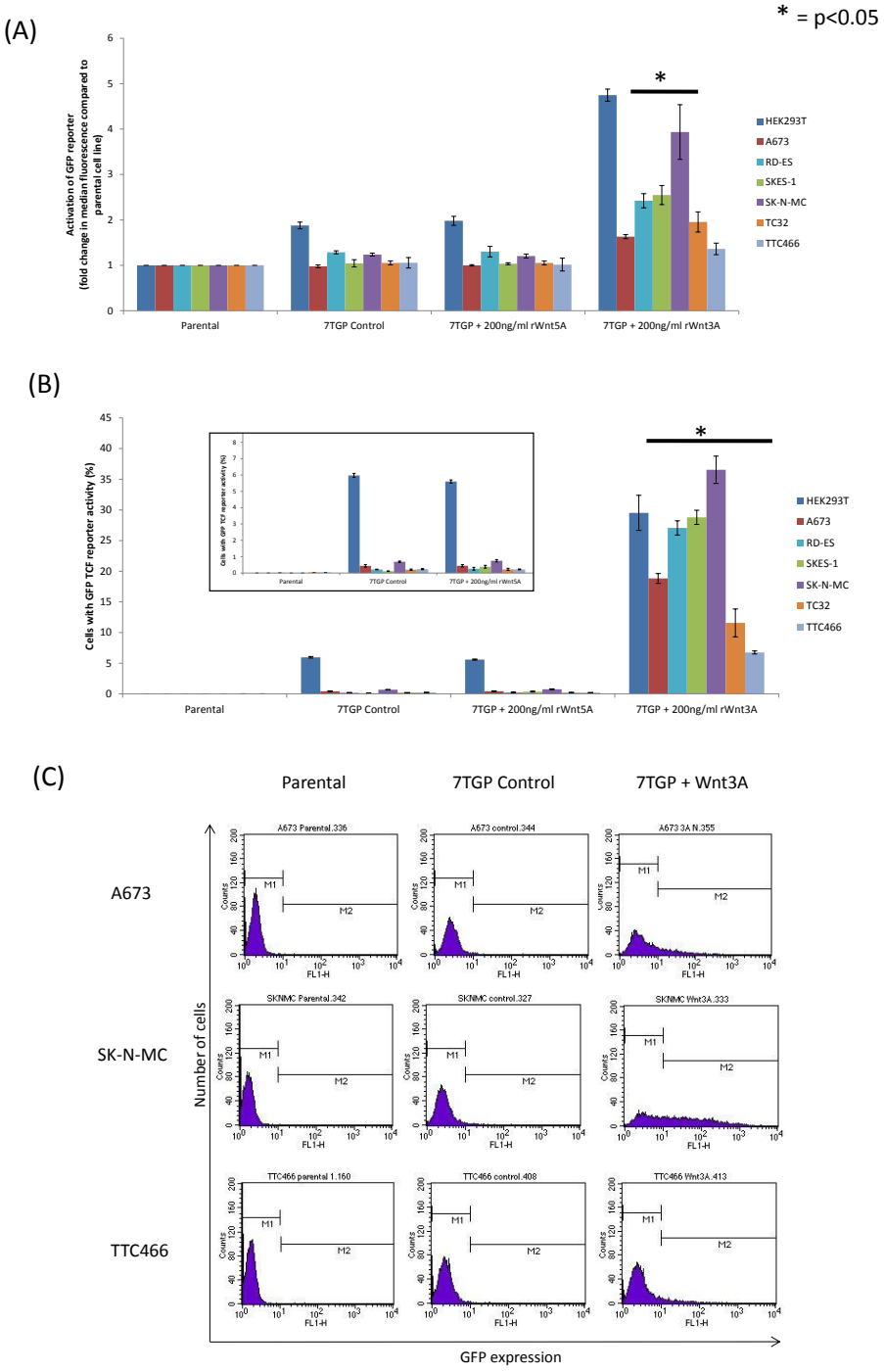

Figure 3.9 GFP reporter activation in ESFT cell lines ESFT-7TGP and HEK293T-7TGP (positive control) cell lines were treated with rWnt5A (200ng/ml) or rWnt3A (200ng/ml) for 24h. Cells were harvested, fixed in 1% PFA and GFP reporter expression analysed by flow cytometry to determine A) median fluorescence and B) percentage cells with GFP expression. Inset shows magnified view of parental, control cells and cells treated with Wnt5A. Data is presented relative to the parental cell line without 7TGP reporter present. Results show the mean of three independent experiments with three replicates per experiment analysing 10,000 events per sample (n=9) (±SEM) C) Representative fluorescence plots for A673, SK-N-MC and TTC466 cell lines showing parental cells, 7TGP control cells and 7TGP cells after treatment with rWnt3A (200ng/ml, 24h). The M1 region designated negative events and M2 region positive events.

3.3.2.2 7TFP reporter activity in ESFT cell lines

Endogenous reporter activity was detected in all ESFT cells transduced with the 7TFP plasmid (Figure 3.10 A, Parental vs. 7TFP Control). This is in contrast to ESFT cells transduced with the 7TGP plasmid where endogenous GFP expression could only be detected in RD-ES and SK-N-MC cell lines, and demonstrates the increased sensitivity of the firefly luciferase reporter. Relative to the parental cell lines with no 7TFP reporter present, endogenous luciferase activity appeared heterogeneous between ESFT cell lines; lowest in SKES-1 (217±24-fold) and highest in A673 (793±20-fold). However, the endogenous activity could not be compared statistically as a viable cell count was not performed, meaning there may have been variation in the number of cells assayed between cell lines. Treatment with rWnt5A (200ng/ml, 24h) did not increase the luciferase activity in any ESFT cell line, consistent with the results observed using the GFP reporter. However, treatment with rWnt3A (200ng/ml, 24h) significantly increased the luciferase reporter activity in all cell lines ($p<0.05$) (Figure 3.10 A). When compared to the level of endogenous reporter activity within each cell line, the increase in luciferase reporter activity was heterogeneous between the cell lines (Figure 3.10 B). Significantly greater stimulation following treatment with Wnt3A was observed in RD-ES (188±14-fold), SKES-1 (167±25-fold) and SK-N-MC (176±24-fold) cell lines ($p<0.01$).

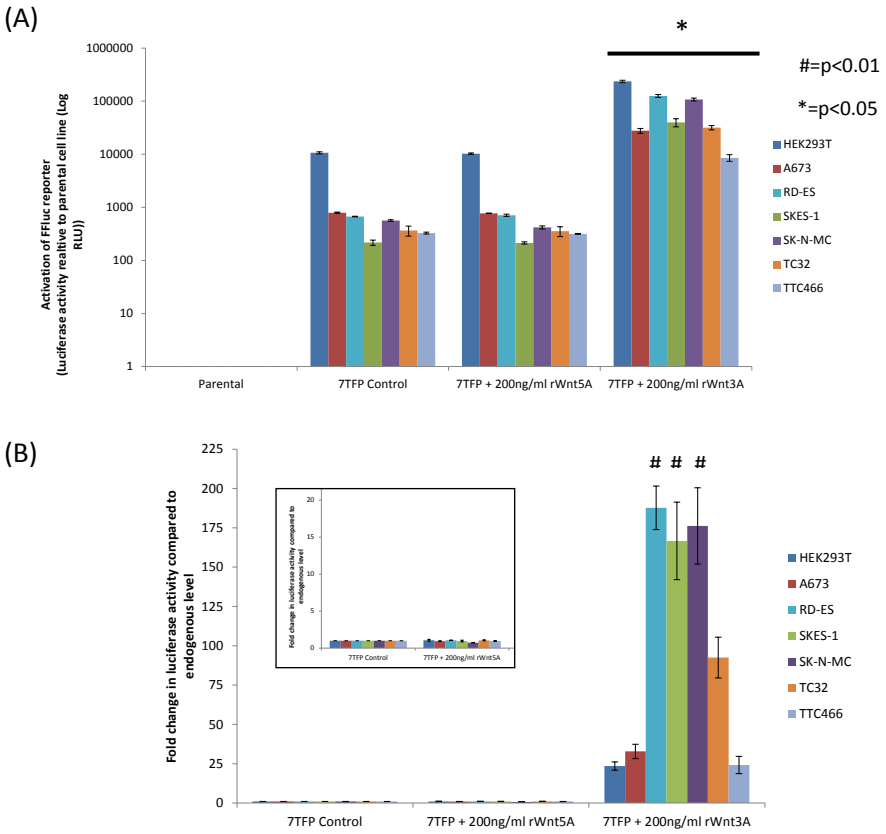

Figure 3.10 Firefly luciferase reporter activation in ESFT cell lines ESFT-7TFP and HEK293T-7TFP (positive control) cell lines were treated with rWnt5A (200ng/ml) or rWnt3A (200ng/ml) for 24h. Luciferase activity was determined using the Luciferase Assay (Section 3.2.5). A) Luciferase activity relative to the parental cell line with no 7TFP plasmid present presented as Log RLU B) Fold increase in luciferase reporter after Wnt treatment relative to 7TFP control (untreated) cells. Inset shows magnified view of control and Wnt5A treated cells. Results presented as the mean of three independent experiments with three replicates per experiment (n=9) (±SEM).

3.3.3 Effect of recombinant Wnt3A and Wnt5A on the viable cell number of ESFT cell lines.

To confirm that the increase in GFP and luciferase reporter activity observed with rWnt3A treatment was not simply due to an increase in the number of viable cells, growth curves were carried out with ESFT cell lines in the presence of rWnt5A (200ng/ml) and rWnt3A (200ng/ml). Treatment with either Wnt3A or Wnt5A for up to 72h had no significant effect on the viable cell number of any ESFT cell line (Figure 3.11 A-F).

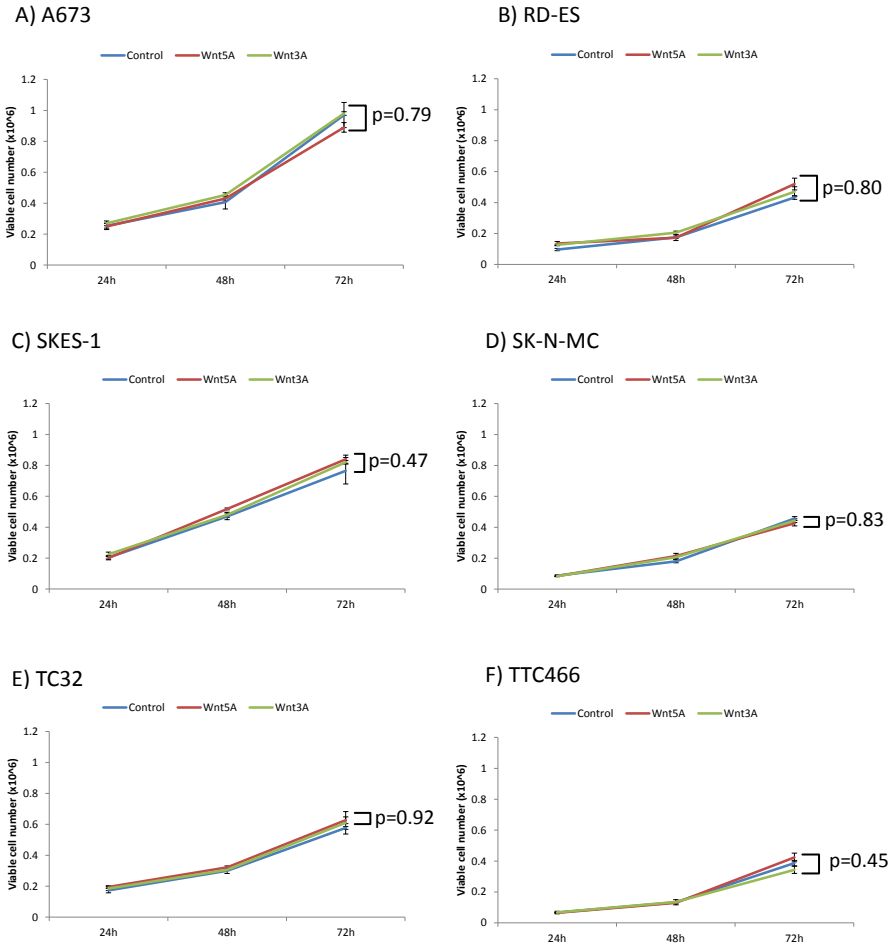

Figure 3.11 ESFT viable cell number after treatment with Wnt3A and Wnt5A ESFT cell lines were seeded into 24 well plates and allowed to adhere for 24 h. Cells were treated with 200ng/ml rWnt3A or 200ng/ml rWnt5A for 24, 48, or 72h. Viable cell number was determined by trypan blue exclusion using the Vi-cell automated cell counter. Results are shown as the mean of two independent experiments with three replicates per experiment (± SEM).

3.3.4 Confirmation of downstream activation of the canonical Wnt signalling pathway

3.3.4.1 Optimising conditions to detect increase in total and active β-catenin after treatment with Wnt3A

To confirm that canonical Wnt signalling was activated by Wnt3A, I measured the levels of both total and active β-catenin in treated cells by western blot. An increase in intracellular β-catenin is known to be a downstream consequence of active canonical Wnt signalling (Gujral, 2010, Hernandez, 2012). Endogenous expression of both total and active (nonphosphorylated) β-catenin was detected in HEK293T cells after treatment with rWnt3A (200ng/ml) (Figure 3.12 A). The level of both active and total β-catenin was increased after 30 min (Figure 3.12 A and B). Densitometry revealed that the peak increase in both active and total β-catenin was observed after 4h treatment with rWnt3A; there was a 6-fold increase in both active (6±0.3) and total (6±0.2) β-catenin. The level of both active (4±0.3-fold) and total (2±0.2-fold) β-catenin remained elevated in HEK293T cells with up to 24h treatment with Wnt3A.

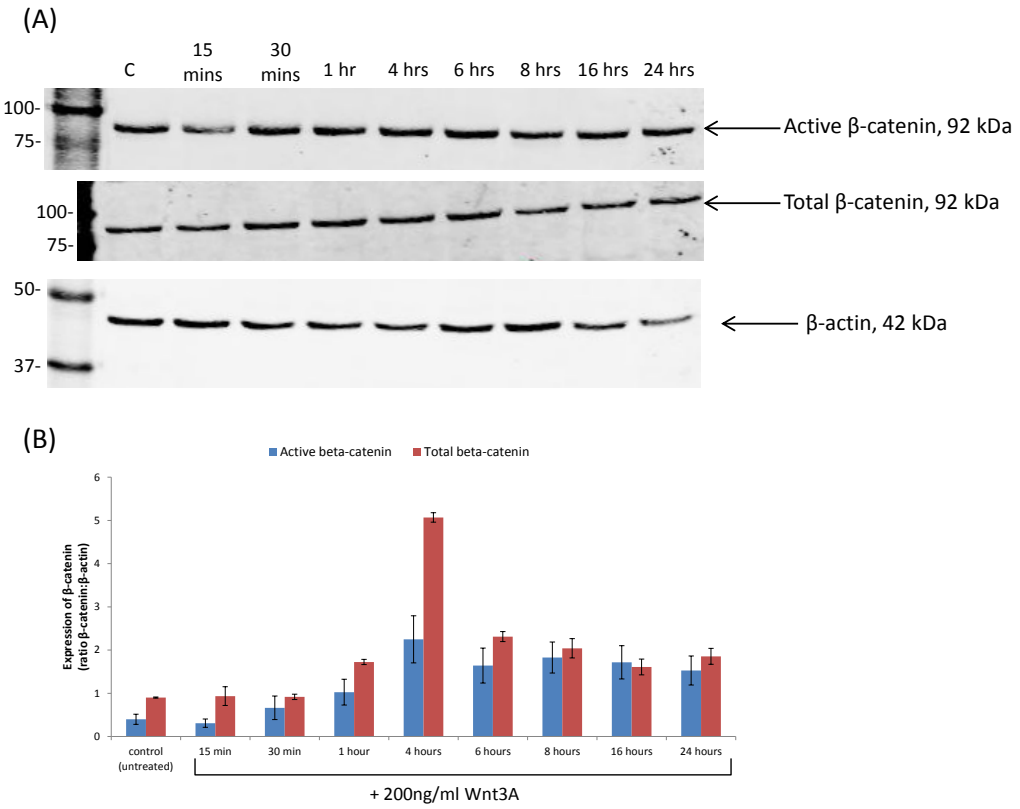

Figure 3.12 Downstream activation of canonical Wnt signalling in HEK293T cells following treatment with Wnt3A HEK293T cells were seeded into 6 well plates and allowed to adhere overnight. Cells were maintained in normal media (control) or treated with 200ng/ml Wnt3A for increasing lengths of time (15 min-24h). A) Total protein was extracted and expression of total and nonphosphorylated (active) β-catenin analysed by western blot. Expression of β-actin was used as a loading control. Representative of two independent repeats. B) Bands were quantified by densitometry and total and active β-catenin expression levels calculated as ratios compared to β-actin expression. Results presented as the mean of two independent experiments (±SEM).

3.3.4.2 Level of total and active β-catenin in ESFT cells after Wnt3A treatment

The expression levels of both total and active β-catenin were investigated by western blot in ESFT cells after treatment with Wnt3A (200ng/ml, 4 h). In addition, expression of cyclin D1 was examined as it is a reported downstream target of canonical Wnt signalling (Shtutman et al. 1999). The level of both total and active β-catenin was increased in HEK293T cells after treatment with Wnt3A, however the 2-fold increase was less than the 6-fold increase observed in previous experiments (Section 3.3.4.1) (Figure 3.13 A,B and C). In ESFT cell lines, an increase in total β-catenin was detected in RD-ES (3.5-fold) and SKES-1 (2.5-fold) following treatment with Wnt3A, but not in the other cells lines (Figure 3.13 A and B). In some cell lines for example A673 and TTC466 there was a decrease in total β-catenin after treatment with Wnt3A. In SK-N-MC cells, total β-catenin levels were increased (1.6-fold) after treatment with Wnt5A (200ng/ml, 4h). An increase in active β-catenin was only observed in SKES-1 cells (1.3-fold) (Figure 3.13 A and C). A slight increase in cyclin D1 expression was detected in RD-ES (1.2-fold), SKES-1 (1.3-fold) and SK-N-MC (1.7-fold) cells after treatment with rWnt3A, however an increase in cyclin D1 expression was also detected after treatment with rWnt5A in A673 (2-fold) and TC32 (1.2-fold) (Figure 3.13 A and D).

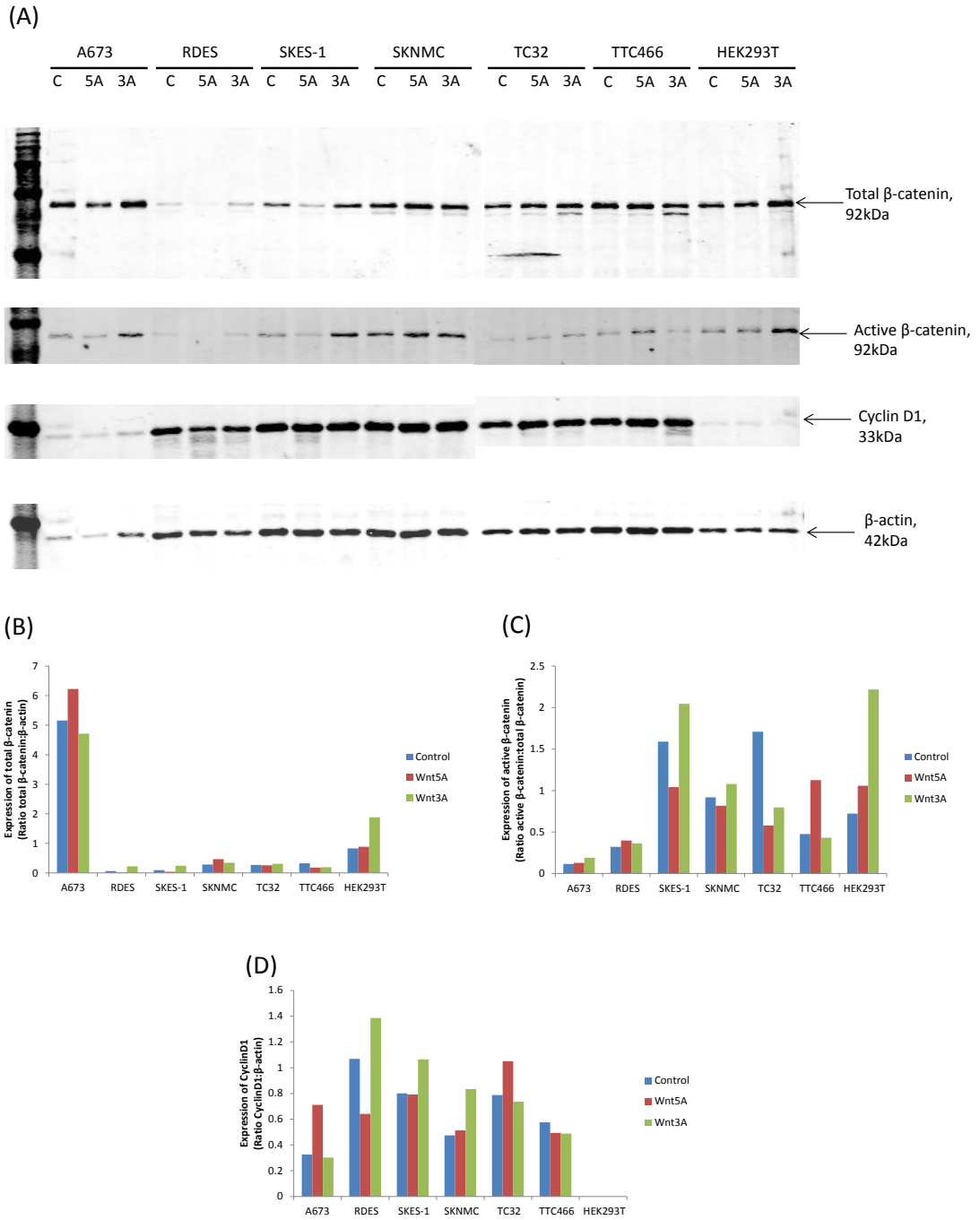

Figure 3.13 Downstream activation of canonical Wnt signalling in ESFT cells after treatment with Wnt3A ESFT and HEK293T (positive control) cells were seeded into 6 well plates. After 24h cells were maintained in normal media (control) or treated with rWnt3A (200ng/ml) or rWnt5A (200ng/ml) for 4h. A) Total protein was extracted and expression of total and nonphosphorylated (active) β-catenin, and cyclinD1 analysed by western blot. Expression of β-actin was used as a loading control. Bands were quantified by densitometry and expression of B) Total β-catenin calculated as the ratio compared to β-actin expression C) Active β-catenin calculated as the ratio compared to total β-catenin expression and D) CycinD1 calculated as the ratio compared to β-actin expression.

3.4 Discussion

In this chapter I have optimised and validated an assay to measure the functional activity of canonical Wnt signalling using a lentiviral luciferase reporter system. Using this assay, endogenous Wnt signalling activity was detected in all ESFT cell lines. This is in concordance with research which was published during the course of the current study, which also demonstrated endogenous canonical Wnt signalling in the CHLA25 ESFT cell line using the 7TFP reporter plasmid (Scannell et al. 2013). These data are in contrast to previous studies in ESFT cells where no or extremely low basal canonical Wnt signalling could be detected, and was not stimulated following treatment with Wnt3A (Hu-Lieskovan et al. 2005, Navarro et al. 2010, Vijayakumar et al. 2011). These differences most probably reflect the use of the less sensitive TOPFlash reporter assay, rather than the luciferase based assay system I have used in my studies.

Consistent with previous studies, ESFT cell lines were successfully infected with lentiviral vectors (McKinsey et al. 2011, Iida et al. 2013). The infection rate of lentiviral particles in TC32 cells was greater than in the other ESFT cell lines. The lentiviral vectors used were pseudotyped with the VSV-G envelope protein which has been shown to increase the infection capabilities of lentiviruses to almost all mammalian cells, including nondividing and difficult to infect cells (Akkina et al. 1996, Naldini et al. 1996). It has recently been shown that low-density lipoprotein receptor (LDLR) is the main receptor for VSV, and therefore the entry method of VSV-G pseudotyped lentiviral vectors into cells (Finkelshtein et al. 2013). Although LDLRs are ubiquitously expressed in all human cells, the level of expression may be heterogeneous, and upregulation of LDLR has been reported in colorectal cancer (Lum et al. 1999). Therefore, ESFT cell lines may have differential expression of the LDLR which may explain the differences observed in infection rates. To compensate for this observation, TC32 cells were infected using a lower MOI than the other cell lines. However this still resulted in greater median GFP expression level in these cells after infection with the pLV-Green plasmid. The consequences of this observation may be important as expression of the reporter plasmids may also be higher in TC32 cells, resulting in a falsely high estimation of canonical Wnt signalling. That said, endogenous canonical Wnt signalling activity measured using the 7TGP and 7TFH reporter plasmids was low in TC32 cells compared to the other ESFT cell lines.

To activate the canonical Wnt signalling pathway in cells and to confirm the specificity of the reporter system, treatment with the canonical Wnt ligand Wnt3A is commonly used. In this study, the activation of canonical Wnt signalling was measured using the 7TGP and

7TFP plasmids in response to both conditioned media from L-cells overexpressing Wnt3A and recombinant Wnt3A protein. An important observation was that the viable cell number of all ESFT cell lines was reduced when cells were grown in L-cell conditioned media. One possible explanation for this reduced cell viability could be that the conditioned media used was DMEM (+10% FCS) and 5 out of 6 of the ESFT cell lines are not normally cultured in this media. However, this cannot be the only explanation since A673 cells are routinely cultured in DMEM (+10% FCS) and yet treatment with L-cell conditioned media also significantly reduced viable cell number. A further consideration is the fact that the conditioned media is collected from L-cells after 4 and 7 days in culture (and subsequently pooled together), and so could have been partially expended and was therefore not optimal for culturing cells in the long time course experiments. Viable cell number was reduced when cells were grown in L-cell (control) and L-Wnt5A conditioned media and furthermore, viable cell number was not reduced in ESFT cell lines cultured in the presence of recombinant Wnt3A protein. This suggests that the decrease in viable cell number is not due to the Wnt3A protein. That said, some cell lines including A673 and RD-ES cells had significantly lower viable cell number after 48h when treated with L-Wnt3A conditioned media compared to when cultured in L-cell control CM. This suggests that Wnt3A may be having an effect on the viable cell number of some cell lines. Since activation of the canonical Wnt signalling pathway by overexpression of Wnt3A can lead to upregulation of other proteins, L-Wnt3A CM also contains other secreted factors (Willert et al. 2003). For example, members of the fibroblast growth factor (FGF) family including FGF4 (Kratochwil et al. 2002) and FGF9 (Hendrix et al. 2006) have been shown to be induced by canonical Wnt signalling. This is potentially important as another FGF family member FGF2, has been shown to induce cell death in ESFT cell lines (Westwood et al. 2002). It would therefore be useful to carry out a protein profile on L-Wnt3A conditioned media to elucidate what else is secreted by these cells. However, taken together my data suggest that conditioned media is not suitable for treating ESFT cell lines, as any change in canonical Wnt signalling may be due to a stress response in cells being cultured in conditions which they do not tolerate or by contaminating factors within the conditioned media and not necessarily Wnt3A itself.

In HEK293T cells transduced with both 7TGP and 7TFP reporter plasmids, canonical Wnt signalling was activated to a greater extent by L-Wnt3A conditioned media than recombinant Wnt3A protein. This is perhaps surprising as the concentration of Wnt3A in the conditioned media has been previously reported to be 200ng/ml (Willert et al. 2003). This is the concentration of recombinant protein used in this study, and increasing the

concentration to 500ng/ml did not increase the activation of canonical Wnt signalling in HEK293T 7TGP cells, to that observed after treatment with L-Wnt3A conditioned media. However, I found that the concentration of Wnt3A in L-Wnt3A conditioned media was almost 600ng/ml, which may explain the differences observed. This could be confirmed by directly comparing the activity of the canonical Wnt signalling pathway when cells are stimulated with 200ng/ml recombinant Wnt3A and L-Wnt3A conditioned media that had been diluted to an equivalent concentration. In addition, the Wnt3A detected in conditioned media had a higher molecular weight than the recombinant Wnt3A protein. Wnt3A is known to be glycosylated and acylated. In particular, the palmitic acid attached to cysteine 77 has been shown to be critical for the activity of Wnt3A (Willert et al. 2003). Therefore, it is possible that recombinant Wnt3A lacks this post-transcriptional modification and this could also explain the differences in activity observed. Finally, as previously mentioned, overexpression of Wnt3A is known to lead to upregulation of factors downstream of canonical Wnt signalling such as FGF proteins, therefore it is possible that some of these factors may also additionally activate canonical Wnt signalling after treatment with L-Wnt3A CM.

In ESFT cells, using the 7TGP (GFP) reporter plasmid, endogenous Wnt signalling could only be detected in RD-ES and SK-N-MC cell lines, whereas using the 7TFP (luciferase) reporter endogenous activity was measured in all cell lines. These data demonstrate that firefly luciferase is a more sensitive reporter gene than GFP. This is in agreement with current literature indicating that luciferase reporter genes can deliver 10- to 1000-fold higher assay sensitivity than GFP (Vidugiriene et al. 2008). Fluorescent reporters such as GFP rely on photons of light to excite the sample and the emission of photons is detected. Fluorometers cannot precisely distinguish between the photon influx and photon emission, meaning there will inherently be low background levels of fluorescence when using GFP reporters, which makes detecting very small changes extremely difficult. In addition, although GFP is not endogenously expressed in mammalian cells, cellular metabolites such as flavins may fluoresce resulting in autofluorescence, which can limit the specificity of the GFP reporter assay. Indeed, autofluorescence was detected in all parental ESFT cell lines that had not been transduced with the 7TGP reporter, limiting the sensitivity of the assay. In contrast, the luciferase assay chemistry is based on an exothermic chemical reaction whereby beetle luciferase is oxidised to oxyluciferin by firfely luciferase, which produces light. As luciferase is not expressed in mammalian cells there is no background and the assay is very specific. In addition, current assay technologies mean that less than 10,000 molecules per sample can be detected, this allows for a large dynamic range with changes

in light production across four to eight orders of magnitude detected in the linear range of the assay (Fan and Wood 2007). Another important consideration is the fact that GFP has a longer half-life (around 26h) compared to luciferase (3-4 h) meaning a GFP reporter is less able to detect dynamic changes in Wnt signalling (Vidugiriene et al. 2008). However, the disadvantage of using a luciferase reporter is that it is not possible to examine the expression in individual cells, therefore differences in canonical Wnt signalling in sub-populations of cells could not be investigated. Since less than 1% of ESFT cells had endogenous canonical Wnt signalling activity detected using the 7TGP reporter this is a limitation.

Using both reporter plasmids the activity of the canonical Wnt signalling pathway was significantly increased in all ESFT cell lines after treatment with recombinant Wnt3A. This is in contrast to a previous study which reported that canonical Wnt signalling could not be stimulated in ESFT cell lines (Navarro et al. 2010). It has been reported that this was because the EWS-FLI1 protein represses canonical Wnt signalling by interacting with β-catenin/TCF complexes. My data suggest this is not the case and this will be further investigated in Chapter 6. In both 7TGP and 7TFP transduced cells, the response to Wnt3A was greatest in RD-ES, SKES-1 and SK-N-MC cell lines and lowest in A673 and TTC466 cell lines (summarised in Table 3.1). This is not consistent with the pattern of active (nonphosphorylated) β-catenin previously observed (in Chapter 2) which was similar between ESFT cell lines, but highest in TC32 cells. High expression of nuclear β-catenin was also detected in A673 and TTC466 cell lines, demonstrating the weaknesses of investigating β-catenin expression and localisation as markers for the activity of the canonical Wnt signalling pathway. In 7TGP transduced cells, the percentage of GFP expressing cells was also significantly increased in all ESFT cells after the addition of recombinant Wnt3A. However the maximum positivity observed was only 37% (in SK-N-MC cells) and GFP expression was only observed in a maximum of 7% of TTC466 cells. In ESFT cell lines the fluorescent plots revealed a peak of negative cells with wide tail, consistent with heterogeneous expression of GFP, some cells with high expression and others with median or low expression. The fact that not all cells had GFP expression may reflect the lack of sensitivity of the GFP reporter or indicate that some ESFT cells within cell lines are not capable of activating Wnt signalling. This could be due to the expression levels of activator and/or inhibitor proteins. For example, canonical Wnt signalling was increased the most in SK-N-MC and SKES-1 cell lines following treatment with Wnt3A, and these cell lines had lower expression of the FRZB inhibitor and higher expression of the activators LEF1 and Wnt10A (in Chapter 2).

Cell Line	Predicated **Canonical or noncanonical** (based on Wnt ligand expression)	**Active β-catenin** expression (ratio to total β-catenin)	**GFP reporter**		**Luciferase reporter**	
			Endogenous activity (median fluorescence/% positive cells)	**Response to Wnt3A** (fold increase in fluorescence/% positive cells)	**Endogenous activity** (Luminescence)	**Response to Wnt3A** (fold increase in luminescence)
A673	Canonical	0.28	0.94/0.4	1.63/19	**Highest** 792.93	32.83
RD-ES	Noncanonical	0.27	**Highest** 1.30/0.2	2.42/27	668.79	**Highest** 187.71
SKES-1	Noncanonical	**Lowest** 0.22	1.12/0.1	2.55/29	**Lowest** 217.03	**Highest** 166.67
SK-N-MC	Canonical	0.32	1.23/0.7	**Highest** 3.94/37	562.86	**Highest** 176.15
TC32	Noncanonical?	**Highest** 0.39	1.06/0.2	1.95/12	365.23	92.48
TTC466	Both?	0.27	**Lowest** 0.85/0.2	**Lowest** 1.36/7	327.97	**Lowest** 24.21

Table 3.1 Summary of results of assays used to measure canonical Wnt signalling in ESFT cell lines ESFT cell lines were predicted to be either canonical or noncanonical based on expression of Wnt1 and Wnt5A (Chapter 2). Expression of active β-catenin was measured by western blot in Chapter 2. Endogenous activity of canonical Wnt signalling in ESFT cell lines was measured using both GFP and firefly luciferase reporters. Canonical Wnt signalling was stimulated by adding 200ng/ml recombinant Wnt3A for 24h.

Recombinant Wnt5A had no effect on activity of either reporter, showing that the assay is specifically detecting canonical Wnt signalling. Previous studies have suggested Wnt5A may inhibit canonical Wnt signalling (Mikels and Nusse 2006), however my data does not demonstrate this. It is important to note that although ESFT cell lines respond to exogenous Wnt3A they do not express Wnt3A (Chapter 2). However, since all cell lines have endogenous active canonical Wnt signalling it is likely that other canonical Wnt ligands such as Wnt1 and Wnt10B which are expressed are endogenously activating the canonical pathway. In Chapter 2 I predicted that A673 cells may have high endogenous canonical Wnt signalling based on the expression of Wnt1 and Wnt5A. Interestingly these cells did have the highest level of canonical signalling in untreated cells, measured using the more sensitive 7TFP reporter. Interestingly in all cell lines, there was no correlation between endogenous canonical signalling activity and stimulation with Wnt3A ligand; SKES-1 had the lowest level of canonical Wnt signalling measured by both the 7TGP and 7TFP reporters, but was stimulated the most by the addition of exogenous Wnt3A (summarised in Table 3.1).

To demonstrate that activation of the GFP and luciferase reporter were truly measuring canonical Wnt signalling, I attempted to measure downstream targets of the pathway. It is not known what downstream factors are activated following activation of the canonical Wnt signalling pathway in ESFT cells. In concordance with previous findings, recombinant Wnt3A did not increase the viable cell number of ESFT cells (Üren et al. 2004). This observation was supported by the lack of consistent increase of cyclin D1 in ESFT cells after treatment with Wnt3A. In HEK293T cells an increase of total and active (nonphosphorylated) β-catenin was observed, reaching a maximum at 4h, and remaining elevated up to 24h consistent with previous reports (Gujral and MacBeath 2010). However, results were less conclusive when active β-catenin was investigated in ESFT cell lines. It may be that the dynamics of β-catenin upregulation is different in ESFT cells, or that detection of total and active β-catenin by western blot is not sensitive enough to detect small changes in expression. It has been reported that Axin2 is universally upregulated in cells following treatment with Wnt3A. Although a specific and sensitive antibody to Axin2 for use in western blots is not available (unpublished observations), expression of Axin2 mRNA has been shown to be increased in ESFT cells after treatment with Wnt3A (Scannell et al. 2013). Therefore future work could use RTqPCR to detect changes in Axin2, β-catenin and possibly other potential downstream targets over a time course after stimulation with Wnt3A.

Further work to validate the reporters used could involve inhibiting components of the Wnt signalling pathway. ESFT cells could be treated with recombinant forms of endogenous inhibitors of the pathway such as sFRP2, to show that this also reduces the activity of the reporter. A disadvantage of these proteins is that they inhibit both canonical and noncanonical Wnt signalling. As an alternative, small molecules have been developed which specifically target the interaction between β-catenin and TCF4 such as iCRT 14 (Gonsalves et al. 2011). Molecules such as this could therefore also be used in ESFT cell lines to show that the reporters are specifically measuring canonical Wnt signalling in these cells.

In summary I have optimised a lentiviral based luciferase assay using the 7TFP plasmid to measure the activation of canonical Wnt signalling at endogenous levels and after treatment with recombinant Wn3A. I have demonstrated that all the ESFT cell lines studied have active canonical Wnt signalling, and this can be further stimulated by treatment with Wnt3A. The downstream consequences of this activation so far remain elusive, as Wnt ligands do not alter the viable cell number of ESFT cells, so further investigation of the effect of Wnt signalling in ESFT cells is required.

4. Developing assays to measure the activity of the noncanonical Wnt signalling pathway in ESFT cells

4.1 Introduction

In the previous chapter I optimised an assay which enabled me to investigate the activity of the canonical Wnt signalling pathway in ESFT cell lines. The aim of the current chapter is to develop assays to measure the activation of the noncanonical Wnt signalling pathway.

Noncanonical Wnt signalling is the term used to describe any pathway that is activated by Wnt proteins but is β-catenin independent. The best described of these are the planar cell polarity (PCP) and calcium (Ca^{2+}) pathways. However, the activity of these noncanonical Wnt signalling pathways is more difficult to measure. Unlike canonical Wnt signalling there are numerous downstream effector molecules that can be activated. In addition, these molecules are often involved in many other signalling pathways making interpretation of results difficult.

In the Ca^{2+} pathway, activation by Wnt5A has been shown to lead to intracellular release of Ca^{2+} thereby activating Ca^{2+} dependent signalling molecules such as PKC and CaMKII (Sheldahl et al. 1999, Kühl et al. 2000, Kang et al. 2007). The phosphatase calcineurin can also stimulate and activate the NFAT transcription factor, which regulates the expression of downstream targets (Saneyoshi et al. 2002). Activation of the Ca^{2+} pathway can therefore be measured by detecting an increase in intracellular Ca^{2+}, by probing for upregulation of these downstream effector proteins and using a NFAT reporter assay.

The PCP pathway has been shown to activate small GTPases of the Rho family including Rac1 as well as downstream kinases such as JNK (Boutros et al. 1998, Habas et al. 2003). In addition, the Ca^{2+} pathway can also activate the small GTPase Cdc42 via PKC (Choi and Han 2002). This means that detection of active GTPases is a useful approach to investigate the activity of multiple branches of the noncanonical Wnt signalling pathway. The Rho family of small GTPases, including Rac1 and Cdc42, act as molecular switches by alternating between an active GTP-bound and inactive GDP-bound state. The Rho family of effector proteins specifically recognise the active GTP-bound form. This has been used experimentally to design pull-down assays using the Cdc42/Rac Interactive Binding (CRIB) region of the effector protein p21 activated kinase I (PAK) (Burbelo et al. 1995). PAK-CRIB has a high affinity for both Rac1 and Cdc42 in their GTP-bound states, making it ideal for

affinity purification of active proteins from cell samples. PAK-CRIB is made as a glutathione-*S*-transferase (GST) fusion protein, coupled to sepharose beads and used to pull-down active (GTP-bound) Rac1 and Cdc42 from lysates (Benard et al. 1999). Although the relationship between noncanonical Wnt signalling and Rho GTPase activation has been primarily described in *Drosophila*, this assay has been successfully used in mammalian cells to detect activation of Rac1 and Cdc42 following treatment of cells with the noncanonical Wnt5A protein (Habas et al. 2001, Habas et al. 2003).

A common function of many of the noncanonical Wnt signalling pathways is to regulate the cytoskeleton to coordinate cell migration and polarity (Hans Clevers 2006). Therefore, assays to measure migration are often used as an indirect measure of the activation of different noncanonical Wnt signalling pathways (Dissanayake et al. 2007). As migration is an important process in the metastatic process of cancer this might suggest that noncanonical Wnt signalling is involved in this process. To understand the potential role of Wnt signalling in migration and metastasis of ESFT cells, I have therefore optimised and utilised a migration assay.

Scratch assays are frequently utilised to investigate migration. A confluent adherent monolayer of cells is manually wounded often using a pipette tip and the time for closure of the wound is then monitored by imaging (Liang et al. 2007). Although convenient, this assay has a number of disadvantages. Firstly it relies upon the generation of confluent adherent monolayers that do not lift off when the scratch is made. Any gaps in the monolayer would obviously affect the results. However, many ESFT cell lines such as SKES-1 and TTC466 grow in colonies and begin to stack when confluent (unpublished observations). Consequently these cells do not form a 100% confluent monolayer and therefore are not suitable for analysis using the scratch assay. In addition, the manual wound formation can be very variable in width (unpublished observations), meaning that many assays need to be performed to get reliable results. The scratch assay is also confounded by cell proliferation rather than migration, especially if assays are run over long periods of time, although the use of tame-lapse microscopy to track individual cells may be possible.

Chemotaxis assays are also commonly used to assess cell migration. Such assays are mostly based on the original Boyden chamber assay (Albini and Noonan 2010) in which single cells in suspension are placed in an upper chamber and media containing an attractant such as a chemokine or growth factor is placed in a lower chamber. A permeable membrane separates the chamber, often coated with matrix proteins such as collagen or fibronectin

to encourage migration of cells from the upper to lower chamber. After a set period of time, the membrane is removed and the number of cells that have migrated onto the lower side quantified. If extracellular matrix such as Matrigel™ is used to coat the membrane then this assay can also be used to quantify invasion of cells through the Matrigel™ in addition to migration. However, the use of enzymatically-digested single cells in these assays means that they do not recapitulate the *in vivo* situation of cells escaping from a tumour in order to migrate.

More recently, 3D models of migration have been developed in an attempt to more closely model the conditions within the tumour and the surrounding microenvironment. For example, nonadherent, heterogeneous aggregates of cells or 'spheroids' have been formed from cancer cell lines that have been shown to contain gradients of cell proliferation oxygen and nutrients (Sutherland et al. 1986, Rodríguez-Enríquez et al. 2008). If these spheroids are then embedded in extracellular matrices such as Collagen I or Matrigel™ or transferred onto plastic coated with a matrix protein, invasion and migration of cells can be observed and quantified (Nowicki et al. 2008, Vinci et al. 2013). These 3D assays are more representative of the metastatic process *in vivo* (Zimmermann et al. 2013).

The aims of this chapter were to;

1. Optimise and validate an assay to measure Rac1/Cdc42 activation after treatment with recombinant Wnt5A.
2. Optimise and validate a migration assay using cell line-derived 3D spheroids.
3. Use these optimised assays to measure the activity of the noncanonical Wnt signalling pathway in ESFT cell lines.

4.2 Materials and Methods

4.2.1 Rac1/Cdc42 pull-down assay

4.2.1.1 Preparing PAK-CRIB protein

Glycerol stocks of BL21(DE3)pLysS competent *E.coli* expressing pGEX GST-PBD were a kind gift from Dr Georgia Mavria (University of Leeds). A loop of glycerol stock was used to inoculate 50ml of LB Medium (containing 100µg/ml amp), and the culture incubated at 37°C for 17h with vigorous shaking. The culture was added to 450ml of LB Medium (+100µg/ml amp) and incubated at 37°C with vigorous shaking until the optical density (OD) of the culture at 600nm was 0.3 (as assessed using a Jenway 6705 Spectrophotometer, supplied by Bibby Scientific). This indicated the bacteria had reached the mid-log growth phase. Expression of GST-PBD was then induced by adding 0.3mM of isopropyl β-D-1-thiogalactopyranoside (IPTG; Sigma-Aldrich) and the culture incubated for a further 3h at 37°C with shaking. Bacteria were harvested by centrifugation at 5163g for 20min at 4°C, and pellets stored at -80°C until required. Bacterial pellets were thawed on ice and lysed with 20ml ice-cold bacterial lysis buffer (10mM $MgCl_2$, 1mM PMSF, 1mM DTT made in 1X Tris-Buffered Saline (TBS; 50mM Tris-HCL, 50mM NaCl, pH 7.5)) and sonicated (Vibra Cell™, Sonics & Materials, Stowmarket, UK) in 30s bursts for a total of 3min (with a 30s incubation on ice in between each sonication). After sonication, Triton X-100 was added to a concentration of 1% (v/v) and the solution incubated for 30min at 4°C with gentle agitation. Lysates were clarified by centrifugation at 12470g for 30min at 4°C and snap-frozen in 5ml aliquots (enough for 12 pull-down samples) at -80°C.

4.2.1.2 Binding GST-PAK-CRIB protein to beads

To generate enough beads to analyse 12 samples, immediately before each pull-down experiment PAK-CRIB lysate (5ml; generated as described in Section 4.2.1.1) was thawed on ice. Meanwhile, 500µl Glutathione Sepharose™ 4B beads (GE Healthcare) (due to slurry this equates to approximately 375µl of beads) were washed with 10ml 1X TBS, centrifuged at 500g for 1min at 4°C, then washed twice with Rac wash buffer (10mM MgCl2, 1mM DTT, 1X cOmplete protease inhibitor cocktail (Roche, Welwyn Garden City, UK) in 1X TBS), followed by centrifugation at 500g for 1min. The prepared beads were then added to the thawed cleared lysate and incubated for 1h at 4°C with gentle agitation. PAK-CRIB bound beads were pelleted by centrifugation at 500g for 1min at 4°C, the supernatant discarded

and beads washed 4 times with Rac wash buffer, and finally centrifuged at 500g for 1min, the buffer discarded and beads aliquoted into 60µl aliquots in screw-capped eppendorfs.

4.2.1.3 Quantification of GST-PAK-CRIB protein bound to beads

To quantify the concentration of PAK-CRIB bound to beads, PAK-CRIB bound beads were prepared as described (Section 4.2.1.2) and 10µl and 25µl of beads (mixed 1:1 with SDS-loading buffer) were loaded onto a 12% acrylamide gel alongside BSA standards (0.5, 1, 2.5, 5, 10 µg) in SDS loading buffer. SDS-PAGE was performed as previously described (Section 2.2.5) and the gel stained with Coomassie blue (0.025% Coomassie Brilliant blue R 250, 40% (v/v) methanol, 7% (v/v) acetic acid in dH_2O) overnight. The gel was destained (40% (v/v) methanol, 7% (v/v) acetic acid in dH_2O) for 3h or until the blue background had disappeared, and the gel scanned using the ChemiDoc™ MP (Bio Rad). Bands were quantified using the ChemiDoc™ MP imaging system and a standard curve generated from the known concentrations on BSA. The curve was used to estimate the concentration of PAK-CRIB in 10µl and 25µl of bead solution.

4.2.1.4 Performing Rac1/Cdc42 pull-down assay

Cells were seeded in $10cm^2$ dishes at an appropriate density to be 70% confluent after 48h; either 1×10^6 (A673), 1.5×10^6 (RD-ES, SKES-1, TC32, TTC466) or 2×10^6 (SK-N-MC). Cells were treated with 5ml of media (control) or media containing 200ng/ml Wnt5A for increasing periods of time (5min-2h; HeLa and SKES-1) or for 30min with increasing concentrations of Wnt5A (50-200ng/ml; SKES-1). ESFT cell lines were treated with 200ng/ml Wnt5A for 30min in cell-line specific media. To harvest cells for detection of active Rac1/Cdc42, media was removed and cells were washed on ice twice with ice-cold 1X TBS. Cells were scraped into ice-cold Rac lysis buffer (900µl; 50mM Tris (pH 7.4), 10% (v/v) glycerol (Sigma-Aldrich), 1% (v/v) Nonidet® P40 substitute (NP-40; Fluka, Sigma-Aldrich), 5mM $MgCl_2$, 100mM NaCl, 1mM DTT, 1X cOmplete protease inhibitor cocktail in dH_2O) using a cell scraper and samples pipetted to ensure complete lysis. To clarify the lysate samples were centrifuged at 12470g for 15min at 4°C. A total protein sample (12.5µl) was removed and mixed 1:1 with loading buffer and used to detect total Rac1/Cdc42. The remaining cleared lysate was added to 60µl GST-PAK-CRIB beads prepared as described (Section 4.2.1.2) and incubated on a rotating wheel for 45min at 4°C. Samples were centrifuged at 500g for 1min at 4°C, the supernatant discarded and the beads washed twice with 1ml Rac wash buffer (Section 4.2.1.2). Finally the wash buffer was discarded and the beads resuspended in 60µl 2X loading buffer and split into two 30µl aliquots for detection of Rac1 and Cdc42. Total protein and pull-down samples were

heated at 95°C for 10min and loaded onto 10% Bis-Tris polyacrylamide gels and SDS-PAGE performed. Initial experiments were carried out using SDS-loading buffer (as described Section 2222), Bis-Tris gels (3.5mM Bis-Tris HCl (pH 6.8), 10% (v/v) acrylamide, 1% (w/v) APS, 0.0025% (v/v) TEMED) using 1X MES-SDS electrophoresis running buffer (GeneFlow) and run at 100V at 4°C. Later experiments were carried out using the Criterion™ XT system (Bio-Rad) using XT sample buffer, 10% Bis-Tris pre-cast XT gels and XT-MES running buffer. Electrophoretic transfer was carried out as previously described (Section 2.2.5). Immunodetection of proteins was carried out (Section 2.2.3.5) using antibodies to Rac1 (1µg/ml; Millipore (05-389)) and Cdc42 (1:1000, Cell Signalling (11A1)).

4.2.1.5 Determining the specificity of Rac1 and Cdc42 antibodies

Total protein from HEK293T cells was extracted (Section 2.2.5). Protein extracts from HEK293T cells over expressing human Rac1 (sc-116394) and human Cdc42 (sc-110467) were purchased from Santa Cruz Biotechnology. Samples were loaded onto 10% acrylamide gels and SDS-PAGE performed (Section 2.2.5), and probed for Rac1 and Cdc42 expression using antibodies (Section 4.2.1.4).

4.2.2 Generation of spheroids from cell lines

Cells were harvested by trypsinsation and counted using the trypan blue exclusion assay and haemocytometer (Section 2.2.5). Cells were suspended in cell-type specific culture medium at 5×10^3 cells/ml and 200µl of cell suspension added to each well of a round-bottomed low adherence 96-well plate (Corning®, supplied by Fisher Scientific) to give 1×10^3 cells per well. PBS was added to empty wells to humidify the plate, and the plate incubated at 37°C for 4 days.

4.2.3 3D migration assay using cell spheroids

The migration assay was adapted from a previously published method (Vinci et al. 2013) Cell spheroids were formed as described previously (Section 4.2.2). For optimisation experiments, Primaria™ flat-bottomed 96-well plates were left uncoated or coated with gelatin from bovine skin (0.1% (w/v; (Sigma-Aldrich) in sterile dH_2O) or Matrigel™ (prepared as described in Section 5.2.1) for 1h at 37°C. Subsequent experiments with ESFT cell lines plates were coated with 0.1% gelatin (see results section 4.3.3.3). After this time the coating substrate was removed and replaced with 200µl of cell-type specific culture medium either untreated (control) or containing 1.5X the required final concentration of Wnt ligand (i.e. 300ng/ml of Wnt5A or 300ng/ml Wnt3A). From the wells containing the cell spheroids, 100µl of media was removed and discarded. The remaining 100µl of media

(containing the cell spheroid) was gently pipetted into the centre of a flat-bottomed coated well. Each well was imaged at 4X magnification at this time point (0h) and then every 24h up to 72h.

Images were analysed using Volocity® software (Perkin Elmer, Cambridge, UK). Using the freehand drawing tool, the outline of the spheroid at 0h was traced to give the area covered (in number of pixels). At each subsequent time point the edge of the central spheroid (if present) was traced as well as the edge of migrating cells (migration zone). The migration zone was taken as the area containing at least 70% of migrating cells, as opposed to the maximum distance migrated by any single cell. The Migration Index (MI) at each time point was calculated as the area of the migration zone at that time point, minus the area of the core at that time point, relative to the area of the core at 0h.

4.2.4 3D invasion assay using cell spheroids

Cell spheroids were formed as previously described (Section 4.2.2). To assess invasion into Matrigel™, an aliquot of Matrigel™ was thawed on ice at 4°C overnight. From the wells containing the spheroids 100µl of media was removed from each well and discarded. Gently, 100µl of Matrigel™ containing 200ng/ml Wnt5A, if required, was added to the well containing the spheroid and allowed to set at 37°C for 1 hr. Once set, 100µl of cell-type specific media containing 200ng/ml Wnt5A, if required, was added to the well.

To assess migration in collagen, a solution containing 4mg/ml collagen type I (Rat tail, BD Biosciences), 0.5X DMEM:F12 and 58mM NaOH was prepared. From the wells containing the spheroids, 190µl media was removed and discarded and 100µl of the collagen solution gently added and incubated at 37°C for 10min to allow to set. Finally, 100µl of cell-type specific culture media containing 2X the final concentration of Wnt5A (i.e. 400ng/ml) if required, was added to the well.

In both conditions, each well was imaged at 4X magnification at this time point (0h) and then every 24h up to 72h.

4.3 Results

4.3.1 Optimisation of Rac1/Cdc42 pull-down assay

4.3.1.1 Quantification of PAK-CRIB protein

The protocol used for active Rac1/Cdc42 pull-down was adapted from Pelligrin and Mellor (2008). Immunoprecipitation of active Rac1/Cdc42 will be dependent on the concentration of PAK-CRIB protein present in each assay, it is recommended that 30-100µg of PAK-CRIB protein is used for each pull-down sample (Pellegrin and Mellor 2008). To quantify the amount of PAK-CRIB protein used per pull-down in my optimised method, samples of GST-PAK-CRIB protein bound to glutathione beads were prepared as described (Section 4.2.1.2) and loaded alongside known concentrations of BSA (Figure 4.1 A). Densitometry was performed and a standard curve of BSA generated so that the concentration of protein in the PAK-CRIB samples could be quantified (Figure 4.1 B). It was calculated that 10µl of sample (i.e. 5µl of beads) contains 3.9µg PAK-CRIB protein which would equate to 47µg PAK-CRIB in each pull-down (using 60µl beads).

(A)

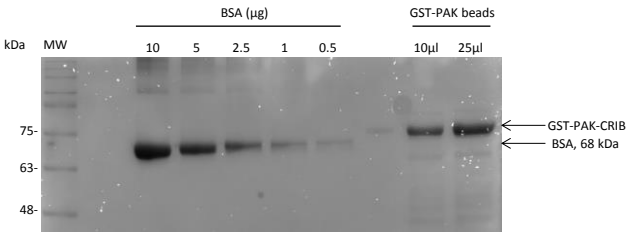

(B)

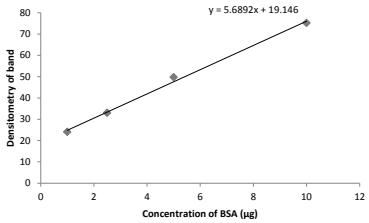

Sample	Densitometry of band	Concentration of PAK-CRIB
10µl beads	41	3.9
25µl beads	74	9.5

Figure 4.1 Quantification of PAK-CRIB bound to glutathione-sepharose beads PAK-CRIB protein was prepared and allowed to bind to glutathione-sepharose beads for 1h at 4°C. A) Beads were washed, mixed 1:1 with SDS-loading buffer and loaded onto a 10% polyacrylamide gel alongside known concentrations of BSA (0.5-10µg). Electrophoresis was performed and the gel stained with Coomassie blue. B) After imaging, densitometry was performed to generate a standard curve for BSA, this was used to quantify the concentration of PAK-CRIB bound to the beads. MW= molecular weight.

4.3.1.2 Validation of Rac1 and Cdc42 antibodies

PAK-CRIB will bind to both active Rac1 and Cdc42, therefore it is possible to pull-down both proteins in the same assay. However, Rac1 and Cdc42 have a similar molecular weight and structure, so it was necessary to test the ability of available antibodies to distinguish between the two proteins. Anti-Rac1 antibody detected a band at 21 kDa corresponding to the predicted molecular weight of Rac1. This band was faint in the HEK293T parental cells, consistent with low level expression (Figure 4.2 A). A strong band was detected in HEK293T cells overexpressing Rac1 (Rac1-293T) but there was no band observed in cells overexpressing Cdc42 (Cdc42-293T). The anti-Cdc42 antibody also detected a band at 21 kDa (Figure 4.2 B). The anti-Cdc42 antibody did not detect a band in the HEK293T cells overexpressing Rac1 (Rac1-293T), but detected a strong band in HEK293T cells overexpressing Cdc42 (Cdc42-293T). These results demonstrate the specificity of both antibodies.

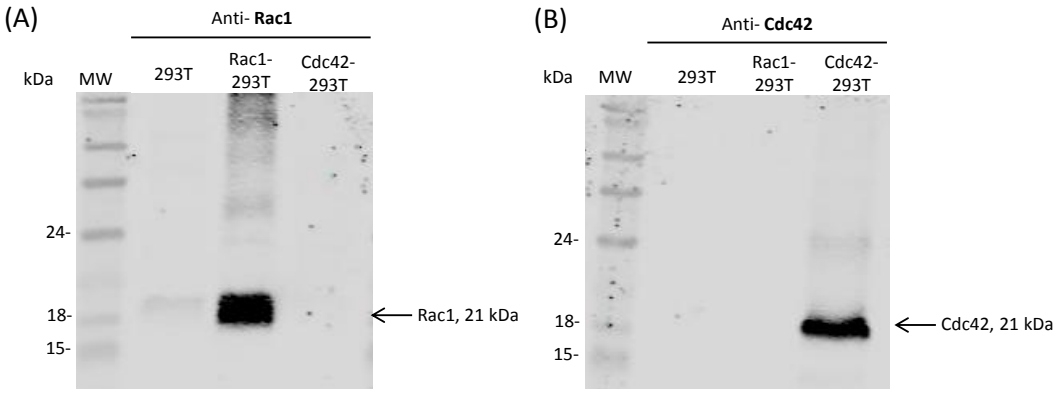

Figure 4.2 Specificity of anti-Rac1 and anti-Cdc42 antibodies HEK293T control extracts and HEK293T cells overexpressing either Rac1 (Rac1-293T) or Cdc42 (Cdc42-293T) were analysed by western blot for expression of both Rac1 and Cdc42 to confirm the antibodies were specific. MW= molecular weight.

4.3.1.3 Stimulation of cells with recombinant Wnt5A

The protocol to measure active Rac1/Cdc42 following treatment with Wnt5A was optimised using HeLa cells (as a positive control). In addition, the SKES-1 cell line was included to confirm that using the optimised method in HeLa cells it was also possible to measure active Rac1/Cdc42 in ESFT cell lines. Densitometry was performed and expression of active Rac1 (21 kDa) expressed relative to the expression of total Rac1 (21 kDa) in each sample. Endogenous active Rac1 was detected in both HeLa and SKES-1 cells (Figure 4.3 A and B). In HeLa cells treatment with Wnt5A (200ng/ml) increased expression of active Rac1 after 5 min, with maximum activation observed after 30min (1.5-fold) (Figure 4.3 C). Wnt5A (200ng/ml) also increased active Rac1 expression in SKES-1 cells after 30 min treatment (1.2-fold).

In SKES-1 cells, there was a dose-dependent increase in active Rac1 expression after 30 min Wnt5A treatment (Figure 4.4 A and B). Greatest activation of Rac1 in SKES-1 cells was observed after treatment with 200ng/ml Wnt5A (1.2-fold) (Figure 4.4 B)

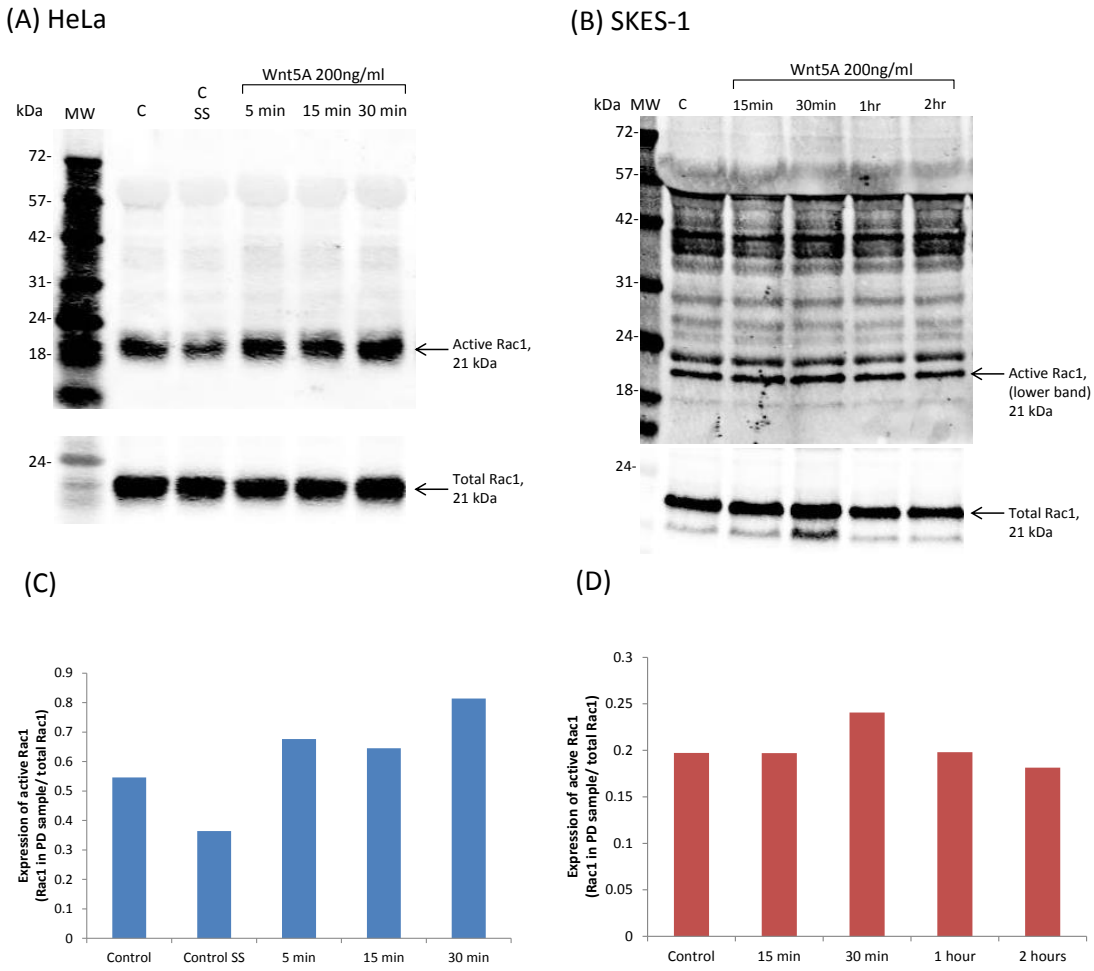

Figure 4.3 Expression of active Rac1 after in HeLa and SKES-1 cells after treatment with Wnt5A over time A) HeLa and B) SKES-1 cells were seeded into 10cm^2 dishes and grown until 70% confluent in normal growth media (containing FCS), then treated with rWnt5A (200ng/ml) for various lengths of time (5min-2h). Cells were harvested, a sample for total protein estimation removed, and active (GTP-bound) Rac1 was precipitated from the remaining sample using glutathione-sepharose beads bound to PAK-CRIB. Expression of active and total Rac1 was determined by western blot using 10% Bis-Tris polyacrylamide gels (for SKES-1 a pre-cast Criterion™ gel was used (BioRad). Densitometry was performed and the ratio of active Rac1/total calculated in C) HeLa and D) SKES-1 cells. MW= molecular weight.

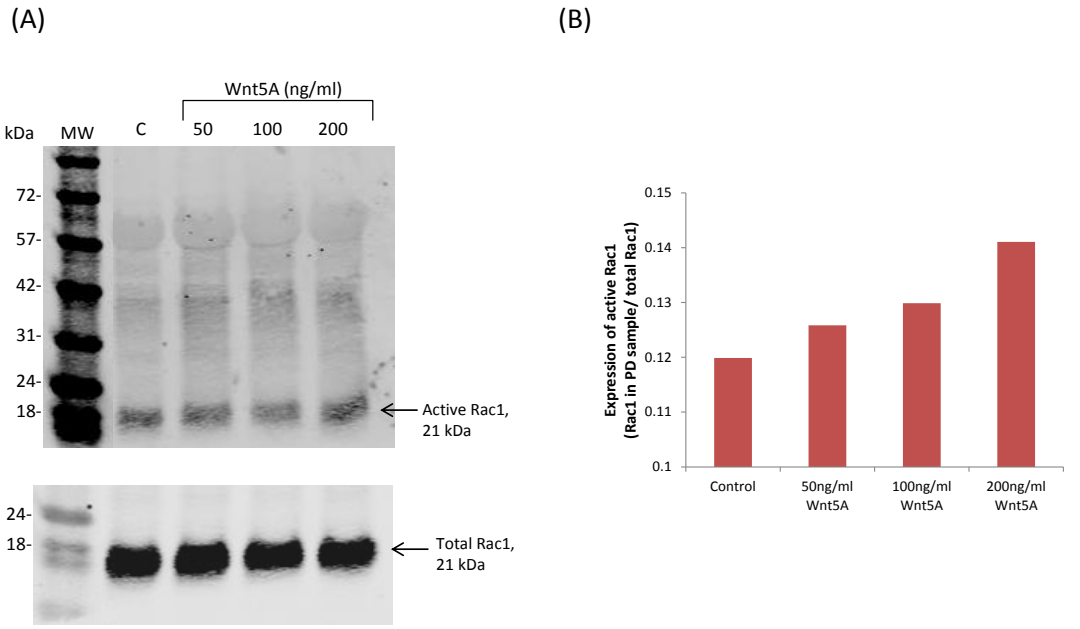

Figure 4.4 Expression of active Rac1 in SKES-1 cells after treatment with increasing concentrations of Wnt5A SKES-1 cells were cultured in 10cm^2 dishes until 70% confluent before treatment with media containing increasing concentrations of rWnt5A (50-200ng/ml) for 30 min. Cells were harvested, a sample for total protein estimation removed, and active (GTP-bound) Rac1 was precipitated from the remaining extract using glutathione-sepharose beads bound to PAK-CRIB. Beads were washed, isolated and resuspended in 2X SDS-loading buffer. A) Expression of Rac1 in pull-down and total protein samples was determined by western blot using a 10% Bis-Tris polyacrylamide gel B) Densitometry was performed and the ratio of active Rac1/total Rac1 calculated. MW= molecular weight in kDa.

4.3.2 Measuring active Rac1/Cdc42 in ESFT cell lines

Expression of both active and total Rac1 were detected in ESFT cell lines. Two bands were observed in pull-down samples when the samples were run on pre-cast Bis-Tris polyacrylamide gels. The lower band was active Rac1, as this was the same molecular weight as total Rac1 (Figure 4.5 A). The level of total Rac1 was heterogeneous between cell lines; equal protein loading was confirmed by staining of the membrane (Figure 4.5 D). SKES-1 cells had the highest level of total Rac1 expression (densitometry= 185) this was 11X higher than total Rac1 expression in A673, which had the lowest expression (densitometry= 17). Endogenous expression of active Rac1 was detected in all ESFT cells, expression was heterogeneous between cell lines (Figure 4.5 A). Densitometry was performed and active Rac1 expression was calculated relative to the expression of total Rac1 in each sample. Results showed that A673 cells had the highest level of endogenous Rac1 activity (Ratio= 2.9) and SKES-1 cells had the lowest activity (Ratio; 0.09). Although not tested statistically, an increase in expression of active of Rac1 was observed after treatment with Wnt5A (200ng/ml, 30min) compared to control (untreated cells) in SKES-1 (3- fold), TTC466 (2-fold) and SKNMC (0.8-fold) cell lines. However, in the other three ESFT cell lines there was a decrease in active-Rac1 expression after Wnt5A stimulation (Figure 4.5 B).

Low levels of both total and active Cdc42 were detected in ESFT cell lines (Figure 4.5 C). The level was so low that densitometry could not be performed though equal loading was confirmed by staining of the membrane (Figure 4.5 D). Active Cdc42 appeared higher in A673 and TTC466 cells, compared to the other cell lines, but no clear increase was measured after treatment with Wnt5A (200ng/ml, 30 min).

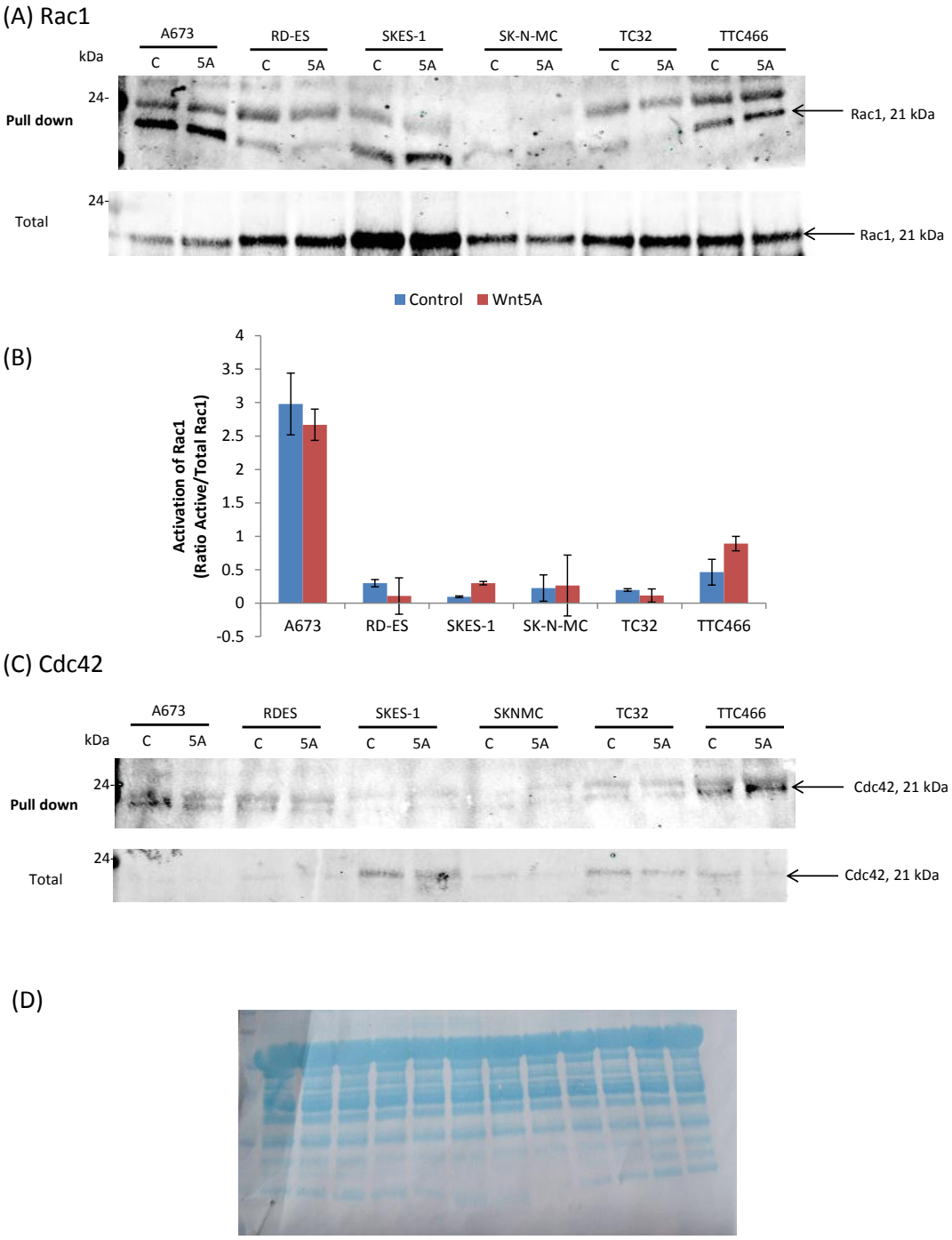

Figure 4.5 Expression of active Rac1 and Cdc42 in ESFT cell lines ESFT cells were cultured in 10cm^2 dishes until 70% confluent then treated with rWnt5A (200ng/ml) for 30min. Cells were harvested, a sample removed for total protein estimation, and active (GTP-bound) Rac1 and Cdc42 precipitated from the remaining extract using glutathione-sepharose beads bound to PAK-CRIB. Beads were washed, isolated and the sample split for analysis of Rac1 and Cdc42. Expression of A) Rac1 and C) Cdc42 in pull-down and total protein samples was determined by western blot using pre-cast Bis-Tris acrylamide gels (BioRad). Images are representative of three independent experiments. B) Densitometry was performed and the ratio of active/total Rac1 calculated. Results show the mean of three independent experiments (±SEM). D) Equal loading of samples was determined by staining the membrane using the Pierce reversible protein stain kit (Section 2.2.3.5).

4.3.3 Optimisation of 3D migration assay

To investigate downstream activation of the noncanonical Wnt signalling in ESFT cells following treatment with Wnt5A protein, a 3-dimensional migration assay was developed.

4.3.3.1 Validation of 3D migration assay in U87MG cells

The migration assay used was developed from a previously published method, using U87MG cells that are known to be highly migratory cells (Vinci et al., 2013). U87MG cells formed compact spheroids; 3D clusters of non-adherent cells, when plated into round-bottomed, ultra-low adherent 96-well plates and cultured for 4 days (Figure 4.6 A). When spheroids were transferred onto 0.1% gelatin-coated flat-bottomed plates, cells migrated out from the central spheroid core in a radial fashion consistent with reports from Vinci et al., (2013). Analysis of migration was performed using Volocity® software (Perkin Elmer). The area covered by the spheroid at 0h (Figure 4.6 B, purple circle) was determined (by the number of pixels). At each time point the migration zone (MZ) was quantified as the area covered by migrating cells (Figure 4.6 B, orange circle) minus the area covered by the spheroid core at that time point (Figure 4.6 B, green circle). The MZ was then normalised to the size of the core at 0h to give the migration index (MI). The average MI in U87MG cells after 72h was 61±8.

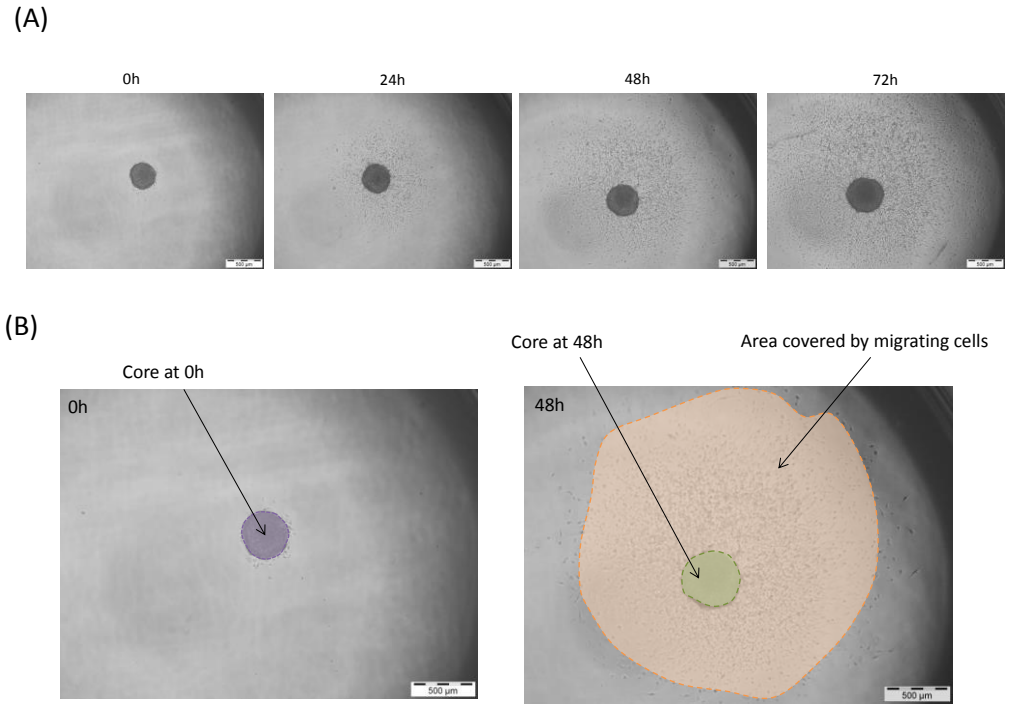

Figure 4.6 Quantifying migration in U87MG cells U87MG cells were seeded (1000 cells/well) into round-bottomed, ultra-low adherence, 96-well plates (CoStar; Corning) to form spheroids. After 4 days, spheroids were transferred to flat-bottomed 96-well plates coated with 0.1% gelatin. A) Cells were imaged every 24h, up to 72h and B) the migration was quantified using Volocity® software. The migration index (MI) at each time point was calculated as the area of the migrating cells minus the area of the core at that time point, relative to the area of the core at 0h.

4.3.3.2 Formation of spheroids from ESFT cell lines

ESFT cell lines formed spheroids when seeded in round-bottomed, ultra-low adherent 96 well plates (1000 cells/well) (Figure 4.7 A). After 4 days the size of the spheroids formed was significantly different between the ESFT cell lines ($p<0.001$). A673 cells formed the largest spheroids (47328±3516 pixels) and RD-ES the smallest spheroids (21232±1939 pixels) (Figure 4.7 B). A673, RD-ES, SK-N-MC and TTC466 cells lines formed compact spheroids with a defined edge, whereas spheroids formed by SKES-1 and TC32 cells were looser with irregular edges, and tended to break apart easily during transfer to flat-bottomed plates (Figure 4.7 A)

(A)

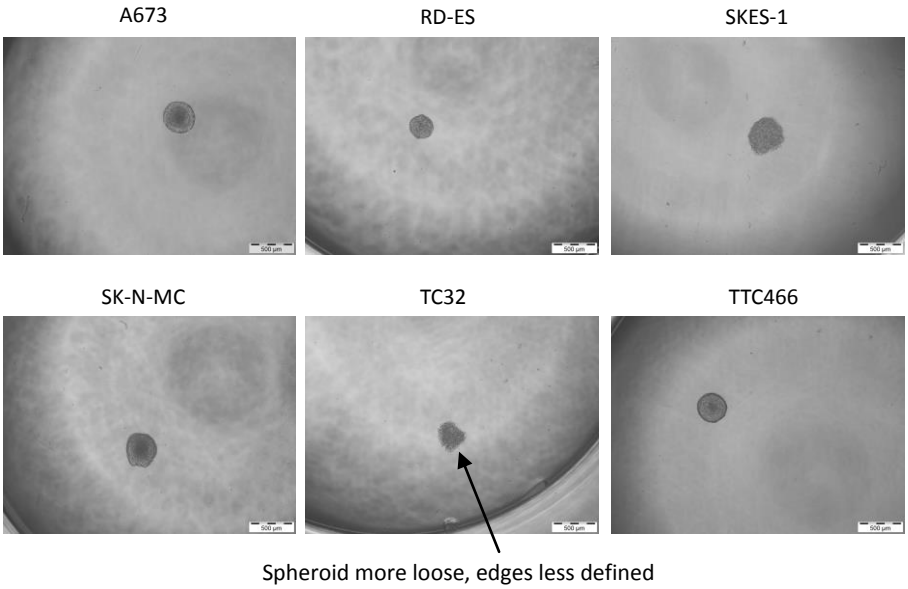

(B)

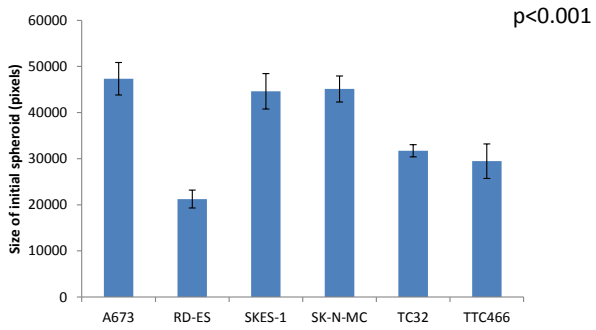

Figure 4.7 Spheroids formed by ESFT cell lines ESFT cell lines were seeded into round-bottomed, ultra-low adherent 96-well plates (1000 cells/well). A) After 4 days spheroids were imaged and B) the area covered by the spheroid quantified using Volocity® software. Results are presented as the mean of three independent experiments with three replicates per experiment (n=9) (±SEM).

4.3.3.3 Migration of ESFT cell lines on different substrates

The 3D migration assay used describes migration on gelatin coated plates. It was investigated if a substrate coating is necessary for ESFT cell line migration, and if so, which is the optimum substrate to use.

All ESFT cell lines studied migrated when plated onto plastic coated with gelatin (0.1%) (Figure 4.8). After 72h, A673 cells migrated the most (MI; 39±3) and SKES-1 the least (MI; 6±0.6). A673 and TC32 cells also migrated on Primaria™ plastic but to a lesser extent (3- and 4-fold less, respectively). Only A673 cells migrated on Matrigel™ coated plastic and this was 2.5-fold less than migration on gelatin (Figure 4.8 A). Therefore, subsequent migration assays were carried out on gelatin coated plastic.

Figure 4.8 ESFT cell migration on different substrates A) A673 B) SKES-1 and C) TC32 ESFT cell lines grown as spheroids were transferred onto flat-bottomed 96 well plates coated with either 0.1% gelatin or Matrigel™ or directly onto Primaria™ plastic (BD). Spheroids were imaged every 24h and the area covered by migrated cells quantified using Volocity® software. Images are 48h post plating. Dotted lines show the edge of migrating cells. Results show the migration index at each time point; the area covered by migrating cells, minus the area of the spheroid at the time point, relative to the size of the spheroid at Day 0. Results show the mean of three wells within one experiment (±SEM).

(A) A673

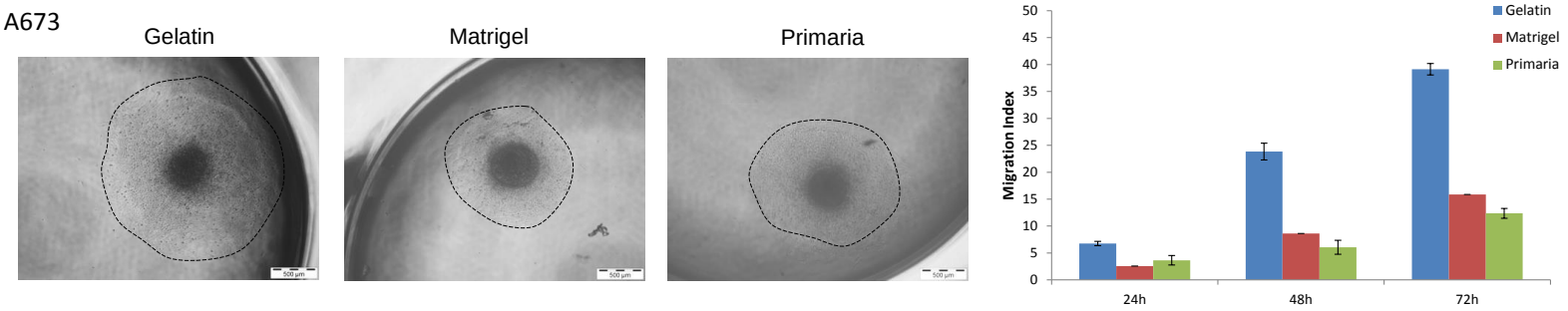

(B) SKES-1

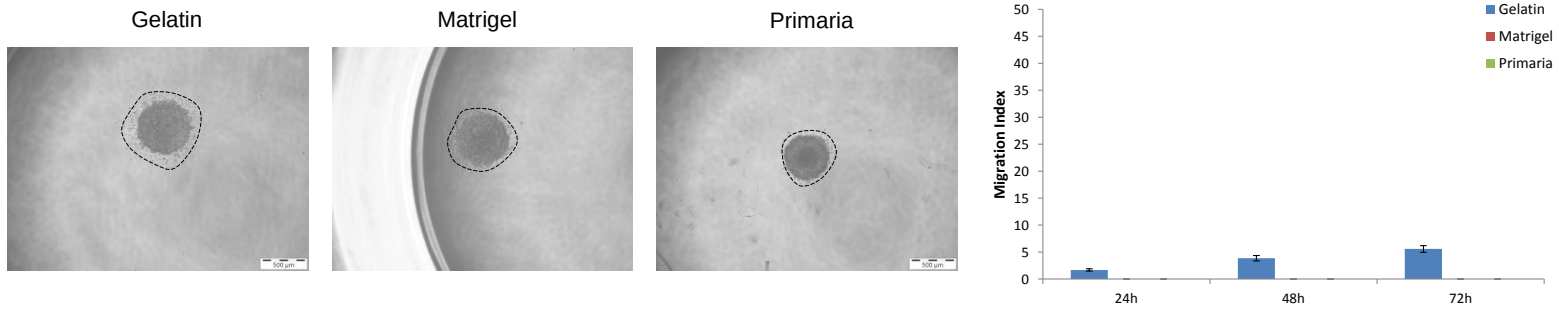

(C) TC32

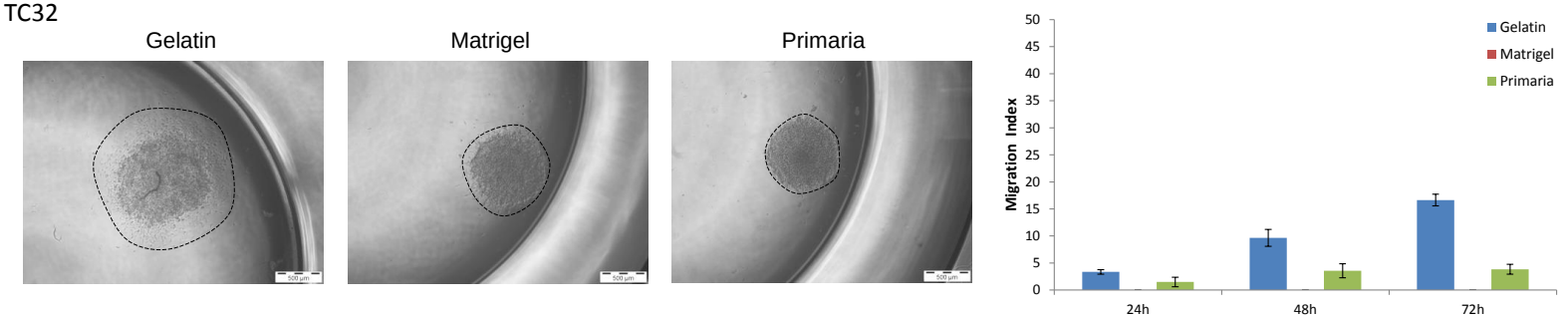

4.3.4 ESFT cell line migration in response to Wnt5A and Wnt3A

All ESFT cell lines grown as spheroids migrated when plated on gelatin coated plastic. The pattern of migration of the cells over 72h was different between cell lines (Table 4.1). In some cell lines such as A673 and TTC466, the cell spheroid could no longer be seen after 24h, and cells migrated radially as a sheet (Figure 4.9 A, lower panels). In contrast, SKES-1 and TC32 maintained a distinct spheroid core, which increased in size over 72h. In TC32 cells, individual cells appeared to migrate from the spheroid core (Figure 4.9 A, middle panels). In untreated (control) cells after 72h, migration was greatest in TTC466 cells (MI; 29±3.9) and A673 (MI; 26±3.6) and was significantly lower in SKES-1 ($p<0.05$, MI; 7±0.4) (Figure 4.9 A and B). Treatment with rWnt5A (200ng/ml) or Wnt3A (200ng/ml) into the media at 0h did not have a significant effect on the MI of any ESFT cell line, or the pattern of migration (Figure 4.9 A and B).

Cell Line	**Appearance of spheroid core (over 72h)**	**Appearance of migrating cells (over 72h)**
A673	Absent by 24h	Sheet of cells migrating radially
RD-ES	Absent by 48h	Sheet of cells migrating radially, with a defined migratory front
SKES-1	Increased in size by 4.4±0.2 - fold	Ring of cells, increasing gradually in size
SK-N-MC	Absent by 48h	Sheet of cells migrating radially with a defined edge
TC32	Increased in size by 10.8±0.7 - fold	Individual cells moving out radially
TTC466	Absent by 24h	Sheet of cells migrating radially with a defined edge

Table 4.1 Phenotype of ESFT cell spheroid migration over 72h ESFT cell lines grown as spheroids for 4 days were plated onto gelatin (0.1%) coated plastic and imaged every 24 h, up to 72h.

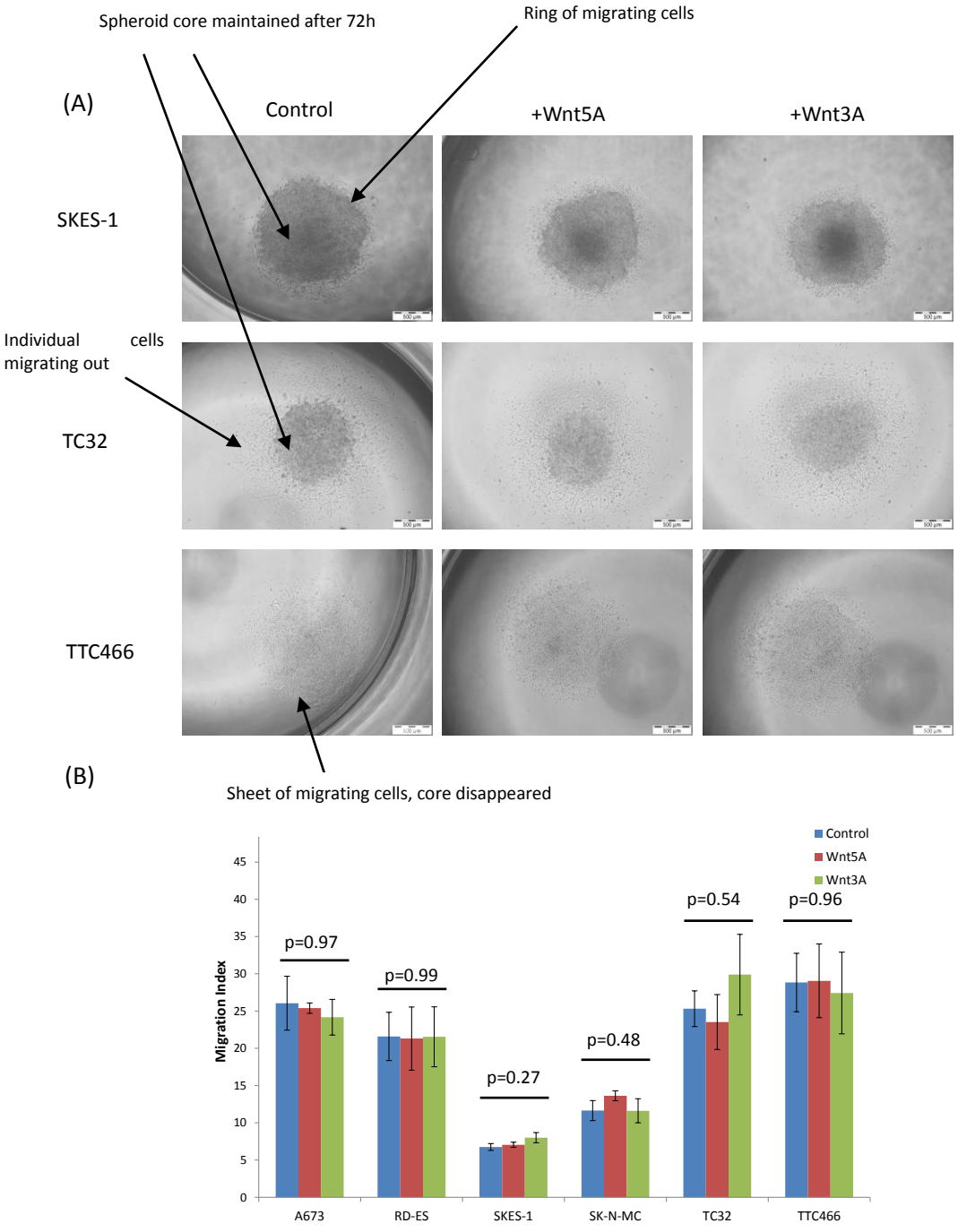

Figure 4.9 Migration of ESFT cell lines with and without treatment with Wnt3A and Wnt5A ESFT cell lines were grown as spheroids and plated onto flat-bottomed 96 well plates coated with 0.1% gelatin, in normal media (control) or media containing a final concentration of 200ng/ml rWnt3A or 200ng/ml rWnt5A. Images were taken every 24h and the area covered by migrating cells quantified using Volocity® software to calculate the migration index (Section 4.2.3) A) Representative images after 72 hrs. B) Results presented as the migration index of three independent experiments with three replicates per experiment (n=9) (±SEM).

4.3.5 Correlation between pull-down and migration assays

There was a very weak correlation between active Rac1 and migration in ESFT cell lines, both endogenous levels (R^2=0.16) and when treated with Wnt5A (200ng/ml; R^2= 0.15) (Figure 4.10 A and B).

(A) Untreated cells

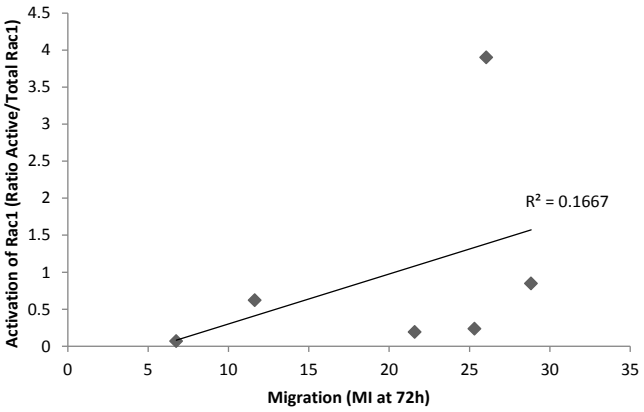

(B) Wnt5A treated cells

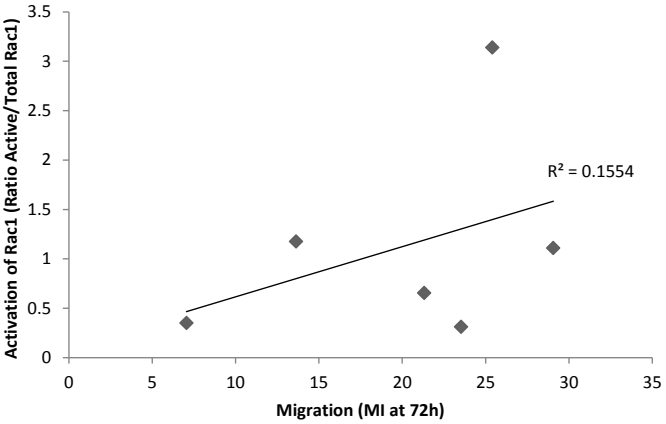

Figure 4.10 Correlation between active Rac1 and migration index ESFT cells There was a weak correlation in the activation of Rac1 measured using the pull-down assay, and the migration index (at 72h) of ESFT cells either when (A) untreated or (B) when cells were treated with 200ng/ml Wnt5A.

4.3.6 Measuring the invasion of ESFT cells

In addition to migration, the invasion of ESFT cells was also investigated as a downstream measure of noncanonical Wnt signalling. To measure the invasion of ESFT cell lines, spheroids were grown for 4 days as previously described and then embedded in collagen or Matrigel™, and imaged every 24h for 3 days. No invasion of ESFT cells was observed, when spheroids were embedded in collagen, with the exception of A673 where a few small processes could be observed (Figure 4.11 A, inset). No invasion was seen when spheroids were embedded in Matrigel™ (Figure 4.11 B). Addition of Wnt5A or Wnt3A to the collagen or Matrigel™ to a final concentration of 200ng/ml did not induce invasion in any ESFT cell line (data not shown).

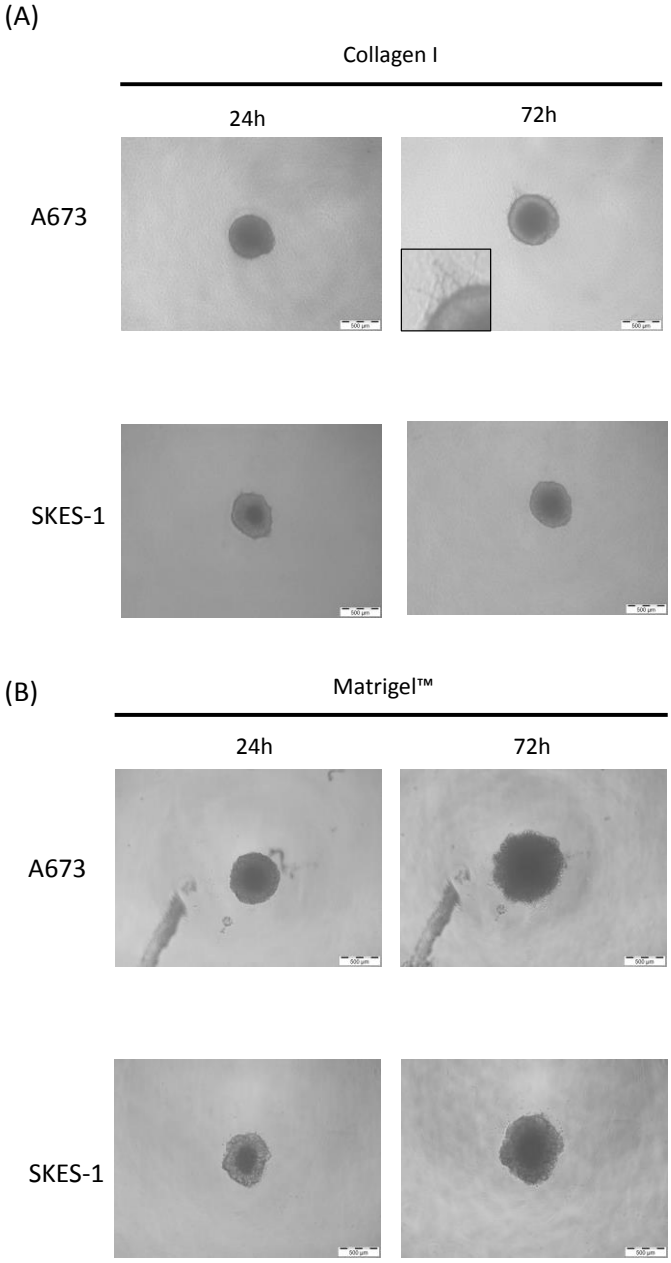

Figure 4.11 Invasion of ESFT cells in Collagen I and Matrigel™ ESFT cell lines were grown as spheroids and then suspended in A) collagen (Type I; rat tail) or B) Matrigel™ and imaged every 24h for up to 72h.

4.4 Discussion

In this chapter I have successfully optimised assays to measure and quantify Rac1/Cdc42 activation and the migration of ESFT cells. However, I have been unable to conclusively determine the activity of noncanonical Wnt signalling in ESFT cell lines using these assays.

The recombinant PAK-CRIB-GST protein was used to pull-down GTP-bound Rac1 and Cdc42 from cell lysates. The ability of this assay to isolate GTP-bound Rac1 was determined using HeLa cells stimulated with EGF. A time-dependent increase in GTP-bound Rac1 could be measured in HeLa cells after treatment with recombinant Wnt5A protein, however this increase was relatively small (1.5-fold). This is similar to a previous study which showed Wnt5A was able to activate Rac1 by 2-fold in HeLa S3 cells (Sato et al. 2010). Although S3 cells are a clonal derivative of the HeLa cell line, they may have different characteristics to the parent line. This may explain the difference in absolute magnitude of effect when cells were treated with Wnt5A. In addition, the concentration of PAK-CRIB used in the study by Sato et al. (2010) has not been given and therefore the differences in the magnitude of response may reflect differences in the concentration of ligand used and the sensitivity of the assay. Also, in the study by Sato et al. (2010) HeLa cells were serum starved for 36h before the addition of Wnt5A. It has been reported in HEK293T cells that serum starvation is necessary to detect Rac1 activation under normal growth conditions because in the presence of serum basal levels of active Rac1 are high (Habas et al. 2001, Habas et al. 2003). Indeed it is often suggested that cells are starved for serum before pull-down assays are performed to ensure low levels of active GTPase in the control condition (Pellegrin and Mellor 2008). However, ESFT cell lines do not tolerate serum starvation well (unpublished observations) and serum starvation was not appropriate in this case since I wanted to detect the levels of active Rac1/Cdc42 in ESFT cell lines under normal growth conditions to determine endogenous noncanonical Wnt signalling.

In ESFT cell lines both total and active (GTP-bound) Rac1 were detected. High levels of total Rac1 did not necessarily correlate to high levels of GTP-bound Rac1; A673 cells had the lowest level of total Rac1 but the highest level of active Rac1. Active Rac1 was heterogeneous between ESFT cell lines suggesting endogenous noncanonical Wnt signalling activation is also heterogeneous.

Another important observation is that the cell lines that had the highest level of endogenous active Rac1 expression were those that had the lowest levels of endogenous Wnt5A protein (Chapter 2), as summarised in Table 4.2. It may be the case that in these

cell lines another noncanonical Wnt such as Wnt11 is responsible for activating noncanonical Wnt signalling; both A673 and TTC466 expressed higher levels of Wnt11 mRNA compared to the other cell lines (Chapter 2). Alternatively, Rac1 activation in these cells may be downstream of other signalling pathways rather than noncanonical Wnt signalling. Indeed, Rac1 has been shown to be activated in the RD-ES and CHLA-10 ESFT cell lines downstream of phosphoinositide 3-kinase (PI3K) signalling (Mendoza-Naranjo et al. 2013, Kamura et al. 2010).

An increase in active Rac1 expression was detected after treatment with Wnt5A but only in SKES-1 and TTC466 cell lines. Small GTPase pull-down assays are usually performed over a short time course of 30s to 10 min (Pellegrin and Mellor 2008), however in the current study Wnt5A was added to the cells for 30 min before the assay was performed. Thirty minutes was optimised from studies using HeLa and SKES-1 cells. It is possible the time course of response to Wnt5A are different in different cell lines. The active Rac1 levels were very low in the cell lines that did not respond to treatment with Wnt5A, and so any small response may be beyond the limits of detection of this assay. Nevertheless to my knowledge this is the first time that activation of Rac1 in response to Wnt5A has been reported in ESFT cells, which suggests noncanonical Wnt signalling is active or at least can be stimulated, in some ESFT cell lines.

In contrast to Rac1, total Cdc42 expression was very low in ESFT cell lines and almost no active Cdc42 was detected. This is in concordance with previous findings in the RD-ES cell line (Kamura et al. 2010) and suggests the small GTPase Rac1 is more important in noncanonical Wnt signalling in ESFT cells.

Although the pull-down method is currently the most convenient and widely used assay to measure Rac1/Cdc42 activation, in agreement with other researchers (Dr Georgia Mavria, personal communication), I have found the method to be problematic and quite variable. These assays also have the disadvantage that they detect Rac1/Cdc42 in total cell populations and so any sub-populations with potentially high noncanonical Wnt signalling may be missed. More recently technologies such as fluorescence resonance energy transfer (FRET) have been used to detect small GTPase activation. In these assays a donor fluorophore is fused to the GTPase, and an acceptor fluorophore fused to the GTPase-binding domain of the effector protein (for example PAK-CRIB). When the GTPase is activated, binding to the effector will bring the two fluorophores close enough together that light emitted by the donor activates the acceptor (Aoki and Matsuda 2009). This assay can be used to observe activation of small GTPases in single cells.

Cell Line	Wnt5A expression			Active Rac1		Migration	
	mRNA ($2^{-\Delta Ct}$)	**Protein by western blot** (ratio to β-actin)	**Protein by flow cytometry** (median fluorescence/% positive)	**Endogenous expression** (ratio to total Rac1 expression)	**Stimulated with Wnt5A** (ratio to total Rac1 expression)	**Migration** (Migration Index at 72h)	**Stimulated with Wnt5A** (Migration index at 72h)
A673	**Lowest** 0.12	0.25	**Lowest** 3.90/67	**Highest** 2.98	**Highest** 2.67	26.2	25.4
RD-ES	**Highest** 2.05	**Highest** 1.04	**Highest** 9.7/46	0.29	**Lowest** 0.11	21.6	21.3
SKES-1	0.94	**Highest** 1.04	4.89/63	**Lowest** 0.09	0.29	**Lowest** 6.76	**Lowest** 7.1
SK-N-MC	0.23	**Lowest** 0.14	5.84/58	0.23	0.27	11.6	13.6
TC32	1.69	0.95	5.7/63	0.19	0.12	25.3	23.5
TTC466	1.32	0.19	6.2/45	0.46	0.89	**Highest** 28.8	**Highest** 29.1

Table 4.2 Summary of the results of the assays used to measure the activity of the noncanonical Wnt signalling pathway in ESFT cell lines Expression of Wnt5A mRNA and protein was determined in Chapter 2. To measure the activity of the noncanonical Wnt signalling pathway; expression of active Rac1 was determined by western blot and the migration of cells was assayed using a 3D migration assay.

In concordance with previous literature (Lawlor et al. 2002), I found ESFT cell lines spontaneously formed spheroids when cultured in low adherence conditions. It has been shown the spheroids formed from ESFT cell lines closely resemble primary ESFT reflected by cell morphology, cell-cell adhesions and kinase activation (Lawlor et al. 2002). In my studies the size and morphology of spheroids formed from ESFT cells was highly variable. This may reflect differences in E-cadherin expression since previous studies in TC32 and TC71 cells have shown that spheroid formation is dependent on E-cadherin and activation of downstream signalling pathways including Ras and PI3K (Kang et al. 2007).

All ESFT cell lines migrated from the spheroids when plated onto a gelatin-coated surface. The pattern and extent of migration was different between cell lines. This may be a result of differences in active noncanonical Wnt signalling since A673 and TTC466 cells which had the highest endogenous level of active Rac1 showed the greatest migration capacity (Table 4.2). However my analysis showed that overall there was no direct correlation between Rac1 activation and migration. Although migration is often used as an end point when attempting to measure the noncanonical Wnt signalling pathway, migration is a highly complex process. For example transcriptional targets of the EWS-FLI1 fusion protein such as CD99 and caveolin-1 have been shown to modulate ESFT cell line migration (Sáinz-Jaspeado et al. 2010, Kreppel et al. 2006). The receptor ERBB4 has also been shown to be highly expressed in ESFT cell lines, activate Rac1 (via PI3K signalling), and promote migration (Mendoza-Naranjo et al. 2013). Therefore, differential expression of these and other proteins may also explain the differences in migration seen.

Migration was not increased in any ESFT cell line by the addition of recombinant Wnt5A protein. This is in contrast to a previous study which showed Wnt5A increased the migration of ESFT cell lines including A673 and RD-ES (Jin et al. 2012). This is perhaps surprising since the study by Jin et al. (2012) used the same cell lines and the same recombinant Wnt5A protein (albeit at a lower concentration). However, the researchers measured chemotaxis using a transwell assay in response to the chemoattractant CXCL12, rather than migration on gelatin. As mentioned previously, chemotaxis assays measure the directional migration of single dissociated cells whereas the assay I have used measures migration from a spheroid. These assay differences could therefore explain the disparities observed. In the previous study in ESFT cell lines, migration was quantified after 18h of Wnt5A treatment (Jin et al. 2012). However, in my assay images to measure migration were taken after a minimum of 24h. Although there was no significant difference in migration in ESFT cell lines after Wnt5A treatment at this time point, it is possible that Wnt5A had an effect earlier in the time course and this was missed in my analysis.

Nevertheless, using the migration assay I have optimised, I failed to show an increase in migration in response to Wnt5A in PC3 and HeLa cells, which has previously been described using the same recombinant protein (Yamamoto et al. 2007, Jin et al. 2013). It would therefore be important to confirm that the recombinant Wnt5A protein used in my experiments is biologically active, which could be done by reproducing precisely the experiments described by Jin et al. (2012) or by using a positive control cell line such as melanoma which is known to migrate in response to Wnt5A (Weeraratna et al. 2002).

In my study migration was analysed by calculating a migration index; the area of the migration zone minus the area of the core. The 'migration zone' was defined as the area covered by at least 70% of cells. Therefore this method of analysis did not take into account the maximum migration of an individual cell. In some cell lines there were individual cells that migrated beyond the migration zone and these were missed from my analysis and this may have affected the results obtained. However, overall, the migration assay is a less informative way to measure noncanonical Wnt signalling since the results of these assays can be confounded by many other factors that can influence migration. The pull down assay is a direct measure of one component of the noncanonical pathway, however there are technical difficulties in measuring this and the assay is not very sensitive.

In contrast to migration, invasion of cells from ESFT spheroids into collagen or Matrigel™ was not observed, either in the presence or absence of Wnt5A. When spheroids were embedded in Matrigel™ they continued to increase in size demonstrating that the cells were still viable, however no invading cells could be seen by light microscopy. Invasion of ESFT cells in transwell assays using Matrigel™ coated membranes has been described previously (Kamura et al. 2010, Mendoza-Naranjo et al. 2013). Again this discrepancy could be attributed to the difference in assaying individual dissociated cells compared to those in a 3D spheroid.

In summary, I have optimised methods to detect active Rac1/Cdc42 in cells, and migration and invasion of cells using a 3D spheroid assay. I have shown that active Rac1 is expressed endogenously in all ESFT cell lines, and in some cell lines can be further activated by the addition of Wnt5A. I have also demonstrated that all ESFT cell lines are migratory, but that Wnt5A does not alter their migration. However the complexity of migration means that this is not suitable as an end-point measure of the noncanonical Wnt signalling pathway. It has been difficult to draw any definitive conclusions regarding the activity of noncanonical Wnt signalling in the ESFT cells lines investigated. As summarised in Table 4.2, in some cell

lines such as A673 and TTC-466 there was a correlation between active Rac1 and migration, thus strengthening the hypothesis that noncanonical Wnt signalling is active in these cells. However overall there was no correlation between active Rac1 and migration in the cell lines, although this may be due to the low sensitivity of the pull-down assay. In addition, there was an inverse correlation between Wnt5A expression in the cell lines, and the activity of noncanonical signalling determined by measuring active Rac1 expression and migration. Taken together these data make it difficult to conclude if noncanonical Wnt signalling is active in these cells. Furthermore, measuring activation of noncanonical Wnt signalling is problematic, as unlike the canonical pathway, there are a number of downstream effector molecules which can be activated, and these are involved in other signalling pathways. For example, as mentioned, Rac1 has been shown to be activated in ESFT cells downstream of PI3K signalling (Kang et al. 2007, Mendoza-Naranjo et al. 2013). Therefore to further understand the role of noncanonical Wnt signalling in ESFT cells it would be necessary to investigate the activation of other effector molecules. For example, phosphorylated JNK, phosphorylated c-Jun (Jin et al. 2012) or phosphorylation of PKC isoforms and subsequent translocation to the plasma membrane after Wnt5A treatment (Dissanayake et al. 2007). Immunofluorescence could also be used to examine changes in the actin cytoskeleton in cells after treatment with noncanonical Wnt ligands. It would also be important to investigate the effect of Wnt5A knock-down on ESFT cells. Wnt5A expression could be inhibited using RNAi, and the effect of this on Rac1 and Cdc42 expression, and on migration could be investigated. This would help to elucidate whether noncanonical Wnt signalling, or other signalling pathways such as PI3K are responsible for the observed phenotypes, such as migration, of ESFT cells.

5. Wnt signalling in reprogrammed ESFT cells

5.1 Introduction

In the previous two chapters I have developed assays to measure the activity of both the canonical and noncanonical Wnt signalling pathways. In this chapter my aim is to use these assays to measure Wnt signalling in reprogrammed ESFT cell lines, in an attempt to understand how Wnt signalling may be important in the initiation and development of ESFT.

Recently it been shown that like normal somatic cells, cancer cells such as chronic myeloid leukaemia (Carette et al. 2010) and gastrointestinal cancers including oesophageal, stomach, colorectal, liver and pancreatic cells (Miyoshi et al. 2010), can also be reprogrammed. As well as providing a renewable source of tumour material to study, it is hoped that reprogramming cancer cells will aid understanding of the cellular programs involved in the initiation and development of disease (Fernandez et al. 2013). For example, it has been recently shown that reprogrammed cells derived from pancreatic ductal adenocarcinoma (PDAC), when injected subcutaneously into mice generated premalignant lesions which later progressed back to invasive cancer (Kim et al. 2013). The ability to study the early stages of tumour development is vitally important and this is extremely difficult in ESFT since the cell(s) of origin are not known, and patients often present with advanced disease (Ross et al. 2013). Therefore, we hope that reprograming ESFT cells will elucidate more about the cancer initiating cell, that is responsible for metastasis and drug resistance, and it may be possible to identify pathways that can be targeted to develop novel therapeutics.

In our laboratory we have reprogrammed an ESFT cell line with a EWS-ERG fusion (TTC466) by transient transfection of one plasmid containing all four OSCK genes (Oct4, Sox2, c-Myc and Klf-4). Three different clones of transfected TTC466 cells have been studied and compared to three clones from a control TTC466 cell line transfected with GFP. In particular one clone, referred to as OSCK4, has been validated and has shown upregulation of stem cell markers, the ability to form embryoid bodies which can be differentiated to various different germ layers, and an increased ability to form subcutaneous tumours *in vivo.*

Reprogrammed cells are maintained in embryonic stem cell culture conditions to maintain their undifferentiated state. This usually involves growing cells on a feeder layer of mouse embryonic fibroblasts (MEFs) (Thomson 1998, Takahashi et al. 2007). However, it is not fully understood how MEF cells support self-renewal. There are undefined components in the media that could influence experimental results and the presence of a feeder layer can be problematic for downstream assays. For these reasons feeder-free culture systems have been developed using various using matrices to replace the feeder cells. In our laboratory, for the culture of hES cells we use Matrigel™ hESC-qualified matrix and mTeSR™1 media. mTesR™1 is a serum-free medium containing a DMEM:F12 base and 12 other defined factors including BSA, FGF2, TGFβ and LiCl (Ludwig et al. 2006, Akopian et al. 2010). It has been shown by the international stem cell initiative consortium to support the maintenance of a panel of embryonic stem cells, and also iPS cell lines (Akopian et al. 2010, Chen et al. 2011).

The aim of this current chapter is to;

1. Develop a feeder-free growth method for optimum maintenance of reprogrammed and control TTC466 cell lines
2. Investigate the activity of the canonical Wnt signalling pathway in reprogrammed ESFT cells using the firefly luciferase reporter system
3. Investigate the activity of the noncanonical Wnt signalling pathway in reprogrammed ESFT cells using Rac1/Cdc42 pull-down and migration assays.

5.2 Materials and methods

5.2.1 Feeder-free stem cell culture

Reprogrammed (OSCK4) cells were maintained in complete mTeSR™1 media (STEMCELL Technologies, Grenoble, France). Complete media was prepared by thawing 5X Supplement (100ml) at 4°C overnight and adding it to 400ml Basal Medium. Complete media was frozen at -20°C in aliquots and working solution stored at 4°C for a maximum of 2 weeks.

5.2.1.1 Coating plastics with hESC-qualified Matrigel™

All culture plastics were coated with Matrigel™ hESC-qualified matrix (BD Biosciences, supplied by VWR) prior to use. Matrigel™ was prepared in single use aliquots in cryovials according to the dilution factor provided by the manufacturer (typical volume range = 270-350µl), stored at -20°C and thawed on ice at 4°C overnight prior to use. To coat plastics, one aliquot of Matrigel™ was added to 25ml of chilled DMEM/F12 in a chilled 50ml Falcon tube, and mixed well. The diluted Matrigel™ was used to completely coat plastics as required (e.g. 2ml per 25 cm^2 flask) and incubated at RT for 1 h. Coated plastics were stored, wrapped in Clingfilm and stored at 4°C for up to 7 days.

5.2.1.2 Routine culture of cells maintained in mTeSR™1

OSCK4 cells were passaged using the same method used for human embryonic stem (hES) cells grown in feeder-free conditions using mTeSR™1. All cells were cultured in 25cm^2 flasks (Nunc™, Fisher Scientific) coated in Matrigel™ as previously described (Section 5.2.1.1). When cell colonies were beginning to merge, mTeSR™1 was aspirated from the flask and replaced with 1.5ml collagenase IV (1mg/ml Gibco™, Life Technologies, in DMEM/F12) and incubated for 5 min at 37°C. In this time, the Matrigel™ was aspirated from pre-coated flasks (Section 5.2.1.1) and replaced with fresh mTeSR™1. The cells were viewed using a light microscope to observe the edges of colonies beginning to detach, at this time the collagenase was aspirated and replaced with 3ml mTeSR™1. Colonies were mechanically dissociated using a fine-tip plastic Pasteur pipette (Alpha laboratories, Eastleigh, UK) whilst being viewed under a light microscope placed in the tissue culture hood. When all colonies had been detached, the solution was pipetted up and down gently 3 times to further dissociate the colonies, and the appropriate volume (depending on the split ratio) placed into the pre-prepared new flasks. Prior to incubation, flasks were gently shaken to ensure an even distribution of cells across the entire flask. Cells were maintained at 37^oC in 5%

CO_2 in 95% air. Media was aspirated and replaced with 5ml fresh mTeSR^{TM}1 daily to inhibit spontaneous differentiation. Cells were routinely split 1:4 every 3-4 days.

5.2.1.3 Formation of single cell suspension from cells maintained in mTeSR™1

Where a single cell suspension was required, OSCK4 cells were washed with 1X PBS and then incubated with 0.2X Trypsin/5mM EDTA (in 1X PBS) for 30s or until cells had completely detached. An equal volume of media containing 10% FCS was added to neutralise the trypsin and the suspension centrifuged at 403g for 3 min. Cells were resuspended in mTeSR™1 and viable cell number was determined using the Neubauer haemocytometer as previously described (Section 2.2.2).

5.2.2 Routine culture of GFP control cells

GFP1, GFP3 and GFP4 cells were maintained on Matrigel™ coated plastic prepared as previously described (Section 5.2.1.1). Cells were maintained in RPMI containing 10% conditioned media, collected from GFP cells and filtered using a 0.2µM membrane prior to use. GFP cells grew as a monolayer and were therefore passaged using trypsinisation as described for the parental TTC466 cell line (Section 2.2.3).

5.2.3 Determining viable cell number of OSCK4 and GFP cell lines

Cells were trypsinised as previously described (GFP, Section 2.2.1; OSCK4, Section 5.2.1.3) and seeded at 2×10^4 cells/well in 24-well Primaria™ plastic plates either uncoated or coated with Matrigel™ as previously described (Section 5.2.1.1). GFP and OSCK4 cells were seeded either in RPMI (+10% conditioned media) or mTeSR™1. After 24, 48 and 72h cells were counted by trypan blue exclusion using the automated vi-cell as previously described (Section 2.2.2). Triplicate wells were counted for each condition, at each time point.

5.2.4 Analysis of Wnt signalling components using RTqPCR

RNA was extracted from three GFP clones (GFP1, GFP3, GFP4) and from OSCK4 cells from confluent 10cm^2 dishes as described previously (Section 2.2.5.1). RNA was extracted at three separate time points to give three biological repeats. Gene expression of components of the Wnt signalling pathway was analysed using the TaqMan® Array Human WNT Pathway 96-well plate (Applied Biosystems), as described (Section 2.2.5.4). Expression of sFRP5, Wnt16, FGF4 and DKK2 was confirmed by specific RTqPCR using TaqMan® Assay-on-Demand™ (Applied Biosystems) primer/probe mixes (Table 5.1). Expression of the housekeeping gene PPIA was used for normalisation as described

previously (Section 2.2.5.5). Results were analysed using the comparative ΔCt method (Section 2.2.5.4).

Gene	Probe exon position	Amplicon length (bp)	Product code
sFRP5	1-2	69	Hs00169366_m1
Wnt16	2-3	104	Hs00365138_m1
FGF4	1-2	130	Hs00999691_m1
DKK2	2-3	88	Hs00205294_m1

Table 5.1 Wnt signalling component TaqMan® Assay-on-Demand primer/probe product information bp=basepair

5.2.5 Cloning of 7TFH vector

5.2.5.1 Plasmid digestion

The 7×Tcf-FFluc.SV40.PuroR (7TFP) plasmid was digested with 20 U (units) SalI-HF (High Fidelity; New England Biolabs (NEB), Hitchin, UK) and the pBABE Hygro plasmid digested with 20 U SalI-HF and 5 U ClaI (NEB). DNA (1µg) was added to a restriction enzyme (RE) mix containing 1X NEBuffer 4 (NEB) and 20 U of RE in nuclease-free H_2O to a total volume of 30µl. Samples were incubated for 2h on a heating block at 37°C. To create blunt ends 3' overhangs were removed and 3' recessed ends filled in using DNA Polymerase I, Large (Klenow) Fragment (NEB). 1.5 U of Klenow was added to the RE mix along with 1mM dNTPs and incubated for 15min at 25°C. To stop the reaction, 10mM EDTA was added and the mix incubated for 20 min at 75°C. Samples were immediately electrophoresed on an agarose gel to separate the fragments.

5.2.5.2 Agarose gel electrophoresis

Agarose (1% (w/v) Invitrogen™) was dissolved in 150ml 1X Tris-Borate-EDTA (TBE) Buffer (90mM Tris, 90mM Orthoboric acid (Sigma-Aldrich) and 2mM EDTA at pH 8) by heating gently in a microwave. The solution was cooled to approximately 60°C and ethidium bromide added (0.5 µg/ml, Sigma-Aldrich) to allow visualisation of the DNA under ultra violet (UV) light. The solution was mixed by gentle agitation and poured into a Horizon™ agarose gel tray (Invitrogen™) and a comb inserted. The gel was incubated at RT for 1h to

solidify and then placed into an electrophoresis tank in 1X TBE buffer. Samples were diluted 1:6 in gel loading buffer (0.4 mM Ficoll (Type 400; Sigma-Aldrich), 17.3 mM SDS, 0.4 mM Bromophenol blue (Sigma-Aldrich) and 5.6 mM Orange G (Sigma-Aldrich)) and loaded into the gel alongside Quick-Load® 1 kilobase (kb) DNA ladder (10 µl containing Bromophenol blue; NEB), to allow for confirmation of the size of DNA fragments. The gel was electrophoresed at 80 V for 90 min. Products were visualised under UV light using a trans-illuminator (BioRad). A nuclease-free H_2O sample was included as a negative control.

5.2.5.3 DNA extraction from an agarose gel

The required fragments of DNA namely the 7TFP vector (minus puromycin, approx. 8000 bp)) and hygromycin resistance gene (approx. 1500 bp) were excised from the agarose gel using a sterile scalpel. DNA was extracted using the GenElute™ kit (Sigma-Aldrich). All solutions are company propriety. Briefly, gel slices were placed in a 1.5ml Eppendorf at 55°C in Gel Solubilisation Solution (3:1) with occasional vortexing until completely dissolved (approximately 10min). Meanwhile, Column Preparation Solution (500µl) was added to a GenElute Binding Column, the column centrifuged (16,000 g for 1min) and the solution discarded. Once the gel had dissolved, isopropanol (100%) was added 1:1, mixed by pipetting and added to the prepared binding column, 700µl at a time, and the column centrifuged (16,000 g for 1min). After all the solubilised gel had been passed through, the column was washed twice with Wash Solution (700µl) and centrifuged as above between each wash. Finally, the empty column was centrifuged to remove any excess ethanol. The column was transferred to a new collection tube and the DNA eluted by centrifugation into 30µl of nuclease-free dH_2O. DNA quality and quantity was determined using the Nanodrop as described previously (Section 2.2.5.2).

5.2.5.4 Calf-intestinal alkaline phosphatase (CIP) treatment

Calf-intestinal alkaline phosphatase (CIP) was used to dephosphorylate the 5’ end of the empty 7TFP vector and therefore prevent religation. CIP was added to extracted 7TFP vector DNA in 1X NEBuffer 3 (NEB) to a final concentration of 0.5 U/µg of DNA and incubated for 1h at 37°C.

5.2.5.5 DNA ligation

The hygromycin resistance gene was ligated into the 7TFP vector at a ratio of 3:1 in a mix containing 1X T4 DNA Ligase Buffer (NEB), 200 U T4 DNA Liagse (NEB) and dH_2O. The mixture was mixed gently by pipetting and incubated at 16°C overnight using the Techne

TC-500 Thermal Cycler. A no hygromycin gene control was included to check for self-ligation of the 7TFP vector.

5.2.5.6 Bacterial Transformation

XL-1 Blue competent cells (Stratagene, supplied by Fisher Scientific) were thawed slowly on ice. For each transformation, 100µl of competent cells were added to a pre-chilled round-bottomed polypropylene tube (Falcon, Fisher Scientific). Ligated DNA (1µl) was added directly and incubated on ice for 20 min. The solution was then placed in a water bath at exactly 42°C for 45s and placed on ice for 2min. Super Optimal broth with Catabolite repression (SOC) medium (250µl) was then added and the tube incubated for 1h at 37°C with vigorous shaking. Transformed bacteria were streaked onto LB Agar plates as previously described (Section 3.2.2.1.1).

5.2.5.7 DNA isolation by minipreparation

Twelve clones were selected from LB Agar plates and minipreparation performed to isolate a small quantify to DNA for analysis. Each colony was picked using a pipette tip and inoculated into 5ml LB medium (+100µg/ml amp) and incubated for 16h at 37°C with vigorous shaking. The GenElute™ Plasmid Miniprep Kit (Sigma-Aldrich) was used to isolate DNA. All reagents are company proprietary. Bacterial cultures (3ml) were transferred to microcentrifuge tubes and the bacteria pelleted by centrifugation (12,000g, 1 min). The pellet was resuspended in 200µl Resuspension Solution and mixed gently by pipetting until clear (5 min). Cell debris was precipitated by adding 350µl Neutralization/Binding Solution and debris pelleted by centrifugation (12,470 g, 10 min). Meanwhile, a GenElute Miniprep Binding Column was prepared by adding 500µl of the Column Preparation Solution followed by centrifugation (12,000 g, 1min), and the flow through discarded. The cleared lysate was then loaded onto the prepared column and the column centrifuged (12,470 g, 1 min), the flow through discarded and the column washed with 750µl Wash Solution (containing ethanol). The column was centrifuged (12,000g, 1 min) and the flow through discarded before centrifuging again (maximum speed, 2 min) to remove any residual ethanol. Finally the column was transferred to a fresh collection tube and the DNA eluted by adding 100µl nuclease-free H_2O to the column and centrifugation (12,000g, 1 min). DNA quantity and quality was measured using the Nanodrop as previously described (Section 2.2.5.2).

5.2.5.8 Identifying correctly cloned vector constructs

To identify which of the 12 clones contained the correct vector contruct, a sample of each clone was digested using restriction enzymes EcoRI and HindIII (Section 5.2.5.1) and separated on an agarose gel (Section 5.2.5.2). Using the vector maps, it was predicted that vector digests should contain unique fragments of 1576 bp and 2040 bp. Clones with these fragments were expanded from the initial 5ml stock produced (Section 5.2.5.7) by adding 200µl bacteria culture to 5ml LB medium (+100µg/ml amp) and incubating for 16h at 37°C with vigourous shaking. After this time the bacterial culture was added to 200ml LB medium (+100µg/ml amp) and incubated for a further 16h in the same conditions. Vector DNA was isolated using the HighSpeed® Plasmid Maxi Kit (Section 3.2.2.1.2).

To confirm that the hygromycin resistance gene was inserted in the correct orientation, the two regions where 7TFP and hygromycin join were sequenced. Sequencing was performed using the BigDye® Terminator v1.1 Cycle Sequencing Kit (Applied Biosystems). Forward and reverse primers were designed to sequence the overlap (Table 5.2). For each primer a BigDye® mix (7.5µl) was prepared containing 500ng vector DNA, 2µl BigDye® Reaction Mix, 1.5µl BigDye® Reaction Buffer, 0.5µl primers (3.2µM) made up in dH_2O. Samples were loaded into a 96-well sequencing plate (Thermo Fisher) and incubated using GeneAmp® PCR System 9700 (Applied Biosystems) for 25 cycles of heating to 96°C for 10s, 55°C for 5s and 60°C for 4min, then cooled to 4°C. To precipitate the DNA, 1µl of sodium acetate (3M, pH 5.2) and 25µl 95% (v/v) ethanol were added to each well and the plate incubated at RT for 30 min. After this time the plate was centrifuged at 1879g for 15min after which the supernatant was removed by gently tipping the plate onto filter paper. Ethanol (75µl of 70% solution) was then added to each well and centrifuged again as described above. After the ethanol had been removed the plate was inverted and centrifuged (420g, 1 min) to remove any excess ethanol. The plate was placed at 95°C for 1 min to evaporate any residual ethanol and finally 15µl of Hi-Di™ Formamide (Applied Biosystems) added to each well. The plate was centrifuged (1879g, 1 min) then placed at 95°C to denature the DNA, then placed on ice before sequencing was performed using the Hitachi 3130xl Genetic Analyzer (Applied Biosystems)

	Primer Sequence	Primer Location
Primer 1	5'-CGTGGATTACGTCGCCAG-3'	Forward from 7TFP into Hygro
Primer 2	5'-CCAGCAGGCAGAAGTATG-3'	Forward after primer 1
Primer 3	5'-CAGAGCTTGGTTGACGGC-3'	Forward from Hygro to 7TFP
Primer 4	5'-CACGCCACGTTGCCTGAC-3'	Reverse from 7TFP into Hygro

Table 5.2 Primers used to sequence clones 7TFH vector The position of the primers in the 7TFH vector is shown in the schematic in Figure 5.6 A.

5.2.6 Generation of cell lines transduced with 7TFH vector

Lentiviral particles containing the newly cloned 7TFH vector were generated in HEK293T cells using the LENTI-Smart kit (Section 3.2.2.2). HEK293T, OSCK4 and GFP3 cell lines were infected with lentiviral supernatant at an MOI of 2 (Section 3.2.2.3) and 48h after infection were selected using media containing 200 µg/ml Hygromycin (Invitrogen™) for 2 weeks. Cells were maintained in Class II conditions (as described in Section 3.2.2.2) for at least 10 days after infection or until the cells had been cultured though at least 2 passages.

5.2.7 Luciferase assay

To test the activity of the 7TFH vector, HEK293T 7TP and HEK293T 7TFH cells were seeded at 5×10^4 cells in 24-well plates. OSCK4 7TFH and GFP3 7TFH cells were seeded at 1×10^5. After 24h the media on cells was replaced with normal growth media (control) or media containing rWnt3A (200ng/ml) or rWnt5A (200ng/ml). After a further 24h luciferase activity was determined using the Luciferase Assay (Section 3.2.5).

5.2.8 Migration assay

OSCK4 and GFP3 cells were grown as spheroids (Section 4.2.2) and the migration assay performed as previously described (Section 4.2.3).

5.2.9 Rac1/Cdc42 pull-down assay

OSCK4 and GFP3 cells were seeded at 2×10^6 cells in $10cm^2$ dishes and treated with normal growth media (control) or media containing 200ng/ml rWnt5A for 30min. Total and active levels of Rac1 and Cdc42 were determined using the pull-down assay as previously described (Section 4.2.1.4).

5.2.10 Statistics

For the Wnt signalling array, the optimal housekeeping gene was selected as previously described (Section 2.2.6). Clustering analysis and analysis to determine if there was a significant difference between expression of Wnt signalling genes in GFP clones and OSCK4 cells was performed by Mr John Alexander (University of Leeds). Differences in expression were analysed using the Limma package (Smyth 2004) using the software R (version 3.0.2 for OS 6). The Limma package uses linear modelling to fit genes from cases (OSCK4) and controls (GFP clones) and find significant differences amongst them. All other statistical analyses were performed as described previously (Section 3.2.11).

5.3 Results

5.3.1 Determining optimal growth conditions for OSCK and GFP cell lines

Previously the OSCK (reprogrammed TTC466) and GFP1, GFP3 and GFP4 (control) cell lines had been generated and maintained on a feeder layer of immortalised MEF cells. However, for the functional assays I have developed to measure the activity of the canonical and noncanonical Wnt signalling pathway it was necessary to transfer the cells to a feeder-free culture system. In addition, to compare results generated from reprogrammed ESFT cells and human embryonic stem (hES) cells with inducible EWS-FLI1 expression (Chapter 6) it was essential that cells were grown in the same culture conditions. I therefore evaluated the viable growth of the OSCK4 and GFP3 cells in mTeSR™1 on a Matrigel™ coated surface (used in our laboratory to maintain hES) to growth on Primaria™ plastic plus RPMI 1640 containing 10% conditioned media (CM), which is used to culture the parent TTC466 cells (Section 2.2.1, Table 2.1)

GFP3 cells did not grow in mTeSR™1; viable cell growth was significantly reduced over 72h when cells were seeded into Primaria™ or Matrigel™ coated 24-well plates ($p<0.0001$) (Figure 5.1 A). Cells appeared rounded and the majority of cells did not adhere to either substrate (Figure 5.2 A). The viable cell number of GFP3 cells increased over 72h when cells were grown in RPMI on both Matrigel™ and Primaria™ coated 24-well plates (Figure 5.1 A) and the appearance of the cells down the light microscope was similar on both substrates (Figure 5.2 A). In contrast, the viable cell growth of OSCK4 cells increased over 72h in all conditions; viable cell growth was greatest when OSCK4 cells were seeded on Matrigel™ coated plates in mTeSR™1 although this difference was not significant ($p=0.16$) (Figure 5.1 B). When seeded on Primaria™ coated plates, OSCK4 cells grew in colonies, with more floating cells compared to growth on Matrigel™ coated plates, where cells grew as a homogenous monolayer (Figure 5.2 B). In optimal conditions, the viable cell growth of OSCK4 cells was significantly slower than that of GFP3 cells ($p<0.0001$). When seeded at the same cellular density, viable cell number after 72h of OSCK4 cells was 0.14×10^6 and of GFP3 cells 0.24×10^6 (Figure 5.1 A and B). In all future experiments, to eliminate any differences in cell behaviour due to substrate, both OSCK4 and GFP3 lines were cultured on Matrigel™ coated plastic. GFP3 cells were cultured in RPMI (+ 10% CM) and OSCK4 cells were cultured in mTeSR™1

(A) GFP3

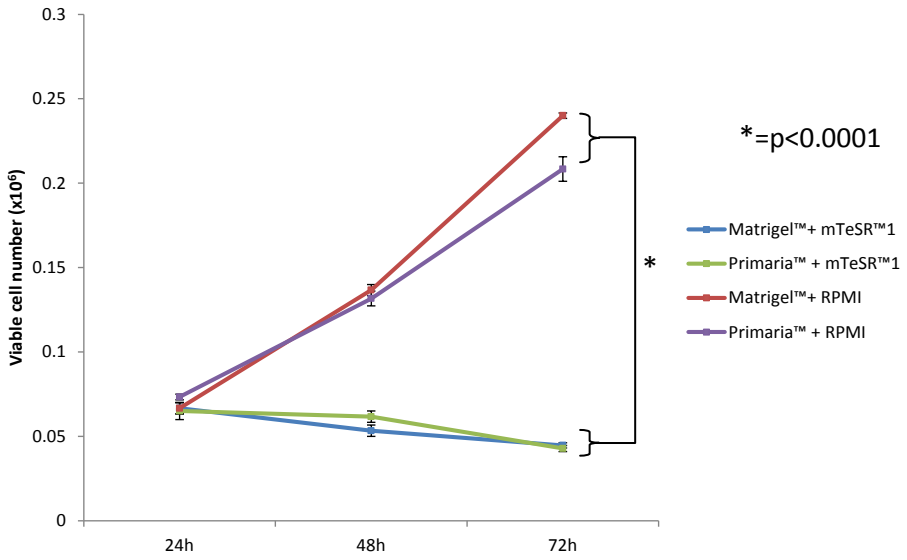

(B) OSCK4

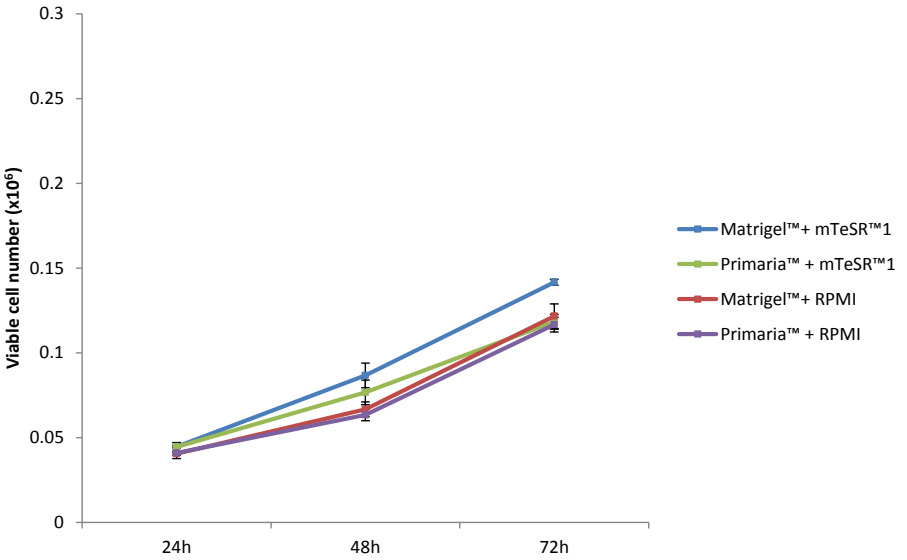

Figure 5.1 Growth of GFP and OSCK cells on different substrates and in different media
(A) GFP and (B) OSCK cells were seeded into 24 well plates either on Primaria™- or Matrigel™-coated plastic and either in RPMI (+10% conditioned media) or mTeSR™1 media. Viable cell number was determined by the trypan blue exclusion assay using an automated Vi-cell, every 24h. Results are the mean of two independent experiments with three replicates in each repeat (n=6) (± SEM).

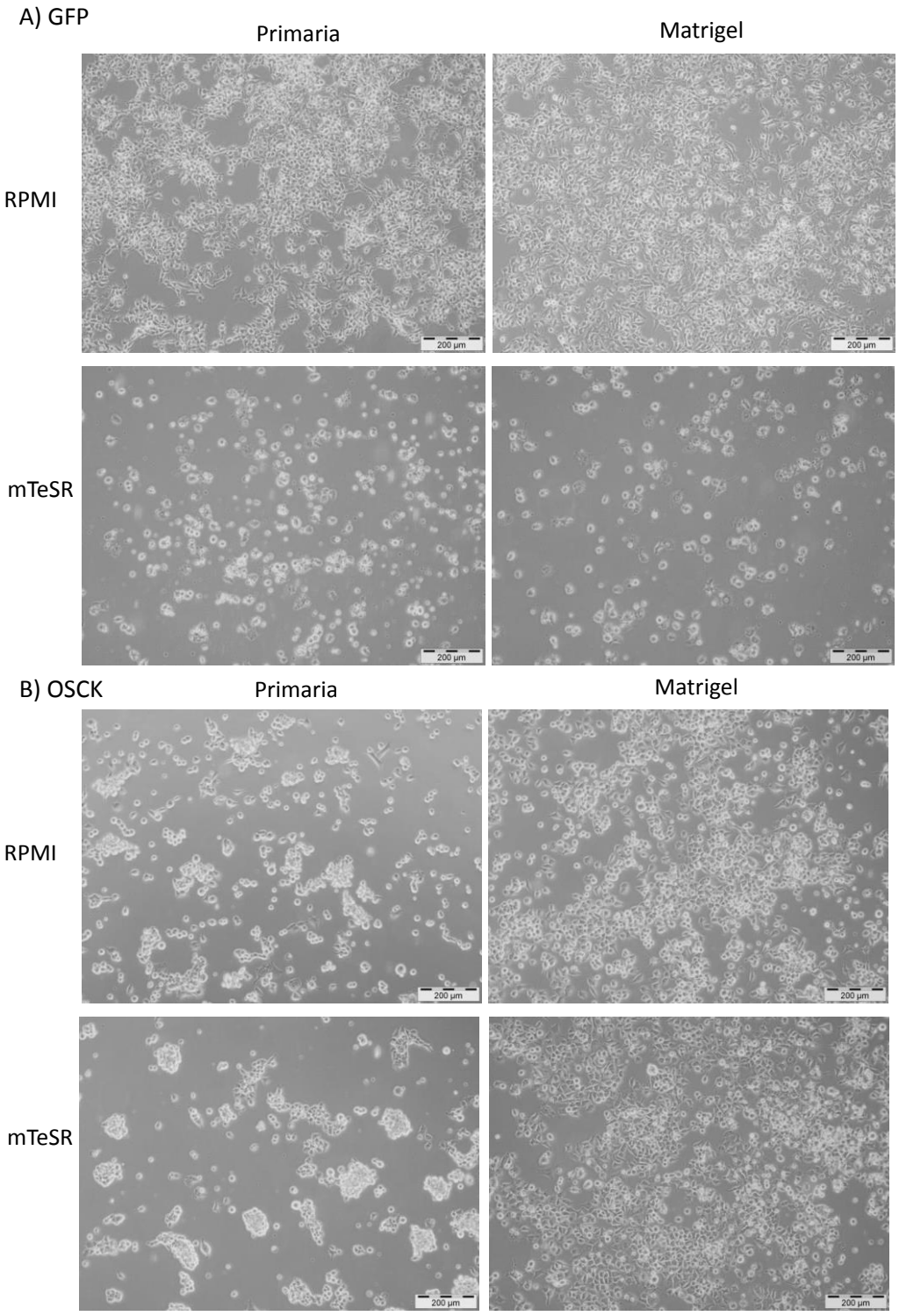

Figure 5.2. Light microscope images of GFP and OSCK cells cultured on different substrates and in different media Representative images 72h after seeding of GFP and OSCK cells grown on Primaria™ or Matrigel™ coated 24 well plates, in either RPMI (+ 10% CM) or mTeSR™1 media.

5.3.2 mRNA expression of Wnt signalling components in OSCK and GFP cells

5.3.2.1 Profile by TaqMan® Wnt Pathway Array

As discussed in Chapter 2, the TaqMan® Wnt Pathway Arrays (Applied Biosystems) contain 4 housekeeping genes. It was necessary to determine which was the appropriate housekeeping gene to use to normalise expression of Wnt signalling components in GFP and OSCK4 cell lines, since this may be different to the housekeeping gene used for the ESFT cell line data. Therefore the expression of HRPT1 and GUSB over each technical replicate for OSCK4, GFP1, GFP3 and GFP4 cells was investigated, to examine the stability of expression across the replicates. Inter-assay variability was determined as previously described (Section 2.2.6). The variance was lowest using the mean of HRPT1 and GUSB (F-value=2.72) compared to using HRPT1 (F-value= 3.60) or GUSB (F-value=3.83) alone. Therefore the mean of HRPT1 and GUSB was used to normalise the data for GFP and OSCK4 cell lines.

RNA was analysed from three different GFP clones; GFP1, GFP3 and GFP4, and from one OSCK clone, OSCK4. Data from our laboratory has demonstrated that the OSCK4 clone has been reprogrammed and generates multiple cell types *in vivo*, and that the variation between the three GFP clones is very low (Andrea Berry, personal communication). Hierarchical clustering revealed that the technical repeats of the GFP clones cluster together, and the OSCK4 repeats cluster separately, consistent with previous observations in the laboratory (Figure 5.4). Of 91 components of the Wnt signalling pathway represented on the array, 88% (80/91) had similar expression in both the OSCK4 and GFP cells (Figure 5.3, Figure 5.4). Genes that were expressed at significantly different levels ($p<0.05$) and were changed by more than 2 Ct values between OSCK4 and GFP cells are shown in Table 5.2. The most significant change was observed in FGF4 ($p<0.001$); expression was increased by more than 6 Ct values in the OSCK4 cells compared to GFP cells. sFRP5 expression was also increased significantly ($p<0.001$) in OSCK4 cells along with 5 Wnt ligands; Wnt16, Wnt8B, Wnt3 (all $p<0.001$), Wnt3A and Wnt1 (both $p<0.05$). In contrast the inhibitor DKK2 had significantly lower expression in OSCK4 cells ($p<0.05$).

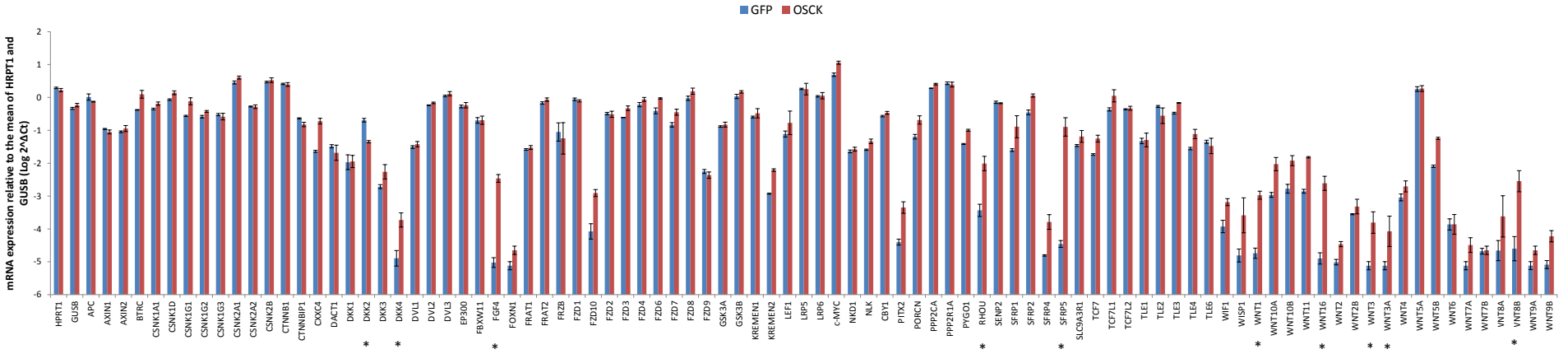

Figure 5.3 RNA expression of components of the Wnt signalling pathway in OSCK and GFP cells. OSCK4, GFP1, GFP3 and GFP4 cells were harvested, total RNA extracted and expression level determined using the Taqman® Wnt signalling gene expression array. Data presented as mRNA expression relative to the mean of the housekeeping genes *HRPT1* and *GUSB*. Results of three independent experiments. Results show mean of all three GFP clones (n=9) and mean of OSCK4 (n=3) (±SEM). *= Genes that were expressed at significantly different levels ($p<0.05$) and were changed by more than 2 Ct values between OSCK4 and GFP cells (see Table 5.2)

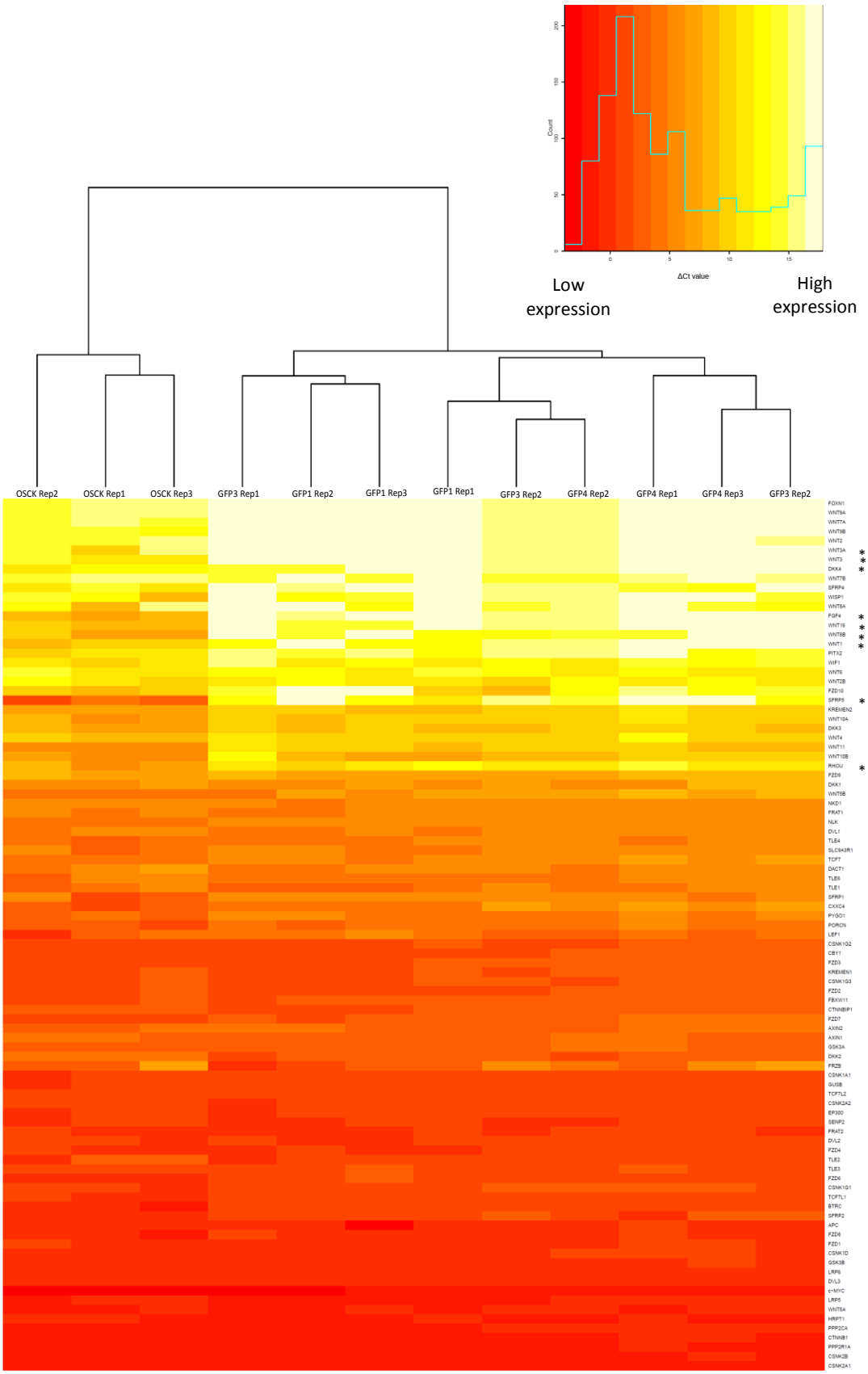
Count
ΔCt value
Low expression
High expression
OSCK Rep2
OSCK Rep1
OSCK Rep3
GFP3 Rep1
GFP1 Rep2
GFP1 Rep3
GFP1 Rep1
GFP3 Rep2
GFP4 Rep2
GFP4 Rep1
GFP4 Rep3
GFP3 Rep2

Figure 5.4 Clustering of Wnt signalling components in OSCK and GFP cells. Expression of Wnt signalling components was determined (Figure 5.3) and hierarchical clustering was performed to generate a heat map. Red indicates low expression and pale yellow high expression. *= Genes that were expressed at significantly different levels ($p<0.05$) and were changed by more than 2 Ct values between OSCK4 and GFP cells (see Table 5.2)

Gene	Significance (P value)	Ct value in GFP	Ct value in OSCK4	Expression in OSCK4 relative to GFP* (Difference in Ct)	Expression directly or indirectly controlled by reprogramming gene(s) (OSCK)?
sFRP5	0.00043	37.8 ±0.7	27.5 ±0.5	-10.3	-No
FGF4	0.000000089	39.7 ±0.2	32.7 ±0.8	-7	-Yes, SOX2 activates FGF4 (Weber et al. 2013)
WNT16	0.000072	36.5 ±0.5	33.2 ±1.1	-3.3	-No
WNT8B	0.001216	38.3 ±0.5	33.1 ±1.4	-5.2	-Yes, Oct4 can activate Wnt8B expression (Katoh 2007)
WNT3	0.000399	40	37.2 ±1.4	-2.8	-No
WNT1	0.001521	38.7 ±0.6	34.4 ±0.4	-4.3	-Yes, Wnt1 can be activated by SOX2 (Chen et al. 2012)
DKK2	0.001723	25.2 ±0.3	29 ±0.4	+3.8	-No
RHOU	0.000399	34.4 ±0.4	31.2 ±1.1	-3.2	-No
DKK4	0.005169	39.2 ±0.4	36.9 ±0.4	-2.3	-No
WNT3A	0.005169	40	38 ±1.9	-2	-No

Table 5.3 Genes with significantly different mRNA expression in OSCK cells compared to GFP cells Expression of genes was determined using the Taqman® Wnt signalling gene expression array and genes with significantly different expression in GFP and OSCK values identified by Limma analysis (Section 5.2.10). Ct values are given for the mean of GFP clones (GFP1, GFP3 and GFP4) and OSCK4 (±SEM). *A lower Ct value means higher expression therefore a reduction in Ct value indicates an increase in expression. A Ct value of 40 is considered no detection.

5.3.2.2 Validation of expression by RTqPCR

The Wnt signalling pathway array only contains one well per target, per plate. Although I have performed three biological repeats it was necessary to validate the significant changes in mRNA expression detected using the Wnt signalling pathway array using RTqPCR for individual genes. The primer and probe mixes were purchased as Assays-on-Demand™ (Applied Biosystems) and were identical to those used in the Wnt signalling pathway array with the exception of FGF4, where a different primer/probe mix was used. The same samples of RNA were used for both the Wnt signalling pathway arrays and validation RTqPCR reactions. However the Wnt signalling array was performed for all three GFP lines, whereas the validation experiments were only performed using GFP3. The pattern of expression was the same for both the Assay-on-Demand and array data; sFRP5, Wnt16 and FGF4 had higher expression in OSCK4 cells, whereas expression of DKK2 was higher in GFP3 cells. However, there were some differences in the magnitude of differences in expression detected using the two methods. When detected using the Assay-on-Demand, expression of sFRP5 was 14.2 Ct values lower in OSCK4 cells then GFP cells (Figure 5.5), whereas expression was only 10.3 Ct values lower when detected using the Wnt signalling pathway array (Table 5.2). In addition using Assays-on-Demand neither Wnt16 or FGF4 mRNA was detected in GFP cells, and the Ct values for OSCK4 cells were higher than those observed in the Wnt signalling array (Table 5.2).

(A)

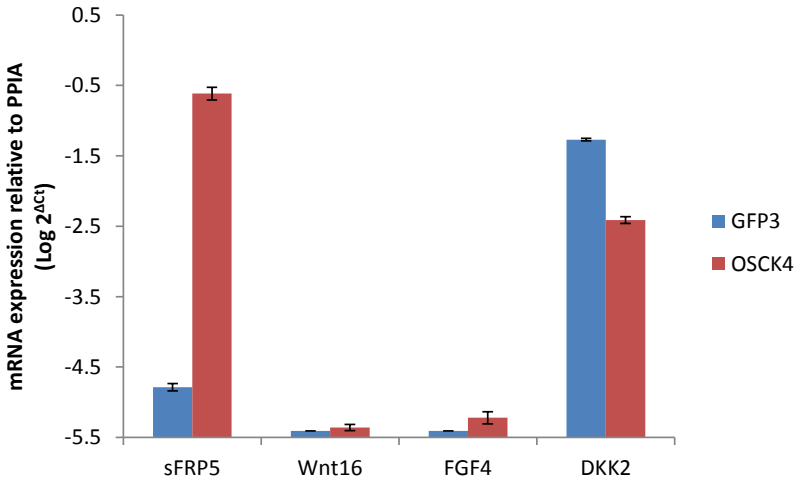

(B)

Gene	GFP3 (Mean Ct value ±SEM)	OSCK4 (Mean Ct value ±SEM)	Expression in OSCK4 relative to GFP (Difference in Ct*)	Wnt signalling array result (Difference in Ct between GFP3 and OSCK4)
sFRP5	37.8 (±0.06)	23.6 (±0.24)	-14.2	-9.8
Wnt16	40	39.4 (±0.12)	-0.6	-6.8
FGF4	40	38.9 (±0.24)	-1.1	-7
DKK2	26.3 (±0.04)	29.6 (±.13)	+3.3	+4
PPIA	22 (±0.15)	22 (±0.14)	0	N/A

Figure 5.5 sFRP5, Wnt16, FGF4 and DKK2 mRNA expression determined by RTqPCR RNA was extracted, RT performed and expression determined by RTqPCR using Assays-on-Demand (Applied Biosystems) A) sFRP5, Wnt16, FGF4 and DKK2 mRNA expression in GFP3 and OSCK4 cell lines using cDNA generated from 10ng RNA. Data presented as target expression relative to the expression of the housekeeping gene PPIA (Log values). Results show the mean of triplicate wells in one experiment. B) Mean Ct values obtained from the RTqPCR. *A higher Ct value corresponds to low expression, a Ct value of 40 is considered no detection.

5.3.3 Activity of the canonical Wnt signalling pathway in OSCK and GFP cells

5.3.3.1 Cloning of Hygromycin resistance gene into 7TFP vector

Previous work has shown that the 7TFP luciferase reporter plasmid can be used as a sensitive measure of canonical Wnt signalling (Chapter 3). This system uses a puromycin resistance gene to select for cells which contain the plasmid to generate a cell population with stable expression. Since the OSCK vector also contains a puromycin resistance gene it was necessary to change the resistance gene in the 7TFP vector to allow selection of the OSCK cells for the luciferase reporter plasmid.

The puromycin resistance gene was removed from the 7TFP vector and replaced with the hygromycin resistance gene from the pBABE Hygro vector (as described in Section 5.2.5). Twelve different clones were produced and each clone was digested with EcoR1 and HindIII to generate multiple fragments (Figure 5.6 B). Based on the restriction enzymes used and the plasmid map it was calculated that the size of full length undigested plasmid was 9581 bp and clones with hygromycin inserted and ligated in the correct orientation should have unique fragments of 1576 bp and 2040 bp. These fragments were identified in clones 1, 4 and 10 and were not present in the other clones (Figure 5.6 B). Clone 10 was expanded and purified plasmid DNA was further validated by sequencing the flanking regions of hygromycin resistance (Appendix). This new plasmid was termed pLenti 7xTcf Ffluc SV40-Hygro (7TFH).

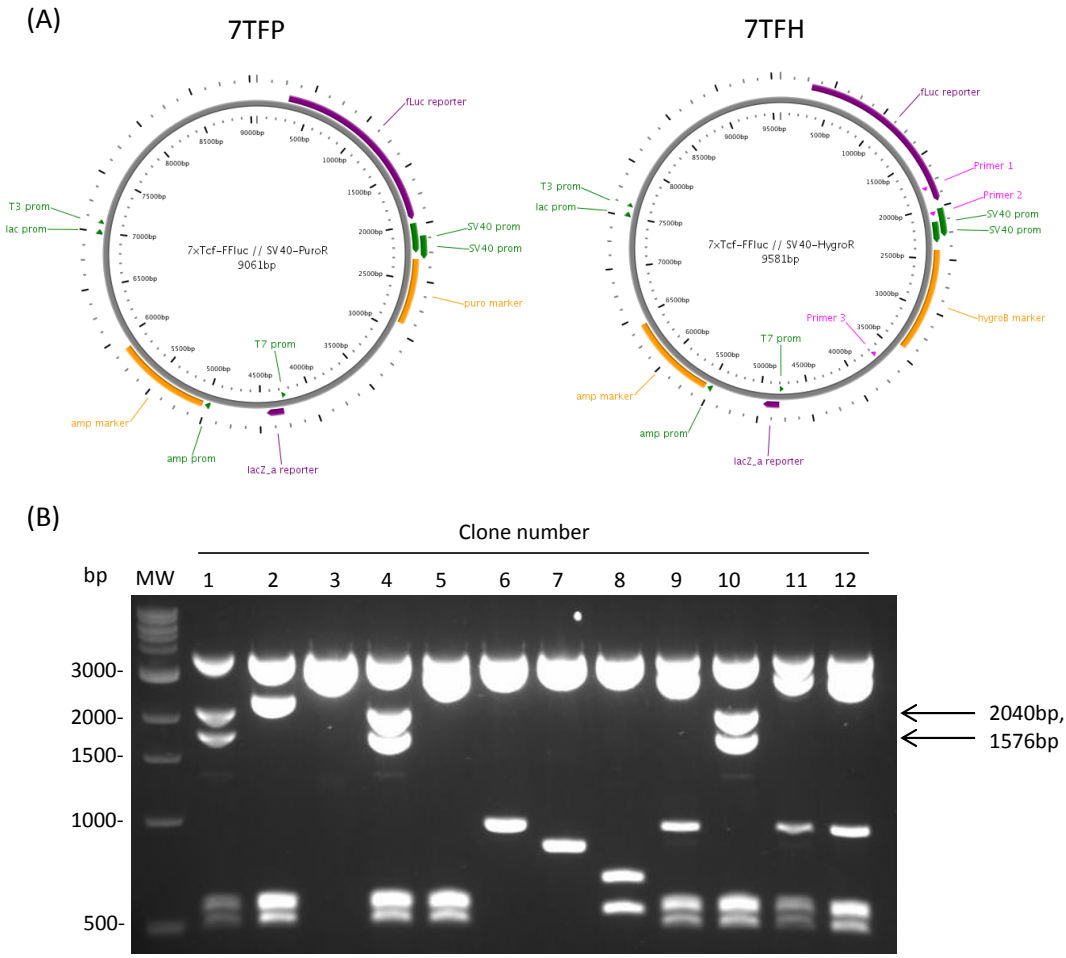

Figure 5.6 Cloning of 7TFH plasmid A) Schematics of expression vectors 7TFP and 7TFH. For 7TFH the position of primers used for sequencing is also shown. Generated using PlasMapper Version 2.0 (Dong et al. 2004). To confirm correct cloning of the 7TFH plasmid, 12 clones were selected, DNA extracted and digested with EcoRI and HindIII. The resulting products were electrophoresed on an agarose gel containing ethidium bromide (0.5µg/ml) and visualised using UV light B) Clones with the correct vector sequence were predicted to have unique bands at 1576 and 2040 bp; lanes 1,4 and 10. Bp= basepair, MW= molecular weight.

5.3.3.2 Confirming the luciferase reporter function of 7TFH plasmid

To test the activity of the newly generated 7TFH vector, the luciferase activity in HEK293T 7TFH cells was compared to that of HEK293T 7TFP cells. Endogenous activity was significantly increased in the 7TFH cells compared to that of the 7TFP by 57±4.4% ($p<0.05$). When stimulated with Wnt3A (200ng/ml for 24h) luciferase activity was significantly increased in both 7TFP and 7TFH cells compared to unstimulated cells, as expected. However, the luciferase activity in 7TFP and 7TFH cells stimulated with Wnt3A was not statistically different from each other (14.6±0.056 $x10^6$ and 15.4±0.048 $x10^6$ RLU, respectively) (Figure 5.7). This demonstrates that the reporter function of the 7TFH vector is equivalent to that of the original vector (7TFP).

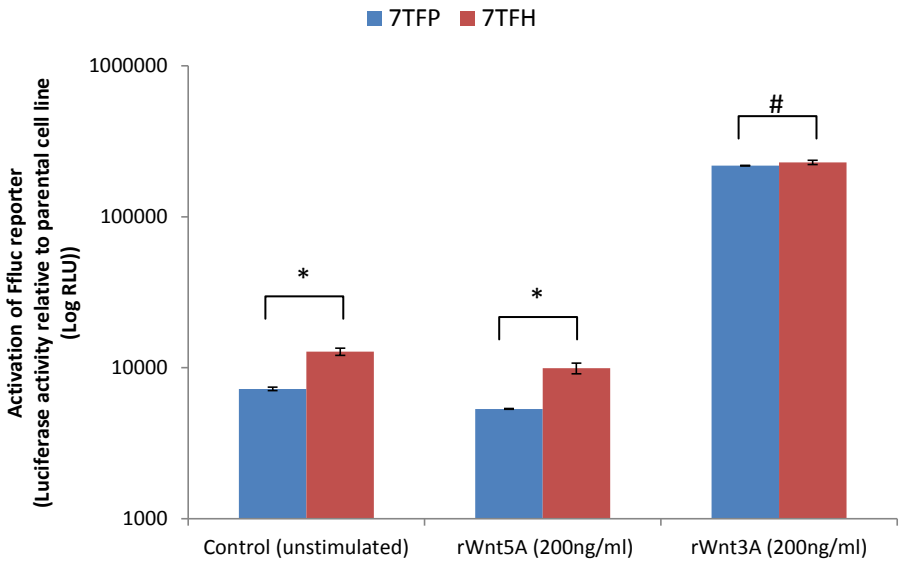

Figure 5.7 Confirming the functional activity of the cloned 7TFH reporter plasmid HEK293T 7TFP and HEK293T 7TFH cell lines were treated with 200ng/ml recombinant Wnt5A or Wnt3A for 24 h. Luciferase activity was determined using the Luciferase Assay (Section 3.2.5). Activation of the firefly luciferase reporter is shown relative to the parental cell line with no reporter plasmid (presented on the Log scale). RLU=Relative Light Units.

5.3.3.3 Measuring the activity of the canonical Wnt signalling pathway in OSCK and GFP cells

Activity of luciferase activity is reported per 10,000 cells. There was no difference in the endogenous activity of the luciferase reporter between GFP3 7TFH and OSCK4 7TFH cells (GFP= 10±3 x10^4 RLU, OSCK=14±3.6 x10^4 RLU). Treatment with rWnt5A (200ng/ml, 24h) had no effect on the luciferase reporter activity in either GFP3 7TFH or OSCK4 7TFH cells. However, there was a significant increase in luciferase activity in both GFP3 7TFH and OSCK4 7TFH cells ($p<0.05$) after stimulation with Wnt3A (200ng/ml, 24h).This stimulation of luciferase reporter activity was greater in OSCK4 cells (150±105-fold) compared to that in GFP3 cells (20±4-fold). Although this difference was substantial it did not reach not significance ($p=0.066$).

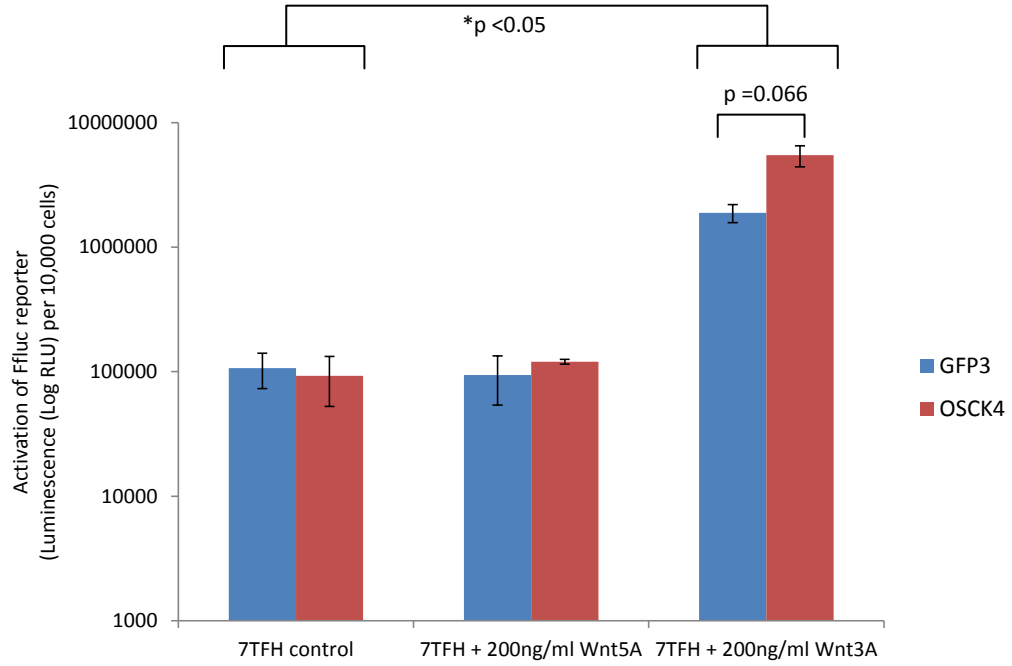

Figure 5.8 Luciferase reporter activity in GFP and OSCK cells. GFP3 7TFH and OSCK4 7TFH cell lines were treated with 200ng/ml recombinant Wnt5A or Wnt3A for 24h. Luciferase activity was determined using the Luciferase Assay (Section 3.2.5). Data presented as luminescence per 10,000 cells (Log scale). Viable cell number was determined from identically treated cells by trypan blue exclusion using the Vi-cell automated cell counter. RLU=Relative Light Units.

5.3.4 Activity of the noncanonical Wnt signalling pathway in OSCK and GFP cells

5.3.4.1 Migration of OSCK and GFP cells

Both GFP3 and OSCK4 cells formed compact spheroids when cultured on ultra-low adherence plastic. However after 4 days, the OSCK4 spheroids were almost double the size (62197±1848 pixels) of that of the GFP3 spheroids (32768±1147 pixels) (Figure 5.9 A and B, left panels).

When spheroids were plated onto gelatin coated plastic, OSCK4 cells migrated out while still maintaining a central spheroid core (Figure 5.9 A). Consistent with previous observations in ESFT cell lines (Chapter 4), migration of OSCK4 cells on gelatin was greater than migration on Matrigel™ coated plastic (data not shown). After 72h, the MI of OSCK cells was 14±1.5 (Figure 5.9 A). In contrast, the GFP3 cells migrated out radially as a flat monolayer, the spheroid core was lost within 24h (Figure 5.8 B). The MI of GFP3 cells was greater than that of OSCK4 cells (36±4). This is also greater than the migration observed in the parental TTC466 cell line (MI; 29 (±4)) (Section 4.3.4). The migration of GFP3 and OSCK4 cells was not increased at any time point by the addition of 200ng/ml recombinant Wnt3A or Wnt5A (Figure 5.9 A and B)

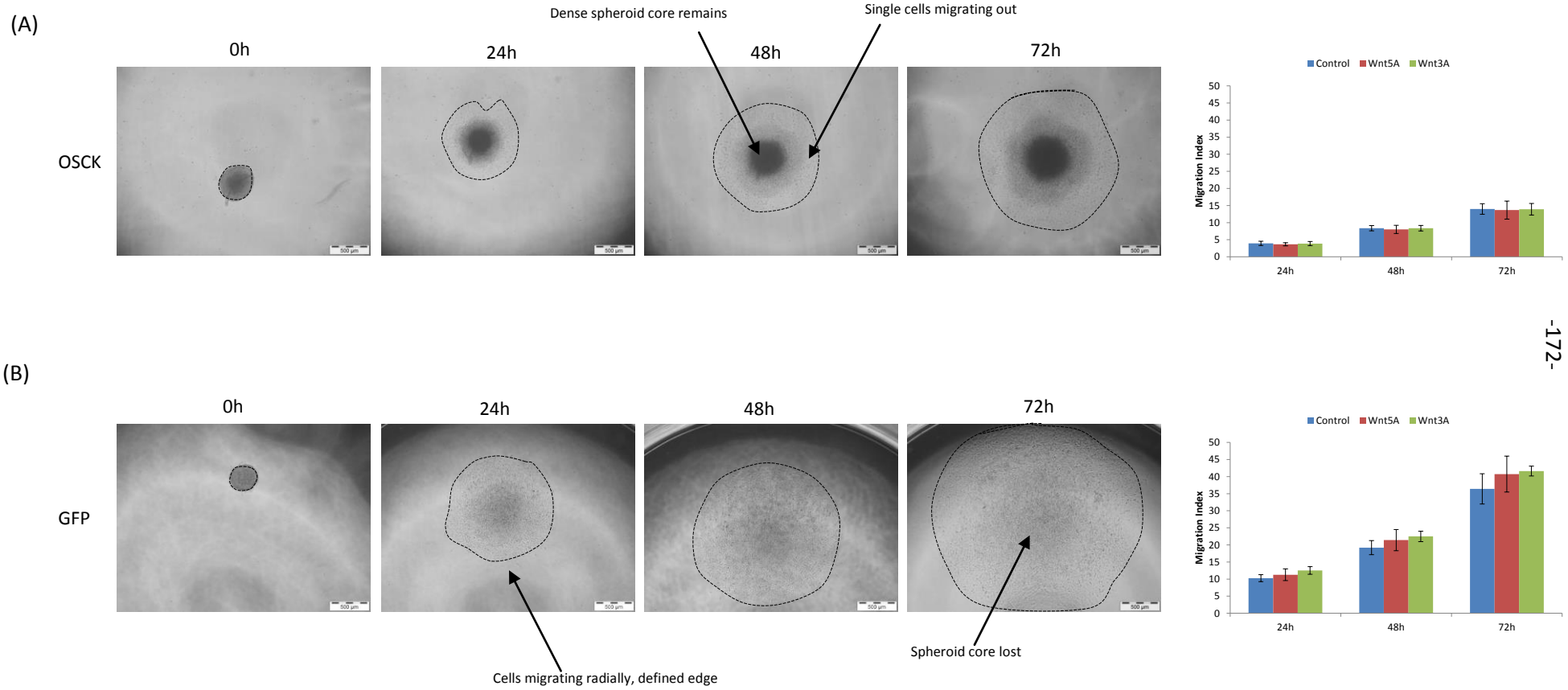

Figure 5.9 Migration of OSCK and GFP cells A) OSCK4 and B) GFP3 cell lines were cultured as spheroids for 4 days and plated onto flat-bottomed 96 well plates coated with 0.1% gelatin in media alone or media containing a final concentration of 200ng/ml recombinant Wnt3A or Wnt5A. Images were taken every 24h and area covered by migrating cells quantified using Velocity software. Graphs show area migrated at 24, 48 and 72h relative to the area of the spheroid at 0h. Representative images are of control cells at 24, 48 and 72 h. Results of three independent experiments (±SEM).

5.3.4.2 Expression of active Rac1/Cdc42 in OSCK and GFP cells

Active Rac1 and Cdc42 were calculated relative to the expression level of total Rac1 and Cdc42 in each sample. Active Rac1 was detected in both OSCK4 and GFP3 cell lines. In control cells, the level of basal active Rac1 was 2.7±0.5-fold higher in OSCK4 cells compared to GFP3 cells (Figure 5.10 A and B). With the addition of rWnt5A for (200ng/ml, 30min) there was an increase in active Rac1 in the GFP3 cells (1.6±0.1-fold) and a slight (1.2±0.1-fold) increase in active Rac1 in OSCK4 cells (Figure 5.10 A and B). Low levels of both total and active Cdc42 were observed in both OSCK4 and GFP3 cells (Figure 5.9 C). Basal active Cdc42 was slightly (1.2±0.2-fold) higher in OSCK4 cells compared to GFP3 cells (Figure 5.10 D). After treatment with rWnt5A for (200ng/ml, 30min), there was an increase in active Cdc42 in both GFP cells (1.4±0.2-fold) and OSCK4 cells (1.5±0.1-fold).

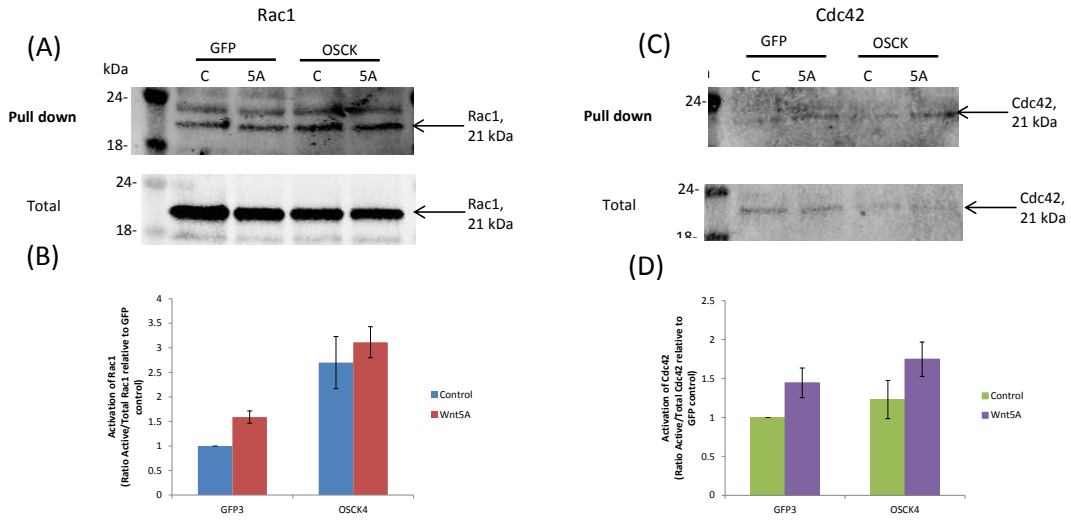

Figure 5.10 Expression of active Rac1 and Cdc42 in GFP and OSCK cell lines GFP3 and OSCK4 cell lines were cultured in 10cm^2 dishes until 70% confluent. Cells were then treated with rWnt5A (200ng/ml) for 30min. Cells were harvested, a sample removed for total protein estimation, and active (GTP-bound) Rac1 and Cdc42 were precipitated from the remaining extract using glutathione-sepharose beads bound to PAK-CRIB. Beads were washed, centrifuged and the sample split for analysis of Rac1 and Cdc42. A) Expression of Rac1 in pull-down and total protein samples was determined by western blot. B) Densitometry was performed and the ratio of active/total Rac1 calculated and expressed relative to expression in GFP control cells. C) Expression of Cdc42 in pull-down and total protein samples was determined by western blot. D) Densitometry was performed and the ratio of active/total Cdc42 calculated and expressed relative to expression in GFP control cells. Error bars on graphs show mean (n=2) (±SEM). Images are representative of 2 independent experiments.

5.4 Discussion

In this chapter I have successfully cultured reprogrammed TTC466 cells using a feeder free system and analysed these cells for activation of Wnt signalling. My data shows that expression of some components of the Wnt signalling pathway are altered in the reprogrammed cells, which may play a role in maintaining the primitive reprogrammed state. However, endogenous canonical Wnt signalling pathway is not upregulated compared to that in control (GFP) cells. Activation of the noncanonical Wnt signalling pathway may be increased in reprogrammed cells, since they have higher level of activated Rac1.

Consistent with previous reports, reprogrammed TTC466 (OSCK4) cells could be maintained in feeder free conditions on hESC-qualified Matrigel™ in mTeSR™1 media (Sun et al. 2009, Chen et al. 2011). In fact, both GFP and OSCK4 cells grew better when cultured on Matrigel™ coated plastic than on Primaria™ plastic. This is not surprising as Matrigel™ is an extract of basement membrane proteins from the murine Engelbreth-Holm-Swarm (EHS) tumour and contains laminin, collagen IV, entactin and heparin sulphate proteoglycan (Kleinman et al. 1982). Matrigel™ has been shown to enhance attachment of normal and cancer cell lines to plastic (Albini et al. 1992), and also been shown to help maintain self-renewal and pluripotency in hES and iPS cells (Xu et al. 2001, Ludwig et al. 2006, Sun et al. 2009). Control (GFP) cell lines did not grow in mTeSR™1 which is consistent with previous observations that ESFT cell lines do not grow in this media (Dr Andrew Gaffney, personal communication). As mentioned previously, mTeSR™1 contains 12 defined factors including FGF2 (200ng/ml), and FGF2 is known to induce cell death in ESFT cells at concentrations greater than 10ng/ml (Westwood et al. 2002). Although OSCK4 cells could tolerate maintenance in RPMI, viable cell number was greatest after culture in mTeSR™1. The ability of OSCK4 cells to grow in stem cell media is an indicator of their reprogrammed state. Data from our laboratory suggests that the OSCK4 population is heterogeneous, therefore growth of these cells in normal TTC466 media (RPMI) may promote outgrowth of partially reprogrammed populations. For these reasons it was concluded that OSCK4 cells should be grown in mTeSR™1 and GFP cells in RPMI. However, I cannot exclude the possibility that maintaining cells in different culture conditions may impact on the downstream assays performed to probe for Wnt signalling activity.

To maintain self-renewal and pluripotency of hES and iPS cells, various feeder free systems have been developed that use different combinations of components to provide the optimal microenvironment for cell growth. It is becoming clear that it is the cross-talk

between key signalling pathways which is important in maintaining hES cells in an undifferentiated state. For example, mTeSR™1 contains TGFβ (23.5pM) which, through the Smad2, 3 pathway, activates downstream targets such as Nanog (Xu et al. 2008). In addition, insulin (3.92μM) potently activates PI3K/Akt signalling (Dalton 2013). mTeSR™1 also contains FGF2 (100ng/ml) which is thought to maintain a basal level of ERK activity and also activate the PI3K pathway (Dalton 2013). Although it is not clear precisely what effect these signalling pathways have on Wnt signalling in hES cells, it is agreed that Wnt signalling plays an important role. It has been suggested that activation of PI3K signalling by FGF2 prevents ERK inactivation of GSK3β, allowing GSK3β to phosphorylate β-catenin to ensuring canonical Wnt signalling is low. Indeed, inhibition of GSK3β or treatment with Wnt3A has been shown to result in activation of the canonical Wnt signalling pathway and subsequently loss of self-renewal and mesodermal differentiation (Davidson et al. 2012, Singh et al. 2012). However, alternative studies have shown that activation of PI3K signalling by FGF2 leads to phosphorylation of GSK3β and therefore activation of Wnt signalling. This is in contrast to other reports which have shown inhibiting GSK3β helps to maintain undifferentiated hESCs (Ding et al. 2010). It is therefore still controversial whether active Wnt signalling promotes or inhibits self-renewal or differentiation in hES cells. Nevertheless, it is clear that growth in mTeSR™1 may have an effect in Wnt signalling in OSCK4 cells and this should be considered when interpreting my data.

However, endogenous canonical Wnt signalling was no different in GFP cells and OSCK4 cells. Both cell lines showed a significant increase in canonical Wnt signalling in response to exogenous Wnt3A protein. Although this response was greater in OSCK4 cells, the difference did not reach statistical significance. Nevertheless this difference may be biologically relevant for example OSCK4 cells may be more primed to respond to Wnt signals due to expression of particular cofactors, or due to decreased expression of inhibitors such as sFRP5 and DKK4. This will be discussed in further detail later.

The OSCK factors have been shown to reprogram normal and cancer cells to a more primitive state, but it is not understood exactly how the factors work. As discussed, Wnt signalling is important in the maintenance of undifferentiated hES cells, therefore it is not surprising that Wnt signalling has also been shown to play a role in the reprogramming process and maintenance of iPS cells. However, as is the case for hES cells, the precise role of Wnt signalling in this process is controversial. Some studies report that Wnt signalling can promote reprogramming. For example, Wnt3A protein has been shown to aid reprogramming in the absence of c-myc (Marson et al. 2008) and activation of canonical

Wnt signalling also promotes reprogramming by somatic nuclear transfer (lluis, 2008). It has been shown that β-catenin binds to Oct4, Sox2 and Klf4, and has been hypothesised that this may help them bind to their endogenous promoters and increase transcription, thus promoting the reprogramming process (Zhang et al. 2014). Conversely however, Oct4 expression has been shown to functionally repress canonical Wnt signalling in both hES cells and non-stem cells (HEK293T) (Davidson et al. 2012). This apparent contradictory role of Wnt signalling could in part be explained by the different components of the canonical pathway. When signalling occurs, β-catenin translocates to the nucleus where it forms a complex with a TCF/LEF family member of transcription factors and also CBP or the closely related homolog p300, leading to expression of downstream target genes (Hecht et al. 2000). It has been suggested that CBP/β-catenin interactions promote stem cell maintenance and p300/β-catenin interactions mediate transcriptional programs leading to differentiation (Teo and Kahn 2010). In addition, the TCF/LEF family is made up of Tcf1, Lef1, Tcf3 (TCF7L1) and Tcf4 and the function of individual TCF/LEF proteins can differ. For example although Tcf3 has been shown to co-occupy promoter regions of pluripotency genes such as Nanog with the factors Oct4 and Sox2 (Cole et al. 2008, Tam et al. 2008, Yi et al. 2008), ablation of Tcf3 has been shown to stimulate Nanog expression (Yi et al. 2011). Therefore it is thought Tcf3 acts as a transcriptional repressor in hESCs, whereas Tcf1 activates transcription in response to β-catenin (Yi et al. 2011). In relation to reprogrammed cells, it has recently been shown that in the early stages of reprogramming, the Wnt signalling pathway is repressed by Tcf3 and Tcf4, and activation of Wnt signalling at this stage leads to a reprogramming block. However, in later stages, Wnt signalling aids reprogramming, and deletion of Tcf3/Tcf4 at this stage enhances iPS formation (Ho et al. 2013).

In the current study, using the Wnt signalling array, significantly higher expression of Tcf1, and lower expression of Tcf3 were detected in OSCK4 cells compared to GFP cells (although these genes were excluded from the analysis as the differences were less than 2 Ct values). Although no difference in canonical Wnt signalling was detected using the Tcf-reporter assay, this assay is not able to distinguish which endogenous Tcf family members are being activated, therefore there may be differences in canonical Wnt signalling between the GFP and OSCK4 cells which are not detectable using this assay. It would therefore be important to look at a panel of downstream Wnt target genes involved in both self-renewal and differentiation such as cyclin D1, survivin, Axin2, c-jun and EphB2 to understand fully what is happening in these cells. However, caution should be taken when

interpreting the results as it is possible Wnt signalling is promoted in OSCK4 cells due to the reprogramming factors themselves, and not related to the ESFT cellular background.

Expression of other components of the Wnt signalling pathway in OSCK4 and GFP cells were also determined using the Wnt signalling array. Some components which had higher expression in OSCK4 cells such as FGF4, Wnt8B and Wnt1 have previously been shown to be activated by at least one of the OSCK factors themselves (Weber et al. 2013, Katoh 2007, Chen et al. 2012). However, other Wnt ligands including Wnt16, Wnt3 and Wnt3A also had increased expression in OSCK4 cells and have not previously been linked to any of the OSCK genes. Other components such as sFRP5 were also highly overexpressed in OSCK4 cells. This is consistent with a previous study showing that sFRP5 is silenced through methylation in ESFT cell lines (Jin et al. 2012). The secreted frizzled-related proteins (sFRPs) are a family of Wnt signalling antagonists that inhibit Wnt signalling by competing with Wnt ligands for binding to Frizzled receptors. My data supports the hypothesis that reprogramming ESFT cells removes this methylation and restores sFRP5 expression. The previous study also demonstrated that treatment of ESFT cells lines with sFRP5 protein reduced migration, and therefore re-expression of sFRP5 in OSCK4 cells may explain the reduced migration observed by these cells in this study.

RHOU (also known as Wrch-1) is a member of the Rho family of GTPases, related to Rac1 and Cdc42, which has been shown to be activated by Wnt1 expression (Tao et al. 2001). Expression of this mRNA was also increased in OSCK4 cells compared to GFP cells. However this could be attributed to the increase in Wnt1 expression observed in OSCK4 cells, which may be the result of induced SOX2 expression. However, RHOU has also been shown to be activated downstream of PCP signalling (Faure and Fort 2011) and therefore may demonstrate activation of the noncanonical Wnt signalling pathway in OSCK4 cells, which corresponds with the increase in active Rac1 observed in these cells. This will be discussed further on in this Chapter.

In contrast to the other Wnt components, expression of DKK2 was lower in OSCK4 cells compared to GFP cells. The DKK family of secreted proteins are generally considered to inhibit Wnt signalling by binding and sequestering the Wnt co-receptors LRP5/6 (Mao et al. 2001, Semënov et al. 2001). However, DKK2 has been shown to either activate or inhibit Wnt signalling, depending on the cellular context (Niehrs 2006). It has been shown previously that DKK2 is highly expressed in ESFT cells compared to other paediatric and small round cell tumours (Miyagawa et al. 2009, Hauer et al. 2013). It has also been demonstrated that EWS-ETS fusion proteins interact with the promoter region of DKK2 to

increase expression (Miyagawa et al. 2009) and that DKK2 expression promotes invasion and migration of ESFT cells (Hauer et al. 2013). Therefore a reduction in DKK2 expression is consistent with reprogramming of the ESFT cells, and again may explain the reduction in migration seen in OSCK4 cells.

Although the Wnt signalling array used in this study is a valuable tool for high-throughput assessment of mRNA expression of components of the pathway, it has some limitations. For example there is only one replicate on each plate (although three biological repeats were performed). Therefore to validate the results of the arrays, individual RTqPCR was performed for four of the Wnt components found to be significantly different between OSCK4 and GFP cells; namely sFRP5, Wnt16, FGF4 and DKK2. RTqPCR was performed using Assays-on-Demand which, except in the case of FGF4, contained the same primer/probe mixes that were used in the array. The same RNA was used for the validation experiments. The results of the individual RTqPCRs were almost identical to the array results for DKK2 and was very similar for sFRP5, except higher expression was observed in OSCK4 cells than had been detected on the array. In the case of Wnt16 and FGF4 however, there was actually less mRNA detected using the Assays-on-Demand. This may reflect some deterioration of the RNA with storage. Nevertheless, the results demonstrate the sensitivity of the Wnt signalling array used in this study to detect components of the Wnt signalling pathway.

To determine if the components I have identified as being differentially expressed in OSCK4 and GFP3 cells have an effect in the reprogramming process to a more primitive cell, it would be necessary to alter the expression of these proteins. Since FGF4, Wnt8B, Wnt1 and sFRP5 had higher expression in OSCK4 cells, expression of these proteins could be knocked down using RNAi. Conversely, DKK2 expression was decreased in OSCK4 cells and therefore this protein could be overexpressed using stable transfection of the gene. The resulting phenotype of the OSCK4 cells could then be investigated using assays such as as proliferation, cell cycle analysis, colony formation and migration.

As previously mentioned, expression of active Rac1 was higher in OSCK4 cells compared to GFP3 cells. It has been demonstrated that the noncanonical PCP pathway, and in particular Rac1 is important in the migration of neural crest stem cells (Mayor and Theveneau 2014). Since it has been hypothesised that ESFT cells may arise from cells of the neural crest (von Levetzow et al. 2011), it is possible this increase in Rac1 is a result of reprogramming of the ESFT cells. However, OSCK4 cells showed reduced migration compared to GFP cells. Although some single cells did migrate out from the spheroid in the migration assay, a

dense core still remained which was more similar to the phenotype observed in hES cells (Chapter 6) and may be explained by the increase in sFRP5 and decrease in DKK2 expression as described previously. As mentioned in Chapter 4, CD99 is known to modulate ESFT cell migration. Interestingly, CD99 expression is maintained in OSCK4 cells but is more heterogeneous, with some cells having low expression (Andrea Berry, personal communication). This may be another explanation for the reduced migration observed in OSCK4 cells. It may be possible to knock down expression of Rac1 in OSCK4 cells, to determine what effect this has on migration. However, since Rac1 is important in other signalling pathways it would still be difficult to link the resulting phenotype to the Wnt signalling pathway. Similarly if inhibitors were used such as BAPTA-AM, a Ca^{2+} chelator or Go6983, an inhibitor of PKC these also often affect other signalling pathways.

In conclusion, it is very difficult to determine the role of Wnt signalling in the initiation of ESFT using reprogrammed cells. Although my data has shown differences in expression of Wnt signalling components in OSCK4 cells and an increased ability to respond to exogenous Wnt3A, the mTeSR™1 media and the OSCK reprogramming factors themselves may affect Wnt signalling and so make interpretation of the results difficult. In addition, using the TCF-reporter it is not possible to identify which TCF family members are being activated, so the effect of Wnt signalling on downstream pathways cannot be definitely concluded. Although the Rac1/Cdc42 pull-down assay only considers one pathway of the noncanonical Wnt signalling pathway my studies have shown increased Rac1 and consequently activation of noncanonical Wnt signalling in OSCK4 cells. Although this did not correlate with the pattern of migration observed, this reflects the limitation of using migration as an end point for noncanonical Wnt signalling. Therefore it is important to utilise alternative models of ESFT initiation in order to investigate the role of Wnt signalling in this process.

6. Wnt signalling in hES cells with inducible EWS-FLI1 expression

6.1 Introduction

In our laboratory we have developed an *in vitro* system to model ESFT initiation in which the EWS-FLI1 fusion protein can be induced in human embryonic stem (hES) cells. hES cells are derived from the inner cell mass of a 4-5 day blastocyst, produced by *in vitro* fertilization (IVF) (Thomson 1998). These cells have unlimited self-renewal capacity and are pluripotent meaning that have the ability to differentiate into all three primary germ layers; mesoderm, endoderm and ectoderm (Thomson 1998). Using this model my goal has been to investigate the potential role of Wnt signalling in the development of the ESFT phenotype.

Expression of EWS-FLI1 in hES cells was achieved using the TetON Advanced inducible expression system (Figure 6.1). This is a tightly regulated, highly responsive system which allows for robust expression of a gene of interest (GOI) using the tetracycline (Tet) derivative doxycycline (DOX) (Gossen et al. 1995, Urlinger et al. 2000). The system components have been modified from bacteria where in the absence of Tet, the Tet Repressor (TetR) blocks expression of genes by binding to tet operator sequences (tetO). In the Advanced TetON system, mutant reverse Tet Repressors (rTetRs) have been produced which along with transactivation domains from herpes simplex virus VP16 protein, form the transactivator, rtTA-Advanced (TetON) (Urlinger et al. 2000). Cells are transfected with two vectors, the first containing the TetON transactivator and the second a Tet Response Element (TRE)-based expression vector containing the GOI. In the presence of DOX, TetON Advanced binds specifically and tightly to tetO sequences in TRE-Tight and activates transcription of the GOI, in this case EWS-FLI1. Since TRE-Tight lacks binding sites for mammalian transcription factors there is extremely low background expression of the GOI.

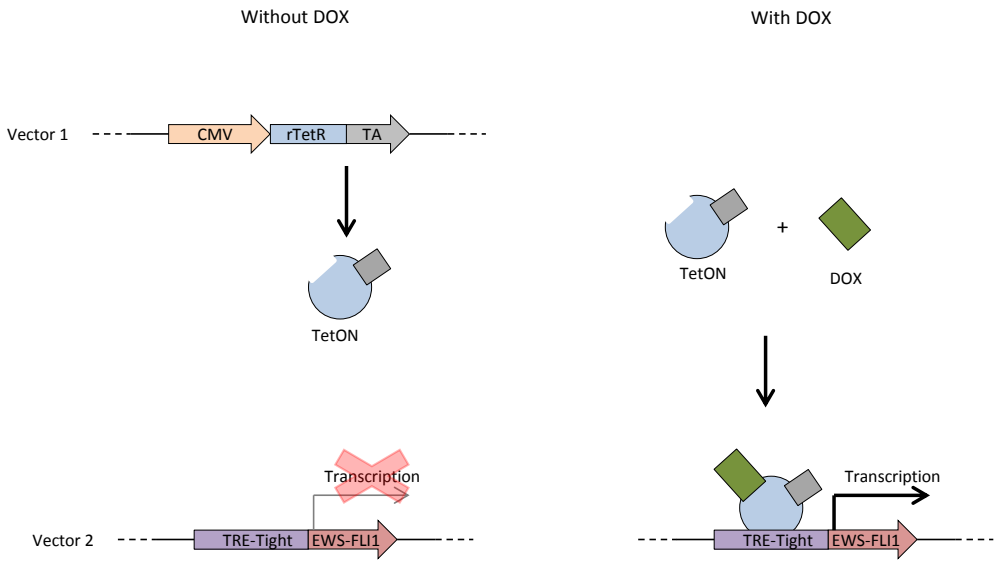

Figure 6.1 Induction of EWS-FLI1 expression using the TetON Advanced inducible expression system Cells are transfected with two vectors. The first vector results in constitutive expression of the rtTA-Advanced transactivator (TetON) containing the reverse Tet Repressor (rTetR) and activation domain (TA). The second vector contains the EWS-FLI1 gene downstream of Tet Response Element (TRE)-Tight containing repeats of the tet operator sequence (tetO) joined to a minimal CMV promoter. Only in the presence of doxycycline (DOX) does TetON bind to TRE which results in the expression of EWS-FLI1. If DOX is not present or is removed, EWS-FLI1 is not expressed. Adapted from the TetON® Advanced Inducible Gene expression system User Manual (Clontech).

The aims of this chapter were to:

1. Investigate the phenotype and growth characteristics of hES cells with inducible EWS-FLI1 expression.
2. Investigate the expression of Wnt signalling components in hES cells with and without EWS-FLI1 expression.
3. Measure the activation of the canonical Wnt signalling pathway in hES cells with and without EWS-FLI1 expression.
4. Measure the activation of the noncanonical Wnt signalling pathway in hES cells with and without EWS-FLI1 expression.

6.2 Materials and Methods

6.2.1 Feeder-free embryonic stem cell culture

Shef4 hES cells were a kind gift from Professor Peter Andrews (University of Sheffield). Parental Shef4 and Shef4$^{EWS\text{-}FLI1.OFF}$ cell lines were maintained in feeder-free culture conditions using Matrigel™ coated plastic and mTesR™1 medium as previously described (Section 5.2.1).

6.2.2 Culture of Shef4$^{EWS\text{-}FLI1.ON}$ cells

6.2.2.1 Inducing EWS-FLI1 expression in Shef4$^{EWS\text{-}FLI1}$ cells

A ready-to-passage flask of Shef4$^{EWS\text{-}FLI1.OFF}$ cells was dissociated into single cells using trypsin/EDTA (Section 5.2.1.3). Cells were seeded onto Matrigel™ coated (Section 5.2.1.1) plastic flasks, dishes or plates as required. The cell density was varied according to the type and length of downstream assay being performed. After 24h, media was replaced with mTeSR™1 containing doxycycline hydrochloride (DOX) (Fisher Scientific). For routine experiments 5µg/ml DOX was used. Media was replaced every 24h until downstream assays were performed, or for stock flasks until cells were 70% confluent.

6.2.2.2 Passage of Shef4$^{EWS\text{-}FLI1.ON}$ cells

Shef4$^{EWS\text{-}FLI1.ON}$ cells maintained in culture grew as an adherent monolayer. Therefore for routine passage cells were trypsinised as previously described (Section 5.2.1.3) and split 1:3 into fresh flasks coated with Matrigel™ (Section 5.2.1.1).

6.2.3 Detection of EWS-FLI1 in Shef4$^{EWS\text{-}FLI1}$ cells

To detect levels of EWS-FLI1, Shef4$^{EWS\text{-}FLI1}$ cells were seeded at 2×10^5 cells/well in 6 well plates or 4×10^5 cells in $T25^2$ flasks as previously described (Section 6.2.2.1). After 24h, cells were treated with normal mTeSR™1 (control) or media containing DOX (range 1-5µg/ml) for up to 72h as required.

6.2.3.1 RTqPCR

To detect EWS-FLI1 mRNA, RNA was extracted from cells (Section 2.2.5.1) and RNA quantity and quality measured using the Nanodrop (Section 2.2.5.2). cDNA was prepared as previously described (Section 2.2.5.3). The RT+ (cDNA) and RT- control samples were added to PCR mixes for amplification of EWS-FLI1 (Table 6.1) and the housekeeping gene PPIA (Section 2.2.5.5, Table 2.5). RTqPCR was performed using the 7500 Real-Time PCR

System (Section 2.2.5.5). For detection of EWS-FLI1 cDNA was incubated at 50°C for 2min, heated to 95°C for 15min followed by 50 cycles of 95°C for 15s, 66°C for 1min and 72°C for 90s. Gene expression was determined using the ΔΔCt method (Section 2.2.5.5) using TC32 cells as the reference sample.

EWS-FLI1 Mix	Volume (µl, per sample)	Final concentration
TaqMan Universal PCR Master Mix	50	1X
20 µM EWS Forward Primer 5'-GTCAACCTCAATCTAGCACAGGG-3'	1	200nM
20 µM FLI1 Reverse Primer 5'-CTGTCGGAGAGCAGCTCCAG -3'	1	200nM
20 µM EWS probe 5'CTCCTACCAGCTATTCCTCTACACAGCCGACT-3'	1	200nM
RNase free H_2O	27	-

Table 6.1 PCR mix reagents for RTqPCR to detect EWS-FLI1

6.2.3.2 Western blot

To detect EWS-FLI1 protein, total protein was extracted and SDS-PAGE performed followed by western blot as previously described (Section 2.2.5). Since no commercial antibody is available for EWS-FLI1, a rabbit anti-FLI1 antibody (Santa Cruz) was used at a concentration of 0.4µg/ml. This antibody detects the C-terminus of FLI1 and therefore detects bands corresponding to wild type FLI1 (51 kDa) as well as EWS-FLI1 (68kDa).

6.2.4 Immunofluorescence

Glass coverslips (22mm × 22mm; VWR) were sterilised by submerging in 100% ethanol and drying in air, this was repeated three times. Each coverslip was placed in one well of a 6-well plate and coated in Matrigel™ (Section 5.2.1.1). Shef4$^{EWS\text{-}FLI1.OFF}$ and Shef4$^{EWS\text{-}FLI1.ON}$ cells were trypsinised (Section 5.2.1.3) and seeded at a density of 4 × 10^4 cells (Shef4$^{EWS\text{-}FLI1.OFF}$) or 6 × 10^4 cells (Shef4$^{EWS\text{-}FLI1.ON}$), suspended in 200µl of growth media. After 6h, once the cells had adhered to the coverslip the well was flooded with 3ml mTeSR™1 (containing 5µg/ml DOX if required) and the cells incubated for a further 48h. If required, media containing rWnt5A (200ng/ml) was added to the well 24h prior to harvesting. To prepare the slides, media was aspirated and cells washed three times in 1X PBS. To fix the cells, 4% PFA was added to the cells for 15 min at RT. Cells were then washed 3 three times with 1X PBS, permeabilised using 0.1% Triton-X (in PBS) and finally washed three more times in 1X PBS. To stain the cytoskeleton (F-actin) cells were incubated with 1 unit of phalloidin (Life

Technologies) and 0.2µg/ml DAPI (Sigma-Aldrich) in 100µl in PBS in the dark for 30min. Cells were washed three more times with 1X PBS and mounted using Dako Faramount Aqueous Mounting Medium Ready-to-use (Dako, Ely, UK). Slides were analysed using the Axioplan 2 fluorescence microscope (Zeiss, Cambridge, UK)

6.2.5 Determining viable cell number of Shef4 cells

Cells which had been pre-treated as required were trypsinised as previously described (Section 5.2.1.3) and seeded at 5×10^4 cells/well in 24-well plates coated with Matrigel™ (Section 5.2.1.1). Cells were seeded either in RPMI (+10% conditioned media) or mTeSR™1 as required. In some experiments after 24h cells were treated with either rWnt3A (200ng/ml) or rWnt5A (200ng/ml). After 24, 48 and 72h cells were counted using the automated vi-cell as previously described (Section 2.2.2). Triplicate wells were counted for each condition, at each time point.

6.2.6 Analysis of Wnt signalling components using RTqPCR

RNA was extracted (Section 2.2.5.1) from Shef4$^{EWS\text{-}FLI1.OFF}$ cells and Shef4$^{EWS\text{-}FLI1.ON}$ cells that has been treated with 5µg/ml DOX for 72h (Section 6.2.2.1). RNA was also extracted from Shef4 parental cells and Shef4 parental cells treated with 5µg/ml DOX for 72h. Gene expression of components of the Wnt signalling pathway were analysed using the TaqMan® Array Human WNT Pathway 96-well plate (Applied Biosystems), as described (Section 2.2.5.4).

6.2.7 Generation of cell lines transduced with 7TFH vector

Shef4$^{EWS\text{-}FLI1}$ and Shef4 parental cells were infected with lentiviral supernatant at an MOI of 2 (Section 3.2.2.3) and 48h after infection were selected using media containing 200 µg/ml hygromycin for 2 weeks. Cells were maintained in Class II conditions (as described in Section 3.2.2.2) for at least 10 days after infection or until at least 2 passages had been performed.

6.2.8 Luciferase assay

Shef4 parental and Shef4$^{EWS\text{-}FLI1}$ cells were dissociated into single cells using trypsin/EDTA (Section 5.2.1.3). Cells were seeded to be approximately 60-70% confluent at the time the luciferase assay was carried out. Therefore the number of cells seeded varied depending on the treatment condition and length of experiment. Shef4 parental and Shef4$^{EWS\text{-}FLI1}$ cells were seeded at 5×10^4 cells/well and assayed after 96h. For Shef4$^{EWS\text{-}FLI1.ON}$ cells the seeding density ranged from 5×10^4 to 1×10^5 and were assayed 24-72h after adding DOX

(5µg/ml). Luciferase was determined using the Luciferase Assay (Section 3.2.5). If required, rWnt3A (200ng/ml) or rWnt5A (200ng/ml) was added 24h prior to the luciferase assay being performed.

6.2.9 Detection of total and active β-catenin by western blot

Cells were seeded in 6-well plates at a density 2×10^5 cells/well. After 24h, cells were treated with normal media (control) or media containing Wnt3A (200ng/ml) or Wnt5A (200ng/ml) for 4h. Total and active β-catenin were determined by western blot as previously described (Section 3.2.10).

6.2.10 Migration assay

Shef4$^{EWS\text{-}FLI1.OFF}$ and Shef4$^{EWS\text{-}FLI1.ON}$ cells that had been cultured in DOX (5µg/ml) for 72h were trypsinised (Section 5.2.1.3) and seeded at 500 cells/well in 96-well plates to form spheroids (Section 4.2.2). For optimisation experiments spheroids were encouraged to form by centrifuging the plate for 4min at 152g or by adding 10µM ROCK inhibitor (Y-27632, Sigma-Aldrich). In optimised conditions ROCK inhibitor (10µM) was added to the cell suspension at day 0. Migration assays were performed to compare migration on different substrates and in response to Wnt ligands and analysed using Volocity® software (Section 4.3.2).

6.2.11 Rac1/Cdc42 pull down assay

Shef4$^{EWS\text{-}FLI1}$ cells were trypsinised (Section 5.2.1.3) and seeded in 10cm^2 dishes at a density of either 1.5×10^6 cells/dish (control) or 3×10^6 cells/dish (treated). After 24h, media containing 5µg/ml DOX was added to the dishes seeded at the higher concentration. After a further 72h the media was replaced with normal growth media (control) or media containing rWnt5A (200ng/ml) for 30 min. Expression of total and active Rac1 and Cdc42 was determined as previously described (Section 4.2.1.4).

6.2.12 Statistics

Analysis of the Wnt signalling array was performed by Mr John Alexander (University of Leeds) as previously described (Section 5.2.10).. All other statistical analyses were performed as described previously (Section 3.2.11).

6.3 Results

6.3.1 Characterising Shef4 cells with inducible EWS-FLI1 expression

6.3.1.1 Expression of EWS-FLI1 mRNA in Shef4$^{EWS-FLI1}$ cells

The expression of EWS-FLI1 in Shef4$^{EWS-FLI1}$ cells after the addition of DOX was confirmed by RTqPCR. EWS-FLI1 mRNA expression was increased in both a dose- and time-dependent manner (Figure 6.2 A and B). Expression of EWS-FLI1 mRNA was greatest after treatment of Shef4$^{EWS-FLI}$ cells with 5 µg/ml DOX for 72h. This level of expression was 1.16±0.18 -times that in the ESFT TC32 cell line (Figure 6.2 B). Expression of EWS-FLI1 was maintained at a similar level when Shef4$^{EWS-FLI.ON}$ cells were cultured continuously in DOX for up to 1 month (Figure 6.2 B).

A)

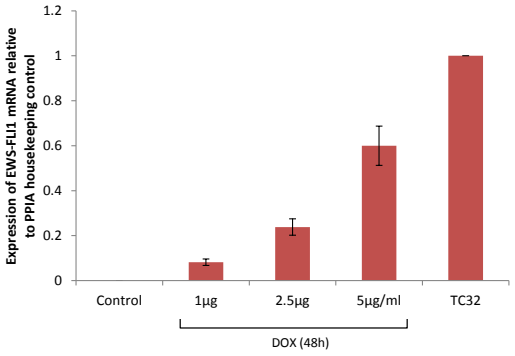

B)

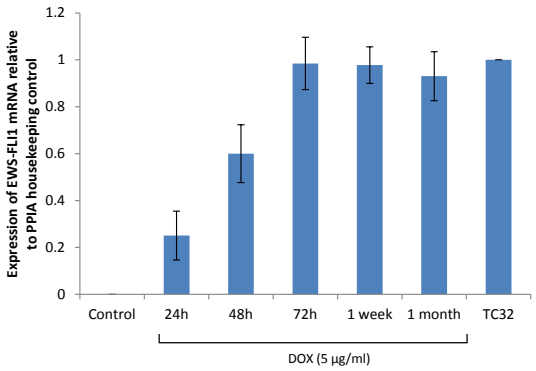

Figure 6.2 Expression of EWS-FLI mRNA in Shef4$^{EWS-FLI}$ cells treated with DOX Shef4$^{EWS-FLI1.OFF}$ (control) cells were treated with A) increasing concentrations of DOX (1,2.5,5 µg/ml) for 48h or B) 5 µg/ml DOX for increasing periods of time (24,48,72 h, 1 week, 1 month). Total RNA was extracted and expression of EWS-FLI1 mRNA determined by RTqPCR. Data are presented as mRNA expression relative to the housekeeping gene PPIA and normalised to expression of EWS-FLI1 in TC32 control cell line. Results show the mean of two independent experiments with three replicates per repeat (n=6) (±SEM).

6.3.1.2 Expression of EWS-FLI1 protein in Shef4$^{EWS\text{-}FLI1}$ cells

Expression of EWS-FLI1 protein in Shef4$^{EWS\text{-}FLI1}$ cells was confirmed by western blot. Since an antibody to EWS-FLI1 is not commercially available, an antibody that recognises the C-terminus of FLI-1 was used to detect the fusion protein (Santa Cruz, sc-356). The antibody detects multiple non-specific bands, in addition to endogenous FLI-1 protein, therefore the EWS-FLI1 band (68 kDa) was confirmed using TC32 positive control cells and TTC466 cells, which contain a different fusion protein (EWS-ERG), as a negative control. EWS-FLI1 protein was induced after DOX treatment in a dose- and time- dependent manner. EWS-FLI1 protein could be detected after treatment with 2.5 and 5µg/ml DOX (Figure 6.3 A). Maximum expression of EWS-FLI1 protein was observed after treatment with 5 µg/ml DOX for 72h (Figure 6.3 B).

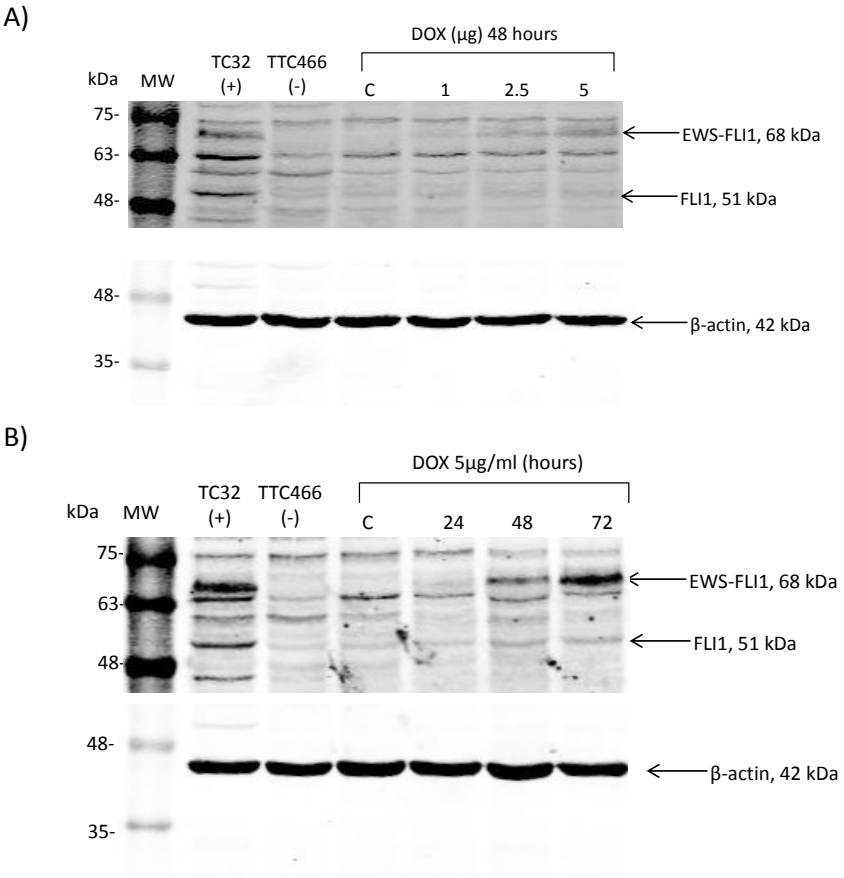

Figure 6.3 Expression of EWS-FLI protein in Shef4$^{EWS\text{-}FLI1}$ cells treated with DOX Shef4$^{EWS\text{-}FLI1.OFF}$ (control) cells were treated with A) Increasing concentrations of DOX (1,2.5,5 µg/ml) for 48h or B) 5 µg/ml DOX for increasing periods of time (24,48,72 h). Total protein was extracted and EWS-FLI1 protein detected by western blot, as a band at 68 kDa present in the TC32 positive control, but not TTC466 negative control. Expression of β-actin was used as a loading control. MW= molecular weight in kDa. Images representative of two independent experiments.

6.3.1.3 Growth characteristics of Shef4$^{EWS\text{-}FLI1}$ cells with EWS-FLI expression

6.3.1.3.1 Phenotype of Shef4$^{EWS\text{-}FLI1}$ cells with and without EWS-FLI1 expression

Over the time period that EWS-FLI1 mRNA and protein was induced (24-72h) the phenotype of the Shef4$^{EWS\text{-}FLI1.ON}$ cells changed. The morphology of non-induced Shef4$^{EWS\text{-}FLI.OFF}$ cells resembled that of the Shef4 parental cell line, cells growing on Matrigel™ coated plastic as undifferentiated stem cell colonies with very defined edges (Figure 6.4 A). Changes in the morphology of Shef4$^{EWS\text{-}FLI1.ON}$ were first noticed approximately 48h after the addition of DOX (5µg/ml). This is also the time point when the EWS-FLI1 protein was detected by western blot (Section 6.3.1.2). After 72h of DOX treatment, the Shef4$^{EWS\text{-}FLI1.ON}$ cells appeared larger and elongated, the colony edges were less defined and single cells migrated out to fill the gaps between colonies, reminiscent of the substrate dependent growth of the ESFT cell lines (Figure 6.4 B). Immunofluorescent staining of the actin cytoskeleton demonstrated Shef4$^{EWS\text{-}FLI1.OFF}$ cells tightly packed with an actin cable surrounding the colonies, and many cell-cell adhesions (Figure 6.5). After 72h DOX treatment, Shef4$^{EWS\text{-}FLI1.ON}$ cells began to lose this organised structure. There appeared to be fewer colonies, less cell-cell adhesions, more single cells and an increase in the number of cells with filapodia (Figure 6.4), although this was not quantified. After continued DOX treatment (1 month) the phenotype of the Shef4$^{EWS\text{-}FLI1.ON}$ continued to change, cells appeared much larger and had more stress fibres, although some smaller cells were still present (Figure 6.5).

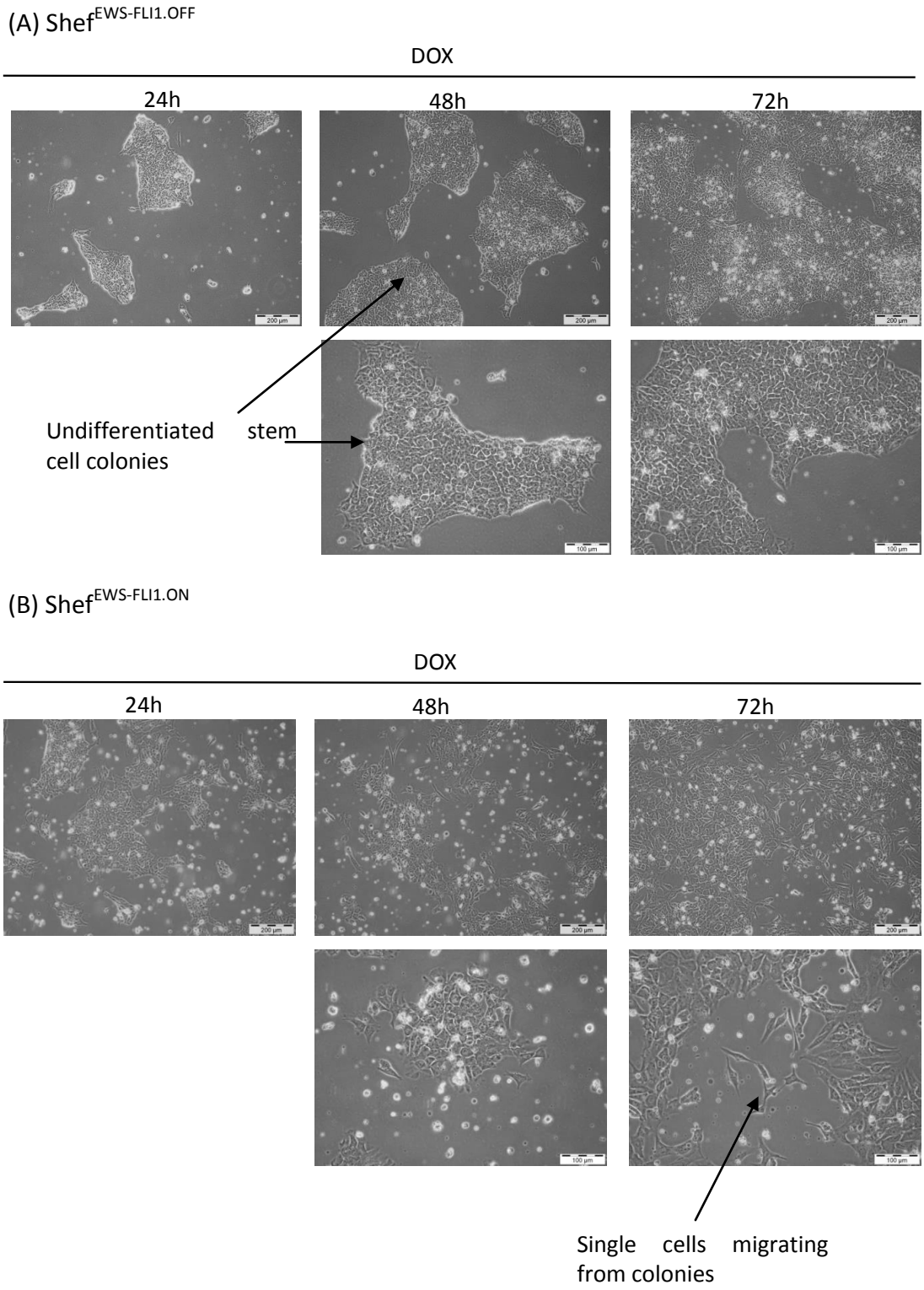

Figure 6.4 Light microscopy of Shef4$^{EWS\text{-}FLI.OFF}$ and Shef4$^{EWS\text{-}FLI.ON}$ cells Shef$^{EWS\text{-}FLI1}$ cells were seeded as a single cell suspension and cultured for 72h in the A) absence or B) presence of 5 µg /ml DOX. Representative images were taken every 24h.

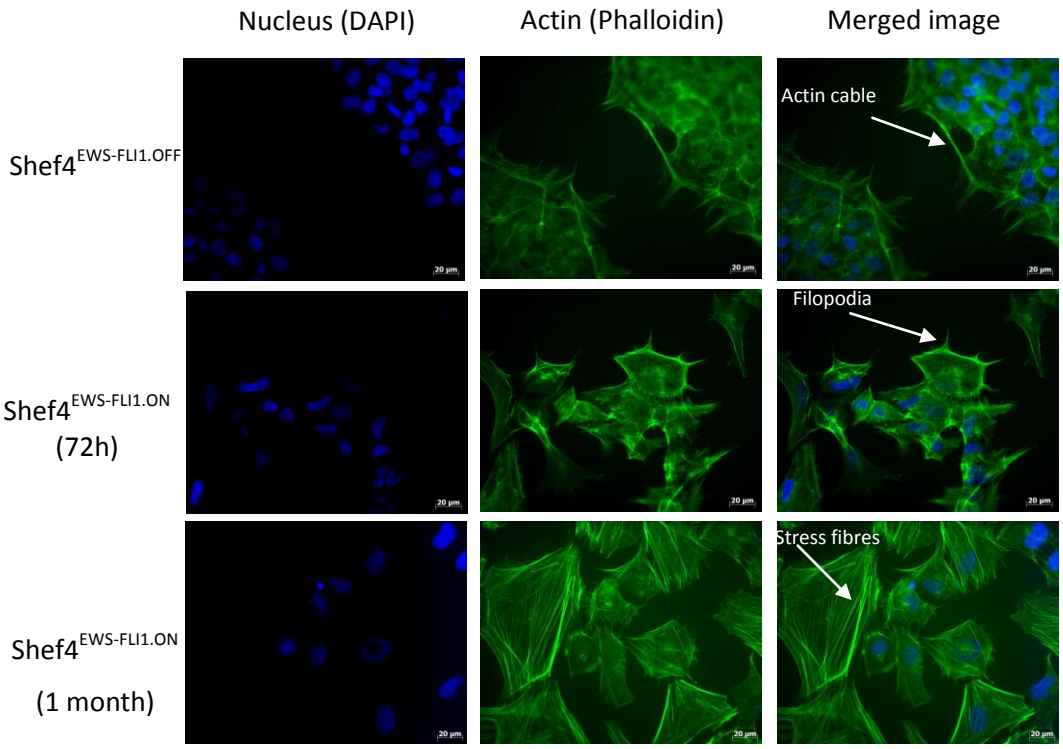

Figure 6.5 Actin cytoskeleton in Shef4$^{\text{EWS-FLI.OFF}}$ and Shef4$^{\text{EWS-FLI.ON}}$ cells Shef4$^{\text{EWS-FLI.OFF}}$, Shef4$^{\text{EWS-FLI.ON}}$ and Shef4$^{\text{EWS-FLI.ON}}$ (1 month) cell lines were seeded as single cells onto glass coverslips coated with Matrigel™. Cells were grown for 48h then fixed with 4% PFA, and stained with DAPI (blue) and phalloidin (green) and imaged using a fluorescent microscope.

6.3.1.3.2 Viable cell growth of Shef4 cells in doxycycline

Following treatment of Shef4$^{EWS\text{-}FLI1}$ cells with DOX, an increase in the number of floating, non-substrate adherent cells was observed. I therefore investigated whether the DOX may be killing some cells. Consistent with this possibility, DOX treatment reduced the viable cell number of Shef4 cell lines (Figure 6.6). The addition of 5 µg/ml DOX for 72h reduced the viable cell number of both Shef4 parental and Shef4$^{EWS\text{-}FLI1\ cells}$ to 42±0.7% and 52±0.16% of the no treated (control) cells, respectively. This suggests the reduction in viable cell number is due to the effect of the DOX itself, not induced expression of the EWS-FLI fusion protein.

When these Shef4 parental cells were re-challenged with DOX (5µg/ml) there was no effect on viable cell number after 72h (Figure 6.7, blue and green lines). In contrast however, Shef4$^{EWS\text{-}FLI1.ON}$ cells re-challenged with DOX (5µg/ml) had significantly reduced viable cell number after 72h ($p<0.0001$). Shef4$^{EWS\text{-}FLI1.ON}$ cells pre-treated with DOX for 1 month had significantly reduced viable cell number than those only pre-treated for 72h ($p<0.05$) (Figure 6.7, orange and red lines). This suggests that in both Shef4 parental and Shef4$^{EWS\text{-}FLI1}$ cells there is a sub-population of cells that are sensitive to DOX and these cells are killed by initial treatment with 5µg/ml DOX for 72h. In Shef4 parental cells the growth of the resistant population is not affected by further exposure to DOX. However, in Shef4$^{EWS\text{-}FLI1.ON}$ cells, even cells resistant to DOX show decrease in viable cell number, suggesting the induced EWS-FLI1 fusion protein is having an effect on the cell cycle of these cells.

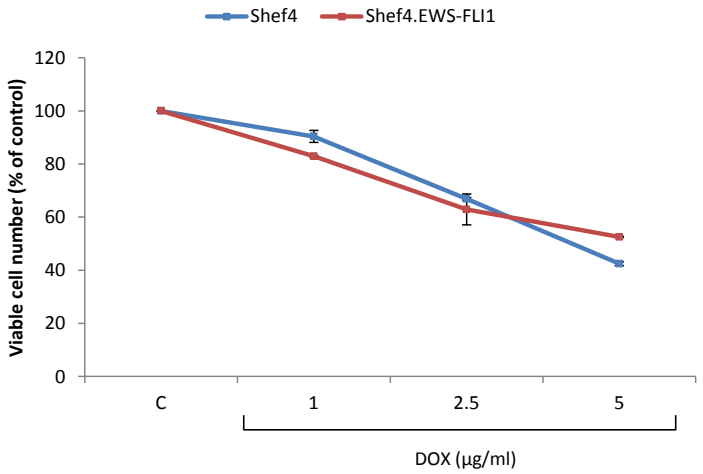

Figure 6.6 Effect of doxycycline on Shef4 and Shef4$^{EWS-FLI1}$ viable growth Shef4 parental and Shef4$^{EWS-FLI1}$ cells were seeded as single cells and cultured in the presence of increasing concentrations of DOX (2,2.5,5 µg/ml) for 72h. Viable cell number was determined by trypan blue exclusion using the Vi-cell automated cell counter. Data presented as a percentage of the viable cell number of control cells not treated with DOX. Results show mean of two independent experiments (±SEM). Stats = NS difference.

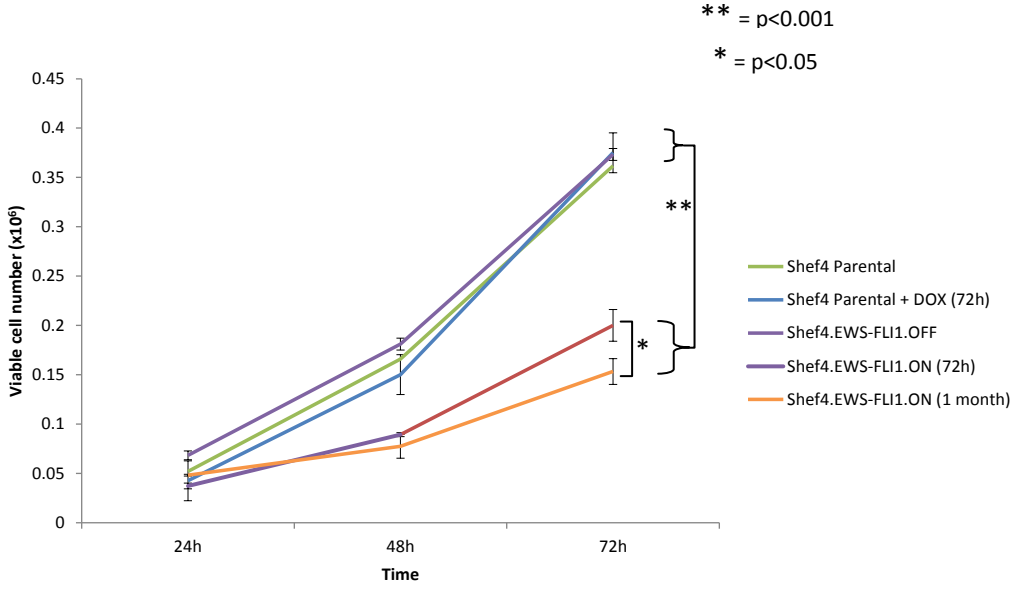

Figure 6.7 Effect of doxycycline treatment on Shef4 viable cell number with time Shef4 parental cells, Shef4 parental cells previously treated with DOX (72h), Shef4$^{EWS-FLI1.OFF}$ and Shef4$^{EWS-FLI1.ON}$ cells that had been previously treated with DOX for 72h or 1 month were seeded in a single cell suspension in 24 well plates. Viable cell number was determined after 24, 48 and 72 h by trypan blue exclusion using the Vi-cell automated cell counter. Results show mean of three independent experiments (±SEM).

6.3.1.3.3 Effect of different media on Shef4$^{EWS\text{-}FLI}$ viable cell number

The reduction in viable cell number over an extended period of time in Shef4$^{EWS\text{-}FLI1.ON}$ cells appeared not to be due to DOX. I therefore tested the hypothesis that the Shef4$^{EWS\text{-}FLI1.ON}$ cells no longer tolerated being cultured in mTeSR™1, which is optimised to maintain undifferentiated embryonic stem cells. By transferring these cells to the growth conditions of ESFT cells I examined if these cells would tolerate the cancer cell media; such an adaption might reflect the development of a more differentiated ESFT-like cell, rather than a stem cell. However, when Shef4$^{EWS\text{-}FLI}$ cells were pre-treated with DOX for 24, 48 or 72h and then seeded into mTeSR™1(+DOX) or RPMI(+DOX), the viable cell number was reduced in the ESFT RPMI culture conditions, regardless of the length of pre-treatment with DOX (Figure 6.8 A-C). In all cases, viable cell number was significantly reduced when Shef4$^{EWS\text{-}FLI1.ON\ cells}$ were grown in RPMI (+ DOX) compared to mTeSR™1(+ DOX) ($p<0.05$).

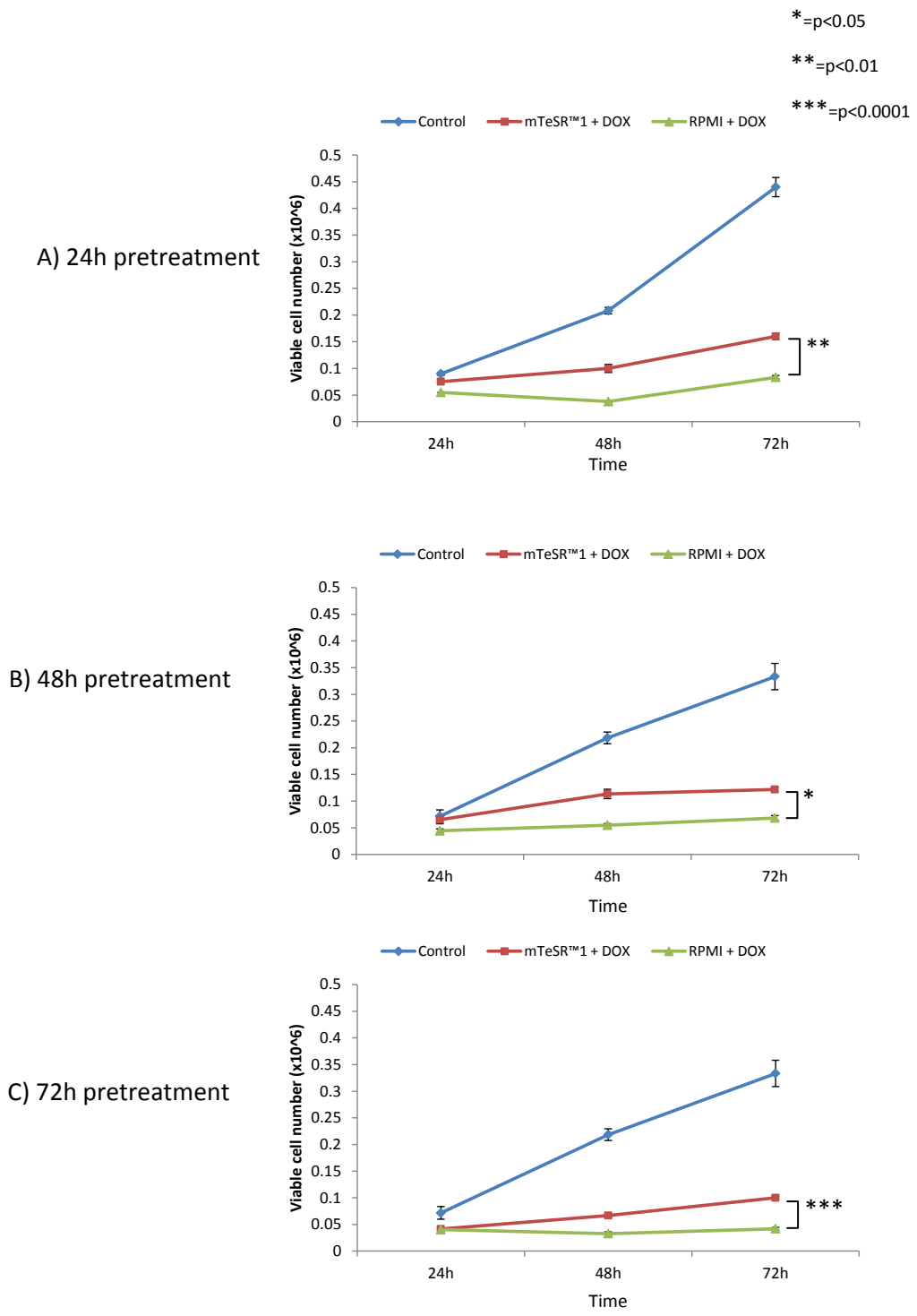

Figure 6.8 Shef4$^{EWS\text{-}FLI1.ON}$ viable cell number in mTeSR-™1 and RPMI Shef4$^{EWS\text{-}FLI1}$ cells were treated with 5µg/ml DOX for either 24, 48 or 72 h. Resulting Shef4$^{EWS\text{-}FLI1.ON}$ cells were trypsinised and seeded in a single cell suspension in mTeSR-™1 or RPMI (+5µg/ml DOX). Viable cell number was determined every 24h up to 72h using the Vi-cell automated cell counter. Growth was compared to Shef4$^{EWS\text{-}FLII1.OFF}$ cells grown in mTeSR™1 (control).

Shef4$^{EWS\text{-}FLI1.ON}$ cells pre-treated with DOX (5µg/ml, 72h) and seeded in mTeSR™1+DOX grew as monolayers with very few colonies. Cells reached confluency after 2-3 days and could be continually passaged using Trypsin/EDTA (0.2X Trypsin/1mM EDTA). These cells did not resemble Shef4$^{EWS\text{-}FLI1.OFF}$ cells when examined down the light microscope; cells appeared larger, elongated and no longer grew in colonies (Figure 6.9 A and B). However, although Shef4$^{EWS\text{-}FLI1.ON}$ cells pre-treated with DOX (5µg/ml, 72h) and seeded in RPMI + DOX had some adherent cells, these did not appear to increase in number even after 5 days of culture (Figure 6.9 C and D). Therefore, Shef4$^{EWS\text{-}FLI1.ON}$ cells which remained in culture were maintained in mTeSR™1(+DOX).

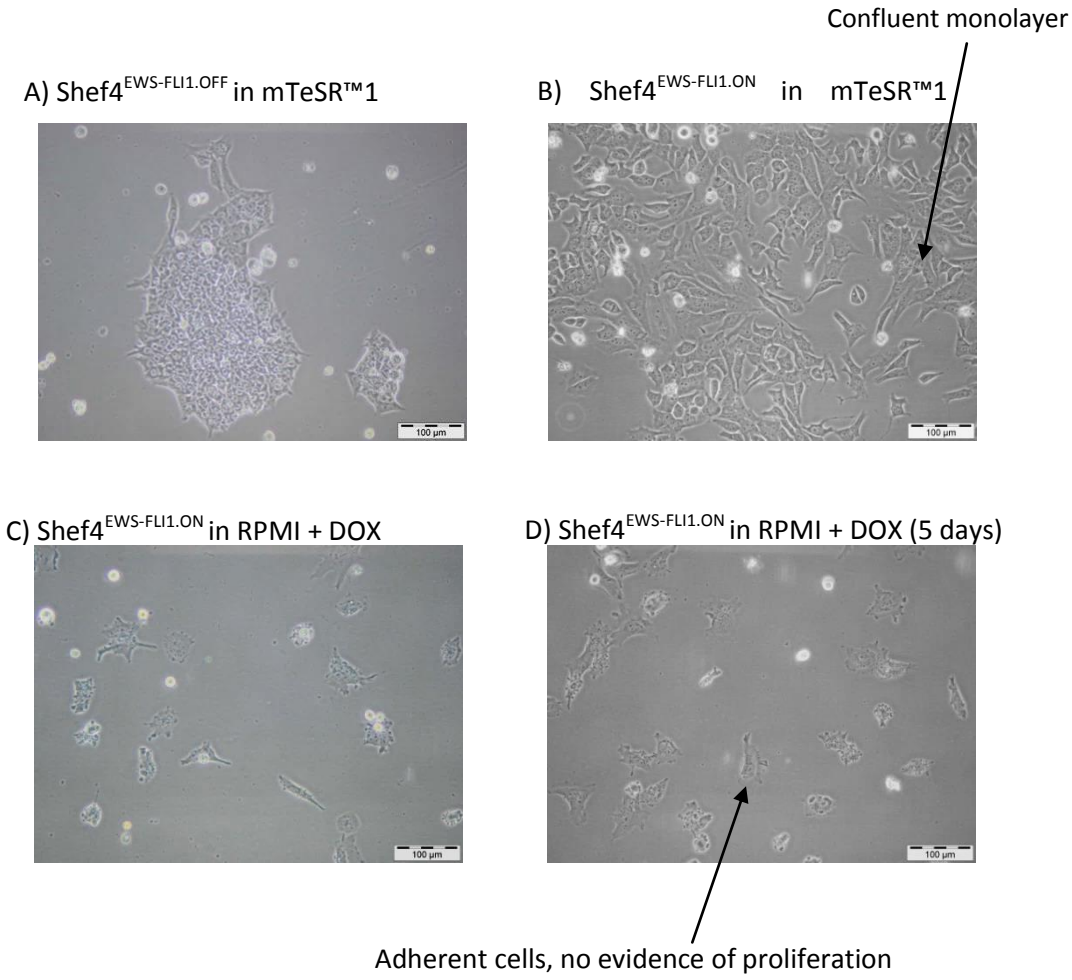

Figure 6.9 Light microscopy of Shef4$^{EWS\text{-}FLI1.ON}$ cells in mTeSR™1 and RPMI Representative images 48h after seeding of A) Shef4$^{EWS\text{-}FLI1.OFF}$ control cells grown in mTeSR™1 and Shef4$^{EWS\text{-}FLI1.ON}$ cells previously cultured in mTeSR™1 + DOX for 72h, then seeded into B) mTeSR™1+DOX or C) RPMI+ DOX. D) Shef4$^{EWS\text{-}FLI1+}$ cells after culture in RPMI +DOX for 5 days.

6.3.2 mRNA expression of Wnt signalling components in Shef4$^{EWS\text{-}FLI1}$ cells

6.3.2.1 Profile by TaqMan® Wnt Pathway Array

RNA from Shef4$^{EWS\text{-}FLI1.OFF}$ cells was compared to RNA from Shef4$^{EWS\text{-}FLI1.ON}$ cells that had been exposed to 5 µg/ml DOX for 72h. Expression of 94.5% (86/91) of Wnt signalling components was unchanged when EWS-FLI1 expression was induced in Shef4 cells (Figure 6.10). Genes where expression changed by more than 2 Ct values are shown in Table 6.2.

After the EWS-FLI1 fusion protein was induced in Shef4$^{EWS\text{-}FLI1}$ cells, there was significantly increased mRNA expression of the Frizzled receptor FZD8 ($p<0.05$), and two noncanonical Wnt ligands Wnt4 and Wnt5A (both $p<0.05$). There was also increased expression of the canonical Wnt inhibitor DKK2 ($p<0.05$) but conversely decreased expression of the related inhibitor DKK4 ($p<0.05$).

Expression of Wnt signalling components was determined for Shef4 parental cells and Shef4 parental cells treated with DOX (5µg/ml) for 72h to confirm that the expression of genes identified in Table 6.2 did not change due to the addition of DOX itself (data not shown).

Gene	P value	Expression in Shef4$^{EWS\text{-}FLI1.OFF}$ (Ct value)	Expression in Shef4$^{EWS\text{-}FLI1.ON}$ (Ct value)	Expression in Shef4$^{EWS\text{-}FLI1.ON}$ relative to Shef4$^{EWS\text{-}FLI1.OFF}$* (Change in Ct value)
FZD8	0.032	28.1±0.6	24.2±0.6	-3.8
DKK2	0.014	32.5±0.4	28.8±0.5	-3.7
DKK4	0.025	27.1±0.1	30.6±1	+3.5
WNT4	0.012	33.3±0.2	30.5±0.4	-2.7
WNT5A	0.013	27.1±0.6	25.1±0.5	-2

Table 6.2 Genes with significantly different mRNA expression in Shef4$^{EWS\text{-}FLI1.ON}$ cells compared to Shef4$^{EWS\text{-}FLI1.OFF}$ Expression of genes was determined using the Taqman® Wnt signalling gene expression array and genes with significantly different expression in Shef4$^{EWS\text{-}FLI1.OFF}$ and Shef4$^{EWS\text{-}FLI1.ON}$ cells identified by Limma analysis (Section 5.2.10). Ct values are given for the mean of two independent experiments (±SEM). *A lower Ct value means higher expression therefore a reduction in Ct value indicates an increase in expression. A Ct value of 40 is considered no detection.

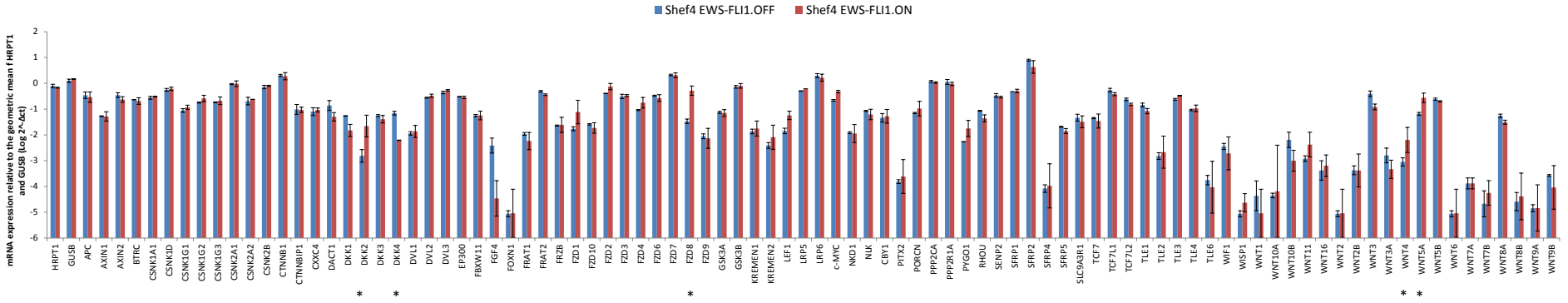

Figure 6.10 RNA expression of components of the Wnt signalling pathway in Shef4$^{\text{EWS-FLI1}}$ cells Shef4$^{\text{EWS-FLI1.OFF}}$ and Shef4$^{\text{EWS-FLI1.ON}}$ cells that had been treated with DOX (5µg/ml) for 72h were harvested, total RNA extracted and expression level determined using the Taqman® Wnt signalling gene expression array. Data presented as mRNA expression relative to the geometric mean of the housekeeping genes HPT1 and GUSB. Results show mean of two independent experiments (±SEM). *= Genes that were expressed at significantly different levels ($p<0.05$) and were changed by more than 2 Ct values between Shef4$^{\text{EWS-FLI1.OFF}}$ and Shef4$^{\text{EWS-FLI1.ON}}$ cells (see Table 6.2)

6.3.3 Activity of the canonical Wnt signalling pathway in Shef4 cells with EWS-FLI1 expression

6.3.3.1 Optimisation of luciferase reporter assay in Shef4 cells

The endogenous activity of the 7TFH luciferase reporter plasmid in Shef4$^{EWS\text{-}FLI1.OFF\ 7TFH}$ cells was very variable and differed up to 15-fold between experimental repeats (range=2735-41985 RLU), unlike in other cell lines studied. For example in the ESFT cell lines the most variation observed was in the TC32 cell line but this difference was only 2.4-fold (range 11711-27989 RLU). It was observed that In Shef4$^{EWS\text{-}FLI1.OFF}$ 7TFH cells the luminescence (measured per 10,000 cells) was higher when the assay was performed 24h after the cells had been seeded (41985 RLU) and reduced in a time dependent manner to 2735 RLU when the assay was performed 96h after seeding (Figure 6.11). This difference was not due to the confluency of the cells, as cell seeding density was optimised so that the viable cell number was similar at the time of each assay (range= 0.25-0.38 x10^6 cells). It was hypothesised therefore that in Shef4 cells, the dissociation of cells by trypsinisation and subsequent plating may affect Wnt signalling. Therefore to control for this luciferase assays in Shef4 cells were always carried out 96h after seeding, regardless of the treatment condition.

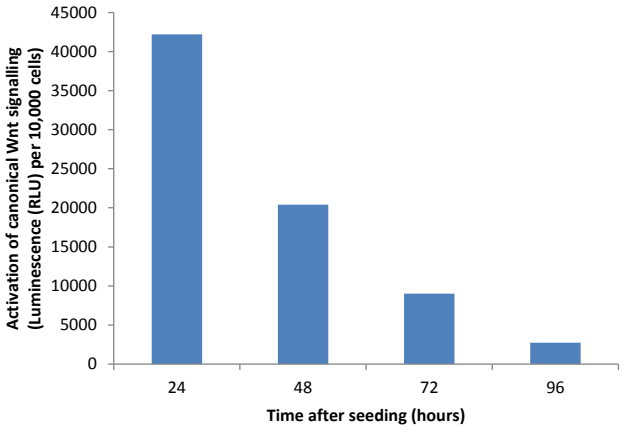

Figure 6.11 Effect of time in culture on the activity of luciferase reporter activity in Shef4 7TFH cells Shef4$^{EWS\text{-}FLI1.OFF}$ cells were trypsinised seeded as a single cell suspension and luminescence determined after 24, 48, 72 and 96 h using the luciferase assay (Section 3.2.5). Cell seeding density was optimised so that cells were 50-60% confluent when assayed. RLU=relative light units.

6.3.3.2 Effect of doxycycline treatment on canonical Wnt signalling activity in Shef4$^{EWS\text{-}FLI1}$ cells with time

The activity of the luciferase reporter plasmid in Shef4$^{EWS\text{-}FLI1.ON}$ 7TFH cells was induced, compared to the level in Shef4$^{EWS\text{-}FLI1.OFF}$ 7TFH control cells, after 56h exposure to DOX (Figure 6.12). After 72h DOX treatment, luciferase activity was 2.6X the level of the control cells. With continued culture in DOX, the activity of the luciferase reporter continued to increase so that after 1 month of DOX treatment the luminescence per 10,000 cells was significantly higher than that of the control cells ($p<0.01$) (Figure 6.12). This suggests that canonical Wnt signalling is activated by the expression of EWS-FLI1.

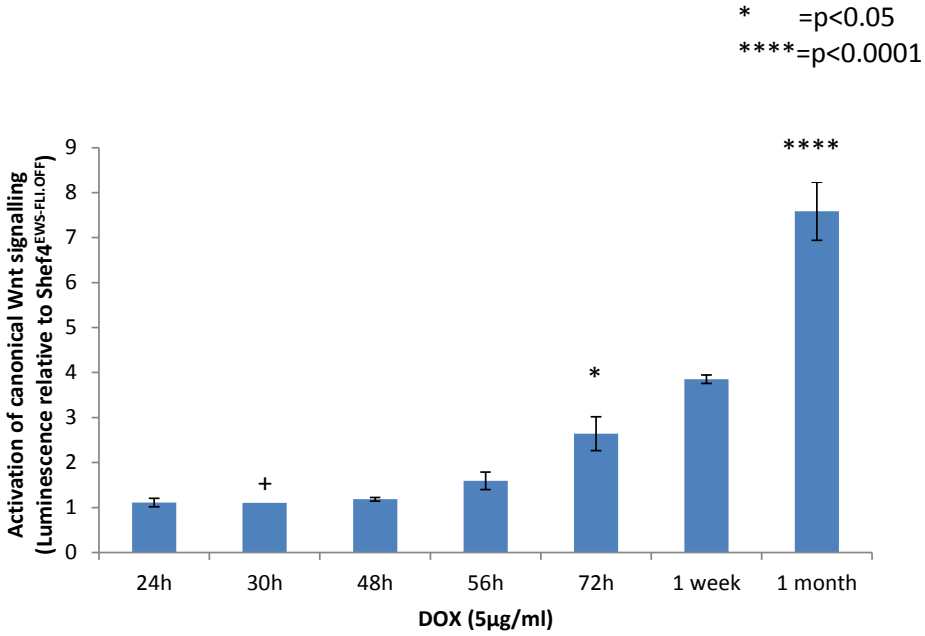

Figure 6.12 Luciferase reporter activity in Shef4$^{EWS\text{-}FLI1.ON}$ cells Shef$^{EWS\text{-}FLI1}$ cells were treated with DOX for increasing periods of time (24h-1month). In all cases luminescence was determined 96h after seeding using the luciferase assay (Section 3.2.5). Luminescence was normalised to the viable cell number which was determined from identically treated wells by trypan blue exclusion using the Vi-cell automated cell counter. Data are presented as luminescence (per 10,000 cells) relative to Shef4$^{EWS\text{-}FLI1.OFF}$ control. Results are of two independent experiments with 3 replicates in each experiment (n=6) presented as mean (±SEM).

+ = only one repeat at 30h (n=3).

6.3.3.3 Activation of canonical Wnt signalling in Shef4 cells with and without EWS-FLI1 expression after treatment with Wnt ligands

As previously described (Section 6.3.3.2), endogenous canonical Wnt signalling was significantly higher in Shef4$^{EWS\text{-}FLI1.ON\ 7TFH}$ cells that had been cultured in DOX for 72h ($p<0.05$) and 1 month ($p<0.0001$), compared to Shef4$^{EWS\text{-}FLI1.OFF}$ 7TFH cells not cultured in DOX. Canonical Wnt signalling was not increased in Shef4$^{EWS\text{-}FLI1.OFF\ 7TFH}$ control cells following treatment with Wnt5A (200ng/ml) or Wnt3A (200ng/ml) for 24h (Figure 6.13, blue bars). However, canonical Wnt signalling was significantly increased in Shef4$^{EWS\text{-}FLI1.ON\ 7TFH}$ cells following the addition of Wnt3A (200ng/ml). This was observed in cells which had been cultured in DOX for 72h ($p<0.01$, red bars) and 1 month ($p<0.05$, green bars).

* =p<0.05
**= p<0.01
**** = p<0.0001

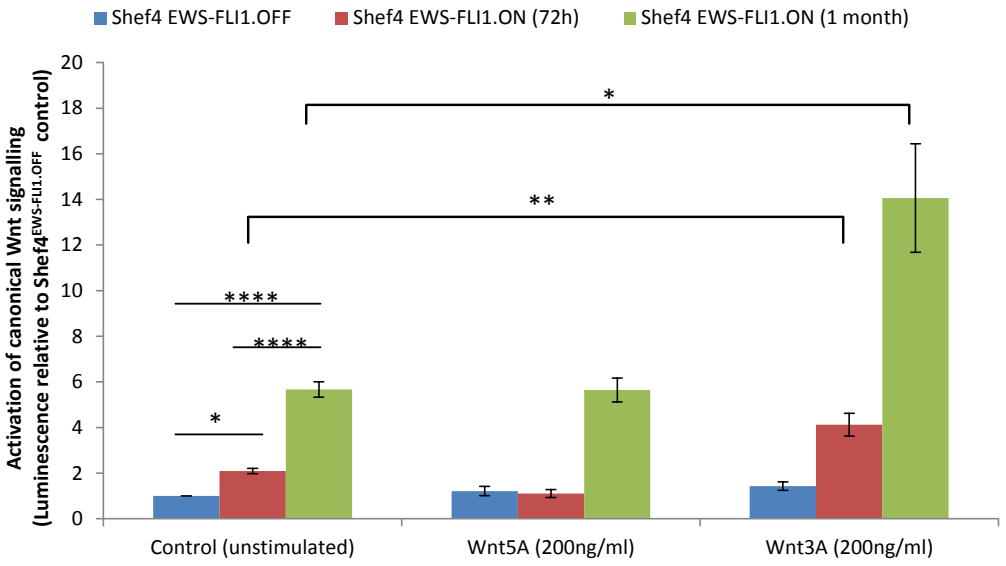

Figure 6.13 Luciferase reporter activity in Shef4 cells with and without EWS-FLI1 expression after treatment with Wnt ligands Shef4$^{EWS\text{-}FLI1.OFF}$ and Shef4$^{EWS\text{-}FLI1.ON}$ cells cultured in DOX for 72h and 1 month were stimulated with 200ng/ml Wnt5A or Wnt3A for 24h. In all cases luminescence was determined 96h after seeding using the luciferase assay (Section 3.2.5). Luminescence was normalised to the viable cell number which was determined from identically treated wells by trypan blue exclusion using the Vi-cell automated cell counter. Data are presented as luminescence (per 10,000 cells) relative to Shef4$^{EWS\text{-}FLI1.OFF}$ control. Results of three independent experiments with 3 replicates per experiment (n=9) showing mean (±SEM). RLU= relative light units.

6.3.3.4 Effect of doxycycline on canonical Wnt signalling in Shef4 parental cells

The addition of increasing concentrations of DOX (1, 2.5,5 µg/ml) or treatment with 5µg/ml DOX plus Wnt5A (200ng/ml) or Wnt3A (200ng/ml) did not increase luciferase reporter activity in Shef4 parental 7TFH cells (Figure 6.14). This suggests that the effects seen in Shef4$^{EWS\text{-}FLI1.ON\ 7TFH}$ cells were due to the EWS-FLI1 fusion protein, not DOX treatment.

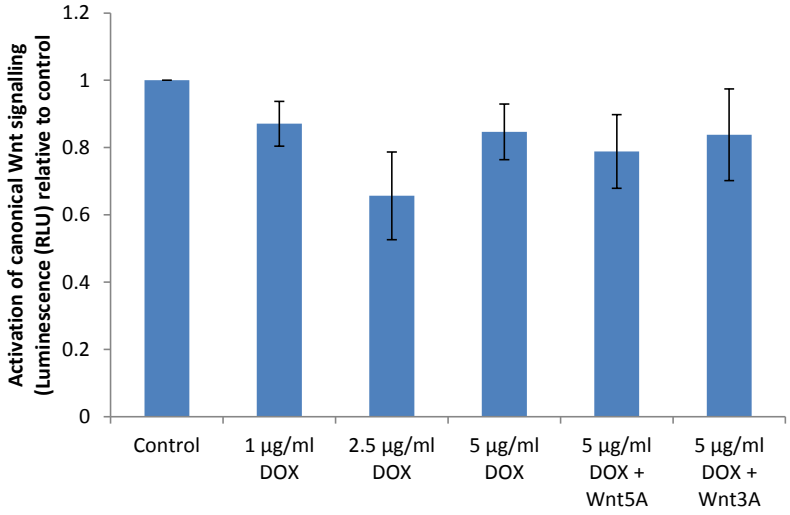

Figure 6.14 Effect of exposure to doxycycline on the activity of luciferase reporter plasmid in Shef4 cells Shef4 parental 7TFH cells were seeded as single cells and 24h later treated with increasing concentrations DOX (1, 2.5 5 µg/ml) for 72h or 5 µg/ml DOX for 48h + 200ng/ml Wnt5A or 200ng/ml Wnt3A (+DOX) for a further 24h. Luminescence was determined using the luciferase assay (Section 3.2.5). Luminescence was normalised to the viable cell number which was determined from identically treated wells by trypan blue exclusion using the Vi-cell automated cell counter. Data are presented as luminescence (per 10,000 cells) relative to Shef4 7TFH control. Results of three independent experiments with three replicates per experiment (n=9) showing the mean (±SEM). RLU= relative light units.

6.3.3.5 Confirmation that stimulation of Wnt signalling in Shef4$^{EWS\text{-}FLI}$ cells activates downstream targets

To confirm the activation of canonical Wnt signalling measured using the firefly luciferase reporter plasmid, expression of downstream targets of canonical Wnt signalling were investigated in Shef4$^{EWS\text{-}FLI1}$ cells. As shown in HEK293T cells (Chapter 3) expression of both active and total β-catenin should increase following activation of canonical Wnt signalling. The endogenous levels of both total (1.5-fold) and active (1.2-fold) β-catenin were increased modestly in Shef4$^{EWS\text{-}FLI1.ON}$ cells compared to Shef4$^{EWS\text{-}FLI1.OFF}$ cells after 1 month culture with DOX (5μg/ml) (Figure 6.15). After treatment with Wnt3A (200ng/ml) for 4h, total (1.3-fold) and active (1.6-fold) β-catenin expression was increased in Shef4$^{EWS\text{-}FLI1.OFF}$ control cells. In Shef4$^{EWS\text{-}FLI1.ON}$ cells after treatment with Wnt3A, total β-catenin was increased 1.5-fold in cells treated with DOX for 72h, but actually decreased in cells treated with DOX for 1 month (Figure 6.15). In contrast active β-catenin was decreased in Shef4$^{EWS\text{-}FLI1.ON}$ cells treated with DOX for 72h and was increased 1.2-fold in cells treated with DOX for 1 month.

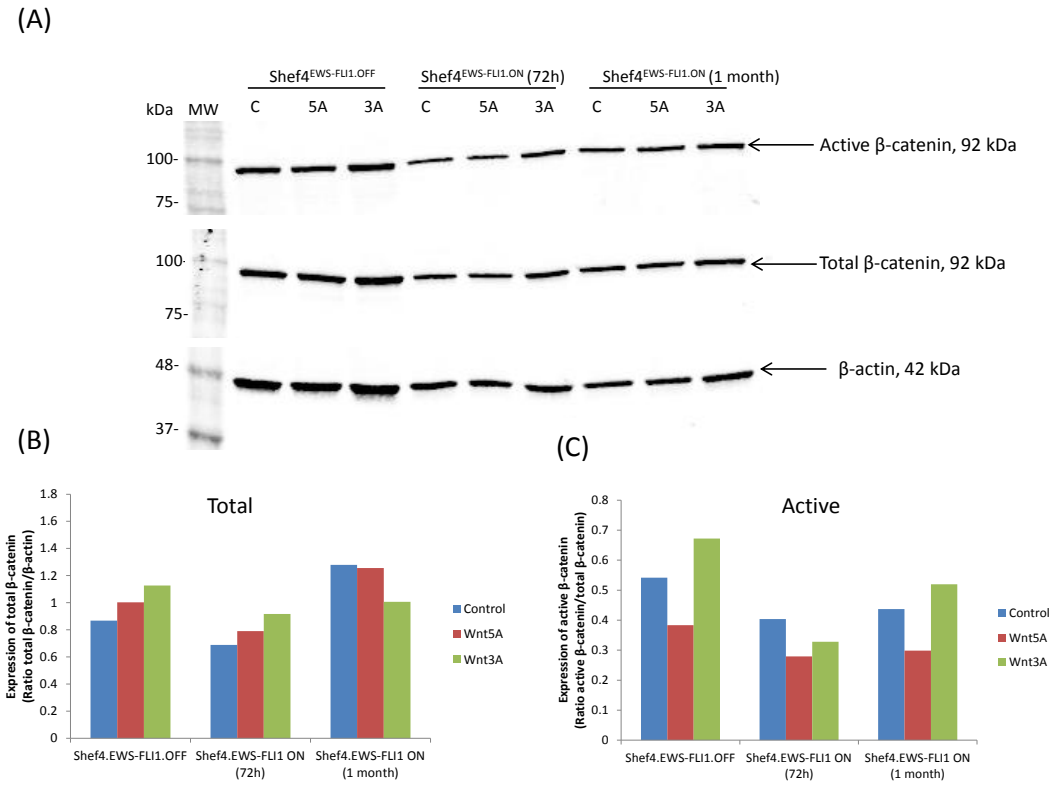

Figure 6.15 Expression of β-catenin in Shef4$^{EWS\text{-}FLI1}$ cells after stimulation with Wnt ligands. Shef4$^{EWS\text{-}FLI1.OFF}$ and Shef4$^{EWS\text{-}FLI1.ON}$ cells cultured in DOX for 72h and 1 month were stimulated with 200ng/ml Wnt5A or 200ng/ml Wnt3A for 4h. A) Total protein was extracted and expression of total and active β-catenin determined by western blot. Expression of β-actin was used as a loading control. Densitometry was performed to quantify the ratio of expression of B) total β-catenin to β-actin expression and C) active β-catenin compared to total β-catenin expression. MW=molecular weight in kDa.

6.3.4 Activity of the noncanonical Wnt signalling pathway in Shef4 cells with EWS-FLI1 expression

6.3.4.1 Migration of Shef4 cells with EWS-FLI1 expression

6.3.4.1.1 Optimisation of migration assay for Shef4 cells

The migration assay I have optimised in Chapter 4 relies upon the initial formation of spheroids from cell lines. However, Shef4 cells plated into ultra-low adherence 96 well round-bottomed plates did not form spheroids; after 4 days of culture, single cells accumulated at the bottom of the well but did not aggregate (Figure 6.16, left panels). Two alternative methods were used to encourage the formation of spheroids by Shef4 cells. Centrifuging the plate (152g, 4 min) immediately after seeding cells did not induce spheroid formation (Figure 6.16, middle panels). Application of a selective Rho-associated kinase (ROCK) inhibitor has been reported to increase survival of dissociated hES cells and promote formation of spheroids also known as 'embryoid bodies' (Watanabe et al. 2007). Indeed, addition of the ROCK inhibitor (Y-27632, 10μM) to the media resulted in the formation of spheroids by both Shef4$^{EWS\text{-}FLI1.OFF}$ and Shef4$^{EWS\text{-}FLI1.ON}$ cells. The spheroids formed by Shef4$^{EWS\text{-}FLI1.ON}$ cells were significantly smaller by, on average, 37±3.5% ($p<0.0001$) Increased amounts of cell debris were visible in the bottom of the well, in which Shef4$^{EWS\text{-}FLI1.ON}$ cells had been cultured which may be attributed to the reduction in cell viability observed when Shef4 cells are treated with DOX (Section 6.3.1.3).

Cells within Shef4$^{EWS\text{-}FLI1.OFF}$ spheroids did not migrate out from the core of the spheroid unless plated onto Matrigel™, which is the substrate used for feeder free culture of Shef4 cells (Figure 6.17 A). After 72h, the maximum MI of Shef4$^{EWS\text{-}FLI1.OFF}$ cells was 54±1.3 (i.e. cells had migrated over an area 54X that of the area covered by the core at 0h). However, cells from Shef4$^{EWS\text{-}FLI1.ON}$ spheroids migrated when plated onto all three substrates. After 72h, the migration index was greatest when spheroids were plated onto gelatin (63±1.7), and smallest when plated onto Primaria™ plastic (13±1.4) (Figure 6.17 B).

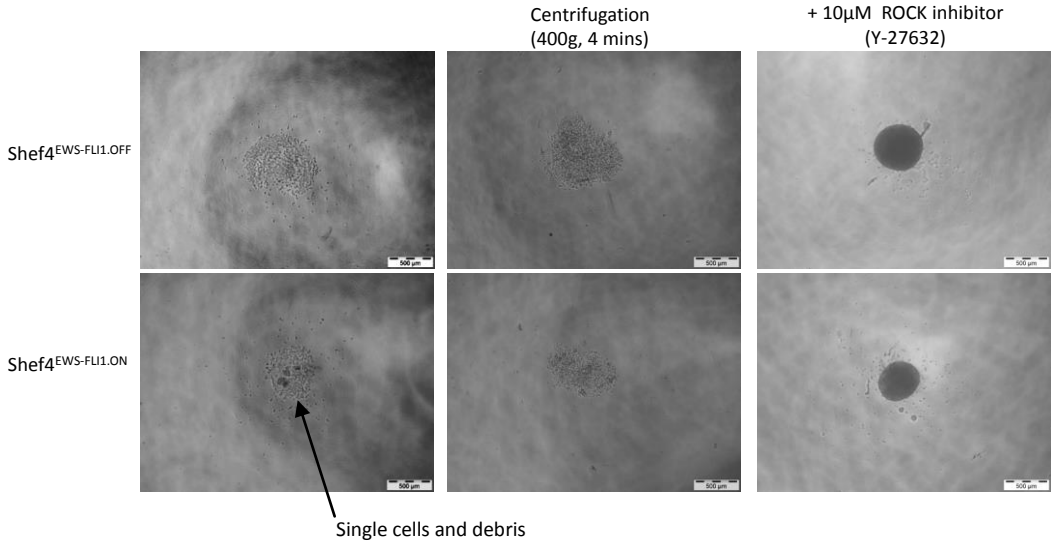

Figure 6.16 Formation of spheroids from Shef4 cells Shef4$^{EWS\text{-}FLI1.OFF}$ and Shef4$^{EWS\text{-}FLI1.ON}$ cells which had been pre-treated with DOX for 72h were seeded into ultra-low adherent 96 well plates (500 cells/well). Plates were either A) placed immediately in the incubator, B) centrifuged at 152g for 4 minutes or C) 10µM ROCK inhibitor (Y-27632) added to the media. Representative images taken after 4 days are shown.

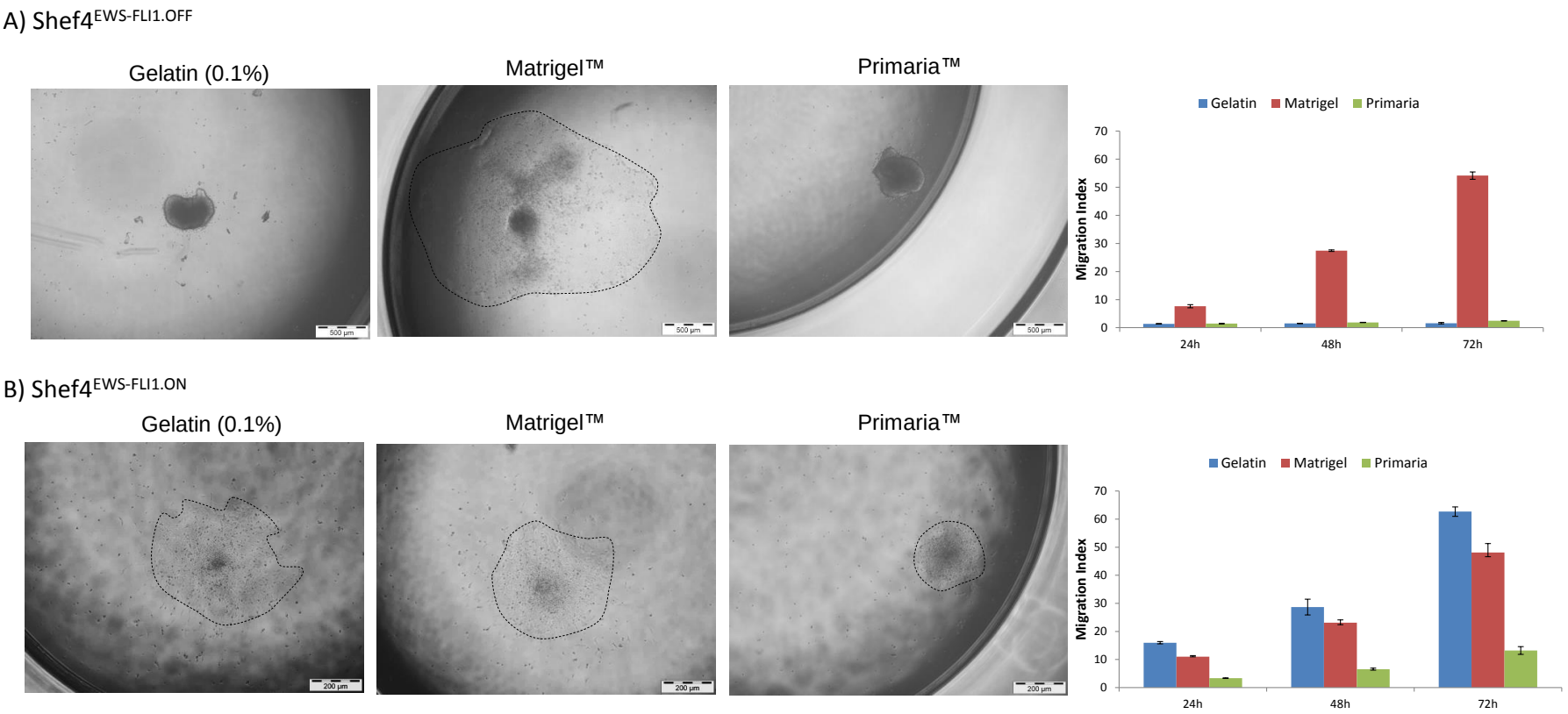

Figure 6.17 Migration of Shef4 cells with and without EWS-FLI1 expression on different substrates. Spheroids were formed from A) Shef4$^{EWS\text{-}FLI1.OFF}$ and B) Shef4$^{EWS\text{-}FLI1.ON}$ cells and transferred into flat-bottomed 96 well plates coated with either 0.1% gelatin, Matrigel™ or directly onto Primaria™ plastic. Spheroids were imaged every 24 h and the area covered by migrated cells quantified using Velocity software. Images show spheroids 48h post seeding. Dotted lines show the boundary of migrating cells. Results are presented as the area covered by migrating cells relative to the size of the spheroid at Day 0 (Migration Index) and given as the mean of three wells within one experiment (n=3) (±SEM)

6.3.4.1.2 Migration of Shef4$^{EWS\text{-}FLI}$ cells in response to Wnt ligands

To enable comparison of the migration of Shef4$^{EWS\text{-}FLI1}$ cells and the migration of ESFT cell lines, Shef4$^{EWS\text{-}FLI1}$ cell spheroids were plated onto gelatin coated plates in the presence of Wnt5A (200ng/ml) or Wnt3A (200ng/ml). Cells within Shef4$^{EWS\text{-}FLI1.OFF}$ spheroids did not migrate out of the core of the spheroid in response to either Wnt5A or Wnt3A (Figure 6.18 A). In contrast, Shef4$^{EWS\text{-}FLI1.ON}$ cells did migrate. After 72h, the migration index of Shef4$^{EWS\text{-}FLI1.ON}$ cells treated with both Wnt5A (44±3.3) and Wnt3A (41±1.7) was increased compared to control cells not treated with Wnt ligand (30±2.4)), however this difference did not reach statistical significance (Figure 6.18 B).

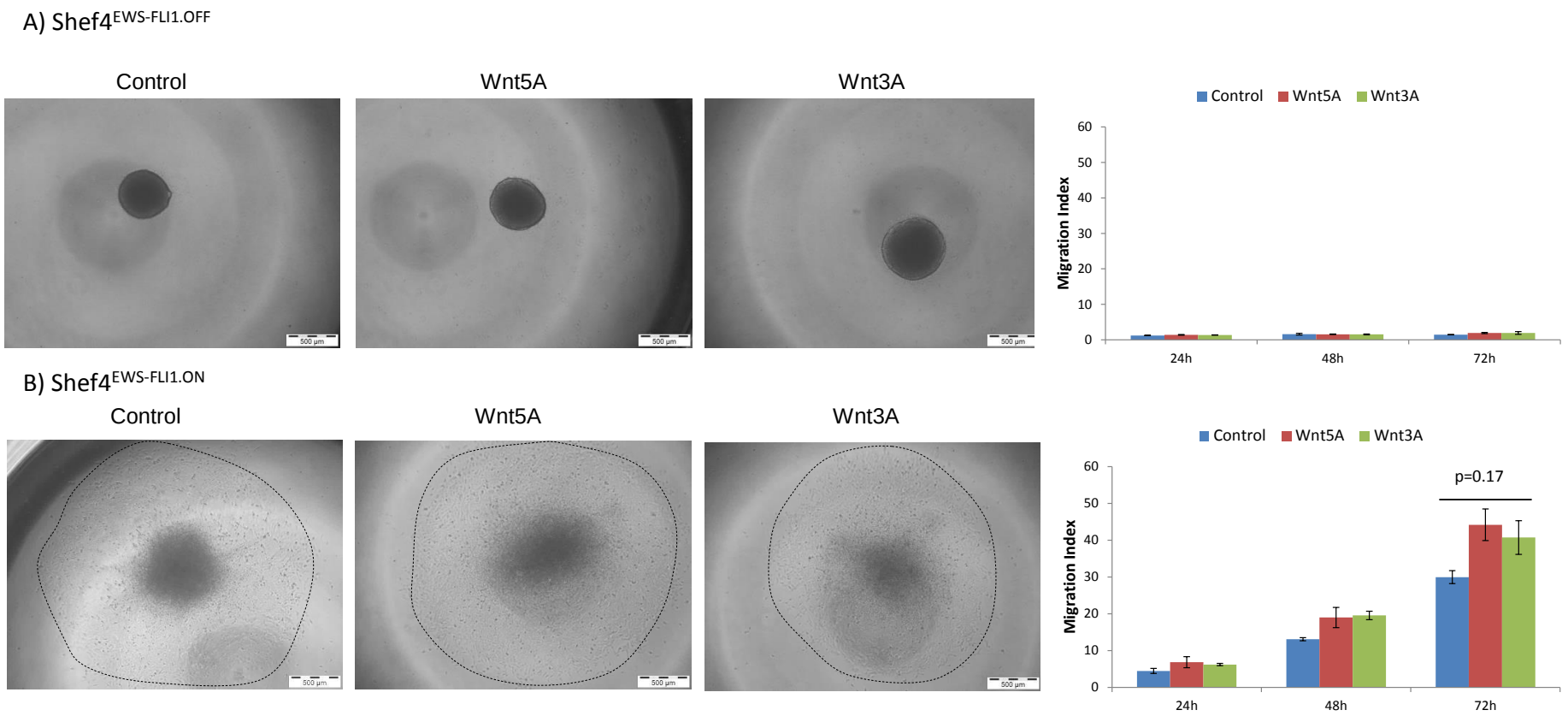

Figure 6.18 Migration of Shef4 cells with and without EWS-FLI1 expression in response to Wnt ligands Spheroids were formed from A) Shef4$^{EWS\text{-}FLI1.OFF}$ and B) Shef4$^{EWS\text{-}FLI1.ON}$ cell lines and plated onto flat-bottomed 96 well plates coated with 0.1% gelatin in mTeSR™1 (+/- DOX) containing a final concentration of 200ng/ml recombinant Wnt3A or 200ng/ml recombinant Wnt5A. Images were taken every 24h and the area covered by migrating cells quantified using Velocity software. Representative images show migration after 72h. Results are presented as the area migrated at each time point relative to the area of the spheroid at 0h (Migration Index) and given as the mean of three independent experiments with three replicates per experiment (n=9)(±SEM).

6.3.4.2 Expression of active Rac1/Cdc42 in Shef4 cells with and without EWS-FLI1 expression

Active Rac1 was detected in both Shef4$^{EWS\text{-}FLI1.OFF}$ and Shef4$^{EWS\text{-}FLI1.ON}$ cells (Figure 6.19 A). The endogenous level of active Rac1 was 1.5±0.1-fold lower in Shef4$^{EWS\text{-}FLI1.ON}$ cells compared to Shef4$^{EWS\text{-}FLI1.OFF}$ (Figure 6.19 B). The expression of active Rac1 was increased in both cell lines following treatment with Wnt5A (200ng/ml) for 30min, however this increase was slightly greater in Shef4$^{EWS\text{-}FLI1.OFF}$ cells (1.6±0.1-fold) than in Shef4$^{EWS\text{-}FLI1.ON}$ cells (1.4±0.1-fold) (Figure 6.19 B). Cdc42 protein could also be detected in Shef4$^{EWS\text{-}FLI1.OFF}$ and Shef4$^{EWS\text{-}FLI1.ON}$ cells (Figure 6.19 C). In contrast to active Rac1, active Cdc42 expression was increased in Shef4$^{EWS\text{-}FLI1.ON}$ cells compared to Shef4EWS$^{-FLI1.OFF}$ cells (1.5±0.07-fold). However, after treatment with Wnt5A (200ng/ml, 30 min) the expression of active Cdc42 decreased in both Shef4$^{EWS\text{-}FLI1.OFF}$ cells (1.8±0.05-fold) and in Shef4$^{EWS\text{-}FLI1.ON}$ cells (2.5±0.14-fold) (Figure 6.19 D).

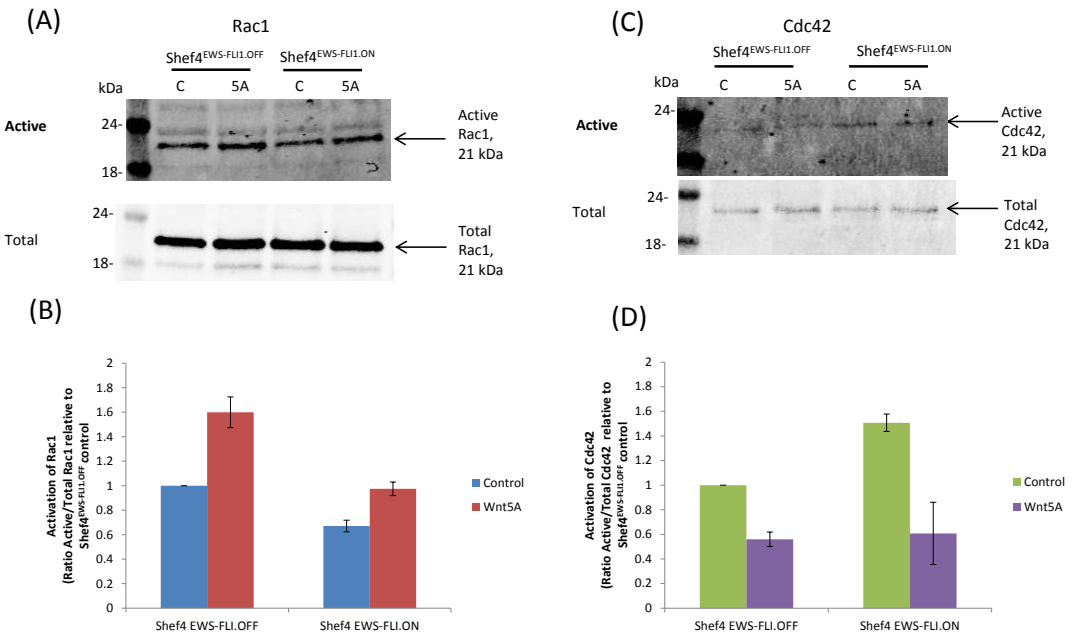

Figure 6.19 Expression of active Rac1 and Cdc42 in Shef4 cells with and without EWS-FLI1 expression Shef4$^{EWS\text{-}FLI1.OFF}$ and Shef4$^{EWS\text{-}FLI1.ON}$ cells were cultured in 10cm^2 dishes until 70% confluent then treated with rWnt5A (200ng/ml) for 30min. Cells were harvested, a sample removed for total protein estimation and active (GTP-bound) Rac1 and Cdc42 were precipitated from the remaining extract using glutathione-sepharose beads bound to PAK-CRIB. Beads were washed, isolated and the sample split for analysis of Rac1 and Cdc42 by western blot. A) Expression of active Rac1 total Rac1 B) Densitometry was performed and the ratio of active/total Rac1 calculated and expressed relative to expression in Shef4EWS$^{-FLI1.OFF}$ control cells. Results show mean of two independent experiments (±SEM). C) Expression of active Cdc42 and total Cdc42. Representative of 2 independent experiments.

6.3.4.2.1 Changes in actin cytoskeleton with Wnt5A

Immunofluorescent staining of the actin cytoskeleton revealed treatment with Wnt5A (200ng/ml, 24h) had no observable effect on the actin cytoskeleton of Shef4$^{EWS\text{-}FLI1.OFF}$ or Shef4$^{EWS\text{-}FLI1.ON}$ cells (Figure 6.20).

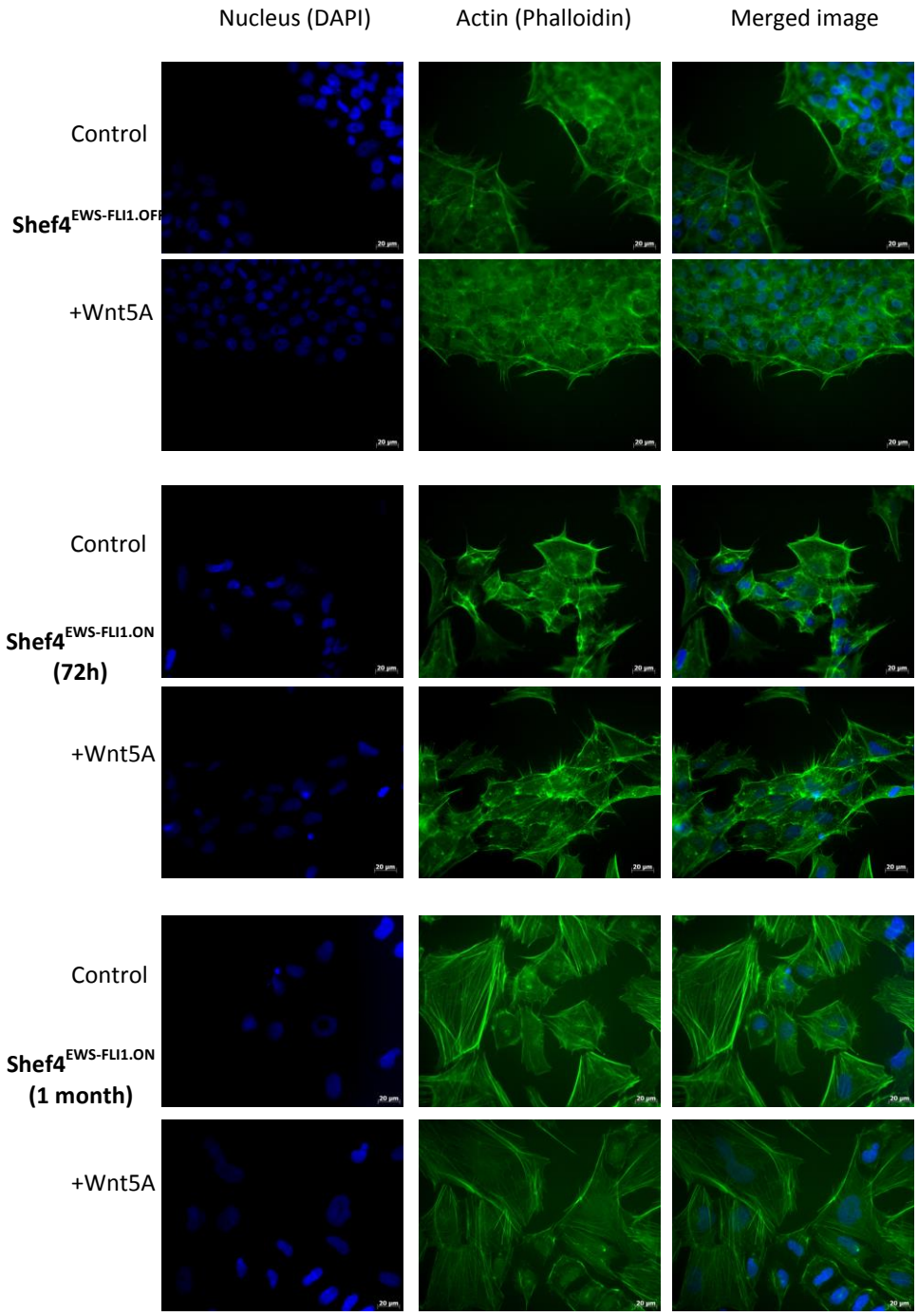

Figure 6.20 Actin cytoskeleton in Shef4$^{EWS\text{-}FLI.OFF}$ and Shef4$^{EWS\text{-}FLI.ON}$ cells treated with Wnt5A Shef4$^{EWS\text{-}FLI.OFF}$, Shef4$^{EWS\text{-}FLI.ON}$ and Shef4$^{EWS\text{-}FLI.ON}$ (1 month) cells were seeded onto glass coverslips coated with Matrigel™. Cells were grown for 24h, then treated with Wnt5A (200ng/ml, fixed with 4% PFA, and stained with DAPI (blue) and phalloidin (green) and imaged using a fluorescent microscope.

6.3.5 Effect of Wnt ligands on the growth of Shef4 cells with and without EWS-FLI1 expression

Recombinant Wnt3A (200ng/ml) and recombinant Wnt5A (200ng/ml) did not increase the viable cell number of the Shef4$^{EWS\text{-}FLI.ON}$ cell line, or on Shef4 parental cell lines (Figure 6.21). Although the viable cell number of Shef4$^{EWS\text{-}FLI1.OFF}$ cells was significantly different after treatment with Wnt ligands ($p<0.05$), treatment with Wnt5A or Wnt3A actually decreased the viable cell number compared to untreated (control) cells (Figure 6.21 A).

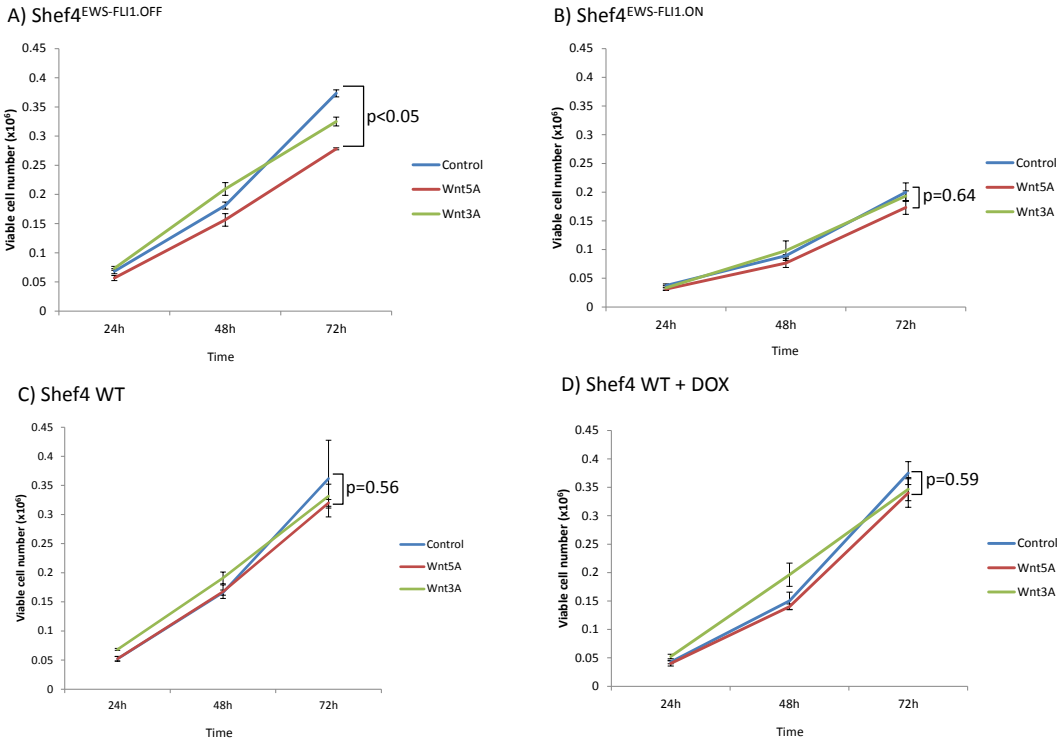

Figure 6.21 Viable cell number of Shef4 cell lines following treatment with Wnt3A and Wnt5A A) Shef4$^{EWS\text{-}FLI1.OFF}$ B) Shef$^{EWS\text{-}FLI1.ON}$ C) Shef4 parental and D) Shef4 parental (treated with DOX) cell lines were seeded as a single cell suspension and allowed to adhere for 24h. Cells were treated with 200ng/ml recombinant Wnt3A or recombinant Wnt5A for 24, 48, or 72h and viable cell number determined by trypan blue exclusion using the Vi-cell automated cell counter. Results show the mean of two independent experiments with three replicates within each experiment (n=6) (± SEM).

6.4 Discussion

In this chapter I have confirmed that expression of EWS-FLI1 can be induced in the Shef4 hES cell line using the TetON Advanced inducible expression system. My data demonstrates that EWS-FLI1 expression alters the growth characteristics and morphology of Shef4 cells. Furthermore, EWS-FLI1 changes the expression of Wnt signalling components and activates a TCF-based luciferase reporter of canonical Wnt signalling in Shef4 cells. EWS-FLI1 expression also increases the migration of Shef4 cells, and increases endogenous expression of active Cdc42. Therefore it is possible that canonical and noncanonical Wnt signalling are activated in these cells.

EWS-FLI mRNA expression could be detected in Shef4$^{EWS\text{-}FLI1}$ cells after only 24h treatment with DOX, and the protein could be detected after 48h. My data confirmed that by 72h Shef4$^{EWS\text{-}FLI1.ON}$ cells expressed EWS-FLI1 mRNA at the same level as the TC32 ESFT cell line, and cells which were maintained in DOX for up to 1 month continued to express EWS-FLI1 at this same level. This confirms that the TetON inducible system is functional for as long as DOX is present in the media. Previous data from our laboratory has shown that expression of EWS-FLI1 in Shef4 cells induced expression of the ESFT marker CD99, as well as significantly increasing mRNA expression of EWS-FLI1 target genes *CAV1, COL11A1, IGF1, NKX2-2* and *NROB1* (Dr Andrew Gaffney, personal communication). These data further support the conclusion that this system is an informative model of ESFT initiation. It is important to note that treatment of Shef4$^{EWS\text{-}FLI1}$ cells with DOX reduced the viable cell number in a dose-dependent manner. It was hypothesised this was because expression of EWS-FLI1 was not tolerated in (at least a sub-population) of Shef4 cells, as has been shown in other cell types (Lessnick et al. 2002). This is consistent with the failure to identify stable EWS-FLI1-expressing Shef4 cells using a constitutive system (Dr Andrew Gaffney, personal communication). However, parental Shef4 cells also had reduced viable cell growth in the same concentrations of DOX. Therefore my data suggests that DOX is toxic to at least a sub-population of Shef4 cells, and the initial reduction in viable cell number is not related to the expression of EWS-FLI1. In this study 5µg/ml DOX was used to induce expression of EWS-FLI. This is higher than the concentration of DOX suggested by Clontech (the manufacturers of the TetON Advanced system). However this high concentration was required to achieve a similar level of EWS-FLI1 expression in Shef4$^{EWS\text{-}FLI1}$ cells to that observed in TC32 cells. Therefore this concentration was used despite the fact that it reduced the viable cell number of Shef4 cells. Despite this, once a resistant population of cells was established, Shef4 parental cells grown in DOX (5µg/ml) had identical growth to

that of Shef4 parental cells not grown in DOX. In contrast, Shef4$^{EWS\text{-}FLI1.ON}$ cells had significantly reduced viable cell growth, and this was further reduced the longer EWS-FLI1 was expressed. My data therefore demonstrates that EWS-FLI does have an effect on the long term growth characteristics of Shef4 cells. This is consistent with a previous study where DOX-induced expression of EWS-FLI1 in mesenchymal stem cells resulted in apoptosis-independent growth inhibition (Miyagawa et al. 2008). Although this previous study did not observe any differences in the cell cycle profile of these cells, further analysis would be required in our hES system to understand the mechanisms behind this growth inhibition.

In addition to the differences in viable growth observed, the phenotype of the Shef4 cells was altered following induction of EWS-FLI1. Shef4$^{EWS\text{-}FLI1.ON\ cell}$ colonies were less tightly packed with an increased number of highly migratory cells. In addition, although not quantified, there were obviously fewer cell-cell adhesions and a greater number of cells which had filopdia. After 1 month of DOX treatment the morphology of Shef4$^{EWS\text{-}FLI1.ON}$ cells had changed even more drastically. Some smaller cells were still observed, however there were many large cells, histologically similar to mesenchymal cells, which contained stress fibres. This observation suggests that although the expression of EWS-FLI1 remains constant over this time, the transformation of Shef4$^{EWS\text{-}FLI1.ON}$ cells is an on-going process. This transition of tightly packed embryonic stem cells to elongated mesodermal-like cells with filamentous actin cytoskeleton has been described previously (Kinney et al. 2014). The change in morphology observed is reminiscent of an EMT. Although commonly investigated in cancer this process is fundamental during development. For example, during gastrulation and when neural crest cells within the dorsal neural epithelium migrate and give rise to the peripheral nervous system and other derivatives (Thiery et al. 2009). To determine if the Shef4$^{EWS\text{-}FLI1.ON}$ cells are truly undergoing mesodermal differentiation it would be necessary to investigate the expression of other markers associated with EMT such as loss of E-cadherin, gain of N-cadherin and gain of vimentin expression. In addition, since spontaneous differentiation to mesodermal-like cells has been demonstrated around the edges of hES cells grown in feeder free conditions (Ullmann et al. 2007), it would be necessary to also stain for EWS-FLI expression to confirm that the cells with this morphology are not simply an outgrowth of cells already present in the Shef4 population and unrelated to the expression of EWS-FLI1.

Shef4 cells were cultured in feeder-free conditions using mTeSR™1 on hES-qualified Matrigel™. As discussed previously (Chapter 5) mTeSR™1 medium is serum-free and

contains a number of defined factors, including FGF2, to maintain self-renewal and pluripotency in hES cells (Ludwig et al. 2006, Akopian et al. 2010). ESFT cells cannot tolerate culture in mTeSR™1 (Dr Andrew Gaffney, personal communication), presumably in part due to the high concentration of FGF2. Therefore it was hypothesised that culture in this media may inhibit the emergence of transformed ESFT-like Shef4$^{EWS\text{-}FLI1.ON}$ cells. For this reason Shef4$^{EWS\text{-}FLI1.ON}$ cell growth in RPMI (typical ESFT media) was investigated to determine if this media more effectively supported the maintenance of Shef4 cells with EWS-FLI1. However, my data showed that this was not the case. Although a subpopulation of cells appeared to adhere, there was no evidence of cell growth after a week. This indicated that despite adopting a phenotype and expression profile similar to that of ESFT cells, Shef4$^{EWS\text{-}FLI1.ON}$ cells are still inherently stem cells which require growth in this defined media. However, growth in RPMI was only investigated after up to 72h after DOX treatment. Since the morphology of Shef4 $^{EWS\text{-}FLI1.ON}$ cells continued to change up to 1 month after DOX treatment, it is possible that there would be a point that Shef4$^{EWS\text{-}FLI1.ON}$ cells could tolerate growth in RPMI, although this was not assessed in this study. The culture media used is clearly important since it has been shown that the expression profile of paediatric MSCs with EWS-FLI1 expression cultured in serum-free knock out (KO) media more closely resembled that of ESFT than the same cells grown in normal FCS-containing media Therefore, for longer term experiments it would be valuable to elucidate the optimal growth media to use for Shef4$^{EWS\text{-}FLI1.ON}$ cells.

To investigate the role of the Wnt signalling pathway in the induction of the ESFT phenotype using the Shef4$^{EWS\text{-}FLI1.OFF}$ and Shef4$^{EWS\text{-}FLI1.ON\ cells}$, initially the Wnt signalling pathway array was performed. Although expression of 95% of components of the pathway were similar in Shef4$^{EWS\text{-}FLI1.OFF}$ and Shef4$^{EWS\text{-}FLI1.ON}$ cells, there was a significant change in expression of a number of genes between the two cell types. Interestingly there was an increase in DKK2 expression and a decrease in DKK4 expression observed in Shef4$^{EWS\text{-}FLI1.ON}$ cells. This is the opposite pattern to that which was observed in the OSCK4 (reprogrammed) ESFT cell line (Chapter 5). This further strengthens the hypothesis that the DKK family play an important role in the initiation of ESFT and will be discussed further in Chapter 7. Interestingly, it has been shown previously that DKK2 expression is increased when EWS-ETS fusion proteins are expressed in mesenchymal progenitor cells (Miyagawa et al. 2009). In Shef4$^{EWS\text{-}FLI1.ON}$ cells there was an increase in expression of the noncanonical Wnt ligands Wnt4 and Wnt5A compared to expression in Shef4$^{EWS\text{-}FLI1.OFF}$ cells. In addition, Shef4$^{EWS\text{-}FLI1.ON}$ cells had increased expression of the FZD8 receptor which is involved in both canonical and noncanonical Wnt signalling and is expressed in ESFT cell lines (Chapter 2).

An increase in expression of FZD8 has also previously been reported in MSCs with inducible EWS-FLI1 expression (Miyagawa et al. 2008). To investigate further if these components play causal role in ESFT development it would be necessary to manipulate their expression, by knock-down and overexpression, and investigate what effect this has on the phenotypes observed after expression of EWS-FLI1.

As in previous chapters, the activity of the canonical Wnt signalling pathway was investigated using the 7TFH luciferase reporter system. It was observed that, consistent with previous reports in other hES cell lines, the endogenous level of canonical Wnt signalling was low in Shef4 cells (Dravid et al. 2005, Davidson et al. 2012). Interestingly, although the raw data was not shown, endogenous canonical Wnt signalling was higher in Shef4$^{EWS\text{-}FLI1.OFF}$ cells compared to Shef4 parental cells. It has previously been reported that endogenous Wnt signalling is heterogeneous in hES cell populations (Blauwkamp et al. 2012). Therefore since the Shef4$^{EWS\text{-}FLI1.OFF}$ cells have been though two rounds of antibiotic selection, it is possible that a sub-population of cells with relatively high canonical Wnt signalling has been selected. It was also observed that endogenous canonical Wnt signalling activity, as measured using the luciferase reporter, was increased after Shef4$^{EWS\text{-}FLI1.OFF}$ cells had been dissociated into single cells by trypsinisation and then plated. It is known that hES cells are extremely sensitive to dissociation into single cells, with replating efficiencies of between 1-5% reported (Amit 2000, Hasegawa et al. 2006). However it has been demonstrated that Wnt signalling can enhance survival of hES cells plated onto Matrigel (Dravid et al. 2005), and specifically increase the replating efficiency of dissociated hES cells (Hasegawa et al. 2006, Blauwkamp et al. 2012). Therefore, it is possible that Shef4 cells transiently increase canonical Wnt signalling when dissociated, which increases their survival. For this reason, canonical Wnt signalling was always assayed in Shef4 cells 96h after seeding to avoid this confounding my results.

My data demonstrate that treatment of Shef4$^{EWS\text{-}FLI1}$ cells with DOX increases luciferase reporter activity in a time-dependent manner between 48-72h. This is consistent with the time that the EWS-FLI1 protein can be detected in these cells, and therefore suggests that EWS-FLI1 is activating the canonical Wnt signalling pathway. However, as previously mentioned hES cells have been shown to have heterogeneous endogenous canonical Wnt signalling, therefore it could be that only Shef4 cells with endogenously high canonical Wnt signalling can tolerate expression of the EWS-FLI1 fusion. That said, luciferase reporter activity was further increased when Shef4$^{EWS\text{-}FLI1.ON}$ cells were cultured in DOX for 1 month. These data suggest therefore that the EWS-FLI1 protein does directly or indirectly activate

canonical Wnt signalling. In contrast to previous reports, the addition of Wnt3A did not increase canonical Wnt signalling in Shef4 $^{EWS\text{-}FLI1.OFF}$ control cells (Dravid et al. 2005, Blauwkamp et al. 2012). However, as previously described Shef4$^{EWS\text{-}FLI1.OFF}$ cells had higher endogenous canonical Wnt signalling than Shef4 parental cells. Therefore it is possible that the canonical Wnt signalling pathway was already maximally stimulated in these cells. In contrast, Wnt3A significantly increased canonical Wnt signalling in Shef4 $^{EWS\text{-}FLI1.ON}$ cells, and this difference was greater when cells had been cultured in DOX for 1 month. This difference in canonical Wnt signalling in Shef4$^{EWS\text{-}FLI1.ON}$ cells cultured for an extended period of time in DOX is consistent with the continued change in morphology that was observed. This data further supports the notion that Shef4$^{EWS\text{-}FLI1.ON}$ cells are undergoing continued adaptation. Importantly, the addition of DOX did not change the activity of canonical Wnt signalling in Shef4 parental cells, further strengthening the hypothesis that EWS-FLI1 (rather than any other confounding factors) affects canonical Wnt signalling. Previous studies modelling the initiation of ESFT have indicated that Wnt signalling may be involved in this process. For example, expression of EWS-FLI1 in MSCs increased expression of FZD4, FZD7, FZD8, TCFL2 and Cdc42 and down regulated DKK1 (Miyagawa et al. 2008). However, my study is the first to provide evidence suggesting that the EWS-FLI1 protein activates canonical Wnt signalling in cells.

I attempted to confirm the increased activation of canonical Wnt signalling in Shef4$^{EWS\text{-}FLI1.ON}$ cells by investigating the expression of total and active β-catenin. Total, but not active, β-catenin was increased in Shef4$^{EWS\text{-}FLI1.ON}$ cells compared to Shef4$^{EWS\text{-}FLI1.OFF}$ cells. However active β-catenin was increased in both Shef4$^{EWS\text{-}FLI1.OFF}$ and Shef4$^{EWS\text{-}FLI1.ON}$ cells after treatment with Wnt3A. These results were therefore inconclusive. As discussed in Chapter 3, detection of β-catenin by western blot may not be sensitive enough to detect subtle changes in expression. There are hundreds of target genes of canonical Wnt signalling and it is not know which of these are up- or down-regulated in this particular cellular situation. However further studies could use RTqPCR to investigate mRNA expression of Axin2 and a panel of other potential target genes to investigate downstream activation of the canonical Wnt signalling pathway.

The migration assay optimised in Chapter 4 was used to investigate migration in hES cells with inducible EWS-FLI1 expression. As previously described, the migration assay used in this study relies on the initial formation of cell spheroids. In the field of hES cells, non-adherent cell aggregates are termed ‘embryoid bodies’ (EBs) and formation of EBs is the first step in many differentiation protocols (Outten et al. 2011). However, as discussed

previously, hES cells are sensitive to single cell dissociation and a selective Rho-associated kinase (ROCK) inhibitor (Y-27632) is widely used to promote EB formation and increase hES cell survival (Watanabe et al. 2007). It has been shown that the activation of Rho is responsible for dissociation-induced hES cell apoptosis by ROCK-mediated myosin light chain phosphorylation (Ohgushi et al. 2010). In agreement with these previous studies, Shef4 $^{EWS\text{-}FLI1.OFF}$ and Shef4$^{EWS\text{-}FLI1.ON}$ cells only formed spheroids in the presence of ROCK inhibitor. Interestingly, the spheroids formed by Shef4$^{EWS\text{-}FLI1.OFF}$ cells were significantly larger than those formed by Shef4$^{EWS\text{-}FLI1.ON}$ cells; this could be explained by the increased viable cell growth of these cells. When the spheroids were plated onto different substrates, Shef4$^{EWS\text{-}FLI1.OFF}$ cells only migrated when plated on hES-cell qualified Matrigel™. This is perhaps not surprising at this is the matrix routinely used for feeder-free growth of Shef4 cells. The Shef4$^{EWS\text{-}FLI1.OFF}$ cells spread out with a clearly defined edge and maintained a tight central core. In contrast Shef4$^{EWS\text{-}FLI1.ON}$ cells migrated the most when plated onto gelatin, as was observed in the ESFT cell lines. In Shef4$^{EWS\text{-}FLI1.ON}$ cells although a spheroid core still remained, highly migratory individual cells were observed. This is consistent with my previous observations that suggested the Shef4$^{EWS\text{-}FLI1.ON}$ cells may have undergone a transition to mesenchymal-like cells, which are known to be highly migratory. This is also consistent with transformation to an ESFT-like cell, as most of the ESFT cell lines studied in Chapter 4 were also highly migratory. Treatment with both Wnt5A and Wnt3A increased the migration of Shef4$^{EWS\text{-}FLI1.ON}$ cells after 72h, however this did not reach statistical significance. Interestingly Wnt5A mRNA expression was increased in Shef4$^{EWS\text{-}FLI1.ON}$ cells and this may in part explain the increase in migration observed in Shef4$^{EWS\text{-}FLI1.ON}$ cells. However, as previously discussed in Chapter 4, many of the downstream targets of EWS-FLI1 have previously been shown to increase migration such as CD99 and caveolin-1 (Sáinz-Jaspeado et al. 2010, Kreppel et al. 2006). Therefore it is not possible to directly link Wnt5A expression or the Wnt signalling pathway to the differences in migration observed. In future studies inhibition of Wnt5A expression by RNAi may increase understanding of the role that this protein is having. To my knowledge this is the first time an increase in migration has been specifically reported in a model where EWS-FLI1 has been induced into mammalian cells.

When Shef4$^{EWS\text{-}FLI1}$ cells were treated with Wnt5A, there was a modest but not statistically significant increase in migration. However, there was no change in the actin cytoskeleton. Importantly, for the immunofluorescence analysis, cells were treated with Wnt5A for 24h. It is therefore possible that changes in the actin cytoskeleton occurred at earlier time points and were missed in my analysis. The pull-down assays used were performed after

30 min of Wnt5A treatment and previous studies have reported Wnt5A has an effect within 1h of exposure (Mikels and Nusse 2006). Future experiments could test this by performing immunofluorescence after shorter treatments with Wnt5A. In addition, by using high throughput automated analysis such as the Operetta® system, which we have access to, easy quantification of parameters could be performed which would give more quantitative results. It is quite possible this would reveal changes to the actin cytoskeleton since an increase in active Rac1 was observed in both Shef4$^{\text{EWS-FLI1.OFF and}}$ Shef4$^{\text{EWS-FLI1.ON}}$ cells after treatment with Wnt5A for 30 min. With regards to differences between Shef4$^{\text{EWS-FLI1.OFF and}}$ Shef4$^{\text{EWS-FLI1.ON}}$ cells, no difference in active Rac1 expression was detected. However, although levels of total Cdc42 were low, there appeared to be in increase in active Cdc42 in Shef4$^{\text{EWS-FLI1.ON}}$ cells. This is interesting since it has been shown that Cdc42 specifically controls the formation of filopida (Samuel and Olson 2011, Yang et al. 2006), and an increase in filopoda was observed in Shef4$^{\text{EWS-FLI1.ON}}$ cells. This change in phenotype was more pronounced after Shef4$^{\text{EWS-FLI1.ON}}$ cells that had been cultured in DOX for 1 month. Therefore, it would be worthwhile to investigate Rac1 and Cdc42 activation in these cells. Rho GTPases including Rac1 and Cdc42 have been shown to play a key role in hES cell survival. This is demonstrated by the fact that that ROCK inhibition greatly increases the replating efficiency of hES cells, as previously discussed. It has been hypothesised that hES cell in colonies are reliant on actomyosin forces from adjacent cells to limit pro-apoptotic signals (Samuel and Olson 2011). Therefore it is evident that Rho GTPase signalling is important in hES cells, independent of Wnt signalling. This means it is more challenging to directly link the changes observed to active noncanonical Wnt signalling. However my data suggest that noncanonical Wnt signalling may also be activated in the initiation of ESFT. It would be interesting to inhibit Wnt signalling, using secreted inhibitors such as sFRP5 and investigate if this has an effect on the morphology of cells after EWS-FLI1 induction.

In summary in this chapter I have validated the model system of EWS-FLI1 expression in Shef4 hES cells, and proved it to be a valuable tool to study ESFT initiation. I have demonstrated that components of the Wnt signalling pathway are altered upon EWS-FLI1 expression. The most exciting result is the strong evidence to suggest that EWS-FLI1 expression increases the activation of the canonical Wnt signalling pathway. This is the first time data has suggested this is the case, and may greatly increase our understanding of how, and in what cell type ESFT develops. In turn this could lead to the development of novel therapeutics to help prevent recurrence and metastasis. The next phase of this research would be to specifically inhibit key proteins such as DKK2, FZD8, Wnt4 and Wnt5A

and overexpress DKK4 (discussed in Chapter 7), which appear to be important, to further elucidate what role Wnt signalling has in the initiation of ESFT.

7. Final Discussion

My hypothesis was that the canonical Wnt signalling pathway is important in the initiation of ESFT, and the noncanonical Wnt signalling pathway becomes dominant during disease progression and metastasis. The specific aims of this thesis were to:

- Examine the expression profile of Wnt signalling components in ESFT cell lines.
- Develop functional assays to measure the activity of both the canonical and noncanonical Wnt signalling pathways.
- Investigate the activity of the Wnt signalling pathways in two model systems of ESFT initiation: in reprogrammed ESFT cells and in hES cells with inducible EWS-FLI1 expression.

The main findings of this thesis are:

- ESFT cells express many key components of the Wnt signalling pathway including the canonical and noncanonical ligands Wnt1 and Wnt5A.
- Canonical Wnt signalling is active in ESFT cell lines, and can be stimulated by the addition of exogenous Wnt3A ligand.
- Expression of EWS-FLI1 activates canonical Wnt signalling in hES cells and changes the expression of Wnt signalling components including FZD8, Wnt4, Wnt5A, DKK4 and DKK2.
- Expression of EWS-FLI1 in hES cells may stimulate noncanonical Wnt signalling since Wnt5A expression, active Cdc42 and cell migration were all increased upon expression of the gene fusion.

These results suggest that EWS-FLI-induced canonical and noncanonical Wnt signalling may be important during the initiation of ESFT. This hypothesis is summarised in Figure 7.1. Although the mechanism for this activation was not elucidated, my data suggests that this may be due to increased expression of FZD8, and decreased expression of DKK4. Since DKK2 expression was also increased in hES cells following induction of EWS-FLI, this may also activate canonical Wnt signalling, in addition to promoting migration. Expression of the noncanonical ligands Wnt4 and Wnt5A were also increased upon expression of EWS-FLI1, however the potential role of the noncanonical Wnt signalling in the initiation of ESFT

was more difficult to determine as there are no assays available to specifically measure the activity of this pathway.

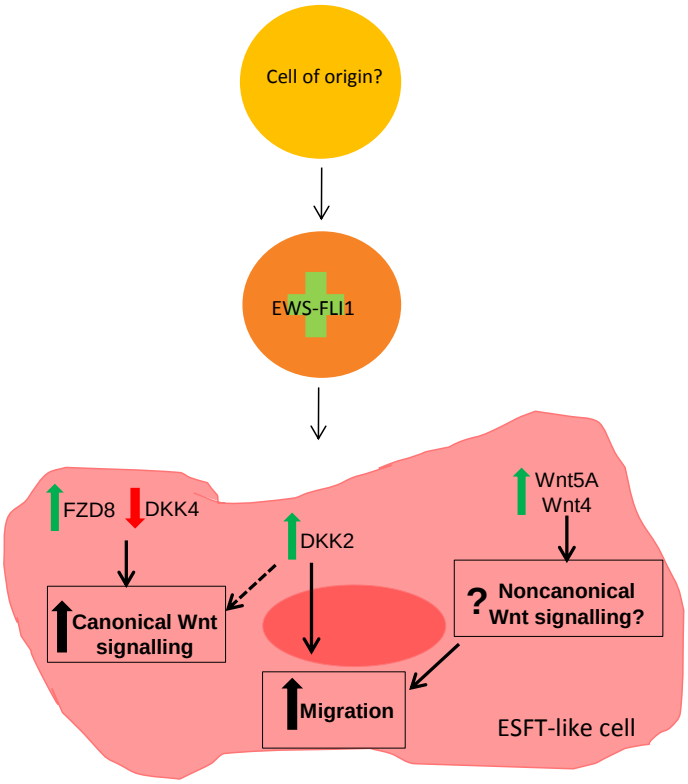

Figure 7.1 Summary of main findings and hypothesised mechanisms of Wnt signalling activation during ESFT initiation

7.1 EWS-FLI1 activates canonical Wnt signalling

To my knowledge this is the first report providing data to suggest that EWS-FLI1 directly activates canonical Wnt signalling. This is an extremely important observation as it suggests that Wnt signalling may be an important pathway in the initiation of ESFT. EWS-ETS fusion proteins are known to be necessary for ESFT initiation, however they are not sufficient to transform all normal cell types. It is believed that a permissive cellular environment is required to support expression of the fusion protein, and that additional mutations or aberrations in certain signalling pathways are also important in the initiation of the tumour phenotype. My results indicate that activation of the canonical Wnt signalling pathway may be important in this initiation process.

The observation that EWS-FLI1 activates canonical Wnt signalling in hES cells is supported by my data to show that active canonical Wnt signalling in all ESFT cell lines studied. Although another recent report has described basal canonical Wnt signalling in the CHLA25 ESFT cell line (Scannell et al. 2013), these data are in contrast to most previous studies in

ESFT cells where no or extremely low basal canonical Wnt signalling could be detected (Hu-Lieskovan et al. 2005, Miyagawa et al. 2009, Navarro et al. 2010, Vijayakumar et al. 2011). This is most probably due to differences in experimental design as previous studies had used the less sensitive TOPFlash reporter assay, rather than the lentiviral vector used in this thesis and in the study by Scannell et al. (2013). However, notably in the paper by Navarro et al. (2010) it was reported that in HEK293T cells transient expression of EWS-FLI1 blocked activation of canonical Wnt signalling, as measured using the TOPFlash reporter system. This directly contradicts my observations in hES cells. One possible explanation for this is that EWS-FLI1 has different effects on Wnt signalling depending on the cellular context, thus highlighting the importance of confirming my observations in other cell types.

In this study I have used pluripotent hES cells to model tumour initiation. It would of course be important to show that activation of canonical Wnt signalling occurs when EWS-FLI1 is expressed in the cell of origin of ESFT. However, the identity of this cell (or cells) has not yet been elucidated. The most widely held hypothesis is that ESFT arise from MSCs (Tirode et al. 2007, Riggi et al. 2008, Riggi et al. 2010). Therefore it would be interesting to differentiate hES cells to a mesenchymal lineage (Outten et al. 2011), prior to inducing EWS-FLI1 expression and observe the effect of this in Wnt signalling activation. In the study by Navarro et al. (2010) the authors also demonstrated that EWS-FLI1 directly binds to LEF1, and hypothesised that the fusion protein may complete with β-catenin for binding, hence the inhibition of canonical Wnt signalling. Although my data disputes the fact that EWS-FLI1 inhibits canonical Wnt signalling, the observation that EWS-FLI1 binds to LEF1 is intriguing. It suggests that EWS-FLI1, behaving in its putative role as an aberrant transcription factor, may directly activate Wnt signalling. It has been estimated that EWS-FLI1 regulates the expression of over 1000 genes, however the fusion protein has only been shown to directly interact with a handful of genes such as such as *NR0B1* (Garcia-Aragoncillo et al. 2008) and *CAV1* (Tirado et al. 2006). In other cases EWS-FLI1 has been shown to indirectly regulate expression; for example the fusion protein upregulates *GLI1* which in turn upregulates *NKX2.2* (Beauchamp et al. 2009). Further studies have attempted to understand the interaction of EWS-FLI1 with its target genes using genome-wide localisation studies such as chromatin immunoprecipitation (ChIP) followed by microarray analysis (ChIP-chip) and have shown that EWS-FLI binds to GGAA-containing microsatellites (Gangwal et al. 2008). It has been reported that these GGAA microsatellites are enriched in the promoters of genes that are upregulated by EWS-FLI1 such as *NR0B1*. Interestingly using this experimental technique over 900 genes were found to directly

interact with EWS-FLI1 including *Wnt10B* and *DKK3* (Gangwal et al. 2008). Although mRNA expression of Wnt10B and DKK3 was not changed in my model systems, in future work techniques such as ChIP-chip and/or ChIP-seq could be employed to investigate whether EWS-FLI1 directly interacts with TCF/LEF and other Wnt signalling components. In the previous study by Navarro et al. (2010) immunoprecipitation (IP) followed by SDS-PAGE was used to identify EWS-FLI1 binding to LEF1, therefore more sensitive methods such as ChIP would provide important data to potentially confirm this interaction.

An alternative hypothesis is that EWS-FLI1 indirectly activates canonical Wnt signalling in hES cells. Interestingly, the morphology of hES cells changed dramatically when EWS-FLI1 was expressed; a transformation reminiscent of an EMT. Future studies staining for specific EMT markers such as loss of E-cadherin, gain of N-cadherin and vimentin expression will be important to examine this possibility. In addition to its role in the Wnt signalling pathway, β-catenin is also important in cell adhesion as a component of adherens junctions, where it is bound to both E-cadherin and the actin cytoskeleton (Adams and Nelson 1998). It has been demonstrated that when E-cadherin expression is reduced (for example during EMT), β-catenin is liberated from this structural complex (Eger et al. 2000). A decrease in E-cadherin expression in pancreatic cancer cells has been reported to lead to increased expression of β-catenin in the nucleus and a subsequent increase in proliferation (Koenig et al. 2006). Therefore it is possible that EWS-FLI1 targets genes that alter the morphology of the cell, thus decreasing E-cadherin expression, and indirectly activating canonical Wnt signalling by increasing intracellular β-catenin. Although EMT often occurs in cancer cells and is linked to invasion and metastasis, this process is vitally important during normal embryonic development (Kalluri and Weinberg 2009). It has been demonstrated that Wnt signalling orchestrates an EMT during gastrulation (Liu et al. 1999) and also when the epithelial cells of the neuroectoderm give rise to migratory neural crest cells (Villanueva et al. 2002). Importantly, in breast cancer canonical Wnt signalling has been shown to regulate both Snail (Yook et al. 2005) and Slug (Wu et al. 2012), via GSK3β mediated phosphorylation. These proteins are both critical regulators of the EMT. Taken together with my data it is also possible that the phenotypic differences observed in hES cells upon EWS-FLI1 expression are a result of the activation of canonical Wnt signalling. Activation of noncanonical Wnt signalling may also have a role in this process and this will be discussed further in Section 7.3.

Expression of the EWS-FLI1 fusion protein in hES cells increased expression of the receptor FZD8 and decreased expression of the inhibitor DKK4. Increased FZD8 expression has been

shown to increase the activity of the canonical Wnt signalling pathway and interestingly has been linked to chemoresistance in both lung (Wang et al. 2012) and triple negative breast cancer (Yin et al. 2013). DKK4 is an antagonist of canonical Wnt signalling (Niehrs 2006, Fatima et al. 2012), therefore the decreased expression in hES cells with EWS-FLI1 expression is consistent with increased canonical Wnt signalling. EWS-FLI1 has previously been reported to regulate the expression of components of the canonical Wnt signalling pathway such as DKK1 (Prieur et al. 2004, Kauer et al. 2009, Miyagawa et al. 2009) and DKK2 (Miyagawa et al. 2009). Therefore it is possible that by altering the expression of these and potentially other components of the Wnt signalling pathway that are as yet undescribed targets of EWS-FLI1, the fusion protein changes the activation of canonical Wnt signalling.

7.2 Role of DKK proteins in the initiation of ESFT

The results of this study highlight a potential role for the DKK family of proteins in ESFT initiation. This is interesting as both DKK1 and DKK2 have been previously identified as targets of EWS-FLI1. DKK1 has been reported to be downregulated by EWS-FLI1 (Prieur et al. 2004, Miyagawa et al. 2009, Navarro et al. 2010), whereas DKK2 is upregulated by the fusion protein (Miyagawa et al. 2009, Hauer et al. 2013). This is consistent with my data which showed higher expression of DKK2 than DKK1 in all ESFT cell lines. In addition, in the reprogrammed TTC466 cells, expression of DKK2 was significantly reduced compared to control (GFP) cells and the opposite was observed in hES cells with EWS-FLI1 expression; a significant increase in expression of DKK2 was observed after induction of expression of the fusion protein. In contrast, no significant difference in DKK1 expression was observed in either model system.

A potential role for DKK2 in the initiation of ESFT has been suggested previously by Miyagawa et al. (2009) who showed that although DKK2 is not expressed in mesenchymal progenitor cells, expression of EWS-ETS fusions in these cells leads to an increase in DKK2 expression. The authors also demonstrated that EWS-ETS fusion proteins directly bind to ETS binding sites in the promoter region of DKK2, thereby activating expression of the gene. This is consistent with my data. However, despite being implicated in the initiation of ESFT, the role of DKK2 in this process is not well understood. In the report by Miyagawa et al. (2009) the authors state that knockdown of DKK2 did not affect cell growth or cell death. However, more recently it has been reported that knockdown of DKK2 in ESFT cells reduced cell migration *in vitro* and also reduced tumour growth and lung metastases when

cells were injected subcutaneously into mice (Hauer et al. 2013). In addition, DKK2 knockdown impaired differentiation into chondrogenic and osteogenic lineages and reduced migration to and infiltration into bone when injected into the tail vein of mice. This suggests that DKK2 may reprogram cells from neuronal to chondro-osseous differentiation. Interestingly, DKK2 has been shown to have a role in terminal osteoblast differentiation (Li et al. 2005), therefore aberrant expression of DKK2 may disrupt the normal differentiation of MSCs during ESFT initiation.

Although DKK2 has been implicated as being important in the initiation of ESFT, only one previous study has linked this to canonical Wnt signalling. The DKK family of secreted proteins are generally considered to inhibit Wnt signalling by binding and sequestering the Wnt co-receptors LRP5/6 (Mao et al. 2001, Semënov et al. 2001). However, DKK2 has been shown to either activate or inhibit Wnt signalling, depending on the cellular context (Niehrs 2006). It has been suggested that in ESFT the latter may be true as it was demonstrated that knockdown of DKK2 in cell lines results in a decrease in canonical Wnt signalling target genes such as cyclin D1, LEF1, ID2 and Jun (Hauer et al. 2013). In my study using the inducible system I have observed an increase in DKK2 mRNA expression, and also an increase in canonical Wnt signalling. However, I cannot conclude from my data whether the increase in Wnt signalling is direct, indirect, or independent of the increase in DKK2 expression. In future experiments an initial step would be to confirm that DKK2 expression is changed at the protein level in my model systems. To confirm that DKK2 is responsible for activating canonical Wnt signalling, it would be necessary to inhibit DKK2 and measure the effect this has on canonical Wnt signalling activity using the luciferase reporter system. We plan to investigate this in collaboration with Dr Guenther Richter from the Functional Genomics and Transplantation Biology Group in Munster, Germany who has developed ESFT cell lines with DKK2 knock-down (Hauer et al. 2013).

Interestingly, expression of DKK4 was also significantly different in both model systems utilised in this study. DKK4 mRNA expression was increased in reprogrammed TTC466 cells and decreased in hES cells with EWS-FLI1 expression, suggesting that repression of DKK4 expression may also be an important step in ESFT initiation. Expression of DKK4 has not previously been reported in ESFT. However it has been recently reported that DKK4 functions as an inhibitor of osteoblastogenesis (Hiramitsu et al. 2013), therefore it would also be of interest to investigate the role of this DKK family member in ESFT initiation and in the activation of canonical Wnt signalling.

7.3 Noncanonical Wnt signalling in ESFT

My original hypothesis was that the noncanonical Wnt signalling pathway is important in ESFT progression through its role in promoting metastasis and invasion. Interestingly, noncanonical Wnt signalling (specifically the Ca^{2+} pathway) has been shown to inhibit the canonical Wnt signalling pathway (Ishitani et al. 2003, Ishitani et al. 1999), and therefore Wnt5A has been described as being tumour suppressive in colorectal cancer (Ying et al. 2008), thyroid cancer (Kremenevskaja et al. 2005) and myeloid leukaemia (Ying et al. 2007, Yuan et al. 2011). However, in my studies, inhibition of the canonical pathway was not evident in either the ESFT cell lines or model systems when treated with Wnt5A, as measured using the luciferase reporter assay. That said, interestingly, the cell lines with the highest level of endogenous active Rac1 expression (indicative of active noncanonical Wnt signalling) had the lowest levels of canonical Wnt signalling, as measured using the GFP and luciferase reporter assays. Therefore I cannot exclude the hypothesis that noncanonical Wnt signalling, activated by endogenous Wnt5A or other noncanonical ligands such as Wnt4 and/or Wnt11, could be acting to inhibit the canonical Wnt signalling pathway in some cell lines.

Developing assays to measure the noncanonical Wnt signalling pathway was more challenging compared to the canonical pathway, since in noncanonical Wnt signalling there is no accepted key mediator, such as β-catenin which can easily be detected and quantified. In this study I therefore developed assays to detect the active form of Rac1 and Cdc42, effector proteins in the PCP and Ca^{2+} pathways, respectively. A pull-down assay was employed to detect the active, GTP-bound forms of these proteins. Although basal levels of active Rac1 could be detected in some ESFT cell lines, this was not consistently increased with the addition of recombinant Wnt5A. Furthermore, basal levels of active Cdc42 were extremely low in ESFT cell lines, although this probably reflects the fact that total levels of Cdc42 were also low. In the inducible model system, expression of active Rac1 was not increased in hES cells after EWS-FLI1 was induced. However, basal levels of active Cdc42 did appear to be increased, although this was difficult to quantify since total levels of Cdc42 were so low. In my hands results from the pull-down assay were highly variable, consistent with observations from my colleagues (Dr Georgia Mavria, personal communication). In addition, this assay is not very sensitive meaning that subtle changes in levels of active Rac1/Cdc42 may have been missed. Pull-down assays are the most commonly used method to detect activation of small GTPases such as Rac1 and Cdc42. However, newer technologies such as FRET could be employed in future studies to more

accurately quantify the activation of Rac1/Cdc42 and also observe this activation in single cells rather than whole cell populations.

Supporting the hypothesis that noncanonical Wnt signalling may be activated during the initiation of ESFT, hES cells with EWS-FLI1 expression showed significantly increased migration *in vitro,* along with increased mRNA expression of the noncanonical Wnt ligands Wnt5A and Wnt4 (Bernard et al. 2008). However, since many of the downstream targets of EWS-FLI1 have previously been shown to increase migration such as CD99 and caveolin-1 (Sáinz-Jaspeado et al. 2010, Kreppel et al. 2006) it was not possible in this study to demonstrate that the increase in migration was due to the activation of noncanonical Wnt signalling. That said, the fact that recombinant Wnt5A increased migration of these cells suggests that noncanonical Wnt signalling may have a role in this process.

As previously discussed, the phenotype of hES cells changed dramatically when EWS-FLI1 was expressed and it is possible that the noncanonical Wnt signalling pathway is important in this process. Noncanonical Wnt signalling, specifically Wnt5A, has been shown to have a role in EMT in ovarian (Qi et al. 2014), pancreatic (Bo et al. 2013) and gastric (Kanzawa et al. 2013) cancers. Noncanonical Wnt signalling is also known to mediate changes in the cytoskeleton through the PCP pathway. Interestingly an increase in Wnt4 expression has been described previously in hES cells differentiated to a neuronal lineage (Elizalde et al. 2011). Therefore the increased expression of Wnt4 in hES cells with EWS-FLI1 expression supports the hypothesis that the fusion protein is responsible for the neuronal characteristics of ESFT.

I originally hypothesised that the noncanonical Wnt signalling pathway may be more important during disease progression and in the process of metastasis. In support of this, Wnt5A expression has previously been reported to be higher in metastatic compared to localised ESFT tumour samples, and exogenous Wnt5A protein shown to increase the migration of ESFT cell lines (Jin et al. 2012). Although I have investigated the effect of Wnt5A on ESFT migration, this thesis has primarily focussed on Wnt signalling in the initiation of ESFT, rather than progression. However a mesenchymal phenotype has been shown to be important for the metastasis of ESFT (Wiles et al. 2013), therefore further understanding of the factors driving the morphological change in hES cells with EWS-FLI1 expression would be important to increase our understanding of ESFT metastasis. Future work could attempt to determine the role of Wnt5A and the noncanonical Wnt signalling pathway on the migration of ESFT cell lines, and the effect of inhibition of noncanonical

Wnt signalling on tumour growth and metastasis *in vivo* when cells are injected subcutaneously and into the tail vein of mice.

7.4 Use of model systems to investigate ESFT initiation

My thesis has used two complementary model systems to investigate ESFT initiation. The first system used TTC466 cells which had been reprogrammed to a more primitive state in an attempt to investigate the cell of origin of ESFT. The second system used pluripotent hES cells in which expression of the EWS-FLI1 fusion could be induced driving hES cells towards an ESFT phenotype. It was hypothesised that by comparing the results generated by these two approaches, the role of Wnt signalling in the initiation of ESFT could be better understood.

Using these models of ESFT initiation, greater differences in Wnt signalling were observed in the inducible system compared to in the reprogrammed cells. Although there were considerable changes in the Wnt signalling mRNA profile in reprogrammed (vs. control) cells, this may be because the factors within the reprogramming vector (Oct4, Sox2, c-Myc and Kfl4) are known to regulate components of the Wnt signalling pathway. Importantly, both DKK2 and DKK4 had significantly differential expression in both model systems. This further strengthens the hypothesis that the DKK family of proteins play an important role in the initiation of ESFT (Section 7.2). The basal activity of the canonical Wnt signalling pathway was increased in the inducible system, but was not changed in the reprogrammed cells. In fact, reprogrammed cells showed an increased response to recombinant Wnt3A protein, compared to control cells. This is perhaps surprising. If the hypothesis is correct that canonical Wnt signalling is increased during the initiation of ESFT, one may expect these more primitive cells would have decreased canonical Wnt signalling. However, my results may be confounded somewhat by the fact that reprogrammed (but not control) cells were cultured in mTeSR®1, which functions to maintain the self-renewal and pluripotency of stem cells (Sun et al. 2009, Chen et al. 2011) and may therefore contain factors which increase Wnt signalling (discussed in Section 5.4). In addition, my hypothesis is that EWS-FLI1 activates canonical Wnt signalling, and reprogrammed cells still express a EWS-ETS fusion protein. It might therefore seem attractive to knock-down expression of the fusion in reprogrammed cells and investigate the effect of this on Wnt signalling. However, these studies may be very challenging as these reprogrammed cells may still depend on the expression of the fusion protein and knock-down may lead to cell death.

A potentially important fact to note is that the inducible system utilised in this study models the effect of EWS-FLI1 expression, whereas the TTC466 (parental reprogrammed) cells contain the EWS-ERG fusion. Interestingly, TTC466 cells had lower basal levels of canonical Wnt signalling, as measured by the GFP and luciferase reporter plasmids, compared to the other ESFT cell lines which all have a EWS-FLI1 fusion. This suggests that the different fusion proteins may differentially regulate the activity of canonical Wnt signalling. Although some studies using cell lines such as NIH/3T3 cells have concluded that there are some functional differences between EWS-FLI1 and EWS-ERG, other studies using cells which more closely resemble the cell of origin of ESFT, such as mesenchymal progenitor cells, have reported that expression of EWS-FLI1 and EWS-ERG in these cells lead to similar expression profiles (Miyagawa et al. 2008). Furthermore data from the Euro-EWING 99 trial showed that the fusion type does not influence prognosis (Le Deley et al. 2010) and tumours with EWS-FLI1 and EWS-ERG are phenotypically indistinguishable (Ginsberg et al. 1999). We might therefore reasonably expect there to be no difference in hES cells expressing EWS-FLI1 and EWS-ERG, justifying the comparison between the induced and reprogrammed models I have made. Nevertheless it would be interesting to investigate the effect of EWS-ERG expression in hES cells to determine if this fusion type has an effect on Wnt signalling.

The use of *in vitro* model systems is essential to further elucidate the process of ESFT initiation. Of the two model systems used in this study the inducible system is potentially most useful as there are no OSCK factors expressed which could potentially have confounding effects on Wnt signalling. In addition, the effect of EWS-FLI1 can be directly measured by inducing expression of this (and potentially other) fusion proteins. The use of model systems is especially important in the case of ESFT where the cell of origin is not known, and where unlike other cancers such as breast and colorectal, there are no known precursor lesions that can be examined. Research in ESFT is also hampered by the lack of a genetic EWS-FLI1 mouse model that accurately recapitulates ESFT without the necessity for additional mutations (Lin et al. 2008, Kovar et al. 2012). My studies have demonstrated that although there are some drawbacks, model systems can provide useful data and there are opportunities to develop these systems further in the future to continue to characterise the process of ESFT initiation, in particular to investigate the impact of genetic and environmental factors on ESFT initiation, and to identify treatments which may prevent relapse (Section 7.6).

7.5 Biological and clinical significance

The data presented in this thesis was all generated using ESFT cell lines or models developed from ESFT or hES cell lines which have been in culture for a number of years, although cells with low passage numbers were used where possible. It is well recognised that cell lines, especially cancer cell lines that may be genetically unstable, will adapt over time when maintained *in vitro* ultimately leading to populations of cells which may differ dramatically to those found in the primary tumours (Schneider and Kulesz-Martin 2004). In the case of the hES cells, although cells with low passage numbers were originally utilised, to generate cells which contained the inducible expression system and luciferase reporter, a number of transfections (including lentiviral infections) and subsequent antibiotic selections were performed. This meant that it was inevitable that cells with higher passage numbers had to be used for the Wnt signalling assays. Although hES cells are karyotypically normal, it has been shown that after 30 passages culture adaptation can occur leading to changes in karyotypes (Amps et al. 2011). In all cases, the selection of cell lines which contained the reporter plasmid using antibiotics meant that the cell lines studied were a subpopulation, which may not be representative of the entire cell population. It would therefore be valuable to repeat my experiments with different clones to confirm the generality of my results.

In this study, my data suggested that the ESFT cell lines may be predominantly canonical or noncanonical. However, as mentioned previously, these cells have been in culture for many years meaning they may not accurately represent the activity of Wnt signalling in the original tumour. Future studies could be performed using primary cell lines established directly from fresh tumour samples to investigate the activity of canonical and noncanonical Wnt signalling in cells which will more closely resemble the tumour *in vivo.* Although primary cell lines are challenging to work with as they are difficult to transfect and have a propensity to senesce, preliminary data has shown that primary ESFT cells can be transduced using lentiviral plasmids making this a potentially exciting avenue for future work. That said, even primary cell lines that are able to grow in *in vitro* culture conditions may not accurately reflect the *in vivo* situation, especially as the role of additional supporting tumour and normal cells is not considered.

It would therefore be important to investigate Wnt signalling in primary tumour tissue. It would be possible to examine the expression of components of the Wnt signalling pathway, identified as potentially important in the initiation of tumour growth, in ESFT sections by immunohistochemistry (IHC) in order to confirm some of the findings of this

study. A commonly used method to investigate activation of canonical Wnt signalling in tumours is to probe for β-catenin and examine its subcellular localisation. Importantly, however it has previously been reported that β-catenin could not be detected in the cytoplasm or the nucleus of ESFT patient samples (Üren et al. 2004). It would therefore be of interest to investigate β-catenin localisation in patient samples using the antibody employed in my study. However, as my results have demonstrated, levels of nuclear and/or nonphosphorylated β-catenin do not always correlate with levels of activated canonical Wnt signalling as measured using a reporter assay, therefore the functional activity of the canonical Wnt signalling pathway could not be determined using this method. Furthermore, quantifying the expression of Wnt ligands and receptors in tumour samples may not be any more informative since the activation of downstream signalling pathways upon Wnt ligand binding has been shown to be dependent on the cellular context rather than the specific ligands and receptors that are expressed. In this study I did not investigate the genetic status of the ESFT cell lines. Recently, using whole-genome sequencing of over 100 ESFT tumours, it has been shown that there are very few recurring mutations found in tumour samples (Tirode et al. 2014). Specifically, mutations in *CTNNB1* (β-catenin) have been shown to be very rare in ESFT (Shukla et al. 2012). Nevertheless, in future, primary ESFT cells could be sequenced to ascertain if any mutations in Wnt signalling components exist, and if this correlates with changes in the activity of the pathway(s). Functional assays such as those I have optimised in this study would still be required to definitively measure Wnt signalling activity in ESFT.

In this study I have demonstrated that canonical and very likely noncanonical Wnt signalling pathways are activated upon expression of EWS-FLI1. An important area of future work would be to understand the biological significance of this activation and what role (if any) Wnt signalling has in the tumorigenesis of ESFT. In the case of canonical Wnt signalling, treatment with Wnt3A did not increase the proliferation of ESFT cell lines, reprogrammed cells or hES cells with EWS-FLI1 expression. This is consistent with previous reports (Üren et al. 2004) and the observation that in ESFT cell lines no increase in cyclin D1 was observed after treatment with Wnt3A. To provide further evidence as to what effect canonical Wnt signalling has on ESFT cells it would be possible to perform large-scale expression profiling of the known targets of canonical Wnt signalling using RNAseq. However this would be time consuming and expensive and would still not provide direct evidence as to the biological effect of Wnt signalling in ESFT cells. Therefore it would be necessary to both activate and inhibit canonical Wnt signalling in ESFT cells to elucidate

what biological effect the observed activation of Wnt signalling is having during ESFT initiation (Section 7.6).

7.6 Wnt signalling inhibition

In order to validate the main results of this study in future work it would be necessary to inhibit Wnt signalling in ESFT cell lines and in my model systems. Many studies have used recombinant endogenous inhibitors of Wnt signalling such as the DKK and sFRP families of proteins in order to inhibit the pathways. However, as discussed, the DKK family have been suggested to be potentially important in ESFT initiation therefore would not be suitable to use as potential inhibitors in these studies. It has also been shown that the sFRP family members can either activate or inhibit Wnt signalling depending on the cellular context (Anastas and Moon 2013). As an alternative, a number of inhibitors of canonical Wnt signalling have been developed. For example iCRT 14 (Gonsalves et al. 2011) and PNU 74654 (Trosset et al. 2006) which both act by inhibiting the interaction between β-catenin and TCF4. Other inhibitors that target other parts of the canonical pathway such as XAV939, which enhances Axin stability through tankyrase inhibition (Huang et al. 2009), have also been developed. To decipher which pathways within noncanonical Wnt signalling are important, specific inhibitors could be used. For example, the Ca^{2+} pathway could be inhibited using BAPTA-AM, a Ca^{2+} chelator or Go6983, an inhibitor of PKC. The PCP pathway could also be inhibited using the JNK-specific inhibitor SP600125. However a limitation of these agents is that they are not very specific and often affect other signalling pathways, therefore it would not be possible to directly link any downstream effects observed to Wnt signalling. A better approach would be to inhibit, using RNAi knockdown, and also overexpress key components which I have identified as being important in the initiation of ESFT, such as DKK2 and Wnt5A. Subsequent phenotypic assay such as proliferation, cell cycle analysis, colony formation and migration could then be performed to elucidate what biological effect the observed activation of Wnt signalling is having during ESFT initiation.

6.4.1 Wnt signalling inhibition in the treatment of ESFT

Although understanding the initiation of ESFT is an important goal, clinically, patients tend to present with advanced and often metastatic disease. ESFT display an aggressive phenotype and up to 50% of patients without clinically detectable metastasis at diagnosis will relapse with distant metastatic disease after surgery if systemic chemotherapy is not given. In addition, despite aggressive treatment the tumour recurs in 30-40% of patients.

Therefore there is a real need to understand the cell or cells that are responsible for this aggressive behaviour. Recently CICs have been identified from ESFT, on the basis of CD133 expression (Suvà et al. 2009). Work in our laboratory has been focussed on characterising CICs from ESFT and our data has revealed that additional markers are required to isolate true CICs. Future studies in our laboratory will attempt to isolate CICs from primary tumour samples, and these cells could also be characterised in terms of Wnt signalling activity. If it is demonstrated that ESFT CICs have active Wnt signalling this could be a target for development of new therapeutics for the treatment of ESFT. Activation of canonical Wnt signalling has been implicated in the maintenance of leukaemic (Jamieson et al. 2004), colorectal cancer (Barker et al. 2009) and breast cancer (Hallett et al. 2012) initiating cells. Unfortunately, direct targeting of Wnt signalling *in vivo* has proven difficult. This is in part due to the lack of specific targets and the redundancy of many of the pathway components. The effectiveness and safety of small molecule inhibitors such as iCRT 14 and PNU 74654 has not yet been evaluated in clinical trials. However other non-specific compounds for example non-steroidal anti-inflammatory drugs (NSAIDS) such as aspirin, and the COX2 inhibitor celecoxib, have been shown to inhibit canonical Wnt signalling in colorectal cancer cells (Dihlmann et al. 2001, Tuynman et al. 2008). Interestingly celecoxib has been shown to inhibit invasion and migration of ESFT *in vitro* (Barlow et al. 2012). In addition, a phase II study investigating celecoxib as an anti-angiogenic agent in ESFT reported that the drug was tolerated and improved event free survival for patients with pulmonary metastasis (Felgenhauer et al. 2013). Therefore, if *in vitro* analysis suggests these agents inhibit growth and/or metastasis of ESFT CICs isolated from tumour samples, my data would support further investigation of these agents to be given to prevent metastasis and/or tumour relapse.

My data has indicated that the DKK family of proteins may have an important role in the initiation of ESFT. Interestingly this family of proteins have been shown to play a role in other bone disorders. For example, DKK1 has been shown to play an important role in myeloma bone disease (Tian et al. 2003) and Paget's disease of the bone (Polyzos et al. 2009). Therefore many DKK1 antibodies have been generated and have shown to be effective in treating bone disease in preclinical models (Pozzi et al. 2013, Zhou et al. 2013) (Miao et al. 2013). If future studies demonstrate that DKK2 is indeed important in the development and/or progression of ESFT then it is likely that anti-DKK2 antibodies could also be development and may prove to be effective in preventing relapse and/or metastasis.

7.7 Final conclusions and future work

In conclusion, the studies described in this thesis have provided interesting data to indicate that activation of the canonical and also noncanonical Wnt signalling pathways may be an important step in the initiation of ESFT. These data could provide further understanding of how ESFT arise, as well as informing future work to develop more effective and less toxic treatment for patients with ESFT, especially those with metastatic disease for whom current treatment options are lacking.

Future studies should specifically investigate:

- **If EWS-FLI1 activates canonical Wnt signalling in hES cells differentiated to a mesenchymal lineage.** To confirm that my results are representative of the events which occur in the putative ESFT-cell of origin, MSCs, it would be important to investigate Wnt signalling activation in mesenchymal cells.
- **What effect inhibiting Wnt signalling has on cells with inducible EWS-FLI1 expression.** To confirm that Wnt signalling is responsible for the phenotypic differences observed when EWS-FLI1 is expressed, it would be important to inhibit Wnt signalling during this process.
- **What effect DKK2 and DKK4 knockdown and/or overexpression have on canonical Wnt signalling in ESFT cell lines, and in cells with inducible EWS-FLI1 expression.** Since my data has suggested that both DKK2 and DKK4 may be important in the initiation of ESFT, it would also be important to both inhibit and overexpress these proteins in cell lines and in my model systems to investigate the phenotypic effects, and the effect on the expression of other components of the Wnt signalling pathway, in order to further investigate what role DKK2 and DKK4 have in this process.
- **If the noncanonical Wnt signalling pathway is responsible for the increased migration observed in cells with inducible EWS-FLI1 expression.** Although an increase in migration was observed when EWS-FLI1 was induced in hES cells it was not possible to directly link this to an increase in noncanonical Wnt signalling. Therefore it would be important to inhibit and overexpress Wnt5A and investigate the effect of this on the migration of inducible cells, in order to ascertain if the noncanonical Wnt signalling pathway is important in this observed phenotype.

- **The activity of canonical and noncanonical Wnt signalling in primary cell lines generated from ESFT samples.** Since my study has only used established cell lines, which may have adapted to *in vitro* culture, it would be important to confirm my results in primary ESFT cell lines. It would also be interesting to sequence primary tumours to determine if any of the components of the Wnt signalling pathway are mutated in ESFT, and what effects this has on the activity of the pathway.
- **The activity of Wnt signalling in CICs isolated from primary ESFT samples, and the effect of Wnt signalling inhibitors on these cells.** CICs have recently been identified in ESFT and they may be responsible for disease relapse and resistance to therapy. Therefore determining if Wnt signalling is active in CICs derived from ESFT, and whether inhibition of the pathway(s) can be used to target these cells, is an important avenue for future work.
- **Developing better assays to measure the activity of the noncanonical Wnt signalling pathway.** The lack of informative assays to measure the noncanonical Wnt signalling pathway meant that I could not draw definite conclusions about the role of this pathway in ESFT initiation. Therefore it would be important to improve the current assays used to measure active Rac1/Cdc42 for example using FRET, and also to develop assays to measure other downstream components of the noncanonical pathways such as a reporter to measure NFAT-mediated activation of gene transcription, and assays to detect activation of PKC and JNK.

Appendix

Sequencing of pLenti 7xTcf Ffluc SV40-Hygro (7TFH)

Primer 1: 5'- CGTGGATTACGTCGCCAG-3'

CCGTGTAATTCTAGAGTCGATCGACCCTGTGGAATGTGTGTCAGTTAGGGTGTGGAAAGTCCCCAG
GCTCCCCAGCAGGCAGAAGTATGCAAAGCATGCATCTCAATTAGTCAGCAACCAGGTGTGGAAAG
TCCCCAGGCTCCCCAGCAGGCAGAAGTATGCAAAGCATGCATCTCAATTAGTCAGCAACCATAGTC
CCGCCCCTAACTCCGCCCATCCCGCCCCTAACTCCGCCCAGTTCCGCCCATTCTCCGCCCCATGGCTG
ACTAATTTTTTTTATTTATGCAGAGGCCGAGGCCGCCTCGGCCTCTGAGCTATTCCAGAAGTAGTGA
GGAGGCTTTTTTGGAGGCCTAGGCTTTTGCAAAAAGCTTGCCAGCTGGGGCGCCCTCTGGTAAGG
TTGGGAAGCCCTGCAGATCTGATCCCGGGGGGCAATGAGATATGAAAAAGCCTGAACTCACCGCG
ACGTCTGTCGAGAAGTTTCTGATCGAAAAGTTCGACAGCGTCTCCGACCTGATGCAGCTCTCGGAG
GGCGAAGAATCTCGTGCTTTCAGCTTCGATGTAGGAGGGCGTGGATATGTCCTGCGGGTAAATAG
CTGCGCCGATGGTTTCTACAAAGATCGTTATGTTTATCGGCACTTTGCATCGGCCGCGCTCCCGATT

Primer 2: 5' – CCAGCAGGCAGAAGTATG-3'

AGTGGAAACCGACGCCCCAGCACTCGTCCGAGGGCAAAGGAATAGAGTAGATGCCGACCGGGAT
CTATCGTCGACAATCAACCTCTGGATTACAAAATTTGTGAAAGATTGACTGGTATTCTTAACTATGT
TGCTCCTTTTACGCTATGTGGATACGCTGCTTTAATGCCTTTGTATCATGCTATTGCTTCCCGTATGG
CTTTCATTTTCTCCTCCTTGTATAAATCCTGGTTGCTGTCTCTTTATGAGGAGTTGTGGCCCGTTGTC
AGGCAACGTGGCGTGGTGTGCACTGTGTTTGCTGACGCAACCCCCACTGGTTGGGGCATTGCCAC
CACCTGTCAGCTCCTTTCCGGGACTTTCGCTTTCCCCCTCCCTATTGCCACGGCGGAACTCATCGCCG
CCTGCCTTGCCCGCTGCTGGACAGGGGCTCGGCTGTTGGGCACTGACAATTCCGTGGTGTTGTCGG
GGAAGCTGACGTCCTTTCCATGGCTGCTCGCCTGTGTTGCCACCTGGATTCTGCGCGGGACGTCCT
TCTGCTACGTCCCTTCGGCCCTCAATCCAGCGGACCTTCCTTCCCGCGGCCTGCTGCCGGCTCTGCG
GCCTCTTCCGCGTCTTCGCCTTCGCCCTCAGACGAGTCGGATCTCCCTTTGGGCCGCCTCCCCG

Primer 3: 5' - CACGCCACGTTGCCTGAC-3'

GCAACATAGTTAAGAATACCAGTCAATCTTTCACAAATTTTGTAATCCAGAGGTTGATTGTCGACGA
TAGATCCCGGTCGGCATCTACTCTATTCCTTTGCCCTCGGACGAGTGCTGGGGCGTCGGTTTCCACT
ATCGGCGAGTACTTCTACACAGCCATCGGTCCAGACGGCCGCGCTTCTGCGGGCGATTTGTGTACG
CCCGACAGTCCCGGCTCCGGATCGGACGATTGCGTCGCATCGACCCTGCGCCCAAGCTGCATCATC
GAAATTGCCGTCAACCAAGCTCTGATAGAGTTGGTCAAGACCAATGCGGAGCATATACGCCCGGA
GCCGCGGCGATCCTGCAAGCTCCGGATGCCTCCGCTCGAAGTAGCGCGTCTGCTGCTCCATACAAG
CCAACCACGGCCTCCAGAAGAAGATGTTGGCGACCTCGTATTGGGAATCCCCGAACATCGCCTCGC
TCCAGTCAATGACCGCTGTTATGCGGCCATTGTCCGTCAGGACATTGTTGGAGCCGAAATCCGCGT
GCACGAGGTGCCGGACTTCGGGGCAGTCCTCGGCCCAAAGCATCAGCTCATCGAGAGCCTGCGCG
ACGGACGCACTGACGGTGTCGTCCATCACAGTTTGCCAGTGATACACATGGGGATCAGCAATCGC

7TFP

HYRGO

References

Akkina, R. K., Walton, R. M., Chen, M. L., Li, Q. X., Planelles, V. and Chen, I. S. (1996) 'High-efficiency gene transfer into CD34+ cells with a human immunodeficiency virus type 1-based retroviral vector pseudotyped with vesicular stomatitis virus envelope glycoprotein G', *Journal of Virology,* 70(4), 2581-5.

Akopian, V., Andrews, P., Beil, S., Benvenisty, N., Brehm, J., Christie, M., Ford, A., Fox, V., Gokhale, P., Healy, L., Holm, F., Hovatta, O., Knowles, B., Ludwig, T., McKay, R. G., Miyazaki, T., Nakatsuji, N., Oh, S. W., Pera, M., Rossant, J., Stacey, G. and Suemori, H. (2010) 'Comparison of defined culture systems for feeder cell free propagation of human embryonic stem cells', *In Vitro Cellular & Developmental Biology - Animal,* 46(3-4), 247-258.

Al-Hajj, M., Wicha, M. S., Benito-Hernandez, A., Morrison, S. J. and Clarke, M. F. (2003) 'Prospective identification of tumorigenic breast cancer cells', *Proc Natl Acad Sci U S A,* 100(7), 3983-8.

Albini, A., Melchiori, A., Garofalo, A., Noonan, D. M., Basolo, F., Taraboletti, G., Chader, G. J. and Gavazzi, R. (1992) 'Matrigel promotes retinoblastoma cell growth in vitro and in vivo', *Int J Cancer,* 52(2), 234-40.

Albini, A. and Noonan, D. M. (2010) 'The ‘chemoinvasion’ assay, 25 years and still going strong: the use of reconstituted basement membranes to study cell invasion and angiogenesis', *Current Opinion in Cell Biology,* 22(5), 677-689.

Alison, M. R., Lin, W.-R., Lim, S. M. L. and Nicholson, L. J. (2012) 'Cancer stem cells: In the line of fire', *Cancer Treatment Reviews,* 38(6), 589-598.

Ambros, I. M., Ambros, P. F., Strehl, S., Kovar, H., Gadner, H. and Salzer-Kuntschik, M. (1991) 'MIC2 is a specific marker for ewing's sarcoma and peripheral primitive neuroectodermal tumors. Evidence for a common histogenesis of ewing's sarcoma and peripheral primitive neuroectodermal tumors from MIC2 expression and specific chromosome aberration', *Cancer,* 67(7), 1886-1893.

Amit, M. (2000) 'Clonally derived human embryonic stem cell lines maintain pluripotency and proliferative potential for prolonged periods of culture', *Dev. Biol.,* 227, 271-278.

Amit, S., Hatzubai, A., Birman, Y., Andersen, J. S., Ben-Shushan, E., Mann, M., Ben-Neriah, Y. and Alkalay, I. (2002) 'Axin-mediated CKI phosphorylation of beta-catenin at Ser 45: a molecular switch for the Wnt pathway', *Genes & Development,* 16(9), 1066-76.

Aoki, K. and Matsuda, M. (2009) 'Visualization of small GTPase activity with fluorescence resonance energy transfer-based biosensors', *Nat. Protocols,* 4(11), 1623-1631.

Barker, L. M., Pendergrass, T. W., Sanders, J. E. and Hawkins, D. S. (2005) 'Survival after recurrence of Ewing's sarcoma family of tumors', *J Clin Oncol,* 23(19), 4354-62.

Benard, V., Bohl, B. P. and Bokoch, G. M. (1999) 'Characterization of Rac and Cdc42 Activation in Chemoattractant-stimulated Human Neutrophils Using a Novel Assay for Active GTPases', *Journal of Biological Chemistry,* 274(19), 13198-13204.

Bernstein, M., Kovar, H., Paulussen, M., Randall, R. L., Schuck, A., Teot, L. A. and Juergensg, H. (2006) 'Ewing's Sarcoma Family of Tumors: Current Management', *The Oncologist,* 11(5), 503-519.

Blanc, E., Roux, G. L., Benard, J. and Raguenez, G. (2005) 'Low expression of Wnt-5a gene is associated with high-risk neuroblastoma', *Oncogene,* 24(7), 1277-83.

Blauwkamp, T. A., Nigam, S., Ardehali, R., Weissman, I. L. and Nusse, R. (2012) 'Endogenous Wnt signalling in human embryonic stem cells generates an equilibrium of distinct lineage-specified progenitors', *Nat Commun,* 3, 1070.

Boland, G. M., Perkins, G., Hall, D. J. and Tuan, R. S. (2004) 'Wnt 3a promotes proliferation and suppresses osteogenic differentiation of adult human mesenchymal stem cells', *Journal of Cellular Biochemistry,* 93(6), 1210-1230.

Bone, H. G., Hosking, D., Devogelaer, J.-P., Tucci, J. R., Emkey, R. D., Tonino, R. P., Rodriguez-Portales, J. A., Downs, R. W., Gupta, J., Santora, A. C. and Liberman, U. A. (2004) 'Ten Years' Experience with Alendronate for Osteoporosis in Postmenopausal Women', *New England Journal of Medicine,* 350(12), 1189-1199.

Bonnet, D. and Dick, J. E. (1997) 'Human acute myeloid leukemia is organized as a hierarchy that originates from a primitive hematopoietic cell', *Nat Med,* 3(7), 730-7.

Boutros, M., Paricio, N., Strutt, D. I. and Mlodzik, M. (1998) 'Dishevelled Activates JNK and Discriminates between JNK Pathways in Planar Polarity and wingless Signaling', *Cell,* 94(1), 109-118.

Bradley, R. S. and Brown, A. M. (1990) 'The proto-oncogene int-1 encodes a secreted protein associated with the extracellular matrix', *EMBO J,* 9(5), 1569-75.

Braun, B. S., Frieden, R., Lessnick, S. L., May, W. A. and Denny, C. T. (1995) 'Identification of target genes for the Ewing's sarcoma EWS/FLI fusion protein by representational difference analysis', *Molecular and Cellular Biology,* 15(8), 4623-30.

Braunreiter, C. L., Hancock, J. D., Coffin, C., Boucher, K. M. and Lessnick, S. L. (2006) 'Expression of EWS-ETS Fusions in NIH3T3 Cells Reveals Significant Differences to Ewing's Sarcoma', *Cell Cycle,* 5(23), 2753-2759.

Brenner, J. C., Feng, F. Y., Han, S., Patel, S., Goyal, S. V., Bou-Maroun, L. M., Liu, M., Lonigro, R., Prensner, J. R., Tomlins, S. A. and Chinnaiyan, A. M. (2012) 'PARP-1 Inhibition as a Targeted Strategy to Treat Ewing's Sarcoma', *Cancer Research,* 72(7), 1608-1613.

Brownhill, S. C., Taylor, C. and Burchill, S. A. (2007) 'Chromosome 9p21 gene copy number and prognostic significance of p16 in ESFT', *Br J Cancer,* 96(12), 1914-23.

Burbelo, P. D., Drechsel, D. and Hall, A. (1995) 'A conserved binding motif defines numerous candidate target proteins for both Cdc42 and Rac GTPases', *J Biol Chem,* 270(49), 29071-4.

Burchill, S. A. (2008) 'Molecular abnormalities in Ewings sarcoma', *Expert Review of Anticancer Therapy,* 8, 1675-1687.

Burkhalter, R. J., Symowicz, J., Hudson, L. G., Gottardi, C. J. and Stack, M. S. (2011) 'Integrin Regulation of β-Catenin Signaling in Ovarian Carcinoma', *Journal of Biological Chemistry,* 286(26), 23467-23475.

Burns, J. C., Friedmann, T., Driever, W., Burrascano, M. and Yee, J. K. (1993) 'Vesicular stomatitis virus G glycoprotein pseudotyped retroviral vectors: concentration to very high titer and efficient gene transfer into mammalian and nonmammalian cells', *Proceedings of the National Academy of Sciences,* 90(17), 8033-8037.

Camilli, T. C. and Weeraratna, A. T. (2010) 'Striking the target in Wnt-y conditions: Intervening in Wnt signaling during cancer progression', *Biochemical Pharmacology,* 80(5), 702-711.

Carette, J. E., Pruszak, J., Varadarajan, M., Blomen, V. A., Gokhale, S., Camargo, F. D., Wernig, M., Jaenisch, R. and Brummelkamp, T. R. (2010) 'Generation of iPSCs from cultured human malignant cells', *Blood,* 115(20), 4039-4042.

Carmon, K. S. and Loose, D. S. (2008) 'Secreted Frizzled-Related Protein 4 Regulates Two Wnt7a Signaling Pathways and Inhibits Proliferation in Endometrial Cancer Cells', *Molecular Cancer Research,* 6(6), 1017-1028.

Cavallo, R. A., Cox, R. T., Moline, M. M., Roose, J., Polevoy, G. A., Clevers, H., Peifer, M. and Bejsovec, A. (1998) 'Drosophila Tcf and Groucho interact to repress Wingless signalling activity', *Nature,* 395(6702), 604-8.

Chaffer, C. L., Brueckmann, I., Scheel, C., Kaestli, A. J., Wiggins, P. A., Rodrigues, L. O., Brooks, M., Reinhardt, F., Su, Y., Polyak, K., Arendt, L. M., Kuperwasser, C., Bierie, B. and Weinberg, R. A. (2011) 'Normal and neoplastic nonstem cells can spontaneously convert to a stem-like state', *Proceedings of the National Academy of Sciences,* 108(19), 7950-7955.

Chang, E. H., Gonda, M. A., Ellis, R. W., Scolnick, E. M. and Lowy, D. R. (1982) 'Human genome contains four genes homologous to transforming genes of Harvey and Kirsten murine sarcoma viruses', *Proceedings of the National Academy of Sciences,* 79(16), 4848-4852.

Cheah, P. Y., Choo, P. H., Yao, J., Eu, K. W. and Seow-Choen, F. (2002) 'A survival–stratification model of human colorectal carcinomas with β-catenin and p27kip1', *Cancer,* 95(12), 2479-2486.

Chen, G., Gulbranson, D. R., Hou, Z., Bolin, J. M., Ruotti, V., Probasco, M. D., Smuga-Otto, K., Howden, S. E., Diol, N. R., Propson, N. E., Wagner, R., Lee, G. O., Antosiewicz-Bourget, J., Teng, J. M. and Thomson, J. A. (2011) 'Chemically defined conditions for human iPSC derivation and culture', *Nat Methods,* 8(5), 424-9.

Chen, S., Xu, Y., Chen, Y., Li, X., Mou, W., Wang, L., Liu, Y., Reisfeld, R. A., Xiang, R., Lv, D. and Li, N. (2012) '*SOX2* Gene Regulates the Transcriptional Network of Oncogenes and Affects Tumorigenesis of Human Lung Cancer Cells', *PLoS ONE,* 7(5), e36326.

Choi, S.-C. and Han, J.-K. (2002) 'Xenopus Cdc42 Regulates Convergent Extension Movements during Gastrulation through Wnt/Ca2+ Signaling Pathway', *Developmental Biology,* 244(2), 342-357.

Clevers, H. (2006) 'Wnt/²-Catenin Signaling in Development and Disease', *Cell,* 127(3), 469-480.

Clevers, H. (2006) 'Wnt/beta-catenin signaling in development and disease', *Cell,* 127(3), 469-80.

Cole, M. F., Johnstone, S. E., Newman, J. J., Kagey, M. H. and Young, R. A. (2008) 'Tcf3 is an integral component of the core regulatory circuitry of embryonic stem cells', *Genes Dev,* 22(6), 746-55.

Collins, A. T., Berry, P. A., Hyde, C., Stower, M. J. and Maitland, N. J. (2005) 'Prospective identification of tumorigenic prostate cancer stem cells', *Cancer Res,* 65(23), 10946-51.

Cotterill, S. J., Ahrens, S., Paulussen, M., Jürgens, H. F., Voûte, P. A., Gadner, H. and Craft, A. W. (2000) 'Prognostic Factors in Ewing' s Tumor of Bone: Analysis of 975 Patients From the European Intergroup Cooperative Ewing' s Sarcoma Study Group', *Journal of Clinical Oncology,* 18(17), 3108-3114.

Cozzio, A., Passegue, E., Ayton, P. M., Karsunky, H., Cleary, M. L. and Weissman, I. L. (2003) 'Similar MLL-associated leukemias arising from self-renewing stem cells and short-lived myeloid progenitors', *Genes Dev,* 17(24), 3029-35.

Dalton, S. (2013) 'Signaling networks in human pluripotent stem cells', *Current Opinion in Cell Biology,* 25(2), 241-246.

Davidson, K. C., Adams, A. M., Goodson, J. M., McDonald, C. E., Potter, J. C., Berndt, J. D., Biechele, T. L., Taylor, R. J. and Moon, R. T. (2012) 'Wnt/β-catenin signaling promotes differentiation, not self-renewal, of human embryonic stem cells and is repressed by Oct4', *Proceedings of the National Academy of Sciences,* 109(12), 4485-4490.

de Alava, E., Antonescu, C. R., Panizo, A., Leung, D., Meyers, P. A., Huvos, A. G., Pardo-Mindan, F. J., Healey, J. H. and Ladanyi, M. (2000) 'Prognostic impact of P53 status in Ewing sarcoma', *Cancer,* 89(4), 783-92.

de Kok, J. B., Roelofs, R. W., Giesendorf, B. A., Pennings, J. L., Waas, E. T., Feuth, T., Swinkels, D. W. and Span, P. N. (2004) 'Normalization of gene expression measurements in tumor tissues: comparison of 13 endogenous control genes', *Lab Invest,* 85(1), 154-159.

Dejmek, J., Dejmek, A., Säfholm, A., Sjölander, A. and Andersson, T. (2005) 'Wnt-5a Protein Expression in Primary Dukes B Colon Cancers Identifies a Subgroup of Patients with Good Prognosis', *Cancer Research,* 65(20), 9142-9146.

Delattre, O., Zucman, J., Plougastel, B., Desmaze, C., Melot, T., Peter, M., Kovar, H., Joubert, I., de Jong, P., Rouleau, G., Aurias, A. and Thomas, G. (1992) 'Gene fusion with an ETS DNA-binding domain caused by chromosome translocation in human tumours', *Nature,* 359(6391), 162-165.

DeVita, V. T. and Chu, E. (2008) 'A History of Cancer Chemotherapy', *Cancer Research,* 68(21), 8643-8653.

Ding, V. M., Ling, L., Natarajan, S., Yap, M. G., Cool, S. M. and Choo, A. B. (2010) 'FGF-2 modulates Wnt signaling in undifferentiated hESC and iPS cells through activated PI3-K/GSK3beta signaling', *J Cell Physiol,* 225(2), 417-28.

Dissanayake, S. K., Wade, M., Johnson, C. E., O'Connell, M. P., Leotlela, P. D., French, A. D., Shah, K. V., Hewitt, K. J., Rosenthal, D. T., Indig, F. E., Jiang, Y., Nickoloff, B. J., Taub, D. D., Trent, J. M., Moon, R. T., Bittner, M. and Weeraratna, A. T. (2007) 'The Wnt5A/protein kinase C pathway mediates motility in melanoma cells via the inhibition of metastasis suppressors and initiation of an epithelial to mesenchymal transition', *J Biol Chem,* 282(23), 17259-71.

Dong, X., Stothard, P., Forsythe, I. J. and Wishart, D. S. (2004) 'PlasMapper: a web server for drawing and auto-annotating plasmid maps', *Nucleic Acids Res,* 32(Web Server issue), W660-4.

Dravid, G., Ye, Z., Hammond, H., Chen, G., Pyle, A., Donovan, P., Yu, X. and Cheng, L. (2005) 'Defining the Role of Wnt/β-Catenin Signaling in the Survival, Proliferation, and Self-Renewal of Human Embryonic Stem Cells', *Stem Cells,* 23(10), 1489-1501.

Dylla, S. J., Beviglia, L., Park, I.-K., Chartier, C., Raval, J., Ngan, L., Pickell, K., Aguilar, J., Lazetic, S., Smith-Berdan, S., Clarke, M. F., Hoey, T., Lewicki, J. and Gurney, A. L. (2008) 'Colorectal Cancer Stem Cells Are Enriched in Xenogeneic Tumors Following Chemotherapy', *PLoS ONE,* 3(6), e2428.

Ellison, D. W., Onilude, O. E., Lindsey, J. C., Lusher, M. E., Weston, C. L., Taylor, R. E., Pearson, A. D. and Clifford, S. C. (2005) 'β-Catenin Status Predicts a Favorable Outcome in Childhood Medulloblastoma: The United Kingdom Children's Cancer Study Group Brain Tumour Committee', *Journal of Clinical Oncology,* 23(31), 7951-7957.

Endo, K., Ueda, T., Ueyama, J., Ohta, T. and Terada, T. (2000) 'Immunoreactive E-cadherin, alpha-catenin, beta-catenin, and gamma-catenin proteins in hepatocellular carcinoma: relationships with tumor grade, clinicopathologic parameters, and patients' survival', *Hum Pathol,* 31(5), 558-65.

Endo, Y., Beauchamp, E., Woods, D., Taylor, W. G., Toretsky, J. A., Uren, A. and Rubin, J. S. (2008) 'Wnt-3a and Dickkopf-1 stimulate neurite outgrowth in Ewing tumor cells via a Frizzled3- and c-Jun N-terminal kinase-dependent mechanism', *Mol Cell Biol,* 28(7), 2368-79.

Erkizan, H. V., Kong, Y., Merchant, M., Schlottmann, S., Barber-Rotenberg, J. S., Yuan, L., Abaan, O. D., Chou, T.-h., Dakshanamurthy, S., Brown, M. L., Uren, A. and Toretsky, J. A. (2009) 'A small molecule blocking oncogenic protein EWS-FLI1 interaction with RNA helicase A inhibits growth of Ewing's sarcoma', *Nat Med,* 15(7), 750-756.

Ewing, J. (1921) 'Diffuse endothelioma of bone', *Proc NY Pathol Soc,* 21, 17-24.

Fan, F. and Wood, K. V. (2007) 'Bioluminescent assays for high-throughput screening', *Assay Drug Dev Technol,* 5(1), 127-36.

Farr, G. H., 3rd, Ferkey, D. M., Yost, C., Pierce, S. B., Weaver, C. and Kimelman, D. (2000) 'Interaction among GSK-3, GBP, axin, and APC in Xenopus axis specification', *The Journal of cell biology,* 148(4), 691-702.

Fattet, S., Haberler, C., Legoix, P., Varlet, P., Lellouch-Tubiana, A., Lair, S., Manie, E., Raquin, M.-A., Bours, D., Carpentier, S., Barillot, E., Grill, J., Doz, F., Puget, S., Janoueix-Lerosey, I. and

Delattre, O. (2009) 'Beta-catenin status in paediatric medulloblastomas: correlation of immunohistochemical expression with mutational status, genetic profiles, and clinical characteristics', *J Pathol,* 218(1), 86-94.

Faure, S. and Fort, P. (2011) 'Atypical RhoV and RhoU GTPases control development of the neural crest', *Small GTPases,* 2(6), 310-313.

Fernandez, T. d. S., de Souza Fernandez, C., Mencalha, A., #xe9 and Luiz (2013) 'Human Induced Pluripotent Stem Cells from Basic Research to Potential Clinical Applications in Cancer', *BioMed Research International,* 2013, 11.

Fidler, I. J. (2003) 'The pathogenesis of cancer metastasis: the 'seed and soil' hypothesis revisited', *Nat Rev Cancer,* 3(6), 453-458.

Finkelshtein, D., Werman, A., Novick, D., Barak, S. and Rubinstein, M. (2013) 'LDL receptor and its family members serve as the cellular receptors for vesicular stomatitis virus', *Proc Natl Acad Sci U S A,* 110(18), 7306-11.

Flaherty, K. T., Puzanov, I., Kim, K. B., Ribas, A., McArthur, G. A., Sosman, J. A., O'Dwyer, P. J., Lee, R. J., Grippo, J. F., Nolop, K. and Chapman, P. B. (2010) 'Inhibition of Mutated, Activated BRAF in Metastatic Melanoma', *New England Journal of Medicine,* 363(9), 809-819.

Foulds, L. (1954) 'The Experimental Study of Tumor Progression: A Review', *Cancer Research,* 14(5), 327-339.

Friedman, D. L., Whitton, J., Leisenring, W., Mertens, A. C., Hammond, S., Stovall, M., Donaldson, S. S., Meadows, A. T., Robison, L. L. and Neglia, J. P. (2010) 'Subsequent Neoplasms in 5-Year Survivors of Childhood Cancer: The Childhood Cancer Survivor Study', *J Natl Cancer Inst,* 102(14), 1083-1095.

Friend, S. H., Horowitz, J. M., Gerber, M. R., Wang, X. F., Bogenmann, E., Li, F. P. and Weinberg, R. A. (1987) 'Deletions of a DNA sequence in retinoblastomas and mesenchymal tumors: organization of the sequence and its encoded protein', *Proceedings of the National Academy of Sciences,* 84(24), 9059-9063.

Fuerer, C. and Nusse, R. (2010) 'Lentiviral vectors to probe and manipulate the Wnt signaling pathway', *PLoS ONE,* 5(2), e9370.

Garnett, M. J., Edelman, E. J., Heidorn, S. J., Greenman, C. D., Dastur, A., Lau, K. W., Greninger, P., Thompson, I. R., Luo, X., Soares, J., Liu, Q., Iorio, F., Surdez, D., Chen, L., Milano, R. J., Bignell, G. R., Tam, A. T., Davies, H., Stevenson, J. A., Barthorpe, S., Lutz, S. R., Kogera, F., Lawrence, K., McLaren-Douglas, A., Mitropoulos, X., Mironenko, T., Thi, H., Richardson, L., Zhou, W., Jewitt, F., Zhang, T., O/'Brien, P., Boisvert, J. L., Price, S., Hur, W., Yang, W., Deng, X., Butler, A., Choi, H. G., Chang, J. W., Baselga, J., Stamenkovic, I., Engelman, J. A., Sharma, S. V., Delattre, O., Saez-Rodriguez, J., Gray, N. S., Settleman, J., Futreal, P. A., Haber, D. A., Stratton, M. R., Ramaswamy, S., McDermott, U. and Benes, C. H. (2012) 'Systematic identification of genomic markers of drug sensitivity in cancer cells', *Nature,* 483(7391), 570-575.

Gerlinger, M., Rowan, A. J., Horswell, S., Larkin, J., Endesfelder, D., Gronroos, E., Martinez, P., Matthews, N., Stewart, A., Tarpey, P., Varela, I., Phillimore, B., Begum, S., McDonald, N. Q., Butler, A., Jones, D., Raine, K., Latimer, C., Santos, C. R., Nohadani, M., Eklund, A. C.,

Spencer-Dene, B., Clark, G., Pickering, L., Stamp, G., Gore, M., Szallasi, Z., Downward, J., Futreal, P. A. and Swanton, C. (2012) 'Intratumor Heterogeneity and Branched Evolution Revealed by Multiregion Sequencing', *New England Journal of Medicine,* 366(10), 883-892.

Gewirtz, D. (1999) 'A critical evaluation of the mechanisms of action proposed for the antitumor effects of the anthracycline antibiotics adriamycin and daunorubicin', *Biochemical Pharmacology,* 57(7), 727-741.

GLOBOCAN (2014) 'GLOBOCAN 2012: Estimated Cancer Incidence, Mortality and Prevalence Worldwide in 2012', [online], available: [accessed

Gonsalves, F. C., Klein, K., Carson, B. B., Katz, S., Ekas, L. A., Evans, S., Nagourney, R., Cardozo, T., Brown, A. M. C. and DasGupta, R. (2011) 'An RNAi-based chemical genetic screen identifies three small-molecule inhibitors of the Wnt/wingless signaling pathway', *Proceedings of the National Academy of Sciences,* 108(15), 5954-5963.

Gossen, M., Freundlieb, S., Bender, G., Muller, G., Hillen, W. and Bujard, H. (1995) 'Transcriptional activation by tetracyclines in mammalian cells', *Science,* 268(5218), 1766-9.

Grier, H. E. (1997) 'THE EWING FAMILY OF TUMORS: Ewing's Sarcoma and Primitive Neuroectodermal Tumors', *Pediatric Clinics of North America,* 44(4), 991-1004.

Grohar, P. J. and Helman, L. J. (2013) 'Prospects and challenges for the development of new therapies for Ewing sarcoma', *Pharmacol Ther,* 137(2), 216-24.

Grohar, P. J., Woldemichael, G. M., Griffin, L. B., Mendoza, A., Chen, Q.-R., Yeung, C., Currier, D. G., Davis, S., Khanna, C., Khan, J., McMahon, J. B. and Helman, L. J. (2011) 'Identification of an Inhibitor of the EWS-FLI1 Oncogenic Transcription Factor by High-Throughput Screening', *J Natl Cancer Inst,* 103(12), 962-978.

Gujral, T. S. and MacBeath, G. (2010) 'A System-Wide Investigation of the Dynamics of Wnt Signaling Reveals Novel Phases of Transcriptional Regulation', *PLoS ONE,* 5(4), e10024.

Habas, R. and Dawid, I. (2005) 'Dishevelled and Wnt signaling: is the nucleus the final frontier?', *Journal of Biology,* 4(1), 2.

Habas, R., Dawid, I. B. and He, X. (2003) 'Coactivation of Rac and Rho by Wnt/Frizzled signaling is required for vertebrate gastrulation', *Genes & Development,* 17(2), 295-309.

Habas, R., Kato, Y. and He, X. (2001) 'Wnt/Frizzled Activation of Rho Regulates Vertebrate Gastrulation and Requires a Novel Formin Homology Protein Daam1', *Cell,* 107(7), 843-854.

Hamburger, A. and Salmon, S. E. (1977) 'Primary bioassay of human myeloma stem cells', *J Clin Invest,* 60(4), 846-54.

Hanahan, D. and Weinberg, R. A. (2000) 'The hallmarks of cancer', *Cell,* 100(1), 57-70.

Hanahan, D. and Weinberg, R. A. (2011) 'Hallmarks of cancer: the next generation', *Cell,* 144(5), 646-74.

Hancock, J. D. and Lessnick, S. L. (2008) 'A transcriptional profiling meta-analysis reveals a core EWS-FLI gene expression signature', *Cell Cycle,* 7(2), 250-256.

Hasegawa, K., Fujioka, T., Nakamura, Y., Nakatsuji, N. and Suemori, H. (2006) 'A Method for the Selection of Human Embryonic Stem Cell Sublines with High Replating Efficiency After Single-Cell Dissociation', *Stem Cells,* 24(12), 2649-2660.

Hashimi, S. T., Fulcher, J. A., Chang, M. H., Gov, L., Wang, S. and Lee, B. (2009) 'MicroRNA profiling identifies miR-34a and miR-21 and their target genes JAG1 and WNT1 in the coordinate regulation of dendritic cell differentiation', *Blood,* 114(2), 404-414.

Hauer, K., Calzada-Wack, J., Steiger, K., Grunewald, T. G., Baumhoer, D., Plehm, S., Buch, T., Prazeres da Costa, O., Esposito, I., Burdach, S. and Richter, G. H. (2013) 'DKK2 mediates osteolysis, invasiveness, and metastatic spread in Ewing sarcoma', *Cancer Res,* 73(2), 967-77.

Hecht, A., Vleminckx, K., Stemmler, M. P., van Roy, F. and Kemler, R. (2000) 'The p300/CBP acetyltransferases function as transcriptional coactivators of beta-catenin in vertebrates', *EMBO J,* 19(8), 1839-50.

Hendrix, N. D., Wu, R., Kuick, R., Schwartz, D. R., Fearon, E. R. and Cho, K. R. (2006) 'Fibroblast Growth Factor 9 Has Oncogenic Activity and Is a Downstream Target of Wnt Signaling in Ovarian Endometrioid Adenocarcinomas', *Cancer Research,* 66(3), 1354-1362.

Hermann, P. C., Huber, S. L., Herrler, T., Aicher, A., Ellwart, J. W., Guba, M., Bruns, C. J. and Heeschen, C. (2007) 'Distinct Populations of Cancer Stem Cells Determine Tumor Growth and Metastatic Activity in Human Pancreatic Cancer', *Cell Stem Cell,* 1(3), 313-323.

Hernandez, A. R., Klein, A. M. and Kirschner, M. W. (2012) 'Kinetic responses of beta-catenin specify the sites of Wnt control', *Science,* 338(6112), 1337-40.

Herrero-Martin, D., Fourtouna, A., Niedan, S., Riedmann, L. T., Schwentner, R. and Aryee, D. N. (2011) 'Factors Affecting EWS-FLI1 Activity in Ewing's Sarcoma', *Sarcoma,* 2011, 352580.

Ho, R., Papp, B., Hoffman, J. A., Merrill, B. J. and Plath, K. (2013) 'Stage-specific regulation of reprogramming to induced pluripotent stem cells by Wnt signaling and T cell factor proteins', *Cell Rep,* 3(6), 2113-26.

Hu-Lieskovan, S., Zhang, J., Wu, L., Shimada, H., Schofield, D. E. and Triche, T. J. (2005) 'EWS-FLI1 Fusion Protein Up-regulates Critical Genes in Neural Crest Development and Is Responsible for the Observed Phenotype of Ewing's Family of Tumors', *Cancer Research,* 65(11), 4633-4644.

Huang, S., Xie, Y., Yang, P., Chen, P. and Zhang, L. (2014) 'HCV Core Protein-Induced Down-Regulation of microRNA-152 Promoted Aberrant Proliferation by Regulating Wnt1 in HepG2 Cells', *PLoS ONE,* 9(1), e81730.

Iida, K., Fukushi, J.-i., Matsumoto, Y., Oda, Y., Takahashi, Y., Fujiwara, T., Fujiwara-Okada, Y., Hatano, M., Nabashima, A., Kamura, S. and Iwamoto, Y. (2013) 'miR-125b develops chemoresistance in Ewing sarcoma/primitive neuroectodermal tumor', *Cancer Cell International,* 13(1), 21.

Inagawa, S., Itabashi, M., Adachi, S., Kawamoto, T., Hori, M., Shimazaki, J., Yoshimi, F. and Fukao, K. (2002) 'Expression and Prognostic Roles of β-Catenin in Hepatocellular Carcinoma', *Clinical Cancer Research,* 8(2), 450-456.

Ishitani, T., Kishida, S., Hyodo-Miura, J., Ueno, N., Yasuda, J., Waterman, M., Shibuya, H., Moon, R. T., Ninomiya-Tsuji, J. and Matsumoto, K. (2003) 'The TAK1-NLK Mitogen-Activated Protein Kinase Cascade Functions in the Wnt-5a/Ca2+ Pathway To Antagonize Wnt/{beta}-Catenin Signaling', *Mol. Cell. Biol.,* 23(1), 131-139.

Jho, E.-h., Zhang, T., Domon, C., Joo, C.-K., Freund, J.-N. and Costantini, F. (2002) 'Wnt/β-Catenin/Tcf Signaling Induces the Transcription of Axin2, a Negative Regulator of the Signaling Pathway', *Molecular and Cellular Biology,* 22(4), 1172-1183.

Jiang, X., Gwye, Y., Russell, D., Cao, C., Douglas, D., Hung, L., Kovar, H., Triche, T. and Lawlor, E. (2010) 'CD133 expression in chemo-resistant Ewing sarcoma cells', *BMC Cancer,* 10(1), 116.

Jin, F., Qu, X., Fan, Q., Wang, L., Tang, T., Hao, Y. and Dai, K. (2013) 'Regulation of prostate cancer cell migration toward bone marrow stromal cell-conditioned medium by Wnt5a signaling', *Mol Med Rep,* 8(5), 1486-92.

Jin, Z., Zhao, C., Han, X. and Han, Y. (2012) 'Wnt5a promotes ewing sarcoma cell migration through upregulating CXCR4 expression', *BMC Cancer,* 12, 480.

Jonsson, M., Dejmek, J., Bendahl, P. O. and Andersson, T. (2002) 'Loss of Wnt-5a protein is associated with early relapse in invasive ductal breast carcinomas', *Cancer Research,* 62(2), 409-16.

Juergens, C., Weston, C., Lewis, I., Whelan, J., Paulussen, M., Oberlin, O., Michon, J., Zoubek, A., Juergens, H. and Craft, A. (2006) 'Safety assessment of intensive induction with vincristine, ifosfamide, doxorubicin, and etoposide (VIDE) in the treatment of Ewing tumors in the EURO-E.W.I.N.G. 99 clinical trial', *Pediatr Blood Cancer,* 47(1), 22-29.

Kamura, S., Matsumoto, Y., Fukushi, J. I., Fujiwara, T., Iida, K., Okada, Y. and Iwamoto, Y. (2010) 'Basic fibroblast growth factor in the bone microenvironment enhances cell motility and invasion of Ewing's sarcoma family of tumours by activating the FGFR1-PI3K-Rac1 pathway', *Br J Cancer,* 103(3), 370-81.

Kang, H.-G., Jenabi, J. M., Zhang, J., Keshelava, N., Shimada, H., May, W. A., Ng, T., Reynolds, C. P., Triche, T. J. and Sorensen, P. H. B. (2007) 'E-Cadherin Cell-Cell Adhesion in Ewing Tumor Cells Mediates Suppression of Anoikis through Activation of the ErbB4 Tyrosine Kinase', *Cancer Research,* 67(7), 3094-3105.

Katoh, M. (2003) 'Expression and regulation of WNT1 in human cancer: up-regulation of WNT1 by beta-estradiol in MCF-7 cells', *Int J Oncol,* 22(1), 209-12.

Katoh, M. (2007) 'Conserved POU/OCT- and GATA-binding sites in 5'-flanking promoter region of mammalian WNT8B orthologs', *Int J Oncol,* 30(5), 1273-7.

Kauer, M., Ban, J., Kofler, R., Walker, B., Davis, S., Meltzer, P. and Kovar, H. (2009) 'A molecular function map of Ewing's sarcoma', *PLoS ONE,* 4(4), e5415.

Kawaguchi-Ihara, N., Murohashi, I., Nara, N. and Tohda, S. (2008) 'Promotion of the self-renewal capacity of human acute leukemia cells by Wnt3A', *Anticancer Research,* 28(5 A), 2701-2704.

Kawano, Y. and Kypta, R. (2003) 'Secreted antagonists of the Wnt signalling pathway', *Journal of Cell Science,* 116(Pt 13), 2627-34.

Kim, J., Hoffman, John P., Alpaugh, R. K., Rhim, Andrew D., Reichert, M., Stanger, Ben Z., Furth, Emma E., Sepulveda, Antonia R., Yuan, C.-X., Won, K.-J., Donahue, G., Sands, J., Gumbs, Andrew A. and Zaret, Kenneth S. (2013) 'An iPSC Line from Human Pancreatic Ductal Adenocarcinoma Undergoes Early to Invasive Stages of Pancreatic Cancer Progression', *Cell Reports,* 3(6), 2088-2099.

Kinney, M. A., Saeed, R. and McDevitt, T. C. (2014) 'Mesenchymal morphogenesis of embryonic stem cells dynamically modulates the biophysical microtissue niche', *Sci Rep,* 4, 4290.

Kleinman, H. K., McGarvey, M. L., Liotta, L. A., Robey, P. G., Tryggvason, K. and Martin, G. R. (1982) 'Isolation and characterization of type IV procollagen, laminin, and heparan sulfate proteoglycan from the EHS sarcoma', *Biochemistry,* 21(24), 6188-93.

Knudson, A. G., Jr. (1971) 'Mutation and cancer: statistical study of retinoblastoma', *Proc Natl Acad Sci U S A,* 68(4), 820-3.

Komekado, H., Yamamoto, H., Chiba, T. and Kikuchi, A. (2007) 'Glycosylation and palmitoylation of Wnt-3a are coupled to produce an active form of Wnt-3a', *Genes to Cells,* 12(4), 521-534.

Korinek, V., Barker, N., Moerer, P., van Donselaar, E., Huls, G., Peters, P. J. and Clevers, H. (1998) 'Depletion of epithelial stem-cell compartments in the small intestine of mice lacking Tcf-4', *Nat Genet,* 19(4), 379-383.

Korinek, V., Barker, N., Morin, P. J., van Wichen, D., de Weger, R., Kinzler, K. W., Vogelstein, B. and Clevers, H. (1997) 'Constitutive Transcriptional Activation by a β-Catenin-Tcf Complex in APC−/− Colon Carcinoma', *Science,* 275(5307), 1784-1787.

Kovar, H., Alonso, J., Aman, P., Aryee, D. N., Ban, J., Burchill, S. A., Burdach, S., De Alava, E., Delattre, O., Dirksen, U., Fourtouna, A., Fulda, S., Helman, L. J., Herrero-Martin, D., Hogendoorn, P. C., Kontny, U., Lawlor, E. R., Lessnick, S. L., Llombart-Bosch, A., Metzler, M., Moriggl, R., Niedan, S., Potratz, J., Redini, F., Richter, G. H., Riedmann, L. T., Rossig, C., Schafer, B. W., Schwentner, R., Scotlandi, K., Sorensen, P. H., Staege, M. S., Tirode, F., Toretsky, J., Ventura, S., Eggert, A. and Ladenstein, R. (2012) 'The first European interdisciplinary ewing sarcoma research summit', *Front Oncol,* 2, 54.

Kratochwil, K., Galceran, J., Tontsch, S., Roth, W. and Grosschedl, R. (2002) 'FGF4, a direct target of LEF1 and Wnt signaling, can rescue the arrest of tooth organogenesis in Lef1−/− mice', *Genes & Development,* 16(24), 3173-3185.

Kremenevskaja, N., von Wasielewski, R., Rao, A. S., Schofl, C., Andersson, T. and Brabant, G. (2005) 'Wnt-5a has tumor suppressor activity in thyroid carcinoma', *Oncogene,* 24(13), 2144-2154.

Kreppel, M., Aryee, D. N., Schaefer, K. L., Amann, G., Kofler, R., Poremba, C. and Kovar, H. (2006) 'Suppression of KCMF1 by constitutive high CD99 expression is involved in the migratory ability of Ewing's sarcoma cells', *Oncogene,* 25(19), 2795-800.

Kuhl, M., Sheldahl, L. C., Malbon, C. C. and Moon, R. T. (2000) 'Ca(2+)/calmodulin-dependent protein kinase II is stimulated by Wnt and Frizzled homologs and promotes ventral cell fates in Xenopus', *J Biol Chem,* 275(17), 12701-11.

Kühl, M., Sheldahl, L. C., Malbon, C. C. and Moon, R. T. (2000) 'Ca2+/Calmodulin-dependent Protein Kinase II Is Stimulated by Wnt and Frizzled Homologs and Promotes Ventral Cell Fates in Xenopus', *Journal of Biological Chemistry,* 275(17), 12701-12711.

Kuhnert, F., Davis, C. R., Wang, H.-T., Chu, P., Lee, M., Yuan, J., Nusse, R. and Kuo, C. J. (2004) 'Essential requirement for Wnt signaling in proliferation of adult small intestine and colon revealed by adenoviral expression of Dickkopf-1', *Proc Natl Acad Sci U S A,* 101(1), 266-271.

Kurayoshi, M., Oue, N., Yamamoto, H., Kishida, M., Inoue, A., Asahara, T., Yasui, W. and Kikuchi, A. (2006) 'Expression of Wnt-5a is correlated with aggressiveness of gastric cancer by stimulating cell migration and invasion', *Cancer Research,* 66(21), 10439-48.

Kurayoshi, M., Yamamoto, H., Izumi, S. and Kikuchi, A. (2007) 'Post-translational palmitoylation and glycosylation of Wnt-5a are necessary for its signalling', *Biochem J,* 402(3), 515-523.

Kuttesch, J. F., Wexler, L. H., Marcus, R. B., Fairclough, D., Weaver-McClure, L., White, M., Mao, L., Delaney, T. F., Pratt, C. B., Horowitz, M. E. and Kun, L. E. (1996) 'Second malignancies after Ewing's sarcoma: radiation dose-dependency of secondary sarcomas', *Journal of Clinical Oncology,* 14(10), 2818-25.

Lagutin, O. V., Zhu, C. C., Kobayashi, D., Topczewski, J., Shimamura, K., Puelles, L., Russell, H. R., McKinnon, P. J., Solnica-Krezel, L. and Oliver, G. (2003) 'Six3 repression of Wnt signaling in the anterior neuroectoderm is essential for vertebrate forebrain development', *Genes Dev,* 17(3), 368-79.

Lane, D. P. and Crawford, L. V. (1979) 'T antigen is bound to a host protein in SV40-transformed cells', *Nature,* 278(5701), 261-3.

Lawlor, E. R., Scheel, C., Irving, J. and Sorensen, P. H. (2002) 'Anchorage-independent multi-cellular spheroids as an in vitro model of growth signaling in Ewing tumors', *Oncogene,* 21(2), 307-18.

Lessnick, S. L., Dacwag, C. S. and Golub, T. R. (2002) 'The Ewing's sarcoma oncoprotein EWS/FLI induces a p53-dependent growth arrest in primary human fibroblasts', *Cancer Cell,* 1(4), 393-401.

Li, C., Heidt, D. G., Dalerba, P., Burant, C. F., Zhang, L., Adsay, V., Wicha, M., Clarke, M. F. and Simeone, D. M. (2007) 'Identification of pancreatic cancer stem cells', *Cancer Res,* 67(3), 1030-7.

Li, J., Yen, C., Liaw, D., Podsypanina, K., Bose, S., Wang, S. I., Puc, J., Miliaresis, C., Rodgers, L., McCombie, R., Bigner, S. H., Giovanella, B. C., Ittmann, M., Tycko, B., Hibshoosh, H., Wigler, M. H. and Parsons, R. (1997) 'PTEN, a Putative Protein Tyrosine Phosphatase Gene Mutated in Human Brain, Breast, and Prostate Cancer', *Science,* 275(5308), 1943-1947.

Li, L., Mao, J., Sun, L., Liu, W. and Wu, D. (2002) 'Second Cysteine-rich Domain of Dickkopf-2 Activates Canonical Wnt Signaling Pathway via LRP-6 Independently of Dishevelled', *Journal of Biological Chemistry,* 277(8), 5977-5981.

Li, X., Lewis, M. T., Huang, J., Gutierrez, C., Osborne, C. K., Wu, M. F., Hilsenbeck, S. G., Pavlick, A., Zhang, X., Chamness, G. C., Wong, H., Rosen, J. and Chang, J. C. (2008) 'Intrinsic resistance of tumorigenic breast cancer cells to chemotherapy', *J Natl Cancer Inst,* 100(9), 672-9.

Li, Y., Welm, B., Podsypanina, K., Huang, S., Chamorro, M., Zhang, X., Rowlands, T., Egeblad, M., Cowin, P., Werb, Z., Tan, L. K., Rosen, J. M. and Varmus, H. E. (2003) 'Evidence that transgenes encoding components of the Wnt signaling pathway preferentially induce mammary cancers from progenitor cells', *Proceedings of the National Academy of Sciences,* 100(26), 15853-15858.

Liang, C.-C., Park, A. Y. and Guan, J.-L. (2007) 'In vitro scratch assay: a convenient and inexpensive method for analysis of cell migration in vitro', *Nat. Protocols,* 2(2), 329-333.

Lin, S.-Y., Xia, W., Wang, J. C., Kwong, K. Y., Spohn, B., Wen, Y., Pestell, R. G. and Hung, M.-C. (2000) 'β-Catenin, a novel prognostic marker for breast cancer: Its roles in cyclin D1 expression and cancer progression', *Proceedings of the National Academy of Sciences,* 97(8), 4262-4266.

Linzer, D. I. and Levine, A. J. (1979) 'Characterization of a 54K dalton cellular SV40 tumor antigen present in SV40-transformed cells and uninfected embryonal carcinoma cells', *Cell,* 17(1), 43-52.

Lipinski, M., Braham, K., Philip, I., Wiels, J., Philip, T., Dellagi, K., Goridis, C., Lenoir, G. M. and Tursz, T. (1986) 'Phenotypic characterization of Ewing sarcoma cell lines with monoclonal antibodies', *Journal of Cellular Biochemistry,* 31(4), 289-296.

Liu, C., Tu, Y., Sun, X., Jiang, J., Jin, X., Bo, X., Li, Z., Bian, A., Wang, X., Liu, D., Wang, Z. and Ding, L. (2011) 'Wnt/beta-Catenin pathway in human glioma: expression pattern and clinical/prognostic correlations', *Clin Exp Med,* 11(2), 105-12.

Livak, K. J. and Schmittgen, T. D. (2001) 'Analysis of Relative Gene Expression Data Using Real-Time Quantitative PCR and the 2−ΔΔCT Method', *Methods,* 25(4), 402-408.

Lopez-Guerrero, J. A., Machado, I., Scotlandi, K., Noguera, R., Pellin, A., Navarro, S., Serra, M., Calabuig-Farinas, S., Picci, P. and Llombart-Bosch, A. (2011) 'Clinicopathological significance of cell cycle regulation markers in a large series of genetically confirmed Ewing's sarcoma family of tumors', *Int J Cancer,* 128(5), 1139-50.

Lopez-Guerrero, J. A., Pellin, A., Noguera, R., Carda, C. and Llombart-Bosch, A. (2001) 'Molecular analysis of the 9p21 locus and p53 genes in Ewing family tumors', *Lab Invest,* 81(6), 803-14.

Lowry, O. H., Rosebrough, N. J., Farr, A. L. and Randall, R. J. (1951) 'Protein measurement with the Folin phenol reagent', *J Biol Chem,* 193(1), 265-75.

Ludwig, T. E., Bergendahl, V., Levenstein, M. E., Yu, J., Probasco, M. D. and Thomson, J. A. (2006) 'Feeder-independent culture of human embryonic stem cells', *Nat Meth,* 3(8), 637-646.

Lum, D. F., McQuaid, K. R., Gilbertson, V. L. and Hughes-Fulford, M. (1999) 'Coordinate up-regulation of low-density lipoprotein receptor and cyclo-oxygenase-2 gene expression in human colorectal cells and in colorectal adenocarcinoma biopsies', *International Journal of Cancer,* 83(2), 162-166.

MacDonald, B. T., Tamai, K. and He, X. (2009) 'Wnt/[beta]-Catenin Signaling: Components, Mechanisms, and Diseases', *Developmental Cell,* 17(1), 9-26.

Maitra, A., Roberts, H., Weinberg, A. G. and Geradts, J. (2001) 'Aberrant expression of tumor suppressor proteins in the Ewing family of tumors', *Arch Pathol Lab Med,* 125(9), 1207-12.

Malanchi, I., Peinado, H., Kassen, D., Hussenet, T., Metzger, D., Chambon, P., Huber, M., Hohl, D., Cano, A., Birchmeier, W. and Huelsken, J. (2008) 'Cutaneous cancer stem cell maintenance is dependent on beta-catenin signalling', *Nature,* 452(7187), 650-3.

Malbon, C. C., Wang, H. and Moon, R. T. (2001) 'Wnt signaling and heterotrimeric G-proteins: strange bedfellows or a classic romance?', *Biochemical and Biophysical Research Communications,* 287(3), 589-93.

Mao, B., Wu, W., Li, Y., Hoppe, D., Stannek, P., Glinka, A. and Niehrs, C. (2001) 'LDL-receptor-related protein 6 is a receptor for Dickkopf proteins', *Nature,* 411(6835), 321-5.

Marson, A., Foreman, R., Chevalier, B., Bilodeau, S., Kahn, M., Young, R. A. and Jaenisch, R. (2008) 'Wnt signaling promotes reprogramming of somatic cells to pluripotency', *Cell Stem Cell,* 3(2), 132-5.

Maurici, D., Perez-Atayde, A., Grier, H. E., Baldini, N., Serra, M. and Fletcher, J. A. (1998) 'Frequency and implications of chromosome 8 and 12 gains in Ewing sarcoma', *Cancer Genet Cytogenet,* 100(2), 106-10.

May, W. A., Gishizky, M. L., Lessnick, S. L., Lunsford, L. B., Lewis, B. C., Delattre, O., Zucman, J., Thomas, G. and Denny, C. T. (1993) 'Ewing sarcoma 11;22 translocation produces a chimeric transcription factor that requires the DNA-binding domain encoded by FLI1 for transformation', *Proceedings of the National Academy of Sciences,* 90(12), 5752-5756.

Mayor, R. and Theveneau, E. (2014) 'The role of the non-canonical Wnt-planar cell polarity pathway in neural crest migration', *Biochem J,* 457(1), 19-26.

McKeon, C., Thiele, C. J., Ross, R. A., Kwan, M., Triche, T. J., Miser, J. S. and Israel, M. A. (1988) 'Indistinguishable patterns of protooncogene expression in two distinct but closely related tumors: Ewing's sarcoma and neuroepithelioma', *Cancer Research,* 48(15), 4307-4311.

McKinsey, E. L., Parrish, J. K., Irwin, A. E., Niemeyer, B. F., Kern, H. B., Birks, D. K. and Jedlicka, P. (2011) 'A novel oncogenic mechanism in Ewing sarcoma involving IGF pathway targeting by EWS/Fli1-regulated microRNAs', *Oncogene,* 30(49), 4910-4920.

McNally, R. J., Blakey, K., Parslow, R., James, P., Pozo, B., Stiller, C., Vincent, T., Norman, P., McKinney, P., Murphy, M., Craft, A. and Feltbower, R. (2012) 'Small-area analyses of bone cancer diagnosed in Great Britain provide clues to aetiology', *BMC Cancer,* 12(1), 270.

Mendoza-Naranjo, A., El-Naggar, A., Wai, D. H., Mistry, P., Lazic, N., Ayala, F. R. R., da Cunha, I. W., Rodriguez-Viciana, P., Cheng, H., Tavares Guerreiro Fregnani, J. H., Reynolds, P., Arceci, R. J., Nicholson, A., Triche, T. J., Soares, F. A., Flanagan, A. M., Wang, Y. Z., Strauss, S. J. and Sorensen, P. H. (2013) 'ERBB4 confers metastatic capacity in Ewing sarcoma', *EMBO Molecular Medicine,* 5(7), 1087-1102.

Mikels, A. J. and Nusse, R. (2006) 'Purified Wnt5a Protein Activates or Inhibits β-Catenin–TCF Signaling Depending on Receptor Context', *PLoS Biol,* 4(4), e115.

Miyagawa, Y., Okita, H., Itagaki, M., Toyoda, M., Katagiri, Y. U., Fujimoto, J., Hata, J., Umezawa, A. and Kiyokawa, N. (2009) 'EWS/ETS regulates the expression of the Dickkopf family in Ewing family tumor cells', *PLoS ONE,* 4(2), e4634.

Miyagawa, Y., Okita, H., Nakaijima, H., Horiuchi, Y., Sato, B., Taguchi, T., Toyoda, M., Katagiri, Y. U., Fujimoto, J., Hata, J.-i., Umezawa, A. and Kiyokawa, N. (2008) 'Inducible Expression of Chimeric EWS/ETS Proteins Confers Ewing's Family Tumor-Like Phenotypes to Human Mesenchymal Progenitor Cells', *Mol. Cell. Biol.,* 28(7), 2125-2137.

Miyoshi, N., Ishii, H., Nagai, K.-i., Hoshino, H., Mimori, K., Tanaka, F., Nagano, H., Sekimoto, M., Doki, Y. and Mori, M. (2010) 'Defined factors induce reprogramming of gastrointestinal cancer cells', *Proceedings of the National Academy of Sciences,* 107(1), 40-45.

Mok, T. S., Wu, Y. L., Thongprasert, S., Yang, C. H., Chu, D. T., Saijo, N., Sunpaweravong, P., Han, B., Margono, B., Ichinose, Y., Nishiwaki, Y., Ohe, Y., Yang, J. J., Chewaskulyong, B., Jiang, H., Duffield, E. L., Watkins, C. L., Armour, A. A. and Fukuoka, M. (2009) 'Gefitinib or carboplatin-paclitaxel in pulmonary adenocarcinoma', *New England Journal of Medicine,* 361(10), 947-957.

Moon, R. T., Kohn, A. D., Ferrari, G. V. D. and Kaykas, A. (2004) 'WNT and [beta]-catenin signalling: diseases and therapies', *Nat Rev Genet,* 5(9), 691-701.

Naing, A., LoRusso, P., Fu, S., Hong, D. S., Anderson, P., Benjamin, R. S., Ludwig, J., Chen, H. X., Doyle, L. A. and Kurzrock, R. (2012) 'Insulin Growth Factor-Receptor (IGF-1R) Antibody Cixutumumab Combined with the mTOR Inhibitor Temsirolimus in Patients with Refractory Ewing's Sarcoma Family Tumors', *Clinical Cancer Research,* 18(9), 2625-2631.

Naldini, L., Blomer, U., Gallay, P., Ory, D., Mulligan, R., Gage, F. H., Verma, I. M. and Trono, D. (1996) 'In vivo gene delivery and stable transduction of nondividing cells by a lentiviral vector', *Science,* 272(5259), 263-7.

Navarro, D., Agra, N., Pestaña, Á., Alonso, J. and González-Sancho, J. M. (2010) 'The EWS/FLI1 oncogenic protein inhibits expression of the Wnt inhibitor DICKKOPF-1 gene and antagonizes β-catenin/TCF-mediated transcription', *Carcinogenesis,* 31(3), 394-401.

Niehrs, C. (2006) 'Function and biological roles of the Dickkopf family of Wnt modulators', *Oncogene,* 25(57), 7469-81.

Nowell, P. C. (1976) 'The clonal evolution of tumor cell populations', *Science,* 194(4260), 23-8.

Nowicki, M. O., Dmitrieva, N., Stein, A. M., Cutter, J. L., Godlewski, J., Saeki, Y., Nita, M., Berens, M. E., Sander, L. M., Newton, H. B., Chiocca, E. A. and Lawler, S. (2008) 'Lithium inhibits

invasion of glioma cells; possible involvement of glycogen synthase kinase-3', *Neuro-Oncology,* 10(5), 690-699.

Nusse, R., van Ooyen, A., Cox, D., Fung, Y. K. and Varmus, H. (1984) 'Mode of proviral activation of a putative mammary oncogene (int-1) on mouse chromosome 15', *Nature,* 307(5947), 131-6.

Nusse, R. and Varmus, H. E. (1982) 'Many tumors induced by the mouse mammary tumor virus contain a provirus integrated in the same region of the host genome', *Cell,* 31(1), 99-109.

O'Brien, C. A., Pollett, A., Gallinger, S. and Dick, J. E. (2007) 'A human colon cancer cell capable of initiating tumour growth in immunodeficient mice', *Nature,* 445(7123), 106-10.

Odri, G. A., Dumoucel, S., Picarda, G., Battaglia, S., Lamoureux, F., Corradini, N., Rousseau, J., Tirode, F., Laud, K., Delattre, O., Gouin, F., Heymann, D. and Redini, F. (2010) 'Zoledronic Acid as a New Adjuvant Therapeutic Strategy for Ewing's Sarcoma Patients', *Cancer Research,* 70(19), 7610-7619.

Ohgushi, M., Matsumura, M., Eiraku, M., Murakami, K., Aramaki, T., Nishiyama, A., Muguruma, K., Nakano, T., Suga, H., Ueno, M., Ishizaki, T., Suemori, H., Narumiya, S., Niwa, H. and Sasai, Y. (2010) 'Molecular Pathway and Cell State Responsible for Dissociation-Induced Apoptosis in Human Pluripotent Stem Cells', *Cell Stem Cell,* 7(2), 225-239.

Oishi, I., Suzuki, H., Onishi, N., Takada, R., Kani, S., Ohkawara, B., Koshida, I., Suzuki, K., Yamada, G., Schwabe, G. C., Mundlos, S., Shibuya, H., Takada, S. and Minami, Y. (2003) 'The receptor tyrosine kinase Ror2 is involved in non-canonical Wnt5a/JNK signalling pathway', *Genes Cells,* 8(7), 645-54.

Outten, J. T., Cheng, X., Gadue, P., French, D. L. and Diamond, S. L. (2011) 'A high-throughput multiplexed screening assay for optimizing serum-free differentiation protocols of human embryonic stem cells', *Stem Cell Research,* 6(2), 129-142.

Palacios, J. and Gamallo, C. (1998) 'Mutations in the β-catenin gene (CTNNB1) in endometrioid ovarian carcinomas', *Cancer Research,* 58(7), 1344-1347.

Pappo, A. S., Patel, S. R., Crowley, J., Reinke, D. K., Kuenkele, K.-P., Chawla, S. P., Toner, G. C., Maki, R. G., Meyers, P. A., Chugh, R., Ganjoo, K. N., Schuetze, S. M., Juergens, H., Leahy, M. G., Geoerger, B., Benjamin, R. S., Helman, L. J. and Baker, L. H. (2011) 'R1507, a Monoclonal Antibody to the Insulin-Like Growth Factor 1 Receptor, in Patients With Recurrent or Refractory Ewing Sarcoma Family of Tumors: Results of a Phase II Sarcoma Alliance for Research Through Collaboration Study', *Journal of Clinical Oncology,* 29(34), 4541-4547.

Paulussen, M., Ahrens, S., Craft, A. W., Dunst, J., Fröhlich, B., Jabar, S., Rübe, C., Winkelmann, W., Wissing, S., Zoubek, A. and Jürgens, H. (1998) 'Ewing's tumors with primary lung metastases: survival analysis of 114 (European Intergroup) Cooperative Ewing's Sarcoma Studies patients', *Journal of Clinical Oncology,* 16(9), 3044-52.

Pelengaris, S. and Khan, M., eds. (2013) *The Molecular Biology of Cancer : a bridge from bench to bedside,* Second Edition ed.*,* Hoboken, NJ: Wiley-Blackwell.

Pellegrin, S. and Mellor, H. (2008) 'Rho GTPase activation assays', *Curr Protoc Cell Biol,* Chapter 14, Unit 14 8.

Peters, J. M., McKay, R. M., McKay, J. P. and Graff, J. M. (1999) 'Casein kinase I transduces Wnt signals', *Nature,* 401(6751), 345-50.

Pleasance, E. D., Cheetham, R. K., Stephens, P. J., McBride, D. J., Humphray, S. J., Greenman, C. D., Varela, I., Lin, M.-L., Ordonez, G. R., Bignell, G. R., Ye, K., Alipaz, J., Bauer, M. J., Beare, D., Butler, A., Carter, R. J., Chen, L., Cox, A. J., Edkins, S., Kokko-Gonzales, P. I., Gormley, N. A., Grocock, R. J., Haudenschild, C. D., Hims, M. M., James, T., Jia, M., Kingsbury, Z., Leroy, C., Marshall, J., Menzies, A., Mudie, L. J., Ning, Z., Royce, T., Schulz-Trieglaff, O. B., Spiridou, A., Stebbings, L. A., Szajkowski, L., Teague, J., Williamson, D., Chin, L., Ross, M. T., Campbell, P. J., Bentley, D. R., Futreal, P. A. and Stratton, M. R. (2010) 'A comprehensive catalogue of somatic mutations from a human cancer genome', *Nature,* 463(7278), 191-196.

Powell, S. M., Zilz, N., Beazer-Barclay, Y., Bryan, T. M., Hamilton, S. R., Thibodeau, S. N., Vogelstein, B. and Kinzler, K. W. (1992) 'APC mutations occur early during colorectal tumorigenesis', *Nature,* 359(6392), 235-237.

Powles, T., McCroskey, E. and Paterson, A. (2006) 'Oral Bisphosphonates as Adjuvant Therapy for Operable Breast Cancer', *Clinical Cancer Research,* 12(20), 6301s-6304s.

Prieur, A., Tirode, F., Cohen, P. and Delattre, O. (2004) 'EWS/FLI-1 Silencing and Gene Profiling of Ewing Cells Reveal Downstream Oncogenic Pathways and a Crucial Role for Repression of Insulin-Like Growth Factor Binding Protein 3', *Molecular and Cellular Biology,* 24(16), 7275-7283.

Qiang, Y.-W., Barlogie, B., Rudikoff, S. and Shaughnessy Jr, J. D. (2008) 'Dkk1-induced inhibition of Wnt signaling in osteoblast differentiation is an underlying mechanism of bone loss in multiple myeloma', *Bone,* 42(4), 669-680.

Radonić, A., Thulke, S., Mackay, I. M., Landt, O., Siegert, W. and Nitsche, A. (2004) 'Guideline to reference gene selection for quantitative real-time PCR', *Biochemical and Biophysical Research Communications,* 313(4), 856-862.

Remon, J., Morán, T., Majem, M., Reguart, N., Dalmau, E., Márquez-Medina, D. and Lianes, P. (2014) 'Acquired resistance to epidermal growth factor receptor tyrosine kinase inhibitors in EGFR-mutant non-small cell lung cancer: A new era begins', *Cancer Treatment Reviews,* 40(1), 93-101.

Riggi, N. and Stamenkovic, I. (2007) 'The Biology of Ewing sarcoma', *Cancer Letters,* 254(1), 1-10.

Riggi, N., Suvà, M.-L., De Vito, C., Provero, P., Stehle, J.-C., Baumer, K., Cironi, L., Janiszewska, M., Petricevic, T., Suvà, D., Tercier, S., Joseph, J.-M., Guillou, L. and Stamenkovic, I. (2010) 'EWS-FLI-1 modulates miRNA145 and SOX2 expression to initiate mesenchymal stem cell reprogramming toward Ewing sarcoma cancer stem cells', *Genes & Development,* 24(9), 916-932.

Riggi, N., Suvà, M.-L., Suvà, D., Cironi, L., Provero, P., Tercier, S., Joseph, J.-M., Stehle, J.-C., Baumer, K., Kindler, V. and Stamenkovic, I. (2008) 'EWS-FLI-1 Expression Triggers a Ewing's Sarcoma Initiation Program in Primary Human Mesenchymal Stem Cells', *Cancer Research,* 68(7), 2176-2185.

Ripka, S., Konig, A., Buchholz, M., Wagner, M., Sipos, B., Kloppel, G., Downward, J., Gress, T. and Michl, P. (2007) 'WNT5A--target of CUTL1 and potent modulator of tumor cell migration and invasion in pancreatic cancer', *Carcinogenesis,* 28(6), 1178-87.

Roberts, P., Burchill, S. A., Brownhill, S., Cullinane, C. J., Johnston, C., Griffiths, M. J., McMullan, D. J., Bown, N. P., Morris, S. P. and Lewis, I. J. (2008) 'Ploidy and karyotype complexity are powerful prognostic indicators in the Ewing's sarcoma family of tumors: a study by the United Kingdom Cancer Cytogenetics and the Children's Cancer and Leukaemia Group', *Genes Chromosomes Cancer,* 47(3), 207-20.

Rodríguez-Enríquez, S., Gallardo-Pérez, J. C., Avilés-Salas, A., Marín-Hernández, A., Carreño-Fuentes, L., Maldonado-Lagunas, V. and Moreno-Sánchez, R. (2008) 'Energy metabolism transition in multi-cellular human tumor spheroids', *Journal of Cellular Physiology,* 216(1), 189-197.

Rorie, C. J., Thomas, V. D., Chen, P., Pierce, H. H., O'Bryan, J. P. and Weissman, B. E. (2004) 'The Ews/Fli-1 Fusion Gene Switches the Differentiation Program of Neuroblastomas to Ewing Sarcoma/Peripheral Primitive Neuroectodermal Tumors', *Cancer Research,* 64(4), 1266-1277.

Rosell, R., Carcereny, E., Gervais, R., Vergnenegre, A., Massuti, B., Felip, E., Palmero, R., Garcia-Gomez, R., Pallares, C., Sanchez, J. M., Porta, R., Cobo, M., Garrido, P., Longo, F., Moran, T., Insa, A., De Marinis, F., Corre, R., Bover, I., Illiano, A., Dansin, E., de Castro, J., Milella, M., Reguart, N., Altavilla, G., Jimenez, U., Provencio, M., Moreno, M. A., Terrasa, J., Muñoz-Langa, J., Valdivia, J., Isla, D., Domine, M., Molinier, O., Mazieres, J., Baize, N., Garcia-Campelo, R., Robinet, G., Rodriguez-Abreu, D., Lopez-Vivanco, G., Gebbia, V., Ferrera-Delgado, L., Bombaron, P., Bernabe, R., Bearz, A., Artal, A., Cortesi, E., Rolfo, C., Sanchez-Ronco, M., Drozdowskyj, A., Queralt, C., de Aguirre, I., Ramirez, J. L., Sanchez, J. J., Molina, M. A., Taron, M. and Paz-Ares, L. (2012) 'Erlotinib versus standard chemotherapy as first-line treatment for European patients with advanced EGFR mutation-positive non-small-cell lung cancer (EURTAC): a multicentre, open-label, randomised phase 3 trial', *The Lancet Oncology,* 13(3), 239-246.

Rosell, R., Moran, T., Queralt, C., Porta, R., Cardenal, F., Camps, C., Majem, M., Lopez-Vivanco, G., Isla, D., Provencio, M., Insa, A., Massuti, B., Gonzalez-Larriba, J. L., Paz-Ares, L., Bover, I., Garcia-Campelo, R., Moreno, M. A., Catot, S., Rolfo, C., Reguart, N., Palmero, R., Sánchez, J. M., Bastus, R., Mayo, C., Bertran-Alamillo, J., Molina, M. A., Sanchez, J. J. and Taron, M. (2009) 'Screening for epidermal growth factor receptor mutations in lung cancer', *New England Journal of Medicine,* 361(10), 958-967.

Ross, K. A., Smyth, N. A., Murawski, C. D. and Kennedy, J. G. (2013) 'The biology of ewing sarcoma', *ISRN Oncol,* 2013, 759725.

Sáinz-Jaspeado, M., Lagares-Tena, L., Lasheras, J., Navid, F., Rodriguez-Galindo, C., Mateo-Lozano, S., Notario, V., Sanjuan, X., Garcia del Muro, X., Fabra, À. and Tirado, O. M. (2010) 'Caveolin-1 Modulates the Ability of Ewing's Sarcoma to Metastasize', *Molecular Cancer Research,* 8(11), 1489-1500.

Salmon, P. (2013) 'Generation of Human Cell Lines Using Lentiviral-Mediated Genetic Engineering' in Randell, S. H. and Fulcher, M. L., eds., *Epithelial Cell Culture Protocols*, Humana Press, 417-448.

Samuel, M. S. and Olson, M. F. (2011) 'Rho-GTPases in Embryonic Stem Cells' in Kallos, M., ed. *Embryonic Stem Cells- Basic Biology to Bioengineering*, In Tech.

Saneyoshi, T., Kume, S., Amasaki, Y. and Mikoshiba, K. (2002) 'The Wnt/calcium pathway activates NF-AT and promotes ventral cell fate in Xenopus embryos', *Nature,* 417(6886), 295-299.

Sato, A., Yamamoto, H., Sakane, H., Koyama, H. and Kikuchi, A. (2010) 'Wnt5a regulates distinct signalling pathways by binding to Frizzled2', *EMBO J,* 29(1), 41-54.

Scannell, C. A., Pedersen, E. A., Mosher, J. T., Krook, M. A., Nicholls, L. A., Wilky, B. A., Loeb, D. M. and Lawlor, E. R. (2013) 'LGR5 is Expressed by Ewing Sarcoma and Potentiates Wnt/beta-Catenin Signaling', *Front Oncol,* 3, 81.

Schaefer, K. L., Eisenacher, M., Braun, Y., Brachwitz, K., Wai, D. H., Dirksen, U., Lanvers-Kaminsky, C., Juergens, H., Herrero, D., Stegmaier, S., Koscielniak, E., Eggert, A., Nathrath, M., Gosheger, G., Schneider, D. T., Bury, C., Diallo-Danebrock, R., Ottaviano, L., Gabbert, H. E. and Poremba, C. (2008) 'Microarray analysis of Ewing's sarcoma family of tumours reveals characteristic gene expression signatures associated with metastasis and resistance to chemotherapy', *Eur J Cancer,* 44(5), 699-709.

Schepers, A. G., Snippert, H. J., Stange, D. E., van den Born, M., van Es, J. H., van de Wetering, M. and Clevers, H. (2012) 'Lineage Tracing Reveals Lgr5+ Stem Cell Activity in Mouse Intestinal Adenomas', *Science,* 337(6095), 730-735.

Schlessinger, K., McManus, E. J. and Hall, A. (2007) 'Cdc42 and noncanonical Wnt signal transduction pathways cooperate to promote cell polarity', *J. Cell Biol.,* 178(3), 355-361.

Schmittgen, T. D. and Zakrajsek, B. A. (2000) 'Effect of experimental treatment on housekeeping gene expression: validation by real-time, quantitative RT-PCR', *Journal of Biochemical and Biophysical Methods,* 46(1–2), 69-81.

Schuck, A., Ahrens, S., Paulussen, M., Kuhlen, M., Könemann, S., Rübe, C., Winkelmann, W., Kotz, R., Dunst, J., Willich, N. and Jürgens, H. (2003) 'Local therapy in localized Ewing tumors: results of 1058 patients treated in the CESS 81, CESS 86, and EICESS 92 trials', *International Journal of Radiation Oncology*Biology*Physics,* 55(1), 168-177.

Scotlandi, K., Benini, S., Sarti, M., Serra, M., Lollini, P.-L., Maurici, D., Picci, P., Manara, M. C. and Baldini, N. (1996) 'Insulin-like Growth Factor I Receptor-mediated Circuit in Ewing's Sarcoma/Peripheral Neuroectodermal Tumor: A Possible Therapeutic Target', *Cancer Research,* 56(20), 4570-4574.

Scotlandi, K., Remondini, D., Castellani, G., Manara, M. C., Nardi, F., Cantiani, L., Francesconi, M., Mercuri, M., Caccuri, A. M., Serra, M., Knuutila, S. and Picci, P. (2009) 'Overcoming Resistance to Conventional Drugs in Ewing Sarcoma and Identification of Molecular Predictors of Outcome', *Journal of Clinical Oncology,* 27(13), 2209-2216.

Semënov, M. V., Tamai, K., Brott, B. K., Kühl, M., Sokol, S. and He, X. (2001) 'Head inducer Dickkopf-1 is a ligand for Wnt coreceptor LRP6', *Current Biology,* 11(12), 951-961.

Shankar, A. G., Ashley, S., Craft, A. W. and Pinkerton, C. R. (2003) 'Outcome after relapse in an unselected cohort of children and adolescents with Ewing sarcoma', *Medical and Pediatric Oncology,* 40(3), 141-147.

Sheldahl, L. C., Park, M., Malbon, C. C. and Moon, R. T. (1999) 'Protein kinase C is differentially stimulated by Wnt and Frizzled homologs in aG-protein-dependent manner', *Current Biology,* 9(13), 695-S1.

Shibamoto, S., Higano, K., Takada, R., Ito, F., Takeichi, M. and Takada, S. (1998) 'Cytoskeletal reorganization by soluble Wnt-3a protein signalling', *Genes Cells,* 3(10), 659-70.

Shtutman, M., Zhurinsky, J., Simcha, I., Albanese, C., D'Amico, M., Pestell, R. and Ben-Ze'ev, A. (1999) 'The cyclin D1 gene is a target of the β-catenin/LEF-1 pathway', *Proceedings of the National Academy of Sciences,* 96(10), 5522-5527.

Shukla, N., Ameur, N., Yilmaz, I., Nafa, K., Lau, C.-Y., Marchetti, A., Borsu, L., Barr, F. G. and Ladanyi, M. (2012) 'Oncogene Mutation Profiling of Pediatric Solid Tumors Reveals Significant Subsets of Embryonal Rhabdomyosarcoma and Neuroblastoma with Mutated Genes in Growth Signaling Pathways', *Clinical Cancer Research,* 18(3), 748-757.

Singh, Amar M., Reynolds, D., Cliff, T., Ohtsuka, S., Mattheyses, Alexa L., Sun, Y., Menendez, L., Kulik, M. and Dalton, S. (2012) 'Signaling Network Crosstalk in Human Pluripotent Cells: A Smad2/3-Regulated Switch that Controls the Balance between Self-Renewal and Differentiation', *Cell Stem Cell,* 10(3), 312-326.

Singh, S. K., Clarke, I. D., Terasaki, M., Bonn, V. E., Hawkins, C., Squire, J. and Dirks, P. B. (2003) 'Identification of a cancer stem cell in human brain tumors', *Cancer Res,* 63(18), 5821-8.

Smit, L., Baas, A., Kuipers, J., Korswagen, H., van de Wetering, M. and Clevers, H. (2004) 'Wnt activates the Tak1/Nemo-like kinase pathway', *J Biol Chem,* 279(17), 17232-40.

Smith, R., Owen, L. A., Trem, D. J., Wong, J. S., Whangbo, J. S., Golub, T. R. and Lessnick, S. L. (2006) 'Expression profiling of EWS/FLI identifies NKX2.2 as a critical target gene in Ewing's sarcoma', *Cancer Cell,* 9(5), 405-416.

Smyth, G. K. (2004) 'Linear models and empirical bayes methods for assessing differential expression in microarray experiments', *Stat Appl Genet Mol Biol,* 3, Article3.

Sparks, A. B., Morin, P. J., Vogelstein, B. and Kinzler, K. W. (1998) 'Mutational Analysis of the APC/β-Catenin/Tcf Pathway in Colorectal Cancer', *Cancer Research,* 58(6), 1130-1134.

Staege, M. S., Hutter, C., Neumann, I., Foja, S., Hattenhorst, U. E., Hansen, G., Afar, D. and Burdach, S. E. G. (2004) 'DNA Microarrays Reveal Relationship of Ewing Family Tumors to Both Endothelial and Fetal Neural Crest-Derived Cells and Define Novel Targets', *Cancer Research,* 64(22), 8213-8221.

Sugimura, R. and Li, L. (2010a) 'Noncanonical Wnt signaling in vertebrate development, stem cells, and diseases', *Birth Defects Research Part C: Embryo Today: Reviews,* 90(4), 243-256.

Sugimura, R. and Li, L. (2010b) 'Shifting in Balance Between Osteogenesis and Adipogenesis Substantially Influences Hematopoiesis', *Journal of Molecular Cell Biology,* 2(2), 61-62.

Sun, N., Panetta, N. J., Gupta, D. M., Wilson, K. D., Lee, A., Jia, F., Hu, S., Cherry, A. M., Robbins, R. C., Longaker, M. T. and Wu, J. C. (2009) 'Feeder-free derivation of induced pluripotent stem cells from adult human adipose stem cells', *Proc Natl Acad Sci U S A,* 106(37), 15720-5.

Sun, Y., Li, Y., Luo, D. and Liao, D. J. (2012) 'Pseudogenes as Weaknesses of ACTB (Actb) and GAPDH (Gapdh) Used as Reference Genes in Reverse Transcription and Polymerase Chain Reactions', *PLoS ONE,* 7(8), e41659.

Sutherland, R. M., Sordat, B., Bamat, J., Gabbert, H., Bourrat, B. and Mueller-Klieser, W. (1986) 'Oxygenation and differentiation in multicellular spheroids of human colon carcinoma', *Cancer Res,* 46(10), 5320-9.

Suvà, M.-L., Riggi, N., Stehle, J.-C., Baumer, K., Tercier, S., Joseph, J.-M., Suvà, D., Clément, V., Provero, P., Cironi, L., Osterheld, M.-C., Guillou, L. and Stamenkovic, I. (2009) 'Identification of Cancer Stem Cells in Ewing's Sarcoma', *Cancer Research,* 69(5), 1776-1781.

Takada, I., Mihara, M., Suzawa, M., Ohtake, F., Kobayashi, S., Igarashi, M., Youn, M.-Y., Takeyama, K.-i., Nakamura, T., Mezaki, Y., Takezawa, S., Yogiashi, Y., Kitagawa, H., Yamada, G., Takada, S., Minami, Y., Shibuya, H., Matsumoto, K. and Kato, S. (2007) 'A histone lysine methyltransferase activated by non-canonical Wnt signalling suppresses PPAR-[gamma] transactivation', *Nat Cell Biol,* 9(11), 1273-1285.

Takada, R., Satomi, Y., Kurata, T., Ueno, N., Norioka, S., Kondoh, H., Takao, T. and Takada, S. (2006) 'Monounsaturated Fatty Acid Modification of Wnt Protein: Its Role in Wnt Secretion', *Developmental Cell,* 11(6), 791-801.

Takahashi-Yanaga, F. and Kahn, M. (2010) 'Targeting Wnt Signaling: Can We Safely Eradicate Cancer Stem Cells?', *Clinical Cancer Research,* 16(12), 3153-3162.

Takahashi, K., Tanabe, K., Ohnuki, M., Narita, M., Ichisaka, T., Tomoda, K. and Yamanaka, S. (2007) 'Induction of Pluripotent Stem Cells from Adult Human Fibroblasts by Defined Factors', *Cell,* 131(5), 861-872.

Takahashi, K. and Yamanaka, S. (2006) 'Induction of pluripotent stem cells from mouse embryonic and adult fibroblast cultures by defined factors', *Cell,* 126(4), 663-76.

Takashima, Y., Era, T., Nakao, K., Kondo, S., Kasuga, M., Smith, A. G. and Nishikawa, S.-I. (2007) 'Neuroepithelial Cells Supply an Initial Transient Wave of MSC Differentiation', *Cell,* 129(7), 1377-1388.

Takemaru, K. I. and Moon, R. T. (2000) 'The transcriptional coactivator CBP interacts with beta-catenin to activate gene expression', *The Journal of cell biology,* 149(2), 249-54.

Tam, W. L., Lim, C. Y., Han, J., Zhang, J., Ang, Y. S., Ng, H. H., Yang, H. and Lim, B. (2008) 'T-cell factor 3 regulates embryonic stem cell pluripotency and self-renewal by the transcriptional control of multiple lineage pathways', *Stem Cells,* 26(8), 2019-31.

Tamai, K., Semenov, M., Kato, Y., Spokony, R., Liu, C., Katsuyama, Y., Hess, F., Saint-Jeannet, J. P. and He, X. (2000) 'LDL-receptor-related proteins in Wnt signal transduction', *Nature,* 407(6803), 530-5.

Tao, W., Pennica, D., Xu, L., Kalejta, R. F. and Levine, A. J. (2001) 'Wrch-1, a novel member of the Rho gene family that is regulated by Wnt-1', *Genes & Development,* 15(14), 1796-1807.

Teng, Y., Wang, X., Wang, Y. and Ma, D. (2010) 'Wnt/β-catenin signaling regulates cancer stem cells in lung cancer A549 cells', *Biochemical and Biophysical Research Communications,* 392(3), 373-379.

Teo, J. L. and Kahn, M. (2010) 'The Wnt signaling pathway in cellular proliferation and differentiation: A tale of two coactivators', *Adv Drug Deliv Rev,* 62(12), 1149-55.

Thacker, M. M., Temple, H. T. and Scully, S. P. (2005) 'Current treatment for Ewing's sarcoma', *Expert Rev Anticancer Ther,* 5(2), 319-31.

Thiery, J. P., Acloque, H., Huang, R. Y. J. and Nieto, M. A. (2009) 'Epithelial-Mesenchymal Transitions in Development and Disease', *Cell,* 139(5), 871-890.

Thomson, J. A. (1998) 'Embryonic stem cell lines derived from human blastocysts', *Science,* 282, 1145-1147.

Tirode, F., Laud-Duval, K., Prieur, A., Delorme, B., Charbord, P. and Delattre, O. (2007) 'Mesenchymal Stem Cell Features of Ewing Tumors', *Cancer Cell,* 11(5), 421-429.

Torchia, E. C., Jaishankar, S. and Baker, S. J. (2003) 'Ewing Tumor Fusion Proteins Block the Differentiation of Pluripotent Marrow Stromal Cells', *Cancer Research,* 63(13), 3464-3468.

Toretsky, J. A., Kalebic, T., Blakesley, V., LeRoith, D. and Helman, L. J. (1997) 'The Insulin-like Growth Factor-I Receptor Is Required for EWS/FLI-1 Transformation of Fibroblasts', *Journal of Biological Chemistry,* 272(49), 30822-30827.

Tso, J. Y., Sun, X. H., Kao, T. H., Reece, K. S. and Wu, R. (1985) 'Isolation and characterization of rat and human glyceraldehyde-3-phosphate dehydrogenase cDNAs: genomic complexity and molecular evolution of the gene', *Nucleic Acids Res,* 13(7), 2485-502.

Tsuchiya, T., Sekine, K., Hinohara, S., Namiki, T., Nobori, T. and Kaneko, Y. (2000) 'Analysis of the p16INK4, p14ARF, p15, TP53, and MDM2 genes and their prognostic implications in osteosarcoma and Ewing sarcoma', *Cancer Genet Cytogenet,* 120(2), 91-8.

Ullmann, U., In't Veld, P., Gilles, C., Sermon, K., De Rycke, M., Van de Velde, H., Van Steirteghem, A. and Liebaers, I. (2007) 'Epithelial–mesenchymal transition process in human embryonic stem cells cultured in feeder-free conditions', *Molecular Human Reproduction,* 13(1), 21-32.

Üren, A., Wolf, V., Sun, Y. F., Azari, A., Rubin, J. S. and Toretsky, J. A. (2004) 'Wnt/Frizzled signaling in Ewing sarcoma', *Pediatr Blood Cancer,* 43(3), 243-249.

Urlinger, S., Baron, U., Thellmann, M., Hasan, M. T., Bujard, H. and Hillen, W. (2000) 'Exploring the sequence space for tetracycline-dependent transcriptional activators: novel mutations yield expanded range and sensitivity', *Proc Natl Acad Sci U S A,* 97(14), 7963-8.

van Amerongen, R., Mikels, A. and Nusse, R. (2008) 'Alternative Wnt Signaling Is Initiated by Distinct Receptors', *Sci. Signal.,* 1(35), re9-.

van Amerongen, R. and Nusse, R. (2009) 'Towards an integrated view of Wnt signaling in development', *Development,* 136(19), 3205-3214.

van Noort, M., Meeldijk, J., van der Zee, R., Destree, O. and Clevers, H. (2002) 'Wnt signaling controls the phosphorylation status of beta-catenin', *J Biol Chem,* 277(20), 17901-5.

Veeman, M. T., Slusarski, D. C., Kaykas, A., Louie, S. H. and Moon, R. T. (2003) 'Zebrafish Prickle, a Modulator of Noncanonical Wnt/Fz Signaling, Regulates Gastrulation Movements', *Current Biology,* 13(8), 680-685.

Vermeulen, L., De Sousa E Melo, F., Van Der Heijden, M., Cameron, K., De Jong, J. H., Borovski, T., Tuynman, J. B., Todaro, M., Merz, C., Rodermond, H., Sprick, M. R., Kemper, K., Richel, D. J., Stassi, G. and Medema, J. P. (2010) 'Wnt activity defines colon cancer stem cells and is regulated by the microenvironment', *Nat Cell Biol,* 12(5), 468-476.

Vidugiriene, J., Schagat, T., Garvin, D. and Vidugris, G. (2008) 'Getting the Most from Your Transfections: Increasing Throughput and Sensitivity', *Promega Notes,* 100, 3-5.

Vijayakumar, S., Liu, G., Rus, I. A., Yao, S., Chen, Y., Akiri, G., Grumolato, L. and Aaronson, S. A. (2011) 'High-frequency canonical Wnt activation in multiple sarcoma subtypes drives proliferation through a TCF/beta-catenin target gene, CDC25A', *Cancer Cell,* 19(5), 601-12.

Vinci, M., Box, C., Zimmermann, M. and Eccles, S. A. (2013) 'Tumor spheroid-based migration assays for evaluation of therapeutic agents', *Methods Mol Biol,* 986, 253-66.

Voeller, H. J., Truica, C. I. and Gelmann, E. P. (1998) 'β-Catenin Mutations in Human Prostate Cancer', *Cancer Research,* 58(12), 2520-2523.

von Levetzow, C., Jiang, X., Gwye, Y., von Levetzow, G., Hung, L., Cooper, A., Hsu, J. H.-R. and Lawlor, E. R. (2011) 'Modeling Initiation of Ewing Sarcoma in Human Neural Crest Cells', *PLoS ONE,* 6(4), e19305.

Wang, Q., Williamson, M., Bott, S., Brookman-Amissah, N., Freeman, A., Nariculam, J., Hubank, M. J., Ahmed, A. and Masters, J. R. (2007) 'Hypomethylation of WNT5A, CRIP1 and S100P in prostate cancer', *Oncogene,* 26(45), 6560-5.

Wang, Y. (2009) 'Wnt/Planar cell polarity signaling: A new paradigm for cancer therapy', *Molecular Cancer Therapeutics,* 8(8), 2103-2109.

Wasilewski-Masker, K., Liu, Q., Yasui, Y., Leisenring, W., Meacham, L. R., Hammond, S., Meadows, A. T., Robison, L. L. and Mertens, A. C. (2009) 'Late Recurrence in Pediatric Cancer: A Report From the Childhood Cancer Survivor Study', *J Natl Cancer Inst,* 101(24), 1709-1720.

Watanabe, K., Ueno, M., Kamiya, D., Nishiyama, A., Matsumura, M., Wataya, T., Takahashi, J. B., Nishikawa, S., Nishikawa, S.-i., Muguruma, K. and Sasai, Y. (2007) 'A ROCK inhibitor permits survival of dissociated human embryonic stem cells', *Nat Biotech,* 25(6), 681-686.

Weber, F. A., Bartolomei, G., Hottiger, M. O. and Cinelli, P. (2013) 'Artd1/Parp1 regulates reprogramming by transcriptional regulation of Fgf4 via Sox2 ADP-ribosylation', *Stem Cells,* 31(11), 2364-73.

Weeraratna, A. T., Jiang, Y., Hostetter, G., Rosenblatt, K., Duray, P., Bittner, M. and Trent, J. M. (2002) 'Wnt5a signaling directly affects cell motility and invasion of metastatic melanoma', *Cancer Cell,* 1(3), 279-88.

Wei, G., Antonescu, C. R., de Alava, E., Leung, D., Huvos, A. G., Meyers, P. A., Healey, J. H. and Ladanyi, M. (2000) 'Prognostic impact of INK4A deletion in Ewing sarcoma', *Cancer,* 89(4), 793-9.

Weidner, N. and Tjoe, J. (1994) 'Immunohistochemical Profile of Monoclonal Antibody 013: Antibody That Recognizes Glycoprotein p30/32MIC2 and is Useful in Diagnosing Ewing's Sarcoma and Peripheral Neuroepithelioma', *The American Journal of Surgical Pathology,* 18(5), 486-494.

Weinberg, R. A. (2014) *The Biology of Cancer,* Second Edition ed.*,* New York: Garland Science.

Welford, S. M., Hebert, S. P., Deneen, B., Arvand, A. and Denny, C. T. (2001) 'DNA Binding Domain-independent Pathways Are Involved in EWS/FLI1-mediated Oncogenesis', *Journal of Biological Chemistry,* 276(45), 41977-41984.

Wells, A., Yates, C. and Shepard, C. R. (2008) 'E-cadherin as an indicator of mesenchymal to epithelial reverting transitions during the metastatic seeding of disseminated carcinomas', *Clinical and Experimental Metastasis,* 25(6), 621-628.

Wend, P., Holland, J. D., Ziebold, U. and Birchmeier, W. (2010) 'Wnt signaling in stem and cancer stem cells', *Seminars in Cell & Developmental Biology,* 21(8), 855-863.

Westwood, G., Dibling, B. C., Cuthbert-Heavens, D. and Burchill, S. A. (2002) 'Basic fibroblast growth factor (bFGF)-induced cell death is mediated through a caspase-dependent and p53-independent cell death receptor pathway', *Oncogene,* 21(5), 809-24.

Willert, K., Brown, J. D., Danenberg, E., Duncan, A. W., Weissman, I. L., Reya, T., Yates, J. R. and Nusse, R. (2003) 'Wnt proteins are lipid-modified and can act as stem cell growth factors', *Nature,* 423(6938), 448-452.

Willert, K. and Nusse, R. (2012) 'Wnt proteins', *Cold Spring Harb Perspect Biol,* 4(9), a007864.

Wong, S. C., Lo, S. F., Lee, K. C., Yam, J. W., Chan, J. K. and Wendy Hsiao, W. L. (2002) 'Expression of frizzled-related protein and Wnt-signalling molecules in invasive human breast tumours', *J Pathol,* 196(2), 145-53.

Wouda, R. R., Bansraj, M. R. K. S., de Jong, A. W. M., Noordermeer, J. N. and Fradkin, L. G. (2008) 'Src family kinases are required for WNT5 signaling through the Derailed/RYK receptor in the Drosophila embryonic central nervous system', *Development,* 135(13), 2277-2287.

Xu, C., Inokuma, M. S., Denham, J., Golds, K., Kundu, P., Gold, J. D. and Carpenter, M. K. (2001) 'Feeder-free growth of undifferentiated human embryonic stem cells', *Nat Biotech,* 19(10), 971-974.

Xu, R. H., Sampsell-Barron, T. L., Gu, F., Root, S., Peck, R. M., Pan, G., Yu, J., Antosiewicz-Bourget, J., Tian, S., Stewart, R. and Thomson, J. A. (2008) 'NANOG is a direct target of TGFbeta/activin-mediated SMAD signaling in human ESCs', *Cell Stem Cell,* 3(2), 196-206.

Yamamoto, H., Yoo, S. K., Nishita, M., Kikuchi, A. and Minami, Y. (2007) 'Wnt5a modulates glycogen synthase kinase 3 to induce phosphorylation of receptor tyrosine kinase Ror2', *Genes to Cells,* 12(11), 1215-1223.

Yang, J., Du, X., Wang, G., Sun, Y., Chen, K., Zhu, X., Lazar, A. J. F., Hunt, K. K., Pollock, R. E. and Zhang, W. (2014) 'Mesenchymal to epithelial transition in sarcomas', *European Journal of Cancer,* 50(3), 593-601.

Yang, L., Wang, L. and Zheng, Y. (2006) 'Gene Targeting of Cdc42 and Cdc42GAP Affirms the Critical Involvement of Cdc42 in Filopodia Induction, Directed Migration, and Proliferation in Primary Mouse Embryonic Fibroblasts', *Molecular Biology of the Cell,* 17(11), 4675-4685.

Yang, W., Yan, H. X., Chen, L., Liu, Q., He, Y. Q., Yu, L. X., Zhang, S. H., Huang, D. D., Tang, L., Kong, X. N., Chen, C., Liu, S. Q., Wu, M. C. and Wang, H. Y. (2008) 'Wnt/beta-catenin signaling contributes to activation of normal and tumorigenic liver progenitor cells', *Cancer Res,* 68(11), 4287-95.

Yee, D., Favoni, R. E., Lebovic, G. S., Lombana, F., Powell, D. R., Reynolds, C. P. and Rosen, N. (1990) 'Insulin-like growth factor I expression by tumors of neuroectodermal origin with the t(11;22) chromosomal translocation. A potential autocrine growth factor', *The Journal of Clinical Investigation,* 86(6), 1806-1814.

Yi, F., Pereira, L., Hoffman, J. A., Shy, B. R., Yuen, C. M., Liu, D. R. and Merrill, B. J. (2011) 'Opposing effects of Tcf3 and Tcf1 control Wnt stimulation of embryonic stem cell self-renewal', *Nat Cell Biol,* 13(7), 762-70.

Yi, F., Pereira, L. and Merrill, B. J. (2008) 'Tcf3 functions as a steady-state limiter of transcriptional programs of mouse embryonic stem cell self-renewal', *Stem Cells,* 26(8), 1951-60.

Ying, J., Li, H., Chen, Y. W., Srivastava, G., Gao, Z. and Tao, Q. (2007) 'WNT5A is epigenetically silenced in hematologic malignancies and inhibits leukemia cell growth as a tumor suppressor', *Blood,* 110(12), 4130-2.

Ying, J., Li, H., Yu, J., Ng, K. M., Poon, F. F., Wong, S. C., Chan, A. T., Sung, J. J. and Tao, Q. (2008) 'WNT5A exhibits tumor-suppressive activity through antagonizing the Wnt/beta-catenin signaling, and is frequently methylated in colorectal cancer', *Clinical cancer research : an official journal of the American Association for Cancer Research,* 14(1), 55-61.

Yost, C., Torres, M., Miller, J. R., Huang, E., Kimelman, D. and Moon, R. T. (1996) 'The axis-inducing activity, stability, and subcellular distribution of beta-catenin is regulated in Xenopus embryos by glycogen synthase kinase 3', *Genes & Development,* 10(12), 1443-54.

Ysebaert, L., Chicanne, G., Demur, C., De Toni, F., Prade-Houdellier, N., Ruidavets, J. B., Mansat-De Mas, V., Rigal-Huguet, F., Laurent, G., Payrastre, B., Manenti, S. and Racaud-Sultan, C. (2006) 'Expression of [beta]-catenin by acute myeloid leukemia cells predicts enhanced clonogenic capacities and poor prognosis', *Leukemia,* 20(7), 1211-1216.

Zecca, M., Basler, K. and Struhl, G. (1996) 'Direct and Long-Range Action of a Wingless Morphogen Gradient', *Cell,* 87(5), 833-844.

Zhang, P., Chang, W.-H., Fong, B., Gao, F., Liu, C., Al Alam, D., Bellusci, S. and Lu, W. (2014) 'Regulation of Induced Pluripotent Stem (iPS) Cell Induction by Wnt/β-Catenin Signaling', *Journal of Biological Chemistry,* 289(13), 9221-9232.

Zhe, J., Chenghai, Z., Xiaorui, H. and Yaxin, H. (2012) 'Wnt5a promotes ewing sarcoma cell migration through upregulating CXCR4 expression', *BMC Cancer,* 12(1), 480.

Zhu, L., Gibson, P., Currle, D. S., Tong, Y., Richardson, R. J., Bayazitov, I. T., Poppleton, H., Zakharenko, S., Ellison, D. W. and Gilbertson, R. J. (2009) 'Prominin 1 marks intestinal stem cells that are susceptible to neoplastic transformation', *Nature,* 457(7229), 603-607.

Zimmermann, M., Box, C. and Eccles, S. A. (2013) 'Two-dimensional vs. three-dimensional in vitro tumor migration and invasion assays', *Methods Mol Biol,* 986, 227-52.

Zufferey, R., Dull, T., Mandel, R. J., Bukovsky, A., Quiroz, D., Naldini, L. and Trono, D. (1998) 'Self-inactivating lentivirus vector for safe and efficient in vivo gene delivery', *J Virol,* 72(12), 9873-80.

Zufferey, R., Nagy, D., Mandel, R. J., Naldini, L. and Trono, D. (1997) 'Multiply attenuated lentiviral vector achieves efficient gene delivery in vivo', *Nat Biotech,* 15(9), 871-875.

Zurawel, R. H., Chiappa, S. A., Allen, C. and Raffel, C. (1998) 'Sporadic medulloblastomas contain oncogenic β-catenin mutations', *Cancer Research,* 58(5), 896-899.